CLINICAL AND GENETIC HETEROGENEITY IN YOUNG ONSET SPORADIC ALZHEIMER'S DISEASE

A thesis submitted to University College London for the Degree of Doctor of Philosophy

Dr Catherine Frances Slattery MA MRCP FHEA

Dementia Research Centre

Department of Neurodegenerative Disease

Institute of Neurology

University College London

2018

Supervisors: Professor Jonathan Schott, Professor Jason Warren

and Professor Nick Fox

For Rosamond, James and Gerard,

all of whom would have liked to read this.

Declaration

I, Catherine Slattery, confirm that the work presented in this thesis is my own. Where information or analyses have been derived from other sources or in collaboration with other researchers I confirm that this has been indicated (please see Statement of Contributions).

Abstract

Alzheimer's disease, the commonest neurodegenerative condition, is characterised by accumulation of amyloid plaques and neurofibrillary tangles, neuronal loss, brain atrophy and cognitive impairment. Sporadic young onset Alzheimer's disease shows marked clinical heterogeneity, with non-memory presentations including the syndromes of posterior cortical atrophy, logopenic aphasia and frontal Alzheimer's disease, seen in around a third of individuals. This variability presents challenges for diagnosis and may confound clinical trial outcomes, but provides an opportunity to explore factors influencing differential selective vulnerability within neural networks which in turn may provide important clues to Alzheimer's disease pathogenesis.

This thesis describes the recruitment of a cohort of a deeply phenotyped patients with sporadic young onset Alzheimer's disease (n=45) and healthy controls (n=24), and a series of genetic, clinical, neuropsychological, and structural, diffusion and functional magnetic resonance imaging experiments to explore disease heterogeneity and its associations.

There are a number of key findings. *APOE* ε4 genotype contributes to, but does not fully explain clinical heterogeneity, with the youngest ages of onset and most atypical presentations seen in ε4-ve individuals. Heterozygosity of the rare *TREM2* genetic variant for late-onset Alzheimer's disease, p.R47H, is shown to confer risk for young onset Alzheimer's disease, driving younger age of onset rather than clinical phenotype. Regional brain atrophy profiles in *APOE* ε4 genotypes are shown to broadly align with the associated neuropsychological deficits. Microstructural damage studied using diffusion tensor imaging, and – applied for the first time to Alzheimer's disease – Neurite Orientation Dispersion and Density Imaging – provides a fine-grained profile of white matter network breakdown, revealing regional differences based on *APOE* ε4 genotype,

and correlations with focal neuropsychological deficits. Finally, activation fMRI using a music paradigm to probe relationships between cognitive performance and brain function is shown to delineate different patterns of brain activation during memory tasks in different Alzheimer's disease phenotypes.

Impact Statement

The analyses presented in this thesis have advanced our knowledge of the clinical and imaging characteristics of young onset Alzheimer's disease and how associated genetic risk factors relate to phenotype. The mechanisms underlying these observations pose questions to be explored in future work. This thesis also applies new techniques to Alzheimer's disease research. Music is used as a tool to investigate aspects of memory processing and network dysfunction, and the NODDI analyses act as proof of concept that the technique can detect microstructural differences in Alzheimer's disease. Both NODDI and fMRI have potential to further inform our understanding of heterogeneity between, as well as within, other neurodegenerative diseases.

Academic impact has been achieved though the scientific papers I have published in peer reviewed journals. I have also given platform presentations at national and international conferences and produced a podcast with the British Neuropsychiatry Association on my work in TREM2. I have lectured UCL undergraduate students on atypical forms of Alzheimer's disease, thereby contributing to the education of future clinicians and academics.

Beyond academia, increased knowledge of heterogeneity in Alzheimer's disease is likely to affect participant recruitment and outcome measure selection for clinical trials. Study of newly identified genetic risk factors, such as TREM2 variants, may lead to new insights into disease pathogenesis and potentially new therapeutic targets, or help select individuals most likely to benefit from certain disease modifying drugs based on their mechanism of action. Imaging techniques such as NODDI may be useful in clinical trials if metrics are shown to be robust, reproducible and capable of tracking disease over time.

The impact may also extend into clinical practice. Much as DTI and fMRI are now used on an individual patient basis in epilepsy surgery to delineate speech areas and visual pathways, NODDI and activation fMRI may be adopted into hospital dementia scanning protocols in conjunction with molecular imaging, to offer people with cognitive symptoms an earlier and more accurate diagnoses. Furthermore, should a disease modifying treatment for early or pre-symptomatic disease be developed, a national NHS screening programme for Alzheimer's would be required to identify those who would most benefit. This may include clinical testing for genetic risk factors, such as APOE and TREM2 to risk stratify individuals, and imaging techniques that can show early structural and/or functional changes will also be important.

Greater public and political awareness of atypical and young onset dementia is important for the design and delivery of dementia healthcare and services. I have worked with Alzheimer's Research UK at their Supporters days and contributed to their blog about Alzheimer's disease being more than just a 'memory problem', I have attended rare dementias support groups, contributed to a BBC Horizon programme that featured some of the work of the YOAD study, and reviewed the content of the NHS Choices dementia website.

Finally, on a personal level the work in this thesis represents the foundations on which I intend to build a career long commitment to research and clinical practice in cognitive neurology.

Table of Contents

Table of Contents **8**

List of Tables **13**

List of Figures **15**

1. Introduction: Alzheimer's disease **22**

1.1 History and epidemiology **22**

1.2 Pathology **23**

1.2.1 Macroscopic pathology 23
1.2.2 Microscopic pathology 23
1.2.3 Neuropathological criteria 25

1.3 Aetiology **28**

1.3.1 Genetic determinants 28
1.3.2 Other Risk Factors 34

1.4 Pathophysiology **34**

1.4.1 The Amyloid Hypothesis 34
1.4.2 Limitations of the amyloid hypothesis and emerging concepts 38

1.5 The Natural History of Alzheimer's disease pathogenesis **40**

1.6 Clinical Presentation **43**

1.7 Clinical Diagnostic Approach **45**

1.7.1 Clinical assessment 46
1.7.2 Neuropsychology 47
1.7.3 Blood tests 47
1.7.4 Neuroimaging 48
1.7.5 CSF biomarkers 50
1.7.6 Neurophysiology 51
1.7.7 Genetics 51

1.8 Treatment **52**

1.8.1 Symptomatic 52
1.8.2 The search for disease modifying therapy 52
1.8.3 A new era of Alzheimer's disease therapeutics 56

2 Pathology to phenotype: Clinical Heterogeneity in Alzheimer's disease **57**

2.1 Early descriptions of Alzheimer's disease heterogeneity: subgroups vs stages **57**

2.2 'Typical Alzheimer's disease' **59**

2.3 'Atypical' Alzheimer's disease **59**

2.3.1 Posterior cortical atrophy 60
2.3.2 Logopenic aphasia 62

2.3.3 Frontal Alzheimer's disease ... 62
2.3.4 Syndromic convergence ... 62
2.4 Research diagnostic criteria ... 64
2.4.1 US National Institute on Aging–Alzheimer's Association criteria ... 64
2.4.2 International working group (IWG) criteria ... 66
2.4.3 NIA-AA 2018 Research Framework ... 69
2.5 Patterns of neuronal injury - evidence for selective vulnerability ... 69
2.5.1 MRI atrophy ... 70
2.5.2 Hypometabolism on ^{18}F-fluorodeoxyglucose (FDG)-PET ... 72
2.6 Drivers of clinical heterogeneity ... 72
2.6.1 Amyloid pathology ... 72
2.6.2 Tau pathology ... 73
2.6.3 Other co-existing pathologies ... 74
2.6.4 Genetic factors ... 75
2.7 Potential mechanisms underlying selective vulnerability ... 76
2.7.1 The network paradigm of neurodegenerative disease ... 77
2.7.2 Nexopathies: from protein abnormality to network signature ... 79
2.7.3 "Catastrophic cliffs" ... 80
2.7.4 Resilience factors ... 80
2.8 The challenge and opportunity of clinical heterogeneity ... 81
3 Neuroimaging in Alzheimer's disease ... 83
3.1 Principles of MRI ... 83
3.2 Volumetric structural MRI ... 84
3.3 Diffusion Tensor Imaging ... 86
3.4 Neurite Orientate Dispersion and Density Imaging ... 90
3.5 Activation functional MRI ... 93
4 Thesis aims and outline ... 96
5 Methods overview - Cohorts ... 98
5.1 The YOAD cohort ... 98
5.1.1 Participants ... 98
5.1.2 Case Selection: inclusion and exclusion criteria ... 100
5.1.3 Consent and Ethical Considerations ... 101
5.1.4 Study design ... 102
5.1.5 Correction for multiple comparisons ... 111
5.1.6 Statistical analyses ... 111
5.1.7 Data storage ... 111
5.2 Other genetic cohorts ... 112
5.2.1 Participants ... 112
5.2.2 Consent and Ethical Considerations ... 113
5.3 Techniques for investigating genetic heterogeneity ... 113
5.3.1 Sanger sequencing ... 113

5.3.2 Next generation sequencing 114

6 Recruitment to the YOAD study 115

6.1 Introduction 115

6.2 Methods 115

6.3 Results 115

6.3.1 Clinical characteristics 115
6.3.2 Neuropsychology 123
6.3.3 Symptomatic treatment for Alzheimer's disease 125

6.4 Discussion 125

7 Genetic heterogeneity in the YOAD cohort 128

7.1 Introduction 128

7.2 Methods 128

7.2.1 Participants 128
7.2.2 Dementia Panel NGS 128
7.2.3 Sanger Sequencing 129
7.2.4 *APOE* ε4 status 129

7.3 Results 129

7.3.1 Autosomal dominant variants 129
7.3.2 *APOE* ε4 status 130

7.4 Discussion 135

8 Rare genetic variants: *TREM2* 138

8.1 Introduction 138

8.2 Methods 139

8.2.1 Cohorts 139
8.2.2 Genetics 141
8.2.3 Clinical phenotyping 141
8.2.4 Imaging 144
8.2.5 Statistics 144

8.3 Results 145

8.3.1 *TREM2* in YOAD cohort 145
8.3.2 *TREM2* in DRC genetics cohort 145
8.3.3 *TREM2* variants are associated with earlier disease onset in Alzheimer's disease 147
8.3.4 R47H variants in Alzheimer's disease: clinical features and neuropsychological profiles 148
8.3.5 Neuroimaging in p.R47H variants 151
8.3.6 Pathology in p.R47H cases 153

8.4 Discussion 153

9 *APOE* and structural brain imaging: brain and grey matter volumes 157

9.1 Introduction 157

9.2 Methods 157

9.2.1 Participants 157
9.2.2 *APOE* genotyoing 158
9.2.3 Imaging acquisition 158
9.2.4 Data analyses 158

9.3 Results 160

9.3.1 Demographics and clinical phenotypes 160
9.3.2 Brain, ventricle and hippocampal volumes 161
9.3.3 Grey matter structural changes: VBM analyses 163

9.4 Discussion 166

10 *APOE* and structural brain imaging: microstructural white matter changes 169

10.1 Introduction 169

10.2 Methods 170

10.2.1 Participants 170
10.2.2 *APOE* genotyping 171
10.2.3 Imaging acquisition 171
10.2.4 Data analyses 172
10.2.5 Neurite density index region of interest analyses 173

10.3 Results 173

10.3.1 Demographics and clinical features 173
10.3.2 Neuropsychological profiles 174
10.3.3 White matter changes by *APOE* ε4 genotype: DTI and NODDI 176
10.3.4 Region of interest NDI correlation with cognitive function 180

10.4 Discussion 183

11 Investigating the functional basis of memory impairment in Alzheimer's disease 189

11.1 Introduction 189

11.2 Methods 193

11.2.1 Participants 193
11.2.2 Assessment of musical background and peripheral hearing function 194
11.2.3 Experimental stimuli and protocol 196
11.2.4 Brain imaging acquisition 200
11.2.5 Post scan behavioural testing 201
11.2.6 Data analyses 202

11.3 Results 206

11.3.1 General characteristics of participant groups 206
11.3.2 Post scan behavioural data 206
11.3.3 Structural neuroanatomical data 207
11.3.4 Functional neuroanatomical data 209

11.4 Discussion 214

12 General discussion 220

12.1 Summary of findings 220
12.2 Limitations 224
12.3 Why clinical heterogeneity matters: Future Directions 229
12.4 Conclusions 235

Statement of contribution 236

Acknowledgements 238

Publications 239

Prizes 241

Appendices 242

Appendix 1: YOAD cohort characteristics and participation by imaging modality 243

Appendix 2: Items used in the musical experience questionnaire 247

Appendix 3: YOAD study – participant folder 248

References 266

List of Tables

Table 1.1 Outcomes of Phase 3 Clinical Trials of Amyloidocentric Drugs 55

Table 2.1 Diagnostic criteria for posterior cortical atrophy 61

Table 2.2 Diagnostic criteria for logopenic variant PPA 63

Table 2.3 NIA-AA 2011 criteria for Probable Alzheimer's Disease Dementia 65

Table 2.4 2014 IWG-2 criteria for typical Alzheimer's disease (A plus B at any stage) 67

Table 2.5 2014 IWG-2 criteria for atypical Alzheimer's disease (A plus B at any stage) 68

Table 5.1 Overview of YOAD study design 102

Table 5.2 MRI sequence parameters 106

Table 5.3 MRI modalities and analyses used by chapter 107

Table 6.1 Reported cognitive, behavioural, neuropsychiatric and motor symptoms in YOAD study participants 118

Table 6.2 Neurological signs in YOAD study participants 120

Table 6.3 Blood pressure of study participants 121

Table 6.4 Neuropsychological characteristics of YOAD study participant groups..... 124

Table 7.1 Variants identified in genes causing autosomal dominant Alzheimer's disease 130

Table 7.2 Expected and observed *APOE* genotype and mean age at onset 131

Table 7.3 Neurological signs in YOAD cohort ε4+ve and ε4-ve individuals 132

Table 7.4 Neuropsychological profiles of YOAD cohort patient participants by APOE ε4 status 134

Table 8.1 Demographics of age and sex matched p.R47H and nil TREM2 variant Alzheimer's disease cases 143

Table 8.2 TREM2 coding variants identified using Sanger sequencing of exon 2 146

Table 8.3 p.R47H TREM2 variants in Alzheimer's disease and frontotemporal dementia 147

Table 8.4 Clinical features of Alzheimer's disease individuals with p.R47H variant... 149

Table 8.5 Leading symptoms and neurological signs in AD patients by p.R47H genotype 150

Table 9.1 Demographics for YOAD study participants included in the grey matter atrophy analyses 160

Table 9.2 Volumetric data for 40 YOAD patient participants and 21 controls 162

Table 10.1 Study Participants' Demographic, Neuropsychological and Clinical Characteristics..... 175

Table 10.2 NODDI metrics in each region of interest..... 180

Table 11.1 Demographic, clinical and behavioural characteristics of participants 195

Table 11.2 Familiar melodies presented in the fMRI experiment 200

Table 11.3 Summary of fMRI data within and between participant groups 211

List of Figures

Figure 1.1 Alois Alzheimer's sketch of neurofibrillary tangles in the advanced stages of Alzheimer's disease 24

Figure 1.2 Photomicrographs of the core pathological lesions observed in Alzheimer's disease 24

Figure 1.3 Spatiotemporal pattern of amyloid plaque deposition according to Thal *et al.* [15] 27

Figure 1.4 Spatiotemporal pattern of neurofibrillary degeneration in Alzheimer's disease 28

Figure 1.5 The genetic landscape of Alzheimer's disease 33

Figure 1.6 The major pathways of amyloid precursor protein processing 35

Figure 1.7 Major pathogenic processes in Alzheimer's disease, as proposed by the Amyloid Hypothesis 37

Figure 1.8 Dynamic biomarkers of the Alzheimer's pathological cascade 43

Figure 1.9 Structural, metabolic and molecular imaging posterior cortical atrophy due to Alzheimer's disease 50

Figure 2.1 Alzheimer's disease atrophy profiles by phenotype 71

Figure 3.1 Diffusion tensor imaging in Alzheimer's disease 88

Figure 3.2 Diffusion tensor imaging (DTI) and neurite orientation dispersion and density imaging (NODDI) models for diffusion weighted MRI 92

Figure 3.3 Neurite Orientation Dispersion and density imaging maps in Alzheimer's disease 93

Figure 5.1 Representative diffusion images for diffusion weighted imaging (top panel) and neurite orientation dispersion and density imaging (lower panels). 109

Figure 8.1 Coronal MRI images in 4 individuals with Alzheimer's disease and p.R47H variant 152

Figure 9.1 Atrophy in young onset Alzheimer's disease relative to controls. Top row: unthresholded t-statistic maps are shown on the left, statistical parametric maps on the right. Bottom row: additional coronal SPM slices 164

Figure 9.2 Atrophy in young onset APOE ε4 positive and negative individuals with Alzheimer's disease relative to controls 165

Figure 9.3 Atrophy differences between ε4–ve and ε4 +ve individuals 166

Figure 10.1 DTI and NODDI metrics in patients with (A) ε4-ve YOAD (n15) and (B) ε4+ve YOAD (n=22) relative to controls (n=23) 177

Figure 10.2 Added sensitivity and specificity of NODDI over DTI 178

Figure 10.3 Coronal (left), sagittal (middle) and axial (right) neurite density index t-statistic maps 179

Figure 10.4 Significant correlations between regional neurite density index and neuropsychological measures in white matter projections from the right (A and B) and left (C) parieto-occipital cortices of patients with YOAD (n=37) 182

Figure 11.1 Anatomical small volumes used in analysis of fMRI data 205

Figure 11.2 Regional grey matter atrophy profiles in the patient groups 208

Figure 11.3 Functional neuroanatomy of musical memory: within-group correlates for patients and healthy controls 212

Figure 11.4 Functional neuroanatomy of musical memory: patients compared with healthy controls 213

Abbreviations

Aβ	amyloid-beta
Aβ42	the 42-aminoacid form of Aβ
AAO	age at clinical disease onset
AChEIs	acetylcholinesterase inhibitors
ADAS-cog	Alzheimer's Disease Assessment Scale–Cognitive Subscale
ADCS-ADL	Alzheimer's Disease Cooperative Study–Activities of Daily Living Inventory
Amyg	amygdala
APP	amyloid precursor protein
APOE	apolipoprotein
AxD	axial diffusivity
BD	twice daily
BOLD	blood oxygenation level dependent
BSI	boundary shift integral
C9orf72	chromosome 9 open reading frame 72
CA1	Cornus ammonis 1 hippocampal subfield
Cblm	cerebellum
Cd	caudate nucleus
CDR-SB	Clinical Dementia Rating–Sum of Boxes
Cg	cingulate cortex
CHMP2B	charged multivesicular body protein 2B gene
CI	confidence interval
Cl	claustrum
CSF	cerebrospinal fluid
CSF1R	colony stimulating factor 1 receptor gene

CT	computed tomography
dNTPs	deoxynucleosidetriphosphates
ddNTPs	di-deoxynucleotidetriphosphates
Die	diencephalon
dir	direction
DKEFS	Delis-Kaplan executive function system
DMARD	disease modifying therapy
DNA	deoxyribonucleic acid
dof	degrees of freedom
DSMT	digit symbol modalities test
DTI	diffusion tensor imaging
DWI	diffusion weighted imaging
EC	entorhinal cortex
EEG	electroencephalomyography
F	female
FA	fractional anisotropy
^{18}FDG	18F-fluorodeoxyglucose FDG
Fiso	fraction of free water
FLIRT	FMRIB's Linear Image Registration Tool
FoV	field of view
FS	FreeSurfer-longitudinal
FSL	FMRIB Software Library
FTD	frontotemporal dementia
FUS	fused in sarcoma gene
FEW	family wise error
GDA	graded difficulty arithmetic test
GDST	graded difficulty spelling test

Gpe	globus pallidus externus
Gpi	globus pallidus internus
GRN	granulin precursor gene
Hipp	hippocampus
Ins	insular cortex
IQR	interquartile range
IV	intravenous
ITM2B	integral membrane protein 2B gene
LL	lower limb
LOAD	late onset Alzheimer's disease
LPA	logopenic progressive aphasia
M	male
MAF	minor allele frequency
MAPT	microtubule-associated protein tau gene
Med	medulla oblongata
Mid	midbrain
MIDAS	Medical Information Display and Analysis
mls	millilitres
MMSE	mini mental state examination
MR	magnetic resonance
n	number
NDI	neurite density index
NFT	neurofibrillary tangles
NODDI	neurite orientation dispersion and density imaging
NOTCH3	neurogenic locus notch homolog protein 3 gene
OD	once daily
ODI	orientation dispersion index

OR	odds ratio
P	probability
PCA	posterior cortical atrophy
PE	phase encoding
PET	positron emission tomography
PIB	^{11}C Pittsburgh Compound B
PLOSL	Polycystic lipomembranous osteodysplasia with sclerosing leukoencephalopathy
Prec	precuneus
PRNP	prion protein gene
PSEN1	presenilin 1 gene
PSEN2	presenilin 2 gene
P-Tau	phosphorylated tau
Put	putamen
RD	radial diffusivity
RMT	recognition memory test
SD	standard deviation
SERPINI1	serpin family I member 1 gene
SIENA	Structural Image Evaluation, using Normalization, of Atrophy
SPM	statistical parametric mapping
SQSTM1	sequestosome-1 gene
TARDBP	TAR DNA-binding protein 43 gene
TBI	traumatic brain injury
TBM	Tensor-Based Morphometry
TE	echo time
TFCE	threshold-free cluster enhancement
TIV	total intracranial volume

TR	repetition time
TREM2	triggering receptor expressed on myeloid cells 2 gene
T-Tau	total tau
TYROBP	TYRO protein tyrosine kinase binding protein gene
UL	upper limb
VCP	valosin-containing protein gene
VOSP	visual object and spatial perception
WASI	Wechsler Abbreviated Scale of intelligence
YOAD	young onset Alzheimer's disease
Yrs	years

1. Introduction: Alzheimer's disease

Alzheimer's disease is a progressive neurodegenerative condition leading invariably to cognitive impairment of sufficient severity to impact on an individual's activities of daily living. It is the commonest cause of dementia worldwide and a major cause of dependence, disability and mortality. The prevalence of dementia is expected to more than triple by 2050 as life expectancy increases and the population ages. It is estimated that without disease modifying treatment 24% of men and 35% of women born in 2015 will develop dementia within their lifetime [1].

1.1 History and epidemiology

In 1906, Alois Alzheimer published on "a peculiar disease of the cerebral cortex" by describing plaques, neurofibrillary tangles and arteriosclerotic changes in the brain of a woman, Auguste D, with presenile dementia who presented at the age of 51 years [2]. She had presented to his clinic with profound language deficits, behavioural disturbance including anxiety and paranoid delusions, and episodic memory loss. In doing so, he described the neuropathology of the disease that was to subsequently bear his name [3]. For the next fifty years the term 'Alzheimer's disease' was restricted to severe forms of presenile dementia with abundant plaques and neurofibrillary tangles until reports based on large clinicopathological series demonstrated that the neuropathological manifestations of presenile and senile dementia were qualitatively the same and hence it was not warranted to define them as separate diseases [4]. Senile dementia was no longer accepted as a 'normal' consequence of aging and Alzheimer's pathology is now recognised as the single biggest cause of dementia, accounting for between 50% to 75% of all cases of dementia.

Age is the single greatest risk factor for sporadic Alzheimer's disease. Incidence of probable Alzheimer's disease for people aged 60 to 69 years is <1% but this increases steadily with age to approximately 7% for those age 85 to 89 years [5]. The prevalence of Alzheimer's disease roughly doubles for every 5 years after age 65 [6]. In the UK, this equates to a prevalence of about 2% for people aged between 65 and 69 years, rising to 20% for those aged between 85 to 89 years [7]. Despite the low incidence of dementia in people under 65 years, over 42,000 people have early-onset dementia in the UK.

1.2 Pathology

1.2.1 Macroscopic pathology

Alzheimer's disease invariably leads to neuronal cell death which manifests macroscopically as atrophy. This atrophy is typically symmetrical resulting in cortical thinning, widening of sulcal spaces and increased size of the ventricles. The rate of brain atrophy varies depending on brain region; the medial temporal lobe structures such as the entorhinal cortex and hippocampus are prominently affected, and the primary motor, sensory and visual cortices and relatively spared until advanced disease.

1.2.2 Microscopic pathology

Alzheimer described the microscopic pathological hallmarks of Alzheimer's disease in his original paper: amyloid plaques and neurofibrillary tangles (Figure 1.1).

Amyloid plaques are dense, extracellular predominantly insoluble deposits of amyloid-β peptide (Aβ1-42), and neurofibrillary tangles are intracellular paired helical filaments composed of hyperphosphorylated microtubule-associated protein tau (Figure 1.2). Neutropil threads, dystrophic neurons, astrogliosis and microglial activation are also seen, and cerebral amyloid angiopathy frequently coexist [8]. These pathological

processes lead to downstream neurodegeneration with progressive loss of neurons and synapses culminating in macroscopic atrophy.

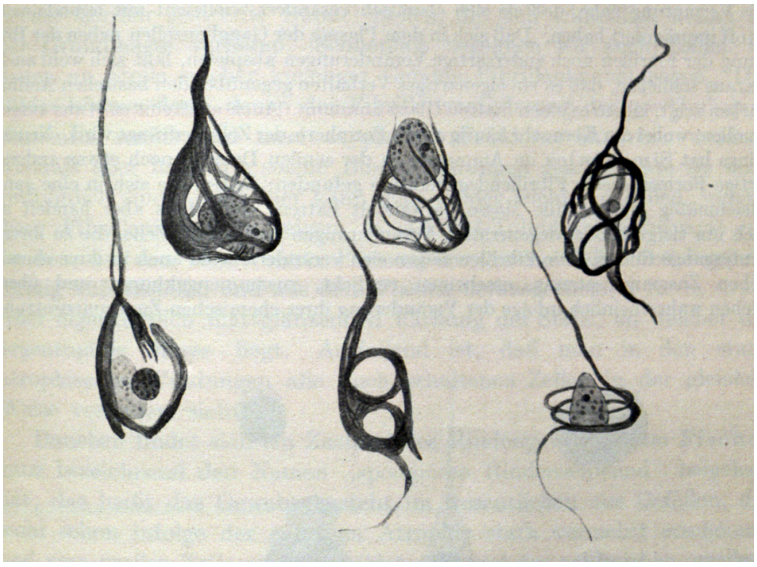

Figure 1.1 Alois Alzheimer's sketch of neurofibrillary tangles in the advanced stages of Alzheimer's disease

From his paper in 1911, published in Zeitschrift für die gesamte Neurologie und Psychiatrie: Originalen.

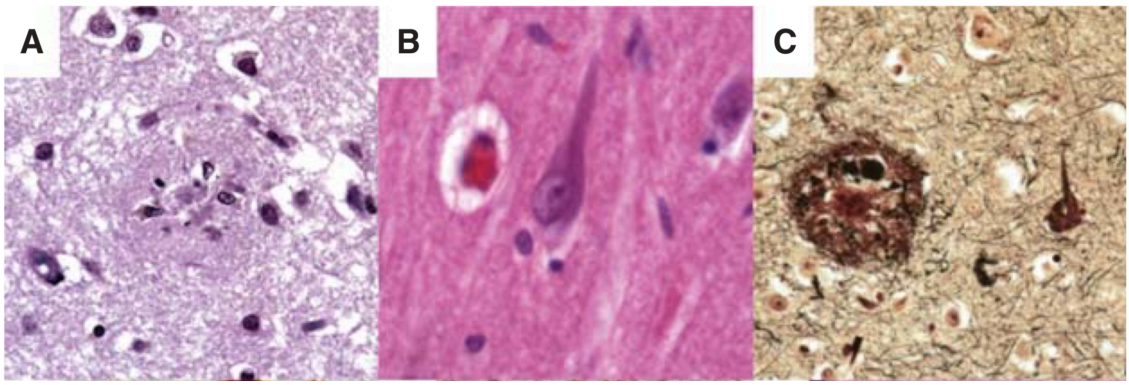

Figure 1.2 Photomicrographs of the core pathological lesions observed in Alzheimer's disease

(A) H&E stained section of frontal cortex showing an amyloid plaque; (B) H&E stained section showing a tangle in a hippocampal pyramidal neuron. (C) Silver stain showing both a plaque and a tangle. Reproduced from Serrano-pozo *et al., 2011 [8].*

Tau is a normal and essential protein expressed in nerves which contributes to their structural and functional integrity by stabilising the cytoskeleton and facilitating axonal transport [9]. It exists in six different isoforms, three of which have three repeats in the extracellular domain ('three-repeat tau', 3R-tau), with the remaining three have four ('four-repeat tau', 4R-tau). Alzheimer's disease is associated with hyperphosphorylation of both 3R-tau and 4R-tau, distinguishing it at the molecular level from other 'tauopathies'; Picks disease is only associated with 3R-tau, and corticobasal degeneration and progressive supranuclear palsy with 4R-tau.

Other pathologies, such as vascular disease, TDP43, and Lew Body Disease often co-exist [10, 11], particularly in older individuals, however it is hard to know what their relative contribution to cognitive impairment for an individual is.

Amyloid and tau are found throughout the brain of people with Alzheimer's disease in broadly predictable distributions. Amyloid plaques are typically found throughout the isocortex, and only involve subcortical structures in advanced disease. Amyloid pathology reaches a plateau early in the symptomatic phase of the disease [12] so tends not to correlate well with clinical features and severity of clinical disease. Tau tangles tend to be found initially in the entorhinal cortex and hippocampus before spreading to the association cortices whereas primary motor, sensory and visual cortex tends to be unaffected. Neurofibrillary tangles parallel synaptic and neuronal loss more closely than amyloid-β [8] and hence tends to correlate with the clinical stage of disease.

1.2.3 Neuropathological criteria

With pathological diagnosis being the 'gold standard' there are several criteria for the neuropathological diagnosis and staging of Alzheimer's disease. Both the Braak criteria [13] and Consortium to Establish a Registry for Alzheimer's Disease (CERAD) criteria [14] quantify the burden of amyloid plaques. The later Thal criteria [15] recognised that

amyloid exists in forms other than plaques, and that deposition in the brain occurs following a distinct sequence in regions that are hierarchically involved (Figure 1.3). Tau pathology is staged using Braak criteria for neurofibrillary tangles [16] (Figure 1.4).

Criteria using only amyloid plaques or NFT have low sensitivity and specificity for Alzheimer's disease [17], so the National Institute of Ageing and the Reagan Institute combined the CERAD neuritic plaque score with the Braak and Braak NFT staging to derive a criteria with three categories of diagnostic certainty: high, intermediate or low likelihood of Alzheimer's disease [18]. The more recent National Institute on Aging and the Alzheimer's Association NIA-AA) [19] neuropathological guidelines also address the potential disconnect between the clinical phenotype and neuropathological changes, as some individuals at post mortem are found to have a high degree of Alzheimer's disease pathology without ever having had clinical symptoms during life.

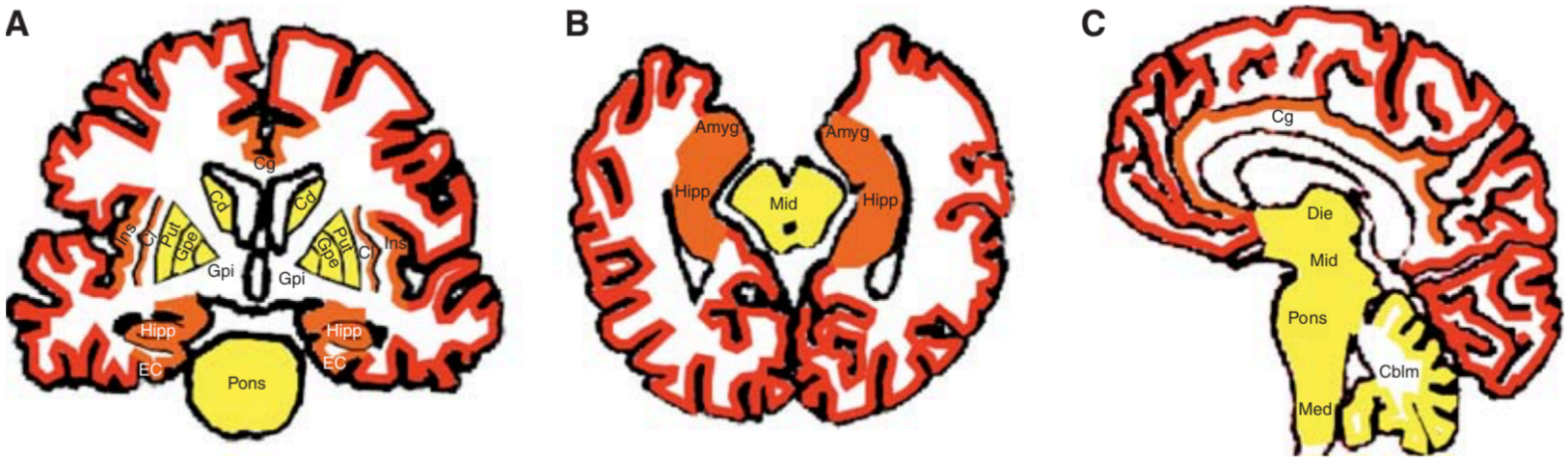

Figure 1.3 Spatiotemporal pattern of amyloid plaque deposition according to Thal *et al.* [15]

Coronal (A), axial (B), and sagittal (C) views of the brain. Five stages of amyloid deposition are summarised in three stages: (i) amyloid deposits accumulate isocortical areas (red), followed by limbic and allocortical structures (orange), and finally in subcortical structures such as the basal ganglia, selected nuclei in the midbrain and medulla and the cerebellar cortex (yellow). Amyg, amygdala; EC, entorhinal cortex; Hipp, hippocampus; Cg, cingulate cortex; Cd, caudate nucleus; Put, putamen; Gpe, globus pallidus externus; Gpi, globus pallidus internus; Cl , claustrum; Ins, insular cortex; Die, diencephalon; Mid, midbrain; Med, medulla oblongata; Cblm, cerebellum. Figure reproduced from Serrane-Pozo *et al.*, 2011 [8].

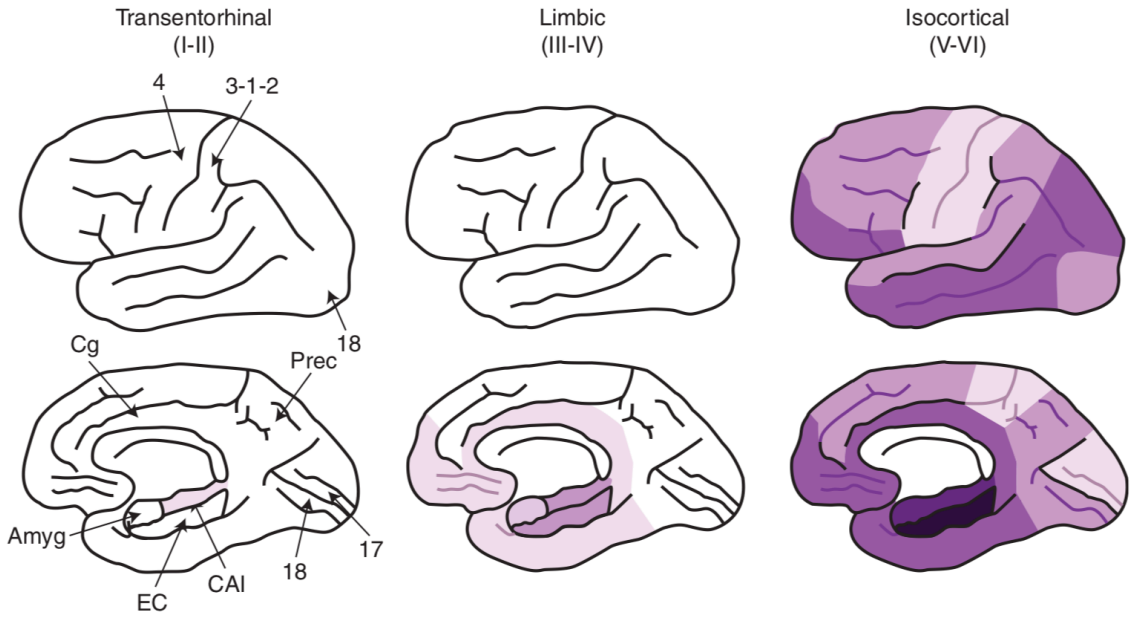

Figure 1.4 Spatiotemporal pattern of neurofibrillary degeneration in Alzheimer's disease

Spatiotemporal pattern of neurofibrillary degeneration in Alzheimer's disease, based on Braak et al., 1991 and 2006 [13, 16]. Shading indicates the distribution of NFTs - darker colours represent increasing densities. Amyg, amygdala; EC, entorhinal cortex; CA1, Cornus ammonis 1 hippocampal subfield; Cg, cingulate cortex; Prec, precuneus; 4, primary motor cortex; 3-1-2, primary sensory cortex; 17, primary visual cortex; 18, associative visual cortex. Figure reproduced from Serrane-Pozo *et al.*, 2011 [8].

1.3 Aetiology

1.3.1 Genetic determinants

Alzheimer's disease has a complex and heterogeneous genetic component. Three genes have been identified as the cause of early onset familial Alzheimer's disease, which represents less than 1% of cases. Early onset familial Alzheimer's disease behaves in an autosomal dominant manner affecting people typically when they are less

than 65 years old, but can be as early as their thirties. In contrast, late onset Alzheimer's disease is typically 'sporadic' with no apparent familial recurrence. The genetic component of this late onset form has been the target of a large number of studies looking to identify genetic risk factors (see below). Furthermore, the genetic architecture of young onset Alzheimer's disease (symptom onset <65 years) occurring in the absence of one of the autosomal dominant mutations remains relatively unknown.

1.3.1.1 Autosomal dominant, causal, genes

In the early 1990s linkage analyses studying families with early onset Alzheimer's disease identified the only fully penetrant mutations known to date to be pathogenic. The localisation of the gene encoding the Aβ precursor protein (APP) to chromosome 21, coupled with the earlier observation that trisomy 21 (Down's syndrome) leads invariably to the neuropathology of Alzheimer's disease [20] set the stage for the proposal that perturbations in Aβ homeostasis are a primary event in Alzheimer's disease pathogenesis. Three genes were found to carry Alzheimer's disease pathogenic mutations: amyloid precursor protein gene (*APP*, chromosome 21q21.3) [21], presenilin 1 gene (*PSEN1,* chromosome 14q24.3) [22] and presenilin 2 gene (*PSEN2*, chromosome 1q31-q42) [23]. More recently duplications of the APP gene have been identified as an additional cause of familial Alzheimer's disease [24].

The identification of these causative genes led to an understanding of the molecular pathology, culminating in the amyloid hypothesis [25] (outlined in the next section) which is also proposed to apply to apparent 'sporadic' disease.

1.3.1.2 Risk factor genes

- *Apolipoprotein ε4: A low frequency variant conferring moderate risk*

The early linkage analyses also identified a strong risk factor for late onset Alzheimer's disease: possession of an ε4 allele of *APOE* (Apolipoprotein E, *APOE*, chromosome 19q13.2) [26]. *APOE* encodes a glycoprotein synthesized predominantly in the liver, brain (by neurons and astrocytes), macrophages and monocytes [27].

The *APOE* gene consists of four exons and three introns and is polymorphic, with three common alleles (epsilon 2, epsilon 3, epsilon 4) coding for three isoforms (ε2, ε3, ε4). The isoforms differ from each other by a single amino acid substitution, and also differ in their binding affinity for *APOE* receptors. The frequencies of the 2, 3, and 4 alleles are estimated at 0.07, 0.79, and 0.14, respectively, but can vary widely among populations (meta-analysis http://www.alzgene.org/ [28]). The ε4 allele confers an increased risk of Alzheimer's disease seen across different ethnic groups of ~3-fold for heterozygous carriers and up to 15-fold for individuals who are ε4 homozygotes relative to ε3homozygotes [29]. *APOE* is known to act in a dose dependent manner: with the risk for Alzheimer's disease increasing, and the mean age of onset decreasing from 84 to 68 years with an increasing number of ε4 alleles [30].

APOE is implicated in mobilisation and redistribution of cholesterol, neuronal growth and repair [31], immunoregulation and activation of enzymes for lipolysis [32]. However, the critical mechanism by which *APOE* ε4 confers a high risk of Alzheimer's disease is unclear. *APOE* ε4 is involved in Aβ transport, and proteins encoded by the different *APOE* polymorphisms have different effects on its clearance. *APOE* ε4 is less effective at clearing Aβ than *APOE* ε2 or 3, so it may be through this effect that the risk of AD is enhanced [33].

The identification of the three autosomal dominant genes, and *APOE* represented a huge leap forward in the understanding of Alzheimer's disease genetics, however these genes have been estimated to account for less than 30% of the genetic variance in early

onset and late onset Alzheimer's disease [34] suggesting that numerous additional Alzheimer's disease risk factor genes exist and environmental factors are important.

- *Genome Wide Association Study: Common variants conferring small increased risk*

The development of whole-genome genotyping platforms has allowed the involvement of common variants conferring low risk in Alzheimer's disease to be studied. Genome wide association studies (GWAS) are large observational studies comparing the DNA of participants with a particular trait or phenotype with individuals who do not. If one genetic locus is more frequent in people with the disease than controls, that region is said to be associated with the disease.

To date over 20 genetic loci with low risk effects for Alzheimer's disease have been identified by GWAS [35], including *CLU*, *PICALM*, *CR1*, *BIN1*, *CD33*, *ABCA7*, *MS4A6A* and *MS4A4E*, *CD2AP*, *EPHA1, HLA-DRB5/DRB1, SORL1, PTK2B, SLC24A4, ZCWPW1, CELF1, FERMT2, CASS4, INPP5D, MEF2C,* and *NME8.* These risk loci implicate some common biological pathways in the pathogenesis of Alzheimer's disease, with clear significant overrepresentation of association signals in pathways related to cholesterol metabolism, the immune response and endosomal vesicle recycling [36].

- *Triggering receptor expressed on myeloid cells 2: A rare variant conferring moderate risk*

In 2013, a rare gene conferring moderate risk for Alzheimer's disease was identified.

Triggering receptor expressed on myeloid cells 2 (*TREM2*) is a transmembrane glycoprotein which associates with *DAP12*; also known as TYRO protein tyrosine kinase binding protein (*TYROBP*). The association between these two proteins controls two streams of signalling to regulate microglial activation. Variants in *TREM2* had

previously been associated with Nasu-Hakola disease, a rare autosomal recessive form of dementia presenting with bone cysts [37]. Prompted by the identification of different rare *TREM2* homozygous mutations causing frontotemporal dementia [38], the role of *TREM2* was investigated in other dementias. In studying Alzheimer's disease cases and controls a heterozygous rare variant (p.R47H) was found to be associated with an increased risk (OR > 3) for the development of Alzheimer's disease [39, 40], making it the most significant, albeit much rarer, risk factor gene for sporadic Alzheimer's disease to be identified since *APOE*. *TREM2* is emerging as a molecular determinant in how the brain responds to Aβ deposition [41, 42].

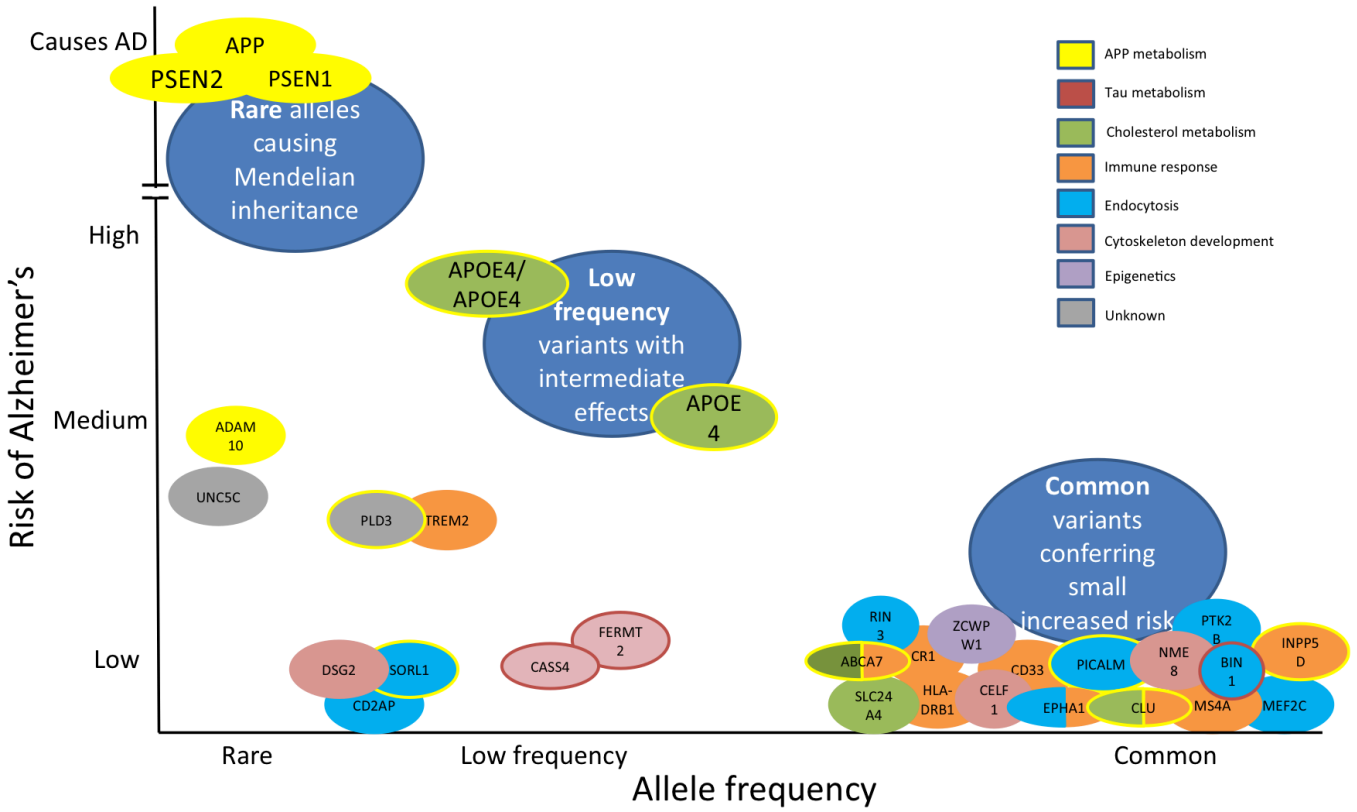

Figure 1.5 The genetic landscape of Alzheimer's disease

The internal colour relates to the current thinking regarding gene function. Where there are two internal colours, the gene has been implicated in more than one pathway. Genes circled in yellow are additionally thought to influence amyloid precursor protein metabolism; genes circled in red are thought to influence tau metabolism. Reproduced from Lane *et al.*, 2018 [43].

1.3.2 Other Risk Factors

There are a number of environmental and life course risk factors that have been associated with sporadic Alzheimer's disease. Risk factors for cardiovascular health in mid-life such as obesity [44], hypertension [45], smoking [46, 47] and hypercholesterolaemia [48] have been associated with higher rates of clinically diagnosed Alzheimer's disease, whilst physical exercise [49, 50] and a diet low in saturated fats may be protective. Remaining socially and cognitive active may also be protective against dementia in general [51], and increased educational and occupational attainment may reduce the risk of incident Alzheimer's disease, perhaps by imparting a reserve that delays the onset of clinical manifestations [52] whilst low educational attainment is a risk factor, perhaps conversely reflecting a lower cognitive reserve.

Numerous case control studies have associated traumatic brain injury (TBI) with an increased risk of Alzheimer's disease, with a systematic review finding that TBI more than doubled the risk of future development of Alzheimer's disease in men [53]: however this has not been replicated in studies looking for association between a history of TBI and neuropathological features of Alzheimer's disease post mortem [54], or with changes in cognition or Alzheimer's disease biomarkers using florbetapir positron emission tomography (PET) scans [55].

1.4 Pathophysiology

1.4.1 The Amyloid Hypothesis

The discovery of mutations in the gene encoding APP led to the development of the amyloid cascade hypothesis [25], which remains the major theory to explain Alzheimer's disease pathophysiology over 25 years later. This hypothesis places dysregulation in

APP processing and the subsequent accumulation of abnormal amyloid plaques as the key initiating event in Alzheimer's disease.

The hypothesized mechanism for erroneous amyloid processing leading to plaque formation is summarised in Figure 1.6. Several enzymes are involved in the cleavage of APP. Normal processing occurs via alpha secretase enzyme cleavage leading to the production of non-amyloidogenic protein product. In Alzheimer's disease there is sequential cleavage of APP by β- and γ-secretases, producing an abnormal protein product which is 42 amino acids in length [56] – Aβ1-42; the major constituent of the extracellular amyloid plaque.

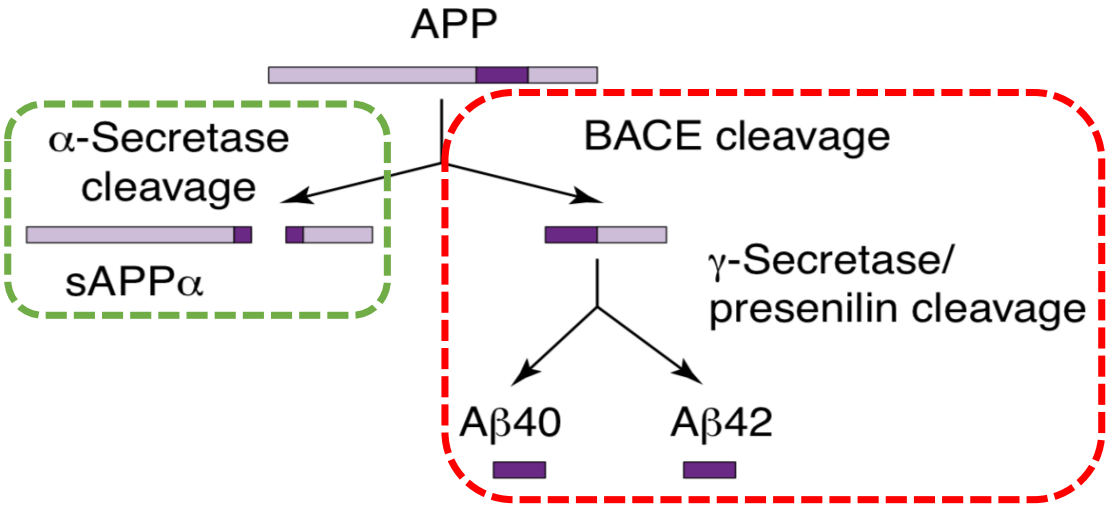

Figure 1.6 The major pathways of amyloid precursor protein processing

Non amyloidogenic pathway (green dashed box): amyloid precursor protein (APP) is cleaved by α-secretase resulting in sAPP-alpha (sAPPα) and a shorter C8 fragment. Amyloidogenic pathway (red dashed box): Sequential cleavage of APP by Aβ cleaving enzyme (BACE) and γ-secretase to yield protein products of varying length, including an abnormal protein product 42 amino acids in length: Aβ1-42. The Aβ1-42 peptides are larger than Aβ1-40 and more prone to self-aggregate. Figure adapted from Mudher and Lovestone, 2002 [57].

Accumulation of these abnormal amyloid protein moieties are thought to trigger a sequence of events leading to synaptic dysfunction, microglial and astrocytic activation, abnormal tau deposition, reduction in neurotransmitters, neuronal death, and atrophy which together causes cognitive symptoms and dementia (Figure 1.7).

Strong genetic support for a central role for Aβ in Alzheimer's disease subsequently came from the realisation that mutations in presenilin genes affect proteins involved in the active catalytic sites of gamma secretase enzymes [58, 59], hence all mutations causing familial Alzheimer's disease result in overproduction of abnormal forms of amyloid. Furthermore, a variant in the APP gene (A673T, a missense mutation) that results in reduced BACE cleavage has been shown to be protective against the development of Alzheimer's disease [60]. The amyloid hypothesis also has mechanistic plausibility for sporadic disease as *APOE* and many of the other risk genes identified (Figure 1.5) are thought to have roles in amyloid clearance.

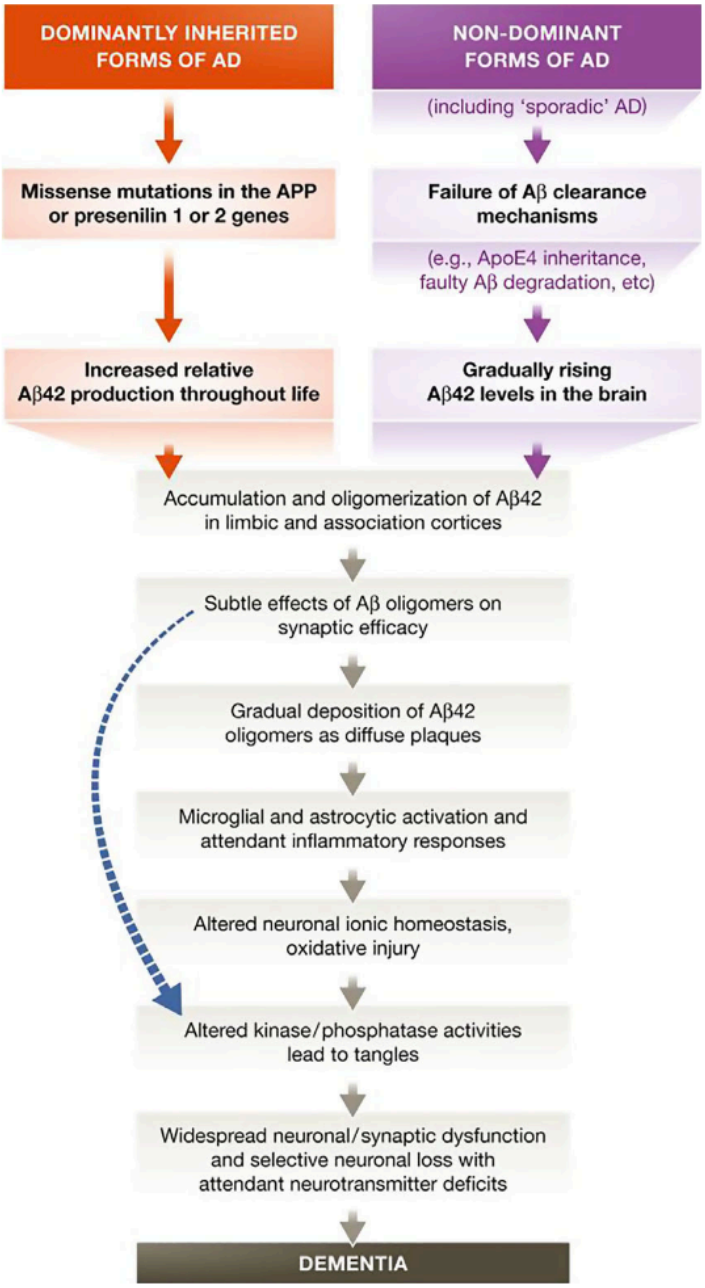

Figure 1.7 Major pathogenic processes in Alzheimer's disease, as proposed by the Amyloid Hypothesis

Aβ oligomers may directly damage synapses and neurites and induce tau hyperphosphorylation directly (indicated by the curved blue arrow), in addition to activating microglia and astrocytes. Diagram reproduced from Selkoe and Hardy, 2016 [61].

1.4.2 Limitations of the amyloid hypothesis and emerging concepts

Whilst the amyloid hypothesis explains much of our current understanding of Alzheimer's disease pathology, there are also many unanswered questions.

The toxic Aβ species

Whilst Aβ1-42 deposition is necessary for a diagnosis of Alzheimer's disease according to neuropathological criteria, a significant proportion of elderly individuals have abundant Aβ1-42 plaques at post mortem without ever having manifest cognitive impairment in life. This indicates that Aβ1-42 deposition alone is not sufficient to cause Alzheimer's disease. Soluble amyloid oligomers may be the more pathological form of amyloid, rather than the plaques containing dense fibrillary amyloid. Aβ oligomers purified from the brains of people with Alzheimer's disease can inhibit long term potentiation, cause synaptic dysfunction and neuronal death when applied to neurons *in vitro* [62]. Plaques may be a 'reservoir' from which amyloid oligomers diffuse. Alternatively, given that individuals with diffuse plaques in the absence of dementia were found to have lower Aβ oligomer levels per plaque than in people with manifest Alzheimer's disease [63], perhaps plaques act as a 'sink' sequestering toxic Aβ species in a non-diffusible less neurotoxic state until a saturation point is reached [61].

The role of tau

Tau is also a vital part of the neuropathological definition of Alzheimer's disease, and the close relationship between regional neurofibrillary tangles and neurodegeneration

indicates it is a key component of pathogenesis. Longitudinal studies have shown that phosphorylated tau pathology in the ventromedial temporal lobe develops prior to the onset of clinical dementia and neurofibrillary tangle density correlates with episodic memory impairment [64].

The tau and tangle hypothesis proposed impairment of the normal role of tau in stabilising microtubules as the primary initiating and pathological event in Alzheimer's disease. However, whilst tau mutations have been found to lead to pathological accumulation of tau and dementias within the frontotemporal dementia spectrum [65], tau mutations alone are not associated with amyloid plaques and do not manifest as Alzheimer's disease. The fact that APP and presenillin mutations give rise to both plaques and tangles strongly suggests that amyloid pathology occurs upstream of the essential coexistent tau pathology. There is emerging evidence that Aβ oligomers can induce hyperphosphorylation of tau in neurons *in vitro* [66] providing one potential mechanism to explain how amyloid and tau interact in Alzheimer's disease pathogenesis, however this relationship remains incompletely understood.

Amyloid plaque burden correlates poorly with cognitive deficits

Amyloid plaque burden does not to correlate as well with the degree of observed cognitive impairment as neurofibrillary tangles do [67]. As the natural history of Alzheimer's disease is becomes better understood, Aβ1-42 deposition is increasing

thought to be an early and widespread event that sets off a downstream cascade of events that ultimately leads to neuronal death and a clinically manifest dementia.

Clinical trials of anti-amyloid agents have not yet lead to a disease modifying therapy

Until recently, the amyloid hypothesis has been the overarching theory for nearly all attempts to develop therapeutics for Alzheimer's disease. Numerous clinical trials of agents altering amyloid production or enhancing amyloid clearance are ongoing but there has been limited success thus far [68, 69] suggesting that either the most relevant targets have not yet been identified, or intervention is not occurring at the optimum stage in the disease process. This may change, as recent preliminary data from a stage 2B trial of BAN2401 (an anti-Aβ1-42 protofibril immunotherapy) shows promising amyloid reduction and a downstream improvement in cognitive function assessed using the ADAS-Cog and ADCOMS composite measure [70] in individuals with mild cognitive impairment due to Alzheimer's disease and mild Alzheimer's disease [71, 72].

No anti-amyloid treatment has yet been licenced for clinical use.

1.5 The Natural History of Alzheimer's disease pathogenesis

Advances in understanding the temporal relationship of pathological and clinical events in Alzheimer's disease have been greatly aided by the development of cerebrospinal fluid (CSF) and imaging biomarkers for amyloid-β pathology and tau related neurodegeneration *in vivo*. The application of these biomarkers to clinical diagnosis is outlined in section 1.7.

CSF biomarkers

Three core CSF biomarkers for Alzheimer's disease have been identified and replicated across many studies [73]: (i) Aβ1-42, which is found at low concentrations in Alzheimer's disease due to cortical amyloid deposition [74], (ii) total tau (T-tau), which is raised due to cortical neuronal loss [75-77], and (iii) phosphorylated tau (P-tau), which is found at high concentration reflecting cortical tangle formation [74, 78]. These CSF biomarkers have good diagnostic accuracy for Alzheimer's disease in life, with sensitivity and specificity of 85-90%, and also for patients with mild cognitive impairment due to underlying Alzheimer's disease pathology [79].

Structural imaging biomarkers

Volumetric structural T1 MRI demonstrates areas of brain atrophy, and serial registered scans can be used to measure rates of atrophy using methods such as the boundary shift integral [80]. Regional brain atrophy profiles in YOAD are further described in chapters 2 and 3.

Positron emission tomography (PET) biomarkers

18F-fluorodeoxyglucose (^{18}FDG) PET visualises cerebral glucose metabolism which increases with regional synaptic activity and decreases with synaptic dysfunction and tau related neurodegeneration.

Amyloid PET ligands bind fibrillar Aβ deposits to detect and quantify Aβ neuritic plaques in the brain during life. Amyloid PET measures of amyloid pathology correlate well with amyloid burden at post mortem [81-83], and amyloid PET can also be used to detect longitudinal change in amyloid plaque load over time [84].

The first PET ligand specific for Aβ was ^{11}C Pittsburgh Compound B (PIB) [85] which has been used in several large multisite studies [86, 87]. The ^{11}C ligand half-life is approximately 20 minutes, which limits it use to imaging centres with an on-site cyclotron.

Subsequently developed ^{18}F amyloid ligands, which include florbetapir, flutemetamol and florbetaben, have a longer half-life of around 2 hours making central production and distribution to other research sites possible.

PET ligands to bind tau have also been developed, such as AV1451 (flortaucipir) [88], and a range of second generation ligands which may be more specific. Regional tau binding recapitulates the topographical distribution of neurofibrillary tangle pathology as described by Braak [89], and regional differences in tau deposition mirror the clinical symptoms and atrophy profiles seen in individuals with atypical phenotypes of Alzheimer's disease [90, 91].

Modelling dynamic biomarkers of the Alzheimer's disease pathological cascade

Longitudinal studies of families carrying autosomal dominant Alzheimer's disease mutations have examined the time course of fluid biomarker, neuroimaging and clinical changes prior to the expect onset of Alzheimer's disease symptoms, based on the age of symptom onset in a parent with the same mutation [92]. Aβ1-42 levels in CSF may first become elevated then decline as early as 25 years before expected clinical symptom onset, followed by PIB-PET evidence of fibrillary amyloid deposits, raised CSF tau levels and progressive brain atrophy on MRI approximately 15 years before symptoms manifest. Neuronal hypometabolism and the earliest detectable clinical memory impairment on neuropsychological assessment appear approximately 10 years before clinical symptoms of severity to fulfil a diagnosis of dementia. Data modelling from a longitudinal study in individuals with sporadic Alzheimer's disease has suggested a similar time course of pre-symptomatic Aβ deposition [93].

Jack *et al.,* have used these biomarker studies to formulate a model for the sequence of pathogenesis in Alzheimer's disease [94, 95] (Figure 1.8).

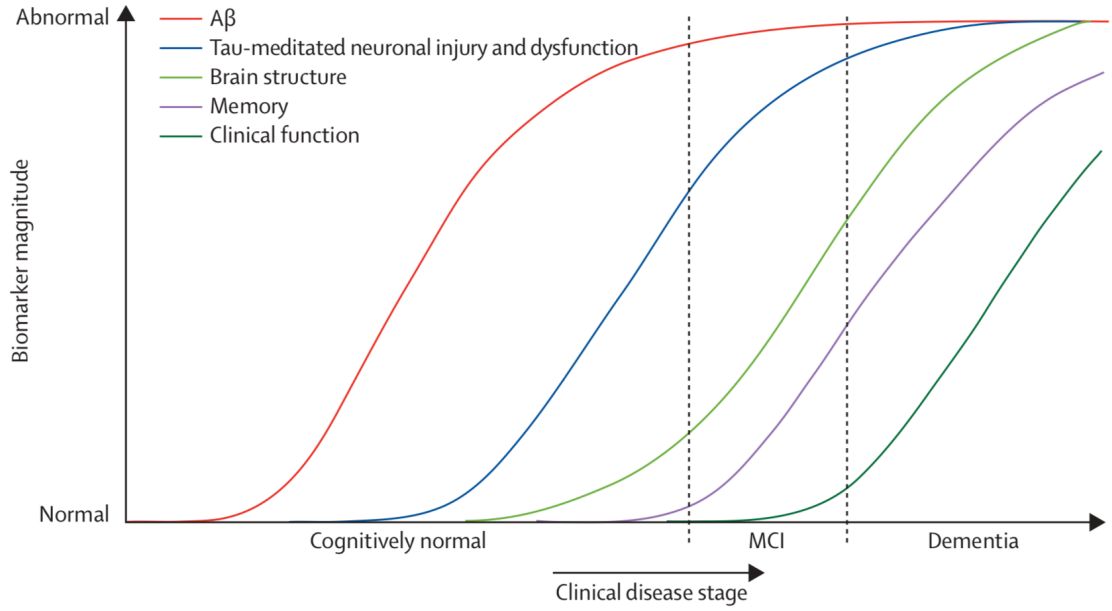

Figure 1.8 Dynamic biomarkers of the Alzheimer's pathological cascade

Aβ is identified using CSF Aβ1-42 or PET amyloid imaging. Tau-mediated neuronal injury and dysfunction is identified by raised CSF tau levels or altered fluorodeoxyglucose-PET. Brain structure is measured using structural MRI. MCI, mild cognitive impairment. Figure reproduced from Jack *et al.*, 2010 [94]

1.6 Clinical Presentation

1.6.1.1 Late onset Alzheimer's disease

Alzheimer's disease typically presents in elderly people with slowly progressive episodic memory impairment, difficulty with route finding and loss of confidence. Cognitive impairment become more severe and spreads to other cortical domains as the disease progresses interfering with activities of daily living and leading to an increasing dependence on care. In advanced Alzheimer's disease people can experience

behavioural and psychological symptoms such as apathy, depression, irritability, agitation and anxiety [96] as well as hallucinations, seizures, falls, and altered sleep patterns. Disease duration in Alzheimer's disease is typically around 8.5 years from clinical presentation to death [97].

1.6.1.2 Young onset Alzheimer's disease

Young onset Alzheimer's disease (defined as symptom onset < 65 years) [98] is markedly less common, but Alzheimer's disease is still the most common cause of young onset dementia. Reported prevalence of young onset Alzheimer's disease within young onset dementia varies across studies but can be up to 67% [99].

People with familial Alzheimer's disease due to an autosomal dominant mutation typically present with memory impairment, but at a much younger age – in their 30s, 40s or 50s. Some autosomal dominant mutations have prominent additional features such as the myoclonus, seizures and spastic paraparesis observed in people carrying PSEN1 variants [100].

Young onset Alzheimer's disease can also occur on an apparent sporadic basis, and these are the individuals studied in this thesis. Atypical (non-memory) syndromes are more commonly seen in this demographic and include posterior cortical atrophy (PCA), logopenic aphasia (LPA) and the frontal variant of Alzheimer's disease. PCA typically presents with breakdown of parieto-occipital function in the context of relatively preserved memory and language functions [101]. Patients have prominent visuospatial and visuoperceptual problems with apraxia, dyscalculia, alexia and agraphia. The language led Alzheimer's disease variant; LPA, is dominated by long word finding pauses, anomia and deficits of working memory [102]. Frontal presentations of Alzheimer's disease are the rarest and characterised by executive impairment,

behavioural change and psychiatric symptoms [103, 104] in the presence of Alzheimer's disease pathology [105, 106].

This clinical heterogeneity and possible underlying mechanisms are discussed further in Chapter 2.

1.7 Clinical Diagnostic Approach

A diagnosis of dementia is based on the clinical history, the pattern of cognitive deficits and neurological signs on examination, and supportive investigations and biomarkers of underlying disease pathology. Accurate and timely diagnoses are important clinically for guiding patient management and prognosis, and will be increasingly important in the future for targeting treatment with the advent of disease modifying therapies.

Diagnosis presents a particular challenge in younger patients who are less than 65 years due to the broad differential diagnosis, increased prevalence of atypical phenotypes and higher burden of genetic causes [98]. Alzheimer's disease needs to be distinguished from both non-neurodegenerative disease mimics such as obstructive sleep apnoea, depression or rarer inflammatory, infective or autoimmune causes, as well as from other neurodegenerative diseases including frontotemporal dementia, dementia with Lewy Bodies and vascular dementia.

Atypical Alzheimer's disease phenotypes pose their own diagnostic challenges, are the subject of this thesis, and are discussed in detail in Chapter 2. Individuals with PCA may have presented to opticians and ophthalmologists reporting visual symptoms, and it can take some time and significant investigation to recognise that their difficulties do not arise from a problem in the anterior visual pathways. Equally individuals with language or frontal variants may initially be diagnosed with frontotemporal dementia, primary psychiatric or functional disorders.

1.7.1 Clinical assessment

The clinical assessment should assess the pattern of cognitive and behavioural deficits, and the impact on the person's life. A good collateral history is essential as patients may lack insight to some of their difficulties. Depression and other psychiatric symptoms should be elicited, and people screened for symptoms suggesting other dementia mimics, such as obstructive sleep apnoea.

A bedside cognitive assessment begins whilst taking a history. For example, a person with episodic memory impairment due to Alzheimer's disease generally has a well preserved social façade but may appear passive during the interview, turning to their partner to answer questions; the 'head turning sign' [107]. The individual's behaviour and interaction with others should be observed as impulsiveness, perseveration, loss of emotional reactivity, or disinhibition suggest a disease processing involving the frontal lobes.

The Mini Mental State Examination (MMSE) [108], Montreal Cognitive Assessment (MOCA) [109] and Addenbrooke's Cognitive Examination (ACE) [110] offer structured tools for assessing different domains of cognitive function. Dyspraxia and a visual apperceptive agnosia suggest organic disease implicating the dominant and non-dominant parietal lobes respectively. Cortical dementias such as Alzheimer's disease are characterised by errors in specific domains with relatively preserved speed of processing, where as profound slowing of cognition and a frontal dysexecutive syndrome is typical of subcortical dementias.

Physical examination should establish any features of 'dementia plus syndromes' [98] which may manifest as neurological signs (e.g. ataxia, pyramidal signs, dystonia, chorea, peripheral neuropathy, myoclonus, gaze palsies, deafness or dysautonomia) or systemic

features (e.g. cataracts, splenomegaly, bone cysts, tendon xanthomas, renal, liver or respiratory failure, anaemia, metabolic or infectious crises, or hyponatraemia).

1.7.2 Neuropsychology

Neuropsychological testing aims to quantitatively assess the extent and pattern of an individual's cognitive impairment using tests of graded difficulty with well-established age related normative data and considering the person's likely premorbid ability (estimated using reading ability which is relatively unaffected by the early stages of Alzheimer's disease, details of educational attainment and employment history). Serial assessment may be used to determine interval change over time, with the caveat that 'practice effects' may need to be taken into account, especially in high functioning individuals.

Although neither 100% sensitive or specific for a given disease, the pattern of cognitive impairment demonstrated can help identify the syndrome.

1.7.3 Blood tests

Blood tests are performed routinely to exclude potentially treatable or reversible causes of dementia, or conditions contributing to cognitive symptoms. The UK NICE clinical guidelines recommend checking a full blood count, renal and liver function, serum electrolytes including calcium, glucose, thyroid function, vitamin B12 and folate [111]. They do not recommend routine testing for syphilis serology or HIV unless there are specific risk factors or suggestive clinical features. Depending on the clinical scenario it may also be appropriate to investigate for other rarer causes of dementia e.g. anti-nuclear antibodies, anti-neuronal antibodies or antibodies implicated in autoimmune encephalitis for patients with rapid-onset dementias or in those with systemic disease, white cell enzymes and very long chain fatty acids to screen for various metabolic

disorders that present in early adulthood, or multiple blood films if neuroacanthocytosis is suspected.

There are currently no Alzheimer's disease specific blood based biomarkers for clinical use [112].

1.7.4 Neuroimaging

Structural, metabolic and molecular imaging are all approved for use in clinical diagnosis of Alzheimer's disease.

1.7.4.1 Structural

Structural imaging with CT or MRI is used to rule out potentially treatable causes of cognitive impairment, such as space occupying lesions and subdural haematomas, and is recommended in the diagnostic work up of all suspected dementias [111].

MRI has the additional benefits of being able to assess the presence and extent of cerebrovascular disease which can mimic or coexist with Alzheimer's disease, and volumetric sequences are being increasingly used in clinical practice to assess regional atrophy profiles in neurodegenerative diseases [98]. Specific patterns of atrophy reflect the characteristic selective neuronal vulnerability in different neurodegenerative diseases, such as focal symmetrical medial temporal lobe atrophy in typical Alzheimer's disease [113] verses atrophy of the frontal and temporal lobes, insula and anterior cingulate cortex atrophy in behavioural variant frontotemporal dementia [114]. Within Alzheimer's disease different phenotypes are associated with different regional atrophy profiles. This is discussed further in Chapter 2.

Longitudinal imaging enables changes over time to be visualised. In clinical practice an interval of one year would be typical to expect to see qualitative change in the degree of atrophy, unless the dementia was very rapidly progressive.

1.7.4.2 Metabolic Imaging

Hypometabolism on ^{18}FDG PET in the parieto-temporal association areas, posterior cingulate and precuneus supports a diagnosis of Alzheimer's disease [115]. Frontal hypometabolism can be useful to identify patients with early frontal lobe dysfunction in whom established atrophy on structural MRI is not clear.

FDG-PET is useful in differentiating Alzheimer's disease from other dementias with specificity higher than 95% in early onset cases where an atrophy profile has not yet developed [41].

1.7.4.3 Molecular Imaging

Amyloid PET imaging has three agents approved by the European Medicines Agency and the US Food and Drug Administration. Florbetapir, flutemetamol and florbetaben all work by binding fibrillary Aβ and PET imaging results closely correlate with pathological Aβ burden at post-mortem [81-83]. Although recognised in diagnostic criteria as evidence of brain β amyloid protein deposition [116, 117] routine clinical access to amyloid PET is limited in the UK. A number of ongoing studies are currently evaluating its clinical utility and cost-effectiveness [118, 119] so its use in clinical practice may expand in the future.

Tau PET imaging, using tracers such as AV1451 [88], is a recent research development which has not yet entered clinical diagnostic practice.

Often a combination of imaging modalities is used to support identification of an Alzheimer's disease syndrome and underlying pathology (Figure 1.9).

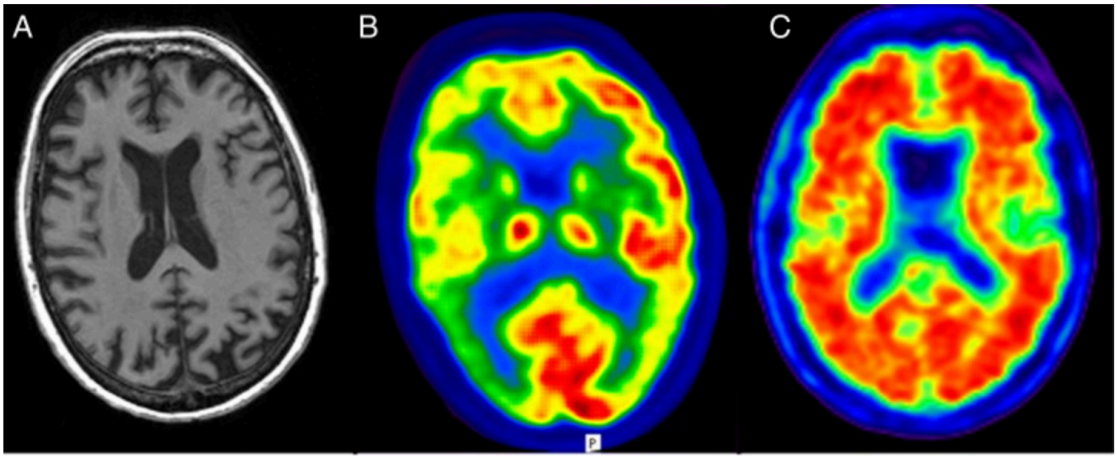

Figure 1.9 Structural, metabolic and molecular imaging posterior cortical atrophy due to Alzheimer's disease

(A) Volumetric T1 MR brain imaging shows prominent posterior volume loss. (B) 18-FDG PET scanning shows cortical hypometabolism (cool colours) most prominent in both parietal lobes. (C) Amyloid PET scanning shows widespread cortical amyloid deposition. For clinical purposes, 18F-florbetapir images are interpreted on a grey (rather than colour) scale. Figure reproduced from Slattery *et al.* [120]

1.7.5 CSF biomarkers

NICE clinical guidelines recommend the use of cerebrospinal fluid examination if Creutzfeldt-Jakob disease (CJD) or other forms of rapidly progressive dementia are suspected [111]. Specifically considering patients with young onset dementia, both the American Academy of Neurology and European Federation of Neurological Societies guidelines recommend CSF examination [121-123].

CSF examination can screen for inflammatory or infective conditions mimicking dementia, and contribute to a positive molecular diagnosis of Alzheimer's disease

pathology. In Alzheimer's disease, the typical pattern is a low Aβ1-42 (due to cortical amyloid deposition), with elevated levels of tau (due to cortical neuronal loss) and phosphorylated tau (reflecting cortical tangle formation). Each of these biomarkers have been reported to differentiate patients with Alzheimer's disease from healthy elderly individuals with 80-90% sensitivity and specificity [124].

1.7.6 Neurophysiology

Electroencephalomyography (EEG) can show early slowing or loss of alpha rhythm in Alzheimer's disease, but arguably is more useful in clinical practice for identifying characteristic EEG changes seen in rarer Alzheimer's disease mimics such as periodic complexes in some prion diseases and subacute sclerosing panencephalitis, or subclinical epileptiform changes in patients having partial seizures that may present as an amnestic syndrome [98].

1.7.7 Genetics

Genetic testing, with appropriate consent, can be used to identify autosomal dominant causes of Alzheimer's disease where these are suspected in clinically affected individuals. Genetic panels using next generation sequencing are increasingly availably and mean large numbers of genes can be tested concurrently at reasonable cost.

Pre-symptomatic testing for autosomal dominant causes of dementia is only undertaken after specific genetic counselling.

Routine testing of genetic risk factors (e.g. *APOE* status) is not currently recommended [123] due to the uncertainty of what this means for an individual.

1.8 Treatment

1.8.1 Symptomatic

Acetylcholinesterase inhibitors (AChEIs) (donepezil, galatamine and rivastigmine) are the mainstay of symptomatic treatment and exert their therapeutic action by inhibiting the enzyme acetylcholinesterase. This increases the brain availability of acetylcholine by preventing its breakdown in the synapse. Several studies have demonstrated AChEIs have modest beneficial effects in mild to moderate Alzheimer's disease with all drugs in the class having similar efficacy [125]. There is also some evidence that cholinesterase inhibitors have some benefit in moderate to severe Alzheimer's disease, as the DOMINO-AD study demonstrated that withdrawal of donepezil lead to increased risk of requiring nursing home placement in the following 12 months [126].

Memantine, a low affinity N-methyl-D-aspartate receptor antagonist, works by reducing L-glutamate excitatory neurotoxicity. It has been shown to have small but clinically significant effects on cognition and function in patients with moderate to severe Alzheimer's disease, and may reduce the likelihood of patients developing agitation [127].

Dual AchEI and memantine therapy appears to lead to some improvement in behavioural symptoms in moderate to severe Alzheimer's disease but there is only weak evidence for improvement in cognition [128].

1.8.2 The search for disease modifying therapy

Models suggest that a disease modifying treatment that could slow dementia progression by 25% would reduce the number of people with severe dementia by almost half [129]. Such a treatment f

or Alzheimer's disease has proved elusive however. There is currently no treatment that can alter the underlying pathology or slow the course of the disease.

A number of major phase 3 clinical trials using monoclonal antibodies targeting cerebral β-amyloid have failed to reach their primary outcome measures leading to scepticism about the validity of the amyloid hypothesis (table 1.1). However, many of these studies have been troubled by concerns about target and patient selection [68], as a proportion of individuals recruited for some of these trials did not have any evidence of underlying Alzheimer's disease pathology [61]. Furthermore, most studies have targeted patients with later-stage Alzheimer's disease, when β-amyloid may no longer be the most appropriate target, or too much irreversible damage may have occurred to change clinical outcomes.

Our better understanding of the natural history of Alzheimer's disease offers an earlier window for intervention.

A trial of aducanumab, targeting Alzheimer's disease at an earlier stage has encouraging preliminary findings showing reduction in amyloid burden and delay in disease progression at 1 year in prodromal and mild Alzheimer's disease patients [130] and there are several other ongoing studies in mild cognitive impairment and mild Alzheimer's disease in progress including the BAN2401 stage 2B trial [71, 131]. Strategies to clear amyloid using immunotherapy or prevent the formation of pathological forms with β-site APP cleaving enzyme (BACE) or γ-secretase inhibitors/modulators are being testing in the pre-clinical phase before any symptoms have manifest. The DIAN-TU [132] and API-ADAD [133] studies are using genetic screening to identify individuals at risk for familial Alzheimer's disease. The Generation study is recruiting *APOE* ε4 individuals [134]; and the A4 study is recruiting healthy elderly individuals with asymptomatic amyloidosis [135].

Drug Name	Proposed Mechanism of Action	Phase 3 Clinical Trial Results
Tramiprosate	Aβ aggregation inhibitor	1,052 mild–moderate AD patients randomized to 3 groups: placebo, 100, 150mg/kg BD for 78 weeks. No significant effects on primary outcome measures on ADAS-cog and CDR-SB [136].
Tarenflurbil	γ-secretase modulator	1,684 mild AD patients randomized to placebo, 800mg BD tarenflurbil for 18 months. No significant effects on primary outcome measures on ADAS-cog and ADCS-ADL [137].
Semagacestat	γ-secretase inhibitor	2,600 mild–moderate AD patients randomized to placebo, 100, 140mg semagacestat OD for 76 weeks in 2 trials (ClinicalTrials.gov identifiers NCT00594568, NTC00762411). Trials were halted after interim analysis showed increased incidence of skin cancer and worsening of cognition and activities of daily living [138].
Bapineuzumab	Humanized monoclonal antibody directed at amino acids 1–5 of Aβ peptide. Amyloid plaque clearance	4,500 mild–moderate AD patients randomized to placebo and 0.5mg/kg IV every 13 weeks for 18 months in APOE4 carriers, and randomized to placebo, 0.5, 1.0mg/kg IV every 13 weeks for 18 months in APOE4 noncarriers in 4 trials (ClinicalTrials.gov identifiers lNCT00575055, NCT00574132, NCT00676143, NCT00667810). Trials were halted after completion of 2 trials

	mediated by microglial activation	demonstrated a failure to meet primary outcome measures on ADAS-cog and activities of daily living [139].
Solanezumab	Humanized monoclonal antibody directed at amino acids 16–24 of Aβ peptide. Amyloid plaque clearance mediated via peripheral sink mechanism	2,000 mild–moderate AD patients randomized to placebo and 400mg solanezumab monthly IV for 18 months (ClinicalTrials.gov identifiers NCT00905372, NCT00904683). Trials failed to meet their primary outcome measures on ADAS-cog and ADCS-ADL. A secondary analysis of mild AD patients pooled from both trials showed a significant effect on cognition [140].
Gammagard	Intravenous immunoglobulin	390 mild–moderate AD patients randomized to 0.2g/kg/2 weeks and 0.4g/kg/2 weeks vs placebo for 18 months (ClinicalTrials.gov Identifier NCT00818662). Gammagard failed to reach its co-primary outcomes of ADAS-cog and ADCS-ADL [141].

Table 1.1 Outcomes of Phase 3 Clinical Trials of Amyloidocentric Drugs

ADAS-cog, Alzheimer's Disease Assessment Scale–Cognitive Subscale; ADCS-ADL, Alzheimer's Disease Cooperative Study–Activities of Daily Living Inventory; BD, twice daily; CDR-SB, Clinical Dementia Rating–Sum of Boxes; CSF, cerebrospinal fluid; IV, intravenous; OD, once per day. Table adapted from Karan and Hardy, 2014 [68].

Alternative targets including tau pathology have also attracted interest, with a number of clinical trials ongoing [142].

Genetic studies have highlighted pathways such as the innate immune system, microglia activation/inflammation and brain cholesterol metabolism as having potential for therapeutic intervention. This may lead to the identification of novel drug targets, however to date there have been no positive clinical trials targeting neuroinflammation [143].

For a review of potential therapies in the current AD treatment pipeline please see Cummings et al., 2018 [144].

1.8.3 A new era of Alzheimer's disease therapeutics

If a disease-modifying treatment with proven clinical benefit is found it will mark a new era in the management of Alzheimer's disease, however will also bring its own challenges for UK healthcare.

A treatment for people with established Alzheimer's disease would need to be affordable and accessible to all those who would benefit, yet this would be a significant challenge for the NHS in its current state to deliver.

A treatment for the pre-clinical phase would require accurate and timely identification of those 'at risk' of Alzheimer's disease through a national screening programme. However, in addition to identifying those 'at risk', we would need risk models and biomarkers to predict when an individual 'at risk' will manifest clinical disease, else it will be difficult to counsel people about the optimal time to start treatment. This will be important initially for treating people within the context of clinical trials, and subsequently if we are able to use a personalised 'preventative medicine' approach to Alzheimer's disease.

2 Pathology to phenotype: Clinical Heterogeneity in Alzheimer's disease

Alzheimer's disease is clinically heterogeneous, but the mechanisms underlying this remain incompletely understood. Selective vulnerability, by which subpopulations of neurons in different brain networks show variable susceptibility to dysfunction and death in response to specific insults, may explain some of the observed phenotypic differences. This chapter reviews attempts to classify the different Alzheimer's disease syndromes and discusses potential means by which the same underpinning neuropathology can manifest in such markedly different clinical presentations.

2.1 Early descriptions of Alzheimer's disease heterogeneity: subgroups vs stages

Alois Alzheimer's first case would now be recognised as having an atypical form of Alzheimer's disease. Auguste D was a 51 year old woman who presented with profound language deficits, behavioural disturbance including anxiety and paranoid delusions. Her episodic memory was impaired, but this was not the most prominent cognitive feature. DNA analyses from the original histological slides prepared in Alzheimer's laboratory have subsequently shown she had pathological c.526T>C PSEN1 variant [145].

Early descriptions of phenotypic heterogeneity in Alzheimer's disease came from observing dementia patients in geriatric hospitals. McDonald noted some individuals had difficulties predominantly with praxis, visual construction, and cortical sensation which he termed a 'parietal group'. Other patients had predominantly memory dysfunction, later age of onset, and slower disease progression than the 'parietal group'. He described them as having 'benign memory dysfunction of aging' [146].

This early classification of subtype variability did not generate widespread recognition however, perhaps as the prevailing theory of the time held that clinical variation arose from observing the disease at different stages of progression ('phase hypothesis'), rather than truly distinct disease phenotypes ('subtype hypothesis') [147].

Regional cerebral glucose metabolism studies using 18F-fluorodeoxyglucose positron emission tomography subsequently lent credence to the 'subtype hypothesis' as they demonstrated that clinically distinct profiles of Alzheimer's disease had distinct topographic patterns of hypometabolism in the brain. Individuals with profound language impairment clinically showed more marked asymmetry with left hemisphere hypometabolism and patients with predominant visuo-constructive dysfunction had a 'hypometabolic focus' in the right parietal cortex [148, 149]. Longitudinal follow up studies went on to demonstrate that different clinical syndromes and their metabolic imaging correlates could still be distinguished with disease progression over time [150].

However, some studies found language predominant presentations were associated with an earlier age of clinical disease onset [151, 152] which could be seen to support the phase hypothesis. Using the CERAD (Consortium to Establish a Registry for Alzheimer's Disease) database, which included standardised neuropsychology assessments, subtypes of Alzheimer's disease were identified [153, 154] showing that individuals with variant presentations, predominantly anomia and impairment of constructional praxis, mirrored the 'left' and 'right' subgroups of the earlier PET studies, respectively. Within the cohort studied, these variant subtypes did not differ significantly in their age of clinical disease onset or duration of illness, strongly suggesting that these observed differences were not alternative stages of disease, but true variants of Alzheimer's disease. As with the PET studies, longitudinal analysis revealed stable subgroup-specific neuropsychological progression patterns, again supporting the idea of true distinct subtypes of disease [155].

It is now recognised that there is significant clinical heterogeneity within Alzheimer's disease. This is particularly apparent in individuals with sporadic young onset Alzheimer's disease (YOAD), defined as symptom onset at less than 65 years [98] and the group studied in this thesis.

2.2 'Typical Alzheimer's disease'

As outlined in Chapter 1, the majority of people with Alzheimer's disease present when over 65 years of age with insidious onset of progressive episodic and topographic memory impairment. Whilst patients may lack insight this typically presents with relatives reporting repeated questioning, losing track of day-to-day events, or becoming disorientated whilst navigating a route. In early to moderate disease, social façade is typically preserved [156]. Some individuals have a very amnestic dominant phenotype and demonstrate the slowest decline in cognition [157], but others can also develop parietal dysfunction, such as problems with praxis and word finding difficulty. Neuropsychology often further reveals poor attention, working memory and executive dysfunction. As the disease progresses other cortical domains become involved leading to widespread cognitive impairment that impairs activities of daily living and an increasing dependence on care. Pathologically, there is a subgroup of patients with the purer amnestic syndrome who have plaques and tangles limited to the medial temporal lobes with little or no spread to the neocortical areas [158].

2.3 'Atypical' Alzheimer's disease

Despite the common underlying histopathology as outlined above, individual patients with Alzheimer's disease have different constellations and degrees of cognitive symptoms. Some have sufficiently unusual phenotypes to be considered as being distinct variants within a continuum.

Whilst an amnestic syndrome is still the commonest in YOAD, some patients present with profound impairment of language, higher order visual symptoms, marked behaviour change and dysexecutive syndrome, or combinations of these features. These atypical presentations of Alzheimer's disease are seen in at least 5% of patients with late onset disease and approximately a third of patients presenting with YOAD [159] and in the absence of autosomal dominant mutations in APP, PS1 or PS2 genes. Three canonical atypical syndromes are described: posterior cortical atrophy (PCA), logopenic aphasia (LPA) and frontal Alzheimer's disease.

2.3.1 Posterior cortical atrophy

PCA is the commonest syndrome of the atypical Alzheimer's disease presentations [159, 160] and presents with breakdown of parieto-occipital function in the context of relatively preserved memory and language functions [101] (see Table 2.1 for the diagnostic criteria for the syndrome of PCA). Patients have combinations of dominant and non-dominant parietal impairment: visuospatial and visual apperceptive agnosias, visual disorientations, apraxia, dyscalculia, alexia and agraphia. They may have features of Balint's syndrome (simultagnosia, oculomotor apraxia, optic apraxia, environmental agnosia) or Gerstmanns syndrome (acalculia, agraphia, left/right disorientation and finger agnosia). Visual field defects, dyspraxia, myoclonus, extrapyramidal features or the motor signs of corticobasal syndrome may be evident on clinical examination [161].

Alzheimer's disease pathology is the most common histological substrate for PCA phenotypes. Pathological series identified Alzheimer's disease pathology in over 60% of cases of PCA [162]. Amyloid PET imaging [163] and CSF neurodegenerative markers [164] are also consistent with Alzheimer's disease in the majority of cases. However, other pathologies can underlie a PCA phenotype, such as corticobasal degeneration, dementia with Lewy Bodies and prion disease [162, 165].

Core features of PCA

- Insidious onset and gradual progression
- Presentation with visual complaints, in the absence of significant primary ocular disease to explain the symptoms
- Absence of stroke or tumour
- Absence of early parkinsonism and hallucinations
- Relative preservation of anterograde memory and insight (early in the disorder)

Plus any of the following symptoms

- Simultagnosia with or without optic ataxia or ocular apraxia
- Constructional dyspraxia
- Visual field defects
- Environmental disorientation
- Any of the elements of Gerstmann syndrome

Supportive clinical features

- Alexia
- Presenile onset
- Ideomotor or dressing apraxia
- Prosopagnosia

Investigations

- Neuropsychological deficits relating to parietal and/or occipital regions
- Focal or asymmetric atrophy in parietal and/or occipital regions on structural imaging
- Focal or asymmetric hypoperfusion or hypometabolism in parietal and/or occipital regions on functional imaging

Table 2.1 Diagnostic criteria for posterior cortical atrophy

Adapted from Tang Wai *et al.*, 2004 [165], the current research criteria during study design and recruitment. In 2017 Crutch *et al.* published an updated consensus classification of posterior cortical atrophy [166].

2.3.2 Logopenic aphasia

The language led Alzheimer's disease variant; LPA, is one of the primary progressive aphasias, and dominated by long word finding pauses (anomia) and impaired phonological short-term memory. On cognitive examination this manifests as reduced auditory digit span and greater difficulty in repeating and comprehending sentences than single words [102]. There is initially relatively preserved episodic memory and non-dominant posterior cortical function. Alzheimer's pathology has been demonstrated in over two thirds of cases [167, 168]. See Table 2.2 for diagnostic criteria for the syndrome of LPA.

2.3.3 Frontal Alzheimer's disease

Frontal presentations of Alzheimer's disease are the rarest and characterised by executive impairment and behavioural change [103, 104] in the presence of Alzheimer's disease pathology [105, 106]. The have proved the most difficult to define, and present a significant diagnostic challenge during life as patients may also fulfil the diagnostic criteria for behavioural variant frontotemporal dementia (bvFTD). The clinical profile is variable but includes aspontaneity, perseveration and psychiatric symptoms. These may coexist with less prominent memory and posterior cortical deficits.

2.3.4 Syndromic convergence

The initial focal deficits of patients with these atypical Alzheimer's disease presentations overlap closely with those that tend to develop in the later stages of typical Alzheimer's disease, and patients with atypical forms usually develop more classic memory deficits as the disease progresses.

Diagnosis of Primary Progressive Aphasia

All three of the following factors must be present:

- The most prominent clinical feature is difficulty with language
- Aphasia should be the most prominent deficit at symptom onset and for the initial phases of the disease
- The language deficits are the principal cause of impairment in daily living activities

All four of the following factors must be absent:

- The pattern of deficits is better accounted for by other non-degenerative nervous system or medical disorders than by PPA
- Cognitive disturbance is better accounted for by a psychiatric diagnosis than by PPA
- Prominent initial episodic memory, visual memory, and visuoperceptual impairments
- Prominent initial behavioural disturbance

Diagnosis of logopenic variant PPA

Both of the following core features must be present:

- Impaired single word retrieval in spontaneous speech and naming
- Impaired repetition of sentences and phrases

At least three of the following four clinical features must be present:

- Speech (phonologic) errors in spontaneous speech and naming
- Spared single-word comprehension and object knowledge
- Spared motor speech
- Absence of frank agrammatism

The clinical diagnosis of logopenic variant PPA can be supported by imaging findings of at least one of the following features:

- Predominant left posterior perisylvian or parietal atrophy on MRI
- Predominant left posterior perisylvian or parietal hypometabolism on single-photon emission CT or PET

Logopenic variant PPA with definite pathology

In patients with a clinical diagnosis of logopenic variant PPA, definite pathology is demonstrated by either of the following features:

- Histopathological evidence of a specific neurodegenerative pathology (including Alzheimer disease, frontotemporal lobar degeneration with tau pathology, frontotemporal lobar degeneration with TDP-43 pathology)
- Presence of a known pathogenic mutation

Table 2.2 Diagnostic criteria for logopenic variant PPA

Adapted from Gorno-Tempini *et al*, 2011 [102].

2.4 Research diagnostic criteria

Both the 2011 US National Institute on Aging–Alzheimer's Association (NIA-AA) [117] and the 2014 International Working Group (IWG) [116] published recommendations for the diagnosis of Alzheimer's disease have recognised and attempted to define the varied clinical phenotypes of Alzheimer's disease.

2.4.1 US National Institute on Aging–Alzheimer's Association criteria

Atypical presentations, including those with early and prominent language, visuospatial and executive impairment, are included in the 2011 criteria for probable Alzheimer's disease dementia (see Table 2.3).

Core clinical criteria for Probable Alzheimer's disease dementia

A. Insidious onset. Symptoms have a gradual onset over months to years, not sudden over hours or days;

B. Clear-cut history of worsening of cognition by report or observation; and

C. The initial and most prominent cognitive deficits are evident on history and examination in one of the following categories:

   i. Amnestic presentation: It is the most common syndromic presentation of Alzheimer's disease dementia. The deficits should include impairment in learning and recall of recently learned information. There should also be evidence of cognitive dysfunction in at least one other cognitive domain, as defined earlier in the text.

   ii.

   iii. Non-amnestic presentations:
      1. Language presentation: The most prominent deficits are in word-finding, but deficits in other cognitive domains should be present.
      2. Visuospatial presentation: The most prominent deficits are in spatial cognition, including object agnosia, impaired face recognition, simultagnosia, and alexia. Deficits in other cognitive domains should be present.
      3. Executive dysfunction: The most prominent deficits are impaired reasoning, judgment, and problem solving. Deficits in other cognitive domains should be present.

D. The diagnosis of probable Alzheimer's disease dementia ***should not*** be applied when there is evidence of:

   (a) substantial concomitant cerebrovascular disease, defined by a history of a stroke temporally related to the onset or worsening of cognitive impairment; or the presence of multiple or extensive infarcts or severe white matter hyperintensity burden; or
   (b) core features of Dementia with Lewy bodies other than dementia itself; or
   (c) prominent features of behavioural variant frontotemporal dementia; or
   (d) prominent features of semantic variant primary progressive aphasia or non-fluent / agrammatic variant primary progressive aphasia; or
   (e) evidence for another concurrent, active neurological disease, or a non-neurological medical comorbidity or use of medication that could have a substantial effect on cognition.

Table 2.3 NIA-AA 2011 criteria for Probable Alzheimer's Disease Dementia

Adapted from McKhann *et al.,* 2011 [117].

2.4.2 International working group (IWG) criteria

IWG criteria for a research diagnosis of typical Alzheimer's disease require the presence of a medical temporal lobe amnestic syndrome, that can be associated with various cognitive or behavioural changes, and evidence indicative of in-vivo Alzheimer's pathology (see Table 2.4).

A diagnosis of atypical Alzheimer's disease can be made in the presence of a clinical phenotype consistent with one of the known atypical presentations (posterior variant, logopenic variant of primary progressive aphasia, frontal variant) and at least one marker of in-vivo Alzheimer's pathology (Table 2.5).

A. Specific clinical phenotype

Presence of an early and significant episodic memory impairment (isolated or associated with other cognitive or behavioural changes that are suggestive of a mild cognitive impairment or of a dementia syndrome) that includes the following features:

- Gradual and progressive change in memory function reported by the patient or the informant over more than 6 months
- Objective evidence of an amnestic syndrome of the hippocampal type, based on significantly impaired performance on an episodic memory test with established specificity for AD, such as cued recall with control of encoding task.

B. In-vivo evidence of Alzheimer's pathology (one of the following)

- Decreased Aß together with increased T-tau or P-tau in CSF
- Increased tracer retention on amyloid PET
- AD autosomal dominant mutation present (in *PSEN1, PSEN2*, or *APP*).

Exclusion criteria for typical AD

History

- Sudden onset
- Early occurrence of the following symptoms: gait disturbance, seizures, major and prevalent behavioural changes

Clinical features

- Focal neurological features
- Early extrapyramidal signs
- Early hallucinations
- Cognitive fluctuations

Other medical conditions severe enough to account for memory and related symptoms

- Non-AD dementia
- Major depression
- Cerebrovascular disease
- Toxic, inflammatory, and metabolic disorders, all of which may require specific investigations
- MRI FLAIR or T2 signal change in the medical temporal lobe that are consistent with infectious or vascular insults.

Table 2.4 2014 IWG-2 criteria for typical Alzheimer's disease (A plus B at any stage)

Reproduced from Dubois *et al*., 2014 [116].

A. Specific clinical phenotype (one of the following)

Posterior variant of AD (including)

- An occipitotemporal variant defined by the presence of an early, predominant, and progressive impairment of visuoperceptual functions or of visual identification of objections, symbols, words or faces
- A biparietal variant defined by the presence of early, predominant and progressive difficulty with visuospatial function, features of Gerstmann syndrome, of Balint syndrome, limb apraxia, or neglect

Logopenic variant of AD defined by the presence of early, predominant, and progressive impairment of single word retrieval and in repetition of sentences, in the context of spared semantic, syntactic, and motor speech abilities

Frontal variant of AD defined by the presence of early predominant, and progressive behavioural changes including association of primary apathy or behavioural disinhibition, or predominant executive dysfunction on cognitive testing.

Down's syndrome variant of AD defined by the occurrence of a dementia characterised by early behavioural changes and executive dysfunction in people with Down's syndrome

B. In-vivo evidence of Alzheimer's pathology (one of the following)

- Decreased Aß together with increased T-tau or P-tau in CSF
- Increased tracer retention on amyloid PET
- AD autosomal dominant mutation present (in *PSEN1, PSEN2*, or *APP*)

Exclusion criteria for atypical AD

History

- Sudden onset
- Early and prevalent episodic memory disorders

Clinical features

- Focal neurological features
- Early extrapyramidal signs
- Early hallucinations
- Cognitive fluctuations

Other medical conditions severe enough to account for memory and related symptoms

- Major depression
- Cerebrovascular disease
- Toxic, inflammatory, and metabolic disorders

Table 2.5 2014 IWG-2 criteria for atypical Alzheimer's disease (A plus B at any stage)

Reproduced from Dubois *et al*., 2014 [116].

2.4.3 NIA-AA 2018 Research Framework

The recent 2018 update to the NIA-AA diagnostic recommendations defines Alzheimer's disease as an "aggregate of neuropathological changes and thus is defined *in vivo* by biomarkers and post-mortem examination, not by clinical symptoms [169]. It shifts the definition of Alzheimer's disease in living people away from the cognitive syndrome to a purely biological construct using biomarkers of Aβ1-42 deposition, pathologic tau, and neurodegeneration [AT(N)]. Cognitive impairment is treated as a symptom and/or sign of disease rather than the definition.

This may help clinical trials, for example, if only individuals with proven Alzheimer's disease pathology are recruited, however the clinical heterogeneity remains important as different imaging and cognitive end points would be needed for individuals with atypical presentations.

2.5 Patterns of neuronal injury - evidence for selective vulnerability

Selective vulnerability in the nervous system may explain differences in the clinical presentation of Alzheimer's disease. It refers to the observation that subpopulations of neurons within different brain systems are show variable susceptibility to dysfunction or cell death in response to specific types of pathological states or injury [170].

Regional neuronal injury, reflecting this selective vulnerability, has been studied in vivo in Alzheimer's disease variants using MRI to examine cross sectional or longitudinal atrophy, and ^{18}F-fluorodeoxyglucose (FDG)-PET to demonstrate areas of brain hypometabolism. These structural and functional imaging studies have shown that the dominant clinical features of atypical Alzheimer's disease syndromes arise fairly predictably from the regional pattern of neurodegeneration.

2.5.1 MRI atrophy

Within Alzheimer's disease, different phenotypes are associated with different regional atrophy profiles (see Figure 2.1).

Patients with late onset disease (manifesting after 65 years of age) typically present with an amnestic syndrome and correspondingly more medial temporal lobe degeneration relative to young onset cases [171]. In contrast, individuals with younger onset disease appear to have more neo-cortical predominant atrophy [172].

Those with an amnestic presentation have bilateral atrophy of the hippocampi and medial temporal lobes, posterior cingulate and precuneus cortices, temporo-parietal cortex, whereas in PCA there is typically parieto-occipital brain atrophy with relative sparing of the hippocampi [101, 173] early in the disease course. Patients with LPA classically have asymmetric involvement of the dominant hemisphere temporo-parietal junction [174-176]. The associated regional atrophy profile of the frontal lobes in people with behavioural or dysexecutive Alzheimer's disease is less striking than the other variant Alzheimer's disease syndromes. Volume loss in the posterior cingulate and precuneus is more prominent in patients with frontal syndromes underpinned by Alzheimer's disease pathology [106, 177] than other diseases causing frontal presentations.

Despite the apparent focality of atrophy, particularly early on in the clinical disease course, there is significant overlap between atrophy in disease variants, and often common involvement of the parieto-temporal and posterior cingulate cortex [178]. Furthermore, as the disease progresses clinically to involve other cognitive domains, the patterns of disease atrophy converge making it more difficult to detect any variant-specific differences [179] and variation between early onset and late onset disease [180].

(a) Typical amnestic Alzheimer's disease

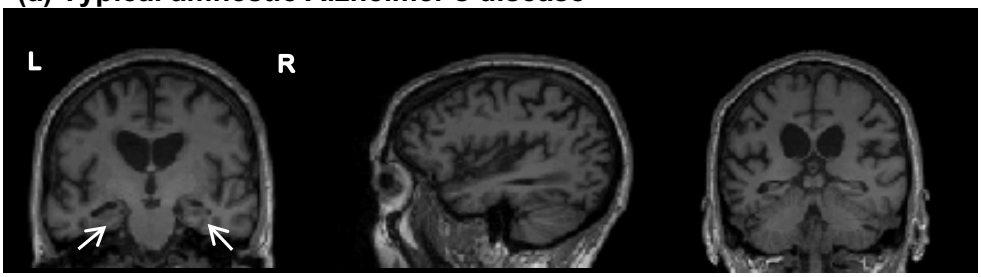

(b) Atypical Alzheimer's disease - Posterior cortical atrophy

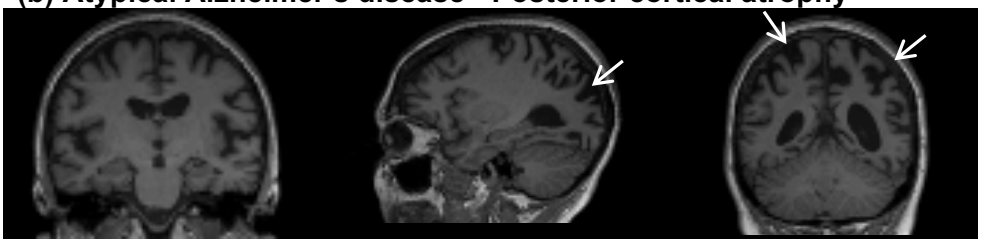

(c)Atypical Alzheimer's disease – logopenic aphasia

(d) Atypical Alzheimer's disease – frontal Alzheimer's

Figure 2.1 Alzheimer's disease atrophy profiles by phenotype

(a) Typical amnestic Alzheimer's disease: A 62 year old man with 6 year symptom duration and CSF tau:Aß ratio suggestive of Alzheimer's disease. MMSE 25/30. (b) Posterior cortical atrophy: A 57 year old woman with 8 year symptom duration and CSF tau:Aß ratio suggestive of Alzheimer's disease. MMSE 22/30. (c) Logopenic aphasia: A 65 year old man with 3 year symptom duration. MMSE 23/30. (d) Frontal Alzheimer's: 53 year old man with 11 year symptom duration and CSF tau:Aß ratio suggestive of Alzheimer's disease. MMSE 15/30. All patients were recruited into the study described in Chapter 5. The right cerebral hemisphere is displayed on the right in all panels.

2.5.2 Hypometabolism on ^{18}F-fluorodeoxyglucose (FDG)-PET

The patterns of regional hypometabolism in Alzheimer's disease variants accord largely with the observed atrophy profiles. Typical Alzheimer's disease is associated with hypometabolism of the hippocampi bilaterally, medial temporal lobe, posterior cingulate, precuneus and temporo-parietal cortex on ^{18}F-fluorodeoxyglucose (FDG)-PET brain imaging. PCA has a parieto-occipital distribution of hypometabolism, as well as relative sparing of the medial temporal lobes, relative to patients with typical Alzheimer's disease —at least early in the disease course [101]. LPA is characterised by left temporo-parietal hypometabolism [181]. Medial and orbital frontal hypometabolism is more pronounced in Alzheimer's disease patients who have prominent behavioural and dysexecutive features [182].

2.6 Drivers of clinical heterogeneity

The histopathological factors and genetic determinants leading to this regional neurodegeneration in Alzheimer's disease are currently incompletely understood, limiting our understanding of the pathogenesis of atypical Alzheimer's disease and how it gives rise to such a diverse repertoire of symptoms.

2.6.1 Amyloid pathology

As discussed in Chapter 1, accumulation of Aβ1-42 is required but not sufficient to lead to clinical manifestations of Alzheimer's disease. However, Aβ1-42 distribution is relatively diffuse throughout the neocortex in people with clinically manifest Alzheimer's disease so appears to explain relatively little about phenotypical variation, and does not mirror clinical symptoms.

Imaging studies using positron emission tomography with (11)C-labelled Pittsburgh compound B in typical amnestic Alzheimer's disease and posterior cortical atrophy have not shown significant differences in amyloid deposition [183-185], and CSF Aβ1-42 levels do not vary significantly between phenotypes [186, 187].

The results of these studies imply that the distribution of amyloid deposition is unlikely to be the key determinant of phenotypic variation in Alzheimer's disease. However, these studies have been performed on individuals with established disease, so given that Aβ1-42 accumulation is an early pathological event in Alzheimer's disease pathogenesis [95] it remains possible that there is regional variation in Aβ1-42 pathology in pre-symptomatic individuals who will go on to develop focal clinical syndromes.

2.6.2 Tau pathology

Pathological studies have shown that tau pathology is more closely correlated with regional neurodegeneration and cognitive impairment than Aβ1-42, suggesting a more causal role in heterogeneity. Even given the tendency for post mortem studies to be performed on patients with longer disease durations (and hence more syndromic convergence) there is some post mortem evidence for regional differences in tau pathology in Alzheimer's disease variants. There is excess deposition of neurofibrillary tangles in occipital and parietal cortices in patients with PCA[165], in the dominant-hemisphere perisylvian language cortices in those with logopenic variant [188, 189] and in the frontal cortex in individuals with frontal variant Alzheimer's disease [105].

CSF phosphorylated tau concentrations correlate with neurofibrillary tangle pathology in Alzheimer's disease [74, 78]. However, this reflects global tau burden in the brain and does not provide any insights to the regional distribution of tau, limiting its usefulness as a biomarker for studying selective vulnerability. It remains unclear whether CSF total and phosphorylated tau vary within Alzheimer's disease phenotypes, with some studies

finding no difference [190] and other suggesting that individuals with posterior cortical atrophy have lower levels of total and phosphorylated tau than those with frontal dysexecutive presentations [187], perhaps reflecting the varying burden of neocortical neuronal injury with PCA being a more focal syndrome than frontal Alzheimer's disease at equivalent disease durations.

The recent advent of advent of the positron emission tomography tracer ^{18}F-AV1451 [88] now enables the regional distribution of tau to be studied during life. Pathological aggregation of tau mirrors patterns of neurodegeneration and clinical manifestations of Alzheimer's disease. Relative to controls, individuals with posterior cortical atrophy show increased ^{18}F-AV1451 uptake in the clinically affected posterior brain regions, those with logopenic aphasia show higher ^{18}F-AV1451 uptake in the left relative to right cerebral hemisphere, and patients with amnestic predominant presentations show highest ^{18}F-AV1451 signal in the medical temporal and lateral temporo-parietal regions[90].

2.6.3 Other co-existing pathologies

Post mortem studies show that very few patients with Alzheimer's disease have 'pure' disease, i.e. coexistent vascular disease, TAR DNA-binding protein 43 and α-synuclein pathologies are highly prevalent alongside Aβ1-42 and tau [10, 191]. It is unclear how these additional pathologies interact and whether for example accumulation of TDP-43 and α-synuclein in neurons could make them more susceptible to damage from tau or amyloid, and how any cognitive impairment arising from these other pathologies clouds the clinical phenotype.

2.6.4 Genetic factors

There is evidence for both autosomal dominant and risk factor genes modifying the clinical phenotype of Alzheimer's disease and the age at which disease manifests.

2.6.4.1 Monogenic 'Familial' Alzheimer's disease

Patients with autosomal dominant mutations account only for a small percentage of the total Alzheimer's disease burden, however they have disproportionate neurobiological significance as an opportunity to gain insight into the much commoner sporadic disease. Mutations in *PSEN1*, *PSEN2* or *APP* genes all alter the intracellular processing of amyloid precursor protein and promote formation and accumulation of Aβ1-42, hence, perhaps unsurprisingly the most striking and consistent phenotypic effect is early symptom onset. Age of clinical disease onset are lowest in families with *PSEN1* mutations, typically falling between 35 and 55 years. *APP* mutations tend to give rise to symptom onset slightly later, between 40 and 65 years and *PSEN2* mutations between 40 and 70 years [192]. However, there is still significant phenotypic heterogeneity with regard to age of onset and clinical features both between families sharing a common mutation and within the affected individuals of a single family.

Despite amyloid not being though to be a principle driver of heterogeneity, and all the autosomal dominant mutations affecting amyloid pathways, there are differences in phenotype observed between the different mutations. Whilst the majority of individuals with familial Alzheimer's disease do have similar clinical presentations to those with sporadic disease, atypical cognitive presentations are seen more commonly in PSEN1 than APP mutations [100]. For reasons not understood, PCA and logopenic aphasia seem very rare in dominantly inherited Alzheimer's disease, however behavioural presentations are described [100, 193].

Myoclonus and seizures tend to occur earlier and more prominently in very young symptomatic patients with dominantly inherited Alzheimer's disease (<40 years) than in individuals with typical sporadic Alzheimer's disease. Spastic paraparesis, parkinsonism and cerebellar ataxia tend to be associated with *PSEN1* mutations that cause severe amyloid plaque deposition in relevant anatomical areas [192].

2.6.4.2 Sporadic Alzheimer's disease: The case of the missing ε4 allele

APOE ε4, the most significant genetic risk factor for Alzheimer's disease is also associated with a younger age of onset in late onset Alzheimer's disease. Individuals homozygous for the ε4 allele can develop Alzheimer's disease up to 10 years earlier than individuals who do not carry an ε4 allele [194]. However, the ε4 allele also appears to have its maximum impact between the ages of 60 and 70 years as it is relatively rarer for people with young onset Alzheimer's disease to carry the *APOE* ε4 allele [195, 196].

Individuals carrying ε4 alleles have more profound memory loss [197, 198] and greater medial temporal lobe vulnerability evidenced by increased atrophy [199-201], more marked FDG PET hypometabolism[202, 203] and post mortem tau pathology compared to non-carriers [204]. Individuals without ε4 alleles are more likely to be predisposed to vulnerability of cerebral networks beyond the medial temporal lobes presenting with non-amnestic phenotypes [205, 206].

2.7 Potential mechanisms underlying selective vulnerability

Potential mechanisms underlying selective vulnerability of neural populations that lead to clinical heterogeneity in Alzheimer's disease need to explain the mismatch between widespread amyloid deposition and more focal downstream neurodegeneration.

2.7.1 The network paradigm of neurodegenerative disease

Alzheimer's disease, and neurodegenerative diseases in general, are characterised by mis-folding of proteins, which may be intraneuronal inclusions (such as tau neurofibrillary tangles), and/or extracellular protein aggregates (such as amyloid plaques) leading ultimately to cell death. The specific clinical phenotype that manifests arises from the individual proteins implicated and the specific pattern of damage across a distributed neural network. This selective 'disconnection' is the basis of the neural network paradigm of neurodegenerative disease [207-210]. Diffusion weighted imaging modalities, such as diffusion tensor imaging (DTI) and neurite orientation and dispersion imaging (NODDI), and functional MRI can be used to study both structural and functional aspects of brain networks. These techniques are described in Chapter 3 and used in Chapters 10 and 11.

Cell models [211], animal models [212] and studies in humans [213] have consistently shown that Aβ1-42 production is related to neuronal activity, and Aβ1-42 largely accumulates in metabolically active highly connected brain regions, including but not limited to those making up the default mode network [214, 215]. This core network has been delineated using resting-state functional MRI. It encompasses the medial temporal limbic structures, their efferent and afferent connections to the anterior and posterior cingulate cortices respectively, posterior temporal cortex, lateral parietal and prefrontal cortices, and thalamic nuclei [210, 216]. Default mode network activity has been linked to task-free activity whilst at rest, hence it's historical definition in 'negative terms' [217]. It is deactivated during various externally driven cognitive tasks and is actively involved in internally focused activity, such as episodic memory retrieval, thinking about the future, daydreaming and inferring the perceptions of others [214].

Dysfunction of this core default mode network may help distinguish Alzheimer's disease

from other neurodegenerative disease, such as frontotemporal dementia [209, 218]. Altered DMN function has also been found in people with mild cognitive impairment with underlying Alzheimer's disease pathology [219], and in pre-symptomatic individuals carrying *APOE* ε4 alleles [220] providing more evidence for its role in Alzheimer's disease pathogenesis.

Furthermore, involvement of the default mode network appears consistent across the spectrum of Alzheimer's disease phenotypes [177, 178, 221] however the extent to which various parts of the network are involved and damaged may differ between phenotypes. This could explain some of the phenotypic differences if the core network is a neuroanatomical and functional chassis on which genetic and environmental factors can modulate the expression of Alzheimer's disease pathology [222].

However, network dysfunction in Alzheimer's disease is also likely to involve functional and/or structural disruption of other networks that closely associate with the default mode network. The extent of such network interactions could vary, and may be another mechanism by which heterogeneity in Alzheimer's disease arises; by different patterns of tau related neuronal injury in specific functional networks. Evidence for this hypothesis comes from the observation that different patterns of neuronal injury in Alzheimer's disease variants broadly map onto established functional brain networks [223]. As discussed earlier, Aβ1-42 aggregation appears to be driven by neuronal activity in highly connected cortical 'hub' regions, hence is diffusely and symmetrically distributed throughout the brain. Noting that tau pathology more closely correlates with regional neurodegeneration patterns, one possibility is that tau develops in specific vulnerable networks and spreads trans-neuronally, perhaps via a prion-like mechanism [224], to interconnected networks, possibly facilitated and augmented by amyloid pathology.

These two theories – differential involvement within a core network, or common

involvement of a core network with selective dysfunction of associated networks – raise a number of further questions. If other networks are implicated, it remains unclear what predisposes them to tau related injury in some individuals but not others. It is also unclear where the neurodegeneration starts – in a specific vulnerable network, or in the hub of the core network which then spreads.

2.7.2 Nexopathies: from protein abnormality to network signature

The molecular nexopathies paradigm attempts to explain how a specific disease phenotype could arise from the interaction between particular characteristics of a vulnerable network and the properties of the abnormal protein that aggregates in that particular neurodegenerative disease [207, 225]. Components of this theory include networks having variable intrinsic vulnerability to due to regional protein expression, or the type of synaptic connections present in a certain network. The pattern of daily activity in a neural network may predispose it to neurodegeneration, for example amyloid deposition in the metabolically active default mode network, and both amyloid and tau trafficking has been shown to change with the perturbations in the sleep wake cycle [226]. A proteinopathy might spread through the local neural circuit by causing connected brain regions to develop the same intracellular protein abnormality, or indirectly by affecting the function of the connected regions.

Pathogenic proteins could promote neural network breakdown by various mechanisms including disruption of synaptic function or repair, axonal transport, cell-cell signalling abnormalities or interruption of downstream trophic functions. Developmental patterns of protein expression or connectivity may make certain networks more vulnerable or resilient to disease effects. Different types of neural connections may vary in their vulnerability to certain pathogenic proteins, for example shorter range dendritic and interneuronal connections appear especially susceptible to damage from some

tauopathies whereas longer range axonal projections appear more likely to be damaged by oligomers from APP [227]. The effect of damage to a network from accumulation of a specific faulty protein may be either a net toxic gain or function or loss of function. The specific interaction between the vulnerable network and the pathogenic protein subsequently gives rise to the observed pattern of regional neurodegeneration and the macroanatomical signature of disease. Specifically, in variant forms of Alzheimer's disease, differential involvement of cortico-cortical projection zones that are part of a core Alzheimer's disease vulnerable network may explain the atypical phenotypes that characterise posterior cortical atrophy and logopenic aphasia.

2.7.3 "Catastrophic cliffs"

Part of the basis of selective vulnerability in neurodegenerative disease is theorised to be due to neurons with specific functions being closer to different types of catastrophic failure, that can be precipitated by downstream effects of particular genetic mutations [228]. For example, in FTD, motor neurons and pyramidal neurons are close to a 'cliff' of ubiquitin proteasome system overload, and that the aberrant products of the *C9orf72* locus overwhelm this system and cause it to fail. In DLB and FTD pyramidal neurons appear to be close to lysosomal failure, and hence are predestined to 'catastrophe' by genetic mutations in the endosome and lysosome system, such as those in GRN and CHMP2B [229]. It is possible that the cholinergic neurons that fail in Alzheimer's disease do so as they tip over a 'catastrophic cliff' relating to directly to APP or tau metabolism, or more indirectly to immune mediated pathways or cholesterol metabolism. How this relates to heterogeneity in sporadic Alzheimer's disease remains to be explored.

2.7.4 Resilience factors

The converse to selective vulnerability is that there may be some individuals who, for whatever genetic or environmental predisposition, have brain networks with connectivity

patterns less susceptible to either the initiation or spread of a proteinopathy. This may help explain the incomplete penetrance of some genetic mutations. Equally, some neurons and brain networks are more resilient to Alzheimer's pathology, for example the primary motor and sensory cortices are relatively spared.

2.8 The challenge and opportunity of clinical heterogeneity

The focus of research in Alzheimer's disease on the 'prototypic' presentation represents the majority of people with the disease, and hence the bulk of the disease burden. However, recognising, characterising and understanding the rare Alzheimer's disease variants and the influence of other common pathologies is important. Much as the study of familial Alzheimer's disease led to the discovery of autosomal dominant genetic mutations and the conception of the amyloid hypothesis, studying common and discordant genetic (and environmental) risk factors for typical and atypical Alzheimer's disease, combined with neuroimaging, cerebrospinal fluid and other biomarkers, may provide fundamental insights into Alzheimer's disease pathogenesis. It is entirely plausible that different risk factors modulate the rate, timing and site of amyloid deposition; whether or when amyloid deposition leads to neurodegeneration; and which neuronal networks bear the brunt of the disease. This in turn may influence how pathology spreads through the brain, and what symptoms predominate.

Armed with this knowledge of syndromic inhomogeneity we may disentangle its confounding effects in clinical trials, as efforts to exclude atypical subtypes are not always successful and can affect outcome measures. Furthermore, understanding the pathogenesis of atypical Alzheimer's disease variants may lead to new targets for therapy and allow us to better tailor existing therapies to individuals.

Finally, from a clinical perspective, clinicians should be alert to the fact that Alzheimer's disease can present with unusual phenotypes and not overlook the existence or

emergence of impairments in visual and other non-memory functions even in patients presenting with amnestic Alzheimer's disease. These are important to recognise to allow prompt diagnosis and appropriate treatment, and tailored support and guidance for an individual patient.

3 Neuroimaging in Alzheimer's disease

One key tool to explore the heterogeneity in Alzheimer's disease, and a technique utilised in this thesis is magnetic resonance imaging (MRI). MRI is a safe, non-invasive and high-resolution imaging modality which utilises the interaction of biological tissue with electromagnetic fields and can be applied to the study of both brain structure and function. It is well established as a key part of the diagnostic work up in the diagnosis of dementia [230] and ongoing technical advances offering higher resolution, new modelling techniques for MRI data and faster acquisition protocols means that MRI continues to be a dominant technique at the forefront of dementia research. Chapters 8 to 11 of this thesis use MRI to investigate aspects of heterogeneity in young onset sporadic Alzheimer's disease. This chapter discusses the principles of MRI and our current understanding of MRI in sporadic YOAD.

3.1 Principles of MRI

In the simplest terms, magnetic resonance imaging is based on the fact that protons placed in a magnetic field and excited by a radiofrequency (RF) pulse emit a radio signal which can be measured and used to construct an image of the brain.

The human body is largely composed of water molecules, each of which contain two hydrogen nuclei, or protons. A person is placed in the magnetic field of an MRI scanner, which generates a magnetic field (B0) typically in the range from 1.5 to 3.0 Tesla, although field strengths up to 7.0 T are now being used in clinical practice. The unpaired protons become aligned with this field depending on the strength of the field and their thermal energy and precess (spin) in the direction of the field with a frequency (f0) determined by the Lamor equation:

$$f0 = gB0$$

where g is the constant defined by the magnetic property of the nuclei. A short RF pulse in the order of 50mT is transmitted at the resonant frequency of the proton and these protons absorb energy and are promoted to a higher energy level (decreasing longitudinal magnetisation) and such that they precess in phase (establishing transverse magnetisation). When the RF pulse is subsequently switched off the excited protons realign with the magnetic field and emit energy in form of radio-waves. The resulting increase in longitudinal magnetisation gives rise to the T1 curve (the time constant T1 is the longitudinal or "spin-lattice" relaxation time) and the loss of transverse magnetisation gives rise to the T2 curve (the time constant T2 is the transverse or "spin-spin" relaxation time and is much shorter than the T1 time constant).

The time from one excitation pulse to the next is denoted as the repetition time (TR) and the time from one pulse to the maximum signal induction is the echo time (TE). As the magnetic field within the scanner is not uniform but instead generated as a gradient, the radio waves emitted from the protons are additionally dependent upon their position within the gradient field, meaning the radio waves can be converted into spatial information.

Altering the MRI acquisition parameters enables the different T1 and T2 properties of tissues to be utilised to generate images highlighting a specific tissue type. T1 is characterised by short TR and short TE, and used in this thesis to image the structure of the brain.

3.2 Volumetric structural MRI

Volumetric structural MRI involves imaging the entire brain as a whole entity, acquiring isotropic voxels or thin slices with high spatial resolution to allow multi-planar

reconstructions in all planes. This thesis uses a Siemens 3D gradient echo sequence: a T1 weighted magnetically prepared rapid acquisition gradient echo sequence (MP-RAGE) [231].

Volumetric structural MRI can be used cross-sectionally to image heterogeneity in regional brain atrophy using visual assessment tools (e.g. Scheltens medial temporal lobe scale [232]), volumetric measures which involve outline a predetermined region of interest on several sequential slices of a volumetric scan, and for voxel based morphometry which employs statistical parametric mapping to study differences in brain tissue composition between groups.

Serial registered scans can be used to measure rates of brain or regional atrophy using methods such as the boundary shift integral (BSI) [80]. This technique determines the total volume through which the boundaries of a given cerebral structure have moved from a baseline to follow up scan, and, hence estimates the volume change, directly from voxel intensities. The mean annual rate of brain atrophy using BSI in people with AD is approximately 2.78% compared with.024% in with healthy controls. Other methods for measuring brain atrophy in longitudinal studies include Structural Image Evaluation, using Normalization, of Atrophy (SIENA) [233], Tensor-Based Morphometry (TBM) [234] and FreeSurfer-longitudinal (FS) [235].

Volumetric structural imaging in young onset Alzheimer's disease

As discussed in section 2.5.1, different AD phenotypes are associated with different regional atrophy profiles (illustrated in Figure 2.1). Volumetric structural imaging is used both in clinical practice to aid diagnosis and in AD research.

Patients with late onset disease tend to have more medial temporal lobe degeneration relative to young onset cases [171] whereas individuals with younger onset disease

appear to have more neo-cortical predominant atrophy [172]. Those with an amnestic presentation have bilateral atrophy of the hippocampi and medial temporal lobes, posterior cingulate and precuneus cortices, temporo-parietal cortex, whereas in PCA there is typically parieto-occipital brain atrophy with relative sparing of the hippocampi [101, 173] early in the disease course. Patients with LPA classically have asymmetric involvement of the dominant hemisphere temporo-parietal junction [174-176]. The associated regional atrophy profile of the frontal lobes in people with behavioural or dysexecutive Alzheimer's disease is less striking than the other variant Alzheimer's disease syndromes. Volume loss in the posterior cingulate and precuneus is more prominent in patients with frontal syndromes underpinned by Alzheimer's disease pathology [106, 177] than other diseases causing frontal presentations.

Despite the apparent focality of atrophy, particularly early on in the clinical disease course, there is significant overlap between atrophy in disease variants, and often common involvement of the parieto-temporal and posterior cingulate cortex [178]. Furthermore, as the disease progresses clinically to involve other cognitive domains, the patterns of disease atrophy converge making it more difficult to detect any variant-specific differences [179] and variation between early onset and late onset disease [180].

3.3 Diffusion Tensor Imaging

Diffusion tensor imaging (DTI) is a magnetic resonance technique for exploring the structural integrity of white matter *in vivo* using water diffusion to distinguish different microstructural environments that has been applied to the study of many neurological diseases[236]. It provides voxel-level estimates of fractional anisotropy (FA), axial diffusivity (AxD) and radial diffusivity (RD) within structural brain networks.

Cerebral white matter consists of myelinated axons which water tends to diffuse along with limited diffusion perpendicularly. A mathematical model to describe this process,

termed the diffusion tensor [237] uses a 3 x 3 matrix to describe the degree and direction of diffusion displacement over time. From the diffusion tensor matrix three eigenvalues (λ1, λ2 and λ3) and their eigenvectors (ε1, ε2 and ε3) are derived. Within each brain voxel the tensor is imagined as an ellipsoid with the eigenvectors defining the principal direction of diffusion along the axis of the ellipsoid and the eigenvalues defining the radius of the ellipsoid.

When a property is highly isotropic (e.g. in water), each eigenvalue will be similar to one another (i.e. λ1≈λ2≈λ3) however when an object is highly anisotropic (e.g. a white matter tract) each eigenvalue will differ in order of magnitude (i.e. λ1>λ2>λ3). To allow us to understand complex 3D changes in both the magnitude and directionality of diffusion a number of scalars have been derived. Fractional anisotropy (FA) describes the degree of directionality of diffusion and is calculated as follows:

$$\mathrm{FA} = \sqrt{\frac{1}{2}} \frac{\sqrt{(\lambda_1 - \lambda_2)^2 + (\lambda_2 - \lambda_3)^2 + (\lambda_3 - \lambda_1)^2}}{\sqrt{\lambda_1^2 + \lambda_2^2 + \lambda_3^2}}$$

Other scalars better represent the magnitude of diffusion such as its average mean diffusivity (MD):

$$\mathrm{MD} = (\lambda_1 + \lambda_2 + \lambda_3)/3$$

Axial diffusivity (AX) is a measure of the magnitude of diffusion parallel to the orientation of the white matter tract being studied, which should be the dominate direction, as diffusion of water in this direction should be relatively unimpeded given the orientation of the structure:

$$AX = \lambda_1$$

Radial diffusivity RD, which is a measure of the magnitude of diffusion perpendicular to the orientation of the white matter tract being studied, should detect only minor diffusion, as the movement of water molecules in this direction is more impeded by tract fibres:

$$RD = \frac{(\lambda_2 + \lambda_3)}{2}$$

FA is the most commonly reported metric within the literature, reflecting the overall integrity of a white matter tract by reporting the degree of isotropy within it (a value approaching one signifies highly anisotropic diffusion of water, often associated with a tract being more structurally intact, whilst lower values signify increasingly isotropic diffusion tending to be associated with tract pathology). However, FA cannot fully explain all the changes within the diffusion tensor, in particular the magnitude of change e.g. increases of similar magnitudes in each eigenvalue can result in no change to FA. Hence it is important to also consider the absolute changes in diffusion as measured by AX, RD and MD.

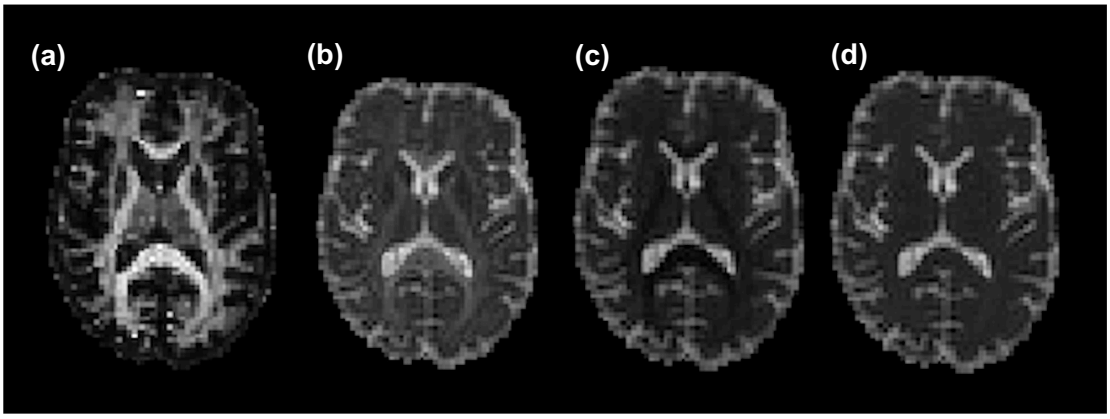

Figure 3.1 Diffusion tensor imaging in Alzheimer's disease

(a) fractional anisotropy, (b) axial diffusivity, (c) radial diffusivity, (d) mean diffusivity. Data are from an individual in this thesis.

Diffusion tensor imaging in young onset Alzheimer's disease

DTI is used as a research tool in AD. Relative to late onset presentations, young onset Alzheimer's disease is associated with more marked and extensive white matter abnormalities, involving the interhemispheric connections, limbic network and major associative tracts, sparing the corticospinal tracts, brainstem and cerebellar white matter. In contrast, individuals with late onset disease showed more localised pattern of white matter damage mainly involving the corpus callosum [238]. White matter diffusion abnormalities in young onset Alzheimer's disease are more extensive than cortical atrophy so have been hypothesised to reflect the pathologic dissemination through structural connections from atrophic to unaffected cortical regions[239].

Diffusion abnormalities between atypical Alzheimer's disease phenotypes show significant spatial overlap in a structural network involving the fornix, corpus callosum, posterior thalamic radiations, superior and inferior longitudinal fasciculi, inferior fronto-occipital fasciculus and uncinate fasciculus [240]. However, syndrome specific signatures of white matter damage are also detected, with diffusion abnormalities particularly in the fornix and cingulum in individuals with memory predominant symptoms, the left inferior fronto-occipital and uncinated fasciculi in those with logopenic aphasia, and the posterior thalamic radiations, superior longitudinal fasciculus, posterior cingulate and splenum of the corpus callosum in those with posterior cortical atrophy.

Limitations of DTI

The DTI model is based on there being a single fibre orientation in each voxel, whereas in the brain the majority of voxels contain fibres of different orientations and crossing fibres. DTI cannot account for this, the scalars reported are summary measures for the voxel. Furthermore, diffusion in is the brain is affected by the presence of membranes and myelin. Whereas in DTI water diffusion is modelled as behaving in a Gaussian

manner, this does not reflect the true hindrance and restriction cause by the underling tissue microstructure [241].

There are several more complex diffusion models of tissue microstructure that try to provide indices closer to what actually happens at the tissue level, one of which uses a three-compartment model and is used in this thesis: neurite orientation dispersion and density imaging (NODDI).

3.4 Neurite Orientate Dispersion and Density Imaging

Neurite orientation dispersion and density imaging (NODDI) [242] is one of a number of advanced diffusion MRI techniques designed to probe tissue microstructure beyond a composite view of each voxel by modelling water diffusion in multiple compartments [243] (Figure 3.2).

(i) Diffusion that is restricted in axons and dendrites – modelled as a set of cylinders with zero radius, reflecting free diffusion along their length and restricted diffusion perpendicularly.

(ii) Hindered in the extra-neurite space i.e. the space around neurites that is occupied by glial cells, the extracellular matrix and neuronal cell bodies in grey matter.

(iii) Isotropic in cerebrospinal fluid (CSF)

NODDI derives a neurite density index (NDI), orientation dispersion index(ODI) and the fraction of free water (F_{iso}). Examples of these NODDI metrics are shown in Figure 3.3 as NODDI maps. NDI is an estimate of neurite density, and may therefore be a useful marker of the axonal loss in Alzheimer's disease that leads to breakdown of brain structural networks and the development of cognitive symptoms.

ODI estimates the spread of dispersion of neurite orientations. It ranges from 0 (all neurites perfectly parallel to 1 (neurites orientated randomly in all possible orientations).

The NODDI model allows axonal loss in white matter (NDI) to be distinguished from altered patterns of axonal organization (ODI) on a voxel-by-voxel basis, thereby disentangling two key factors contributing to changes in FA.

A key strength of NODDI, compared to alternative multi-compartment techniques, is the use of standard MRI acquisition similar to DTI, making it accessible for routine clinical studies. To date, it is the only multi-compartment technique whose utility has been widely demonstrated in a broad range of applications, including Parkinson's disease [244], epilepsy [245], normal ageing [246], brain development [247], and neurogenetic disorders [248].

At the time of investigation during this PhD, NODDI had not been applied to Alzheimer's disease.

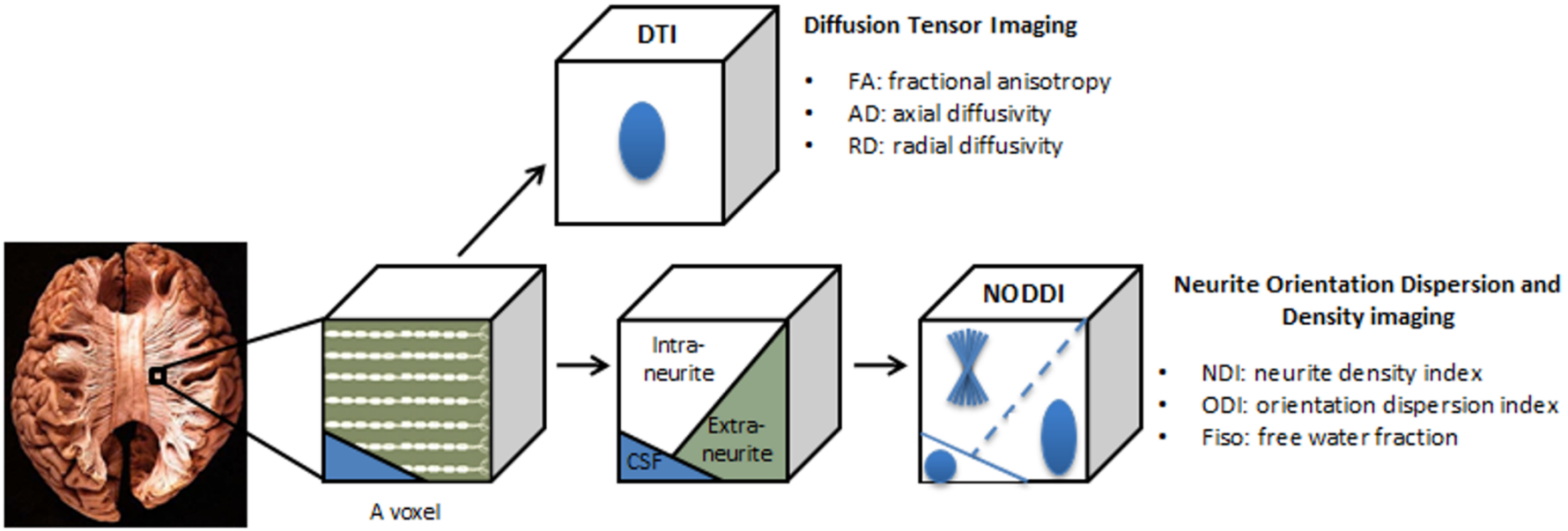

Figure 3.2 Diffusion tensor imaging (DTI) and neurite orientation dispersion and density imaging (NODDI) models for diffusion weighted MRI

DTI models each voxel using a single tensor, hence gives a composite view of tissue microstructure. NODDI models each voxel as three compartments: intraneurite (restricted diffusion), extraneurite (hindered diffusion) and cerebrospinal fluid (isotropic diffusion). Dendrites and axons, collectively known as 'neurites', are projections of neurons. NODDI can estimate neurite density index (NDI) and orientation dispersion index (ODI), specifically in the intraneurite compartment, without partial volume effects from free water.

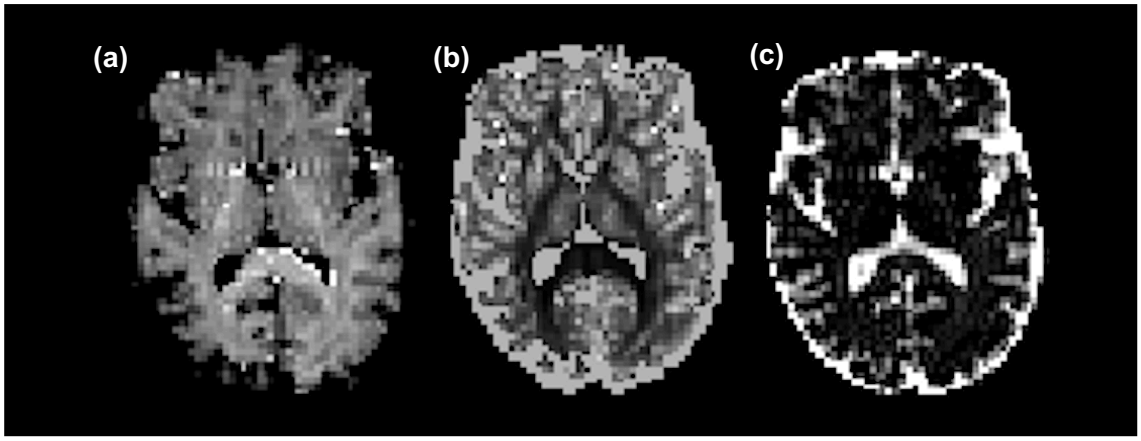

Figure 3.3 Neurite Orientation Dispersion and density imaging maps in Alzheimer's disease

(a) neurite density index, NDI (b) orientation dispersion index, ODI (c) fraction of free water, F_{iso}. Data are from an individual in the YOAD cohort.

3.5 Activation functional MRI

Functional MRI (fMRI) estimates and localises brain activation using the blood oxygenation level dependent signal (BOLD).

This BOLD signal results from dynamic changes in blood flow and oxygenation (the ratio of deoxyhaemoglobin to oxyhaemoglobin) due to neuronal and synaptic activity, and as such is an indirect measure of neural activity [249].

Regional changes in the BOLD signal influence the transverse relaxation rate T2 and T2*. Reduction of local magnetic gradients and increased blood volume prolong parenchymal T2*, which is recorded as a 'positive' BOLD signal by means of T2* weighted MRI.

Fluctuations in BOLD without an external trigger, the so-called resting state fMRI, allows indirect inference about intrinsic brain connectivity. Haemodynamic responses due to

experimental external events result in task-activated BOLD fMRI from which inferences have been made with regard to cognitive function.

Functional MRI has three potential advantages over structural MRI:

(i) It may be more sensitive than conventional structural metrics and can hence detect disease-associated functional alterations prior to the onset of irrecoverable brain damage [94].

(ii) It can measure functional connections between brain regions which may occur via indirect structural connections and would otherwise not be appreciated.

(iii) As well as identifying areas of decreased brain activity, it can uncover disease mediated aberrant and compensatory increases.

Functional fMRI is well hence suited for studying the mechanisms by which brain networks break down in dementia and for testing specific pathophysiological hypotheses such as the relevance of pathogenic protein deposition[250].

Limitations of activation fMRI

There are also a number of challenges in using this technique including a lack of methodological consistency between studies, the presence of physiological noise, and unclear applicability to individual participants. Furthermore, the application of task based fMRI to patients with cognitive impairment can be challenging and usually requires customised protocols based on short scanning sessions and minimal in scanner task demands, (e.g. in Chapter 11 I use a task free paradigm).

Activation fMRI studies in Alzheimer's disease

As memory impairment and hippocampal atrophy are the commonest findings in patients with Alzheimer's disease, most fMRI studies of task related activity in Alzheimer's disease have focused on memory tasks and memory related brain activation. Reduced hippocampal activation in Alzheimer's disease patients verses controls has been demonstrated in several studies using memory encoding tasks [251-254]. However, increased hippocampal activity is also reported, especially in studies looking at patients with early stages of disease [255]. Furthermore, whilst hippocampal activity may be diminished in later disease, coexistent hyperactivation is seen in other parts of the DMN, such as the parietal and posterior cingulate regions[254]. The nature of this hyperactivation compared to control participants remains debated. Hippocampal hyperactivity may be a compensatory mechanism which occurs early in the disease process, followed by hippocampal failure as the disease progresses, or may vary between individuals reflecting the degree, load and spatial profile of pathology within the wider DMN.

4 Thesis aims and outline

The aims of this thesis are to describe clinical and genetic heterogeneity in a deeply phenotyped prospectively recruited cohort of individuals with young onset sporadic Alzheimer's disease (YOAD).

Chapter 5 outlines how the YOAD study was set up to recruit a cohort to explore this heterogeneity.

Chapter 6 describes the clinical and neuropsychological features of the YOAD cohort.

Chapters 7 and 8 explore genetic underpinnings of YOAD. The presence of any autosomal dominant mutations and *APOE* ε4 status for individuals in the YOAD cohort are reported in Chapter 7. Chapter 8 addresses the prevalence of p.R47H: a rare genetic variant in *TREM2* and a moderate genetic risk factor for Alzheimer's disease first described during the timespan of this thesis, in both the YOAD cohort and a larger genetic cohort of individuals with dementia using Sanger Sequencing. The clinical phenotype of individuals with Alzheimer's disease carrying an R47H variant is also described.

Chapter 9 investigates macrostructural brain changes associated with different *APOE* ε4 statuses including brain and hippocampal volumes and voxel based morphometry.

Chapter 10 looks into microstructural changes derived from diffusion imaging – including diffusion tensor imaging (DTI) and neurite orientation dispersion and density imaging (NODDI), relationships with *APOE* ε4 status, and between regional metrics and cognitive performance.

Finally, Chapter 11 seeks to understand the brain basis of memory impairment in Alzheimer's disease by using behavioral measures and activation fMRI to investigate the neuroanatomical basis of musical memory in individuals with memory led and visual led presentations of young onset Alzheimer's disease.

5 Methods overview - Cohorts

The data analysed in this thesis is drawn from both the young onset Alzheimer's disease (YOAD) study cohort – a new cohort set up and run as part of the work of this thesis (Chapters 7-11) and the pre-existing UCL Department of Neurodegenerative disease genetics cohort (Chapter 8).

5.1 The YOAD cohort

The YOAD Study was designed to explore phenotypic differences in a population of individuals with sporadic young onset Alzheimer's disease using multimodal imaging and correlative neuropsychology, genetic and cerebrospinal fluid biomarker data. The aim was to recruit ~50 patients with mild to moderate Alzheimer's disease representing a variety of disease phenotypes, and ~25 age and sex matched controls.

Work preceding the analyses in this thesis included writing study protocols, information sheets, data capture sheets, trialling imaging protocols and successful application for approval from Ethics and Research and Development committees.

5.1.1 Participants

Individuals with YOAD

All patients were recruited from the Specialist Cognitive Disorders Clinic at the National Hospital for Neurology and Neurosurgery: a national referral centre for patients with cognitive disorders with a particular expertise in young onset dementia and genetic forms of dementia.

All patients approached about the study had previously indicated that they would be interested in research or completed a Data Protection Act form to be included on the

UCL Dementia Research Centre Research Register. All patients had a diagnosis of Alzheimer's disease, which had been explained to them and their next of kin.

Prior to recruitment to the study, patients underwent thorough neurological assessments as part of their clinical care. This included a detailed medical history and collateral history from someone who knows them well, and general medical and neurological examinations. Patients also underwent detailed neuropsychological testing to map the pattern of cognitive deficits and an MRI brain to exclude space occupying lesions, subdural haematoma and/or significant vascular disease as alternative causes for their cognitive presentations. Standard screening blood tests including renal and liver function, vitamin B12 levels and thyroid function (in addition to any further felt necessary by the clinical consultant) to exclude other treatable causes of cognitive impairment were done.

Patients with cerebrospinal fluid biomarker evidence of underlying Alzheimer's disease pathology were preferentially, but not exclusively, recruited. As part of their clinical work up, selected patients had cerebrospinal fluid samples for neurodegenerative markers collected in polypropylene tubes between 9am and 3pm according to local protocols. Total tau (T-Tau) and Aβ1-42 were analysed using INNOTEST enzyme-linked immunosorbent assays (ELISAs) (Fujirebio Europe N.V., Gent, Belgium). Assays were carried out in batches according to local clinical NHNN neuroimmunology laboratory standard operating procedures to achieve coefficient of variation of <10%. A tau/ Aβ1-42 ratio cut-off of 0.52, shown to provide good sensitivity and specificity of underlying Alzheimer's disease pathology [256] was used to guide decisions about patient eligibility for the study, in combination with a CSF Aβ1-42 <550pg/ml (based on patient and control CSF normative valves used locally).

All patients recruited had a prior diagnosis of Alzheimer's disease that had been explained to them and their next of kin.

Informants

Patient participants were asked to identify a family member or friend who knew them well to act as an informant. Informants were invited together with the participant to complete a number of questionnaires relating to the participant's health and wellbeing and their own experiences of caring for a person with dementia. This involvement was independent of participation in the study as a healthy control.

Healthy controls

Unaffected partners of study patient participants were preferentially recruited as healthy controls for practical reasons and to aid accurate matching of the groups in terms of background, age and education.

Partners of other patients seen at the Cognitive Disorders Clinic or attending the Rare Dementias Support Group (http://www.ucl.ac.uk/drc/support-groups), or people directly contacting the UCL Dementia Research Centre to volunteer were also recruited as study controls.

5.1.2 Case Selection: inclusion and exclusion criteria

Inclusion criteria for patient participants included:

- age at reported symptom onset < 65 years;
- fulfils criteria for probable Alzheimer's disease dementia of intermediate or high certainty based on NIA-AD criteria incorporating biomarkers[117];
- has capacity to give informed consent and be able to attend with a carer;
- MMSE score [108] at recruitment of >12/30;

- on the basis of a medical history and physical examination the participant is considered to be otherwise healthy;
- be a fluent English speaker;
- stable for at least 3 weeks on any medication for dementia (cholinesterase inhibitors and/or memantine).

Inclusion criteria for control participants included:

- age and sex matched individuals willing to participate and give informed consent;
- no known neurological or severe psychiatric disorders;
- and no history of significant cognitive decline.

Exclusion criteria for all participants included:

- inability to tolerate MRI scanning;
- any contraindication to MRI scanning;
- member of a known autosomal dominant dementia family testing positive for a disease-causing mutation;
- trisomy of chromosome 21;
- and for patients, current or recent (<6 months) participation in a clinical trial of an investigation medicinal product for Alzheimer's disease.

5.1.3 Consent and Ethical Considerations

This study was approved by the local research ethics committee at The National Hospital for Neurology and Neurosurgery, Queen Square, London (13/LO/0005). Informed written consent was obtained from all participants. Participants were all informed that taking part in the study was entirely voluntary and that they could withdraw at any time. It was emphasized that participants would not be provided with individual results, however if their MRI revealed an unrelated but clinically significant abnormality such as

a cerebral neoplasm their general practitioner would be informed. All patient participants had capacity to consent at enrolment to the study.

Data was stored in accordance with the Data Protection Act 1998.

5.1.4 Study design

The YOAD study involved assessment at baseline with additional assessment for interval change after one year (Table 5.1). The longitudinal data analyses are beyond the scope of this thesis and not further considered here.

	Baseline visit	One year visit
Clinical Assessment	x	x
Neuropsychology	x	x
MMSE	x	x
Neuroimaging		
3D T1	x	x
Diffusion tensor imaging	x	x
Neurite orientation dispersion and density imaging	x	x
Activation fMRI	x	
Blood sample for genetic analyses	x	

Table 5.1 Overview of YOAD study design

5.1.4.1 Clinical assessment

All study participants underwent a structured clinical assessment and physical examination. This included a structured interview to assess any current cognitive symptoms and relevant background medical information. With their permission, patients were interviewed in the presence of their consultee to ensure accurate data collection, noting some patients had significant memory impairment and/or lack of insight.

Specific information collected for all subjects included age, sex, handedness, level of educational attainment, occupation, smoking history, alcohol consumption and medical comorbidities. An estimate of clinical symptom onset was made for patients from the history and from past medical notes available, and information about the use of symptomatic treatment (cholinesterase inhibitors or memantine) was collected. Patients and their consultee were asked what their first noted symptom was (noting this may be vulnerable to recall bias, and patients often use the phrase 'memory problems' to describe a variety of cognitive symptoms). All participants were asked to grade any current cognitive, behavioural, neuropsychiatric, or motor symptoms.

Neurological examination recorded whether abnormalities were demonstrable in the following domains: visual fields, eye movements, limb tone, limb reflexes, plantar response and gait. The presence or absence of visual inattention, optic ataxia, myoclonus, rest tremor, postural tremor, bradykinesia, ataxia and/or dystonia was specifically noted. Limb and orofacial praxis was assessed using subtest 3 of the Adult Battery for Adults (ABA-2) [257]. General physical examination recorded lying and standing blood pressure using a digital sphygmomanometer, height and weight. Body mass index (BMI) was estimated calculated according to the formula: weight/(height)^2.

All participants were assessed using the MMSE [108]: a widely used 30-point screening tool for cognitive impairment within clinical practice assessing multiple cognitive domains including (i) orientation to time and place (10 points); (ii) registration (3 points); (iii) attention ± calculation (5 points); recall (3 points); (v) language (2 points); (vi) repetition (1 point); (vii) reading (1 point); (ix) visuospatial function (1 point); and (x) following a three stage command (3 points). The modified Hachinski ischaemic score[258] was also calculated for patient participants – this scale ranges from 0 to 12, with vascular risk factors leading to an increased score (contained in YOAD study folder, see appendix 3).

5.1.4.2 Neuropsychology

A neuropsychology battery was specifically designed to capture cognitive deficits in domains affected by both typical and atypical Alzheimer's disease presentations. The battery was designed to be implemented in less than two hours, to be applicable to both patients with mild to moderate Alzheimer's disease and controls. Material was presented both verbally and in written format (where applicable) to control for confounds due to e.g. language impairment on tests not primarily assessing language in patients with LPA, and visual impairment on tests not primarily assessing vision in PCA patients.

The battery included assessment of general intellect (vocabulary and matrices subtests of the Wechsler Abbreviated Scale of Intelligence, WASI[259]), episodic memory (Recognition Memory Test - faces and words subtests, RMT [260]; Camden Paired Associate Learning test [261]), working memory (digit span from the Wechsler Memory Scale Revised [262]), word retrieval (Graded Naming Test [263]), calculation (Graded Difficulty Arithmetic, GDA [264]), spelling (Graded Difficulty Spelling Test, GDST [265]), visuospatial and visuoperceptual performance (Visual Object and Spatial Perception battery, VOSP[266]), speed of processing and executive function (design fluency and category fluency from the Delis-Kaplan Executive Function System, DKEFS [267]; Digit Symbol Modalities Test, DSMT [268]).

5.1.4.3 Phenotype

Phenotype for each patient participant was determined according to research criteria in use at the time of recruitment, as discussed in Chapter 2 [102, 116, 165].

5.1.4.4 Genetics

Patient participants gave separate specific consent to donate blood for genetic analyses. Twenty millilitres of blood were collected by venepuncture and DNA extracted using

standard techniques. Patient participant samples were tested for *APOE* ε4 genotype, the presence of any autosomal dominant causes of neurodegenerative disease using next generation sequencing, and known risk factor single nucleotide polymorphisms. The techniques and results are detailed in Chapters 7 and 8.

5.1.4.5 Neuroimaging

Participants underwent MRI scanning so that group differences in brain structure and function could be studied.

All imaging was acquired on a 3T TIM Trio whole-body MRI scanner (Siemens Healthcare, Erlangen, Germany). A 32-channel receiver phased-array head coil was used for all modalities, except the activation fMRI protocol (a 12-channel head coil was substituted as the participant was required to wear headphones during this sequence).

Sequences acquired included:

(i) High resolution 3D T1-weighted volumetric scans;

(ii) Multi-shell high angular resolution diffusion-weighted MRI (DW MRI);

(iii) Gradient-echo echo-planar image (GE-EPI) volumes as part of an activation functional MRI paradigm.

An additional B0 field map was also acquired for distortion correction of the DW MRI and GE-EPI volumes. Full details for the acquisition parameters are shown in Table 5.2.

The technical detail of the acquisitions, image processing and data analyses are described in Chapters 8 to 11. The techniques used in each chapter are shown in table 5.3.

	MPRAGE (3D T1)	*DTI*	*NODDI*	*Diffusion field map*	*Act-fMRI*	*Act-fMRI field map*
Voxel resolution (mm^3)	1.1x1.1x1.1	2.5x2.5x2.5	2.5x2.5x2.5	3.0x3.0x3.0	2.0x2.0x2.0	3.0x3.0x3.0
Matrix size	256x256x208	96x96x55	96x96x55	64x64x55	96x96x48	80x80x48
FOV (read x PE) (mm)	282x282	240x240	240x240	192x192	192x192	192x192
Slice coverage (mm)	229	137.5	137.5	165	144	144
Orientation	sagittal	transversal	transversal	transversal	transversal	transversal
PE direction	A>>P	A>>P	A>>P	R>>L	A>>P	A>>P
TE (ms)	2.9	91	91.6	4.92; 7.38	30	4.92; 7.38
TR (ms)	2200	6900	7000	688	11340	688
Flip angle (°)	10	90/180/180	90/180/180	60	90	60
Acq Bandwidth (Hz/pix)	240	1578	1578	260	2264	259
Sequence specific comments	TI=900ms	1st run: 4 interleaved b=0; b=1000 s/mm^2 64 dir 2nd run: 5 interleaved b=0; b=1000 s/mm^2 64 dir (same 64 dir as 1st run) Parallel imaging acquisition (GRAPPA with iPAT factor 2)	3 non-zero b-values B=300 s/mm^2 8 dir B=700 s/mm^2 36 dir B=2000 s/mm^2 72 dir 13 interleaved b=0 Parallel imaging acquisition (GRAPPA with iPAT factor 2)		92 volumes in each run Parallel imaging acquisition (GRAPPA with iPAT factor 2)	
Total scan time	9min 23s	16min 29s	16min 32s	1 min 31s	35min 58s (2 runs 17min 59 s)	1min 53s

Table 5.2 MRI sequence parameters

MRI modality	Analysis technique	Chapter
Volumetric T1	Qualitative descriptive	8
	Brain, hippocampal and total intracranial volumes	8, 9
	Voxel based morphometry	9, 11
Diffusion weighted imaging	Tract based spatial statistics for DTI and NODDI	10
	ROI analysis for NODDI indices	10
Activation fMRI	Statistical parametric mapping	11

Table 5.3 MRI modalities and analyses used by chapter

3D volumetric T1-weighted

3D T1-weighted volumetric brain images were acquired using a sagittal 3-D magnetization prepared rapid gradient echo (MPRAGE) sequence[269] optimised to provide strong contrast between white matter and grey matter (repetition time/echo time = 2200/2.9ms, dimensions 256x 256x208, voxel size 1.1x1.1x1.1 mm).

All scans were reviewed by an experienced rater for overall quality and suitability for the analysis methods used. 3D T1 scans were specifically checked for blurring, image wrap around and contrast problems.

T1 scans were segmented and brain volumes calculated (see methods in Chapter 9) and used for voxel based morphometry (Chapter 9).

Diffusion-weighted MRI

Two identical Diffusion Weighted Imaging (DWI) acquisitions were performed using a single-shot, spin-echo echo planar imaging sequence (64 diffusion-weighted directions, b=1000 s/mm^2; 9 b=0 s/mm^2 images (referred to as 'b0' images); 55 slices; voxel size 2.5x2.5x2.5mm^3; TR/TE=6900/91ms; total acquisition time for both sequences=16:29 minutes). A three-shell diffusion sequence optimised for NODDI was acquired (64, 32, and 8 diffusion-weighted directions at b=2000, 700 and 300 s/mm^2; 14 b=0 images; 55

slices; voxel size 2.5x2.5x2.5mm^3; TR/TE=7000/92ms; total acquisition time=16:32 minutes). Both single-shell (DTI) and multi-shell (NODDI) diffusion weighted sequences utilised twice-refocused spin echo to minimise distortion effects from eddy-currents.

Visual review of diffusion imaging was performed for identification of poor quality images by checking for full brain coverage, inter-acquisition motion (using motion plots over the acquisition), sufficient correction of geometric distortion and slice-wise signal dropout (using correlation plots between adjacent slices).

Diffusion Tensor Imaging (DTI)

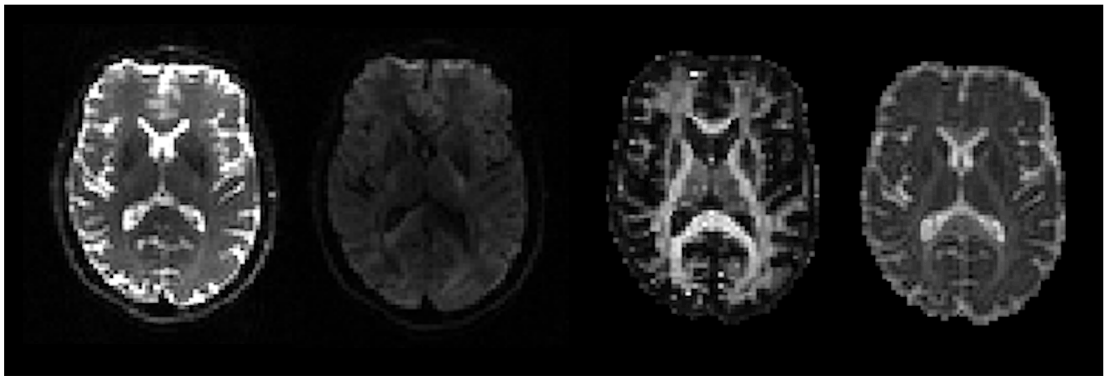

Neurite Orientation Dispersion and Density Imaging (NODDI)

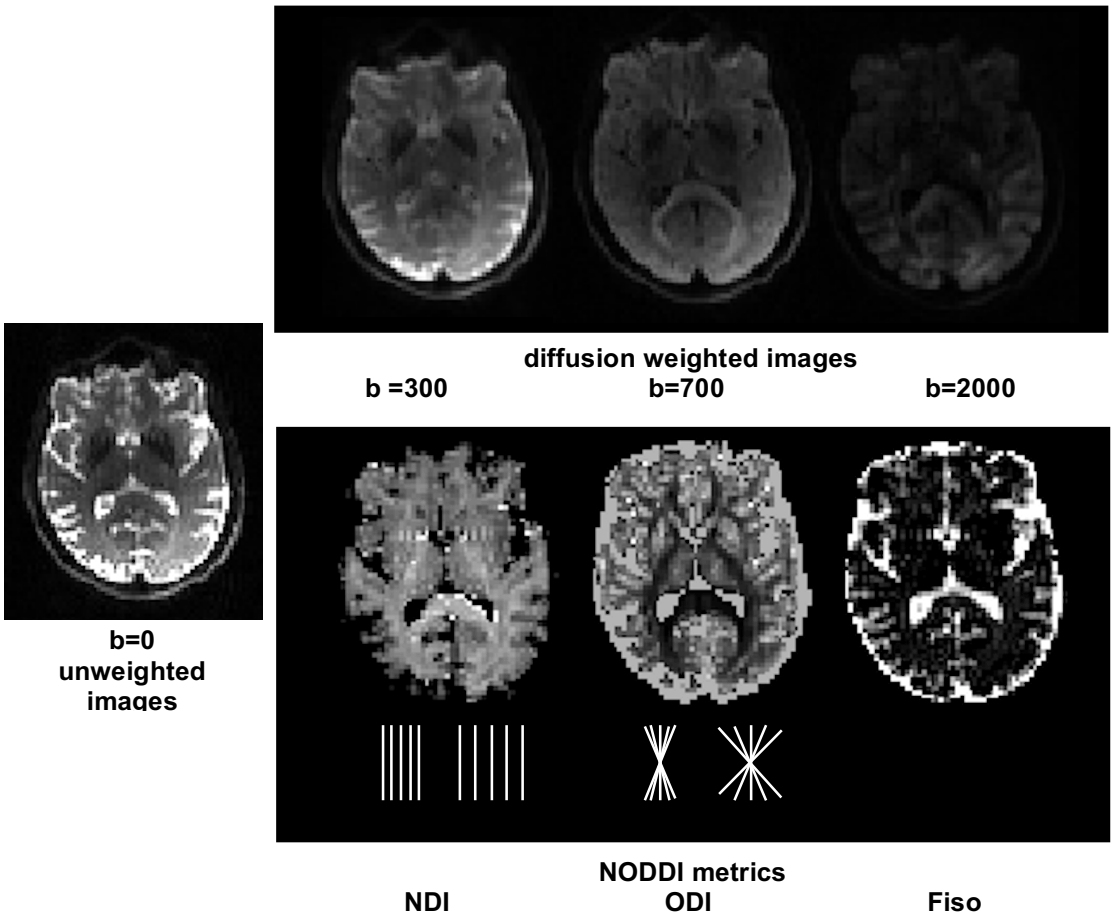

Figure 5.1 Representative diffusion images for diffusion weighted imaging (top panel) and neurite orientation dispersion and density imaging (lower panels).

Pre-processing involved correction for motion by rigidly registering each diffusion-weighted image to the first b0 image using FLIRT [270, 271]. Diffusion tensor volumes were spatially normalized with DTI-TK (http://dti-tk.sourceforge.net) which bootstraps a population-specific tensor template from the input tensor volumes and aligns them to the template in an iterative fashion [272] with a tensor-based registration algorithm[273]. This framework has been shown to improve white matter alignment compared to conventional FA-based registration [274]. DTI metrics (FA, AxD, RD) were estimated using FSL [275]. NODDI metrics (NDI, ODI, F_{iso}) were estimated using the NODDI Matlab toolbox (http://www.nitrc.org/projects/noddi_toolbox).

Activation functional MRI

MRI data were acquired on a 3T TIM Trio whole-body MRI scanner (Siemens Healthcare, Erlangen, Germany). 92 gradient-echo echo-planar image (GE-EPI) volumes were acquired in each run using a 12-channel RF receive head and body transmit coil in sparse (TR 11.3 seconds) acquisition mode (to reduce any interaction between scanner acoustic noise and auditory stimulus presentations). Each EPI volume comprised 48 oblique transverse slices with slice thickness 2mm, inter-slice gap 1mm and 2x2mm in-plane resolution (TR/TE=11340/30ms; echo spacing=0.69ms; matrix size=96x96 pixels; FoV=192x192mm, GRAPPA factor 2 in anterior-posterior phase encoding direction). The initial two brain volumes were discarded to allow for equilibrium of longitudinal T1 magnetization. B0 field-maps were acquired using two gradient echo sequences (TR=688ms; TE1/TE2=4.92/7.38ms, 3x3x3mm resolution, no inter-slice gap; matrix size=80x80pixels; FoV=192x192mm; phase encoding anterior-posterior) to allow correction of field inhomogeneity.

Visual review of fMRI acquisitions was performed for identification of poor quality images

Data from the fMRI experiment were pre-processed using SPM8. In brief, scans for each participant were realigned using the first image as a reference, and un-warped incorporating field-map distortion information. DARTEL processing was used to spatially normalise individual scans to a group mean template image in MNI space. Normalised images were smoothed using a Gaussian smoothing kernel 6mm full-width at half-maximum.

Pre-processed images were entered into a first-level and second-level design matrices to assess effects of specific contrasts within and between participant groups (see Chapter 11 for more detail of experimental conditions and contrasts).

5.1.5 Correction for multiple comparisons

Conducting a large number of voxel-wise t-tests in SPM or FSL creates a risk of type 1 error. Family-wise error correction was used to account for these multiple comparisons, either across the whole brain or in study-specific predefined small volumes in the VBM and activation FMRI analyses.

Threshold free cluster enhancement (TFCE) was used in the diffusion imaging analyses.

5.1.6 Statistical analyses

STATA version 12 (Stata Corporation, College Station, Texas, 2003) was used to perform standard parametric and non-parametric tests to investigate basic linear regression and test between group differences for demographics and neuropsychological data.

5.1.7 Data storage

Study data was stored electronically on a secure password protected database on a UCL secure server protected by comprehensive firewalls.

Hard copy study data was securely stored within the Dementia Research Centre.

Personal identifying details were removed from MRI scans and replaced with a unique study ID. All brain imaging was then uploaded to a customised open source imaging informatics software platform (www.xnat.org) hosted on the Dementia Research Centre secure servers.

The YOAD study was registered with the UCL Data Protection Office. All personal information was safeguarded in accordance with the UCLH NHS Trust Information Governance policy and the Data Protection Act (1998).

5.2 Other genetic cohorts

In order to investigate other genetic risk factors with rare or with a small effect, a larger University College London Department of Neurodegenerative disease genetic cohort was used in Chapter 8 sourced from multiple sites and studies.

5.2.1 Participants

Alzheimer's disease (n=1002) and FTD (n=358) cases were recruited via tertiary specialist clinics at the National Hospital for Neurology and Neurosurgery, London. Clinical diagnoses of Alzheimer's disease and FTD were supported by participation in longitudinal research studies at University College London and the University of Cambridge, however as these sample collections were acquired over two decades the comprehensive use of research diagnostic criteria cannot be confirmed and some samples were assigned to these diagnostic categories based on clinical diagnoses only.

All patients of known non-white ethnicity were excluded. Individuals known to have pathogenic disease-causing variants in the amyloid precursor protein, *APP*; Presenillin

1, *PSEN1*; Presenillin 2, *PSEN2*; prion protein, *PRNP*, chromosome 9 open reading frame 72, *C9orf72*; microtubule associated protein tau, *MAPT*; or progranulin, PGRN genes were excluded although the entire sample collection was only partially screened for mutations in these genes.

Control samples were obtained from the Human Random Control panel (European Collection of Cell Cultures *n=534)* and the UK 1958 Birth cohort (n=2381) (University of Leicester).

5.2.2 Consent and Ethical Considerations

All participants gave written informed consent at the recruiting centre.

5.3 Techniques for investigating genetic heterogeneity

5.3.1 Sanger sequencing

Sanger sequencing[276] is based on the selective incorporation of chain-terminating dideoxynucleotides by DNA polymerase during in vitro DNA replication, and useful for sequencing single genes (e.g. in Chapter 8 looking for *TREM2* variants in patient cohorts)

The method requires a single-stranded DNA template (to be sequenced), a short DNA primer complementary to the template DNA, DNA polymerase, standard deoxynucleosidetriphosphates (dNTPs), and modified di-deoxynucleotidetriphosphates (ddNTPs) which terminate DNA strand elongation and may be radioactively or fluorescently labelled. After many rounds of template DNA extension there are DNA fragments terminated by labelled ddNTPs of many different lengths. The DNA fragments are heat denatured and separated by size using gel electrophoresis in a DNA sequencer. The fragments migrate according to size and each is detected as it passes a laser beam

at the bottom of the gel. Each type of labelled ddNTP emits coloured light of a characteristic wave length and is recorded as a coloured band on a simulated gel image. This is then interpreted by a computer program to output an electrophergram with each coloured peak representing each letter in the sequence. Variants in the sequence can then be identified.

5.3.2 Next generation sequencing

Next-generation sequencing (NGS), or 'high-throughput sequencing', is the term used to describe a number of different modern sequencing technologies that allow longer DNA and RNA templates to be sequenced much more quickly and cheaply than Sanger sequencing.

In contrast to Sanger Sequencing, Ion torrent NGS (as used in Chapter 7) does not use optical signals. Instead, the method utilises the fact that addition of a dNTP to a DNA polymer releases an H^+ ion. The DNA sequencing machine records tiny changes in pH to determine which bases have been added at each point in the template replication.

6 Recruitment to the YOAD study

6.1 Introduction

The aim of this work described in this Chapter was to recruit 50 patients with young onset sporadic Alzheimer's disease and 25 controls, and to define this cohort in detail using a range of clinical measures, standardised batteries and neuropsychological testing.

6.2 Methods

Detailed methods including inclusion and exclusion criteria, clinical and neurological assessments are described in Chapter 5.

6.3 Results

In total, 45 patients with young onset Alzheimer's disease and 24 controls were recruited over a two-year period. One additional patient and one additional control were assessed but did not take participate further as they were unable to tolerate the first MRI scan due to claustrophobia. Recruitment was closed at this point to allow sufficient time for analysis of data during the lifetime of this PhD.

6.3.1 Clinical characteristics

Baseline clinical characteristics of each participant are shown in appendix 1.

6.3.1.1 All Participants

Age

The mean age at entry to the study was 60.6 (SD 5.8; range 48.8-68.1) years for controls and 61.7 (SD 5.1; range 51.8-73.8) years for patients with young onset Alzheimer's disease (no significant difference).

Sex

Of the 24 controls, 11 (48%) were male, and of the 45 patients, 20 (44%) were male (no significant difference).

Handedness

There was no significant difference in the rate of left-handedness between the groups; 3/24 (13%) controls were left-handed, compared with 2/45 (4%) of patients (p=0.47, Fisher's exact test).

Education

Both groups had a high level of education, with 15/24 (63%) controls and 20/45 (44%) patients having a university degree; controls had a mean of 16.7 (SD 3.0, range 11-22) years of education, and patients with YOAD a mean of 15.1 (SD 2.9, range 10-20), p=0.05 (t-test).

Employment

The majority of controls were in full time employment (18/24, 75%), whereas the majority of patients were not (5/45, 11% employed) p<0.0001 (Fisher's exact test). The patients still in work were all under 65 years and tended to be in self-employed roles (freelance journalist, socialist party treasurer, partner in the family business, shop owner, priest).

Smoking

Of the controls, 15/24 (63%) were life-long non-smokers. There was no significant difference with the YOAD cohort: 29/45 (64%) (p=1.00, Fisher's exact test).

Alcohol consumption

More controls than patients exceeded the recommended weekly alcohol consumption (≥14 units per week): male participants - 7/11 (64%) controls vs 7/20 (35%) patients, p=0.15; female participants - 6/13 (46%) controls vs 3/25 (12%) patients, p=0.04.

Medical comorbidities

There were no significant differences between controls and patients (cardiac disease, p=0.12; head injury, p=0.73; stroke, p=1.00; diabetes mellitus, p=0.61; psychiatric diagnoses, p=1.0; hypertension, p=0.50; hypercholesterolaemia, p=0.09; all Fisher's exact test).

Cognitive symptoms

Controls reported no or very mild symptoms in all domains apart from 3 individuals who reported mild depression, 2 individuals with mild anxiety and 1 with moderate anxiety. As expected, patients with YOAD had a wide range of cognitive symptoms; and higher level of anxiety, apathy and depression (Table 6.1)

Symptom	Absent		Very mild		Mild		Moderate		Severe	
	n	(%)	n	%	n	%	n	%	n	%
Controls										
Cognitive										
Memory impairment	19	(79)	5	(21)	0	(0)	0	(0)	0	(0)
Language impairment	23	(96)	1	(4)	0	(0)	0	(0)	0	(0)
Behavioural										
Apathy	21	(88)	3	(12)	0	(0)	0	(0)	0	(0)
Neuropsychiatric										
Depression	17	(71)	4	(17)	3	(12)	0	(0)	0	(0)
Anxiety	16	(67)	5	(21)	2	(8)	1	(4)	0	(0)
Motor										
Tremor	23	(96)	1	(4)	0	(0)	0	(0)	0	(0)
Slowness	23	(96)	1	(4)	0	(0)	0	(0)	0	(0)
Weakness	22	(92)	2	(8)	0	(0)	0	(0)	0	(0)
YOAD patients										
Cognitive										
Memory impairment	4	(9)	1	(2)	14	(31)	18	(40)	8	(18)
Language impairment	15	(33)	2	(4)	8	(18)	17	(38)	3	(7)
Visuoperceptual/ visuospatial	9	(20)	2	(4)	9	(20)	19	(42)	15	(33)
Dyspraxia	22	(49)	5	(11)	6	(13)	7	(16)	5	(11)
Impaired judgement/ problem solving	11	(24)	2	(4)	6	(13)	17	(38)	8	(18)
Impaired attention/ concentration	6	(13)	5	(11)	13	(29)	15	(33)	6	(13)
Behavioural										
Disinhibition	36	(80)	2	(4)	2	(4)	3	(7)	1	(2)
Apathy	16	(36)	5	(11)	14	(31)	7	(16)	3	(7)
Loss of sympathy/ empathy	34	(76)	3	(7)	2	(4)	1	(2)	4	(9)
Ritualistic/ compulsive behaviour	32	(71)	3	(7)	6	(13)	1	(2)	2	(4)
Hyperorality/ appetite changes	34	(76)	3	(7)	5	(11)	2	(4)	0	(0)
Neuropsychiatric										
Visual hallucinations	40	(89)	3	(7)	0	(0)	2	(4)	0	(0)
Auditory hallucinations	44	(98)	1	(2)	0	(0)	0	(0)	0	(0)
Tactile hallucinations	44	(98)	1	(2)	0	(0)	0	(0)	0	(0)
Delusions	44	(98)	1	(2)	0	(0)	0	(0)	0	(0)
Depression	25	(56)	7	(16)	8	(18)	4	(9)	1	(2)
Anxiety	17	(38)	6	(13)	8	(18)	10	(22)	4	(9)
Motor										
Dysarthria	35	(78)	4	(9)	3	(7)	3	(7)	0	(0)
Tremor	41	(91)	2	(4)	1	(2)	1	(2)	0	(0)
Slowness	40	(89)	0	(0)	2	(4)	3	(7)	0	(0)
Weakness	44	(98)	0	(0)	1	(2)	0	(0)	0	(0)
Gait disorder	42	(93)	1	(2)	1	(2)	1	(2)	0	(0)
Falls	41	(91)	2	(4)	2	(4)	0	(0)	0	(0)

Table 6.1 Reported cognitive, behavioural, neuropsychiatric and motor symptoms in YOAD study participants

Mini Mental State Examination (MMSE, maximum score 30)

Controls had a mean MMSE score of 29.5 (SD 0.7, range 28-30); patients with YOAD had a mean MMSE score of 21.5 (SD 4.6, range 13-29); the difference (as expected) was highly significant ($p<0.0001$, t-test). Within the patient group, 18 individuals scored between 10/30 and 20/30 indicating moderate dementia (within this group, 2 individuals had moderately severe dementia, scoring between 10-14/30), 16 individuals scored between 21/30 and 16/30 indicating mild dementia [277]. There were 9 individuals who scored between 27/30 and 29/30 which would be classified as a 'normal' MMSE score, but these individuals fulfilled research criteria for Alzheimer's disease [117] so were included.

No individual scored less than 12/30, as per the study inclusion criteria.

Neurological signs

Neurological signs in patients and controls are shown in Table 6.2. The commonest neurological findings in patients were visual extinction (10/45, 22%), optic ataxia (9/45, 20%), and postural tremor (8/45, 18%), all of which were significantly different to the frequency observed in the control group ($p=0.01$, $p=0.02$ and $p=0.04$ respectively, Fisher's exact test).

One control had an eye movement abnormality (broken smooth pursuit) and one control had brisk upper limb reflexes, but no other upper motor neuron signs

	Control n=24		YOAD n=45		P
	n	(%)	n	(%)	
Field defect	0	(0)	5	(11)	0.16
Optic ataxia	0	(0)	9	(20)	**0.02**
Visual extinction	0	(0)	10	(22)	**0.01**
Eye movement abnormality	1	(4)	6	(13)	0.41
Myoclonus	0	(0)	5	(11)	0.16
Rest tremor	0	(0)	0	(0)	n/a
Postural tremor	0	(0)	8	(18)	**0.04**
Bradykinesia	0	(0)	1	(2)	1.00
Ataxia	0	(0)	3	(7)	0.55
Dystonia	0	(0)	0	(0)	n/a
UL spasticity	0	(0)	0	(0)	n/a
LL spasticity	0	(0)	1	(2)	1.00
UL hyper-reflexia	1	(4)	4	(9)	0.65
LL hyper-reflexia	0	(0)	2	(4)	0.54
Up-going plantars	0	(0)	0	(0)	n/a
Abnormal gait	0	(0)	0	(0)	n/a

Table 6.2 Neurological signs in YOAD study participants

Apraxia

All 24 controls scored 50/50 on the apraxia score (right upper limb, left upper limb and orofacial). Patients were significantly impaired relative to controls on apraxia scores of the right upper limb (mean 48.5, SD 2.5, range 40-50, p=0.0002), left upper limb (mean 48.1, SD 3.3, range 34-50, p=0.0001), and for orofacial movements (mean 49.2, SD 1.8, range 42-50, p=0.009), (Wilcoxon rank sum).

Blood pressure

Blood pressure was recorded for and 24 controls and 44 patients. There were no significant groups differences in mean lying systolic (p=0.4), diastolic blood pressure (p=0.2), or mean arterial pressure (diastolic + 1/3 (systolic – diastolic)) (p=0.3, all t tests). The observation there is no excess hypertension in the patient group supports there being no excess cardiovascular disease.

	n	Mean systolic BP mmHg	Mean diastolic BP mmHg	Mean Arterial Pressure mmHg
Controls	24	138 (26)	76 (11)	97 (15)
Patients	44	134 (19)	73 (11)	93 (13)

Table 6.3 Blood pressure of study participants

Body mass index

Body mass index (BMI) was recorded for 24 controls and 44 patients. The mean for controls was 27.6 (SD 4.4, range 21.8-36.2), and for the patients 25.2 (SD 3.9, range 18.9-36.8). Patients had significantly lower BMIs than controls (p=0.03, t-test).

6.3.1.2 Patients

The following information was collected only for the patient group.

Age at clinical disease onset

The mean age of symptom onset, as reported retrospectively by the patient and corroborated by their consultee, was 56 yrs (SD 4.7, range 42-64).

Years of symptoms

The mean clinical disease duration (i.e. time elapsed between age of clinical symptom onset and recruitment to the study) was 5.7 (SD 2.9, range 1.5-14.5) years. The individual with the longest disease duration was a 70 year old female who experienced visuospatial and visuoperceptual difficulties from age 56 years and had a PCA phenotype. She was *APOE* ε3ε4 genotype and scored 22/30 on the MMSE at entry to the study.

Modified Hachinski ischaemic score

No YOAD participant had significant vascular risk: 3/45 (7%) had a score of 0; 19/45 (42%) had a score of 1; 15/45 (33%) had a score of 2; 5/45 (11%) had a score of 3; and 3/45 (7%) had a score of 4.

Cerebrospinal fluid

35/45 (78%) patients recruited had clinical CSF samples done prior to recruitment to the study. An additional 5 participants had CSF taken as part of the YOAD study. Of these patients only one patient had a clinical CSF sample that did not have a raised tau:Aβ1-42 ratio (Aβ1-42 511 pg/ml, tau 203 pg/ml, tau:Aβ1-42 ratio 0.40). She presented with a phenotype clinically consistent with Alzheimer's disease: her first reported symptom was dyscalculia, neuropsychology showed memory, naming, executive, speed and attention deficits, and there was bilateral hippocampal atrophy on her clinical MRI scan. Her Aβ1-42 was low (i.e. in keeping with Ab deposition in the brain) for someone aged 62 years, but her tau was not raised. The referring clinician and study PI confirmed that this was consistent with Alzheimer's disease.

Leading symptom

The most common leading symptom, as retrospectively reported by the patient and their consultee was memory problems (24/45, 53%). Other leading symptoms were higher visual problems (12/45, 27%), language impairment (3/45, 7%), difficulty with manual dexterity (2/45, 4%) and impaired judgement and/or problem solving (2/45 4%). For two patients (4%), memory problems and impaired judgement and problem solving were reported to have started simultaneously.

Phenotype according to research criteria

28/45 (63%) patients met criteria for typical amnestic Alzheimer's disease, and the remaining 17 (38%) had an atypical presentation: 14 (31%) met criteria for posterior cortical atrophy, 2 (4%) had a primary progressive aphasia, and 1 (2%) had a behavioural / dysexecutive syndrome.

6.3.2 Neuropsychology

As expected, there were significant differences between the number of patients and controls individuals performing at or below the 5% centile relative to published norms in the following cognitive domains: episodic memory, working memory, word retrieval, calculation, visuospatial and visuoperceptual function, and executive and speed of information processing. These are illustrated in Table 6.4.

	Controls				YOAD				P†
	n	Mean (SD)	(< 5% centile) n	(%)	n	Mean (SD)	(< 5% centile) n	(%)	
Episodic Memory									
RMT – words (/25)	24	24 (1)	1	(4)	44	18 (4)	30	(68)	<0.0001
RMT – faces (/25)	24	25 (1)	0	(0)	45	20 (4)	12	(27)	0.006
Camden Paired Associates learning (/24)	24	20 (3)	0	(0)	44	5 (6)	27	(61)	<0.0001
Working memory									
WMS-R Digit Span Forwards (/12)	24	9 (2)	0	(0)	45	6 (3)	13	(29)	0.003
WMS-R Digit Span Backwards (/12)	24	8 (1)	0	(0)	44	4 (2)	12	(27)	0.006
Word Retrieval									
Graded naming test (/30)	24	25 (4)	1	(4)	45	16 (9)	17	(38)	0.003
Calculation									
Graded arithmetic test (oral) (/24)	24	14 (7)	2	(8)	43	3 (5)	28	(65)	<0.0001
Spelling									
Graded difficulty spelling test (oral) (/30)	24	26 (4)	0	(0)	43	14 (9)	6	(14)	0.08
Visuospatial and visuoperceptual performance									
VOSP – object decision (/20)	24	18 (1)	0	(0)	45	14 (4)	16	(36)	0.0006
VOSP figure ground discrimination (/20)	23	19 (1)	4	(17)	42	18 (2)	22	(52)	0.008
VOSP dot counting (/10)	24	10 (0)	0	(0)	42	7 (3)	19	(45)	<0.0001
VOSP fragmented letters (/20)	23	20 (1)	0	(0)	42	11 (7)	28	(67)	<0.0001
Executive and speed of information processing									
Category fluency (animals, n)	24	23 (5)	0	(0)	44	11 (5)	29	(66)	<0.0001
WAIS-R Digit Symbol (n)	24	54 (11)	1	(4)	41	14 (16)	36	(88)	<0.0001
A Cancellation (s)	24	21 (6)	1	(4)	42	52 (25)	35	(83)	<0.0001

Table 6.4 Neuropsychological characteristics of YOAD study participant groups

Mean (standard deviation) values show raw data; maximum scores on neuropsychological tests are given in parentheses. † Fisher's exact test.

6.3.3 Symptomatic treatment for Alzheimer's disease

All but one of the patients (44/45, 98%) was on a symptomatic treatment for Alzheimer's disease (40 on a cholinesterase inhibitor, one on memantine, three on dual cholinesterase inhibitor and memantine).

6.4 Discussion

The patient and control cohorts recruited were well matched for the key demographics, with comparable and non-significant differences in age, sex-ratios, handedness, blood pressure, smoking history and levels of educations. However, as expected there were clear differences in performances on tests of cognition, with the patient group performing less well on both the screening MMSE and on a wide range of formal neuropsychological tests.

Both the control group and patient groups recruited were highly educated. This is consistent with other studies run locally through the Dementia Research Centre, and perhaps reflects high-functioning individuals (or those with high-functioning spouses) being motivated to find research studies to participate in. There was a trend towards the patients having a slightly lower number of years of education, which could be seen to be consistent with epidemiological studies that report higher levels of education being associated with a lower risk of developing dementia, perhaps through increased cognitive reserve [52].

As previously discussed, a definitive diagnosis of Alzheimer's disease is not possible without histopathological confirmation. Diagnosis in life therefore relies on the use of diagnostic criteria, the most commonly and recently updated criteria used at the time this study was set up was the NIA-AA 2011 criteria for Probable Alzheimer's disease Dementia [117]. All patients recruited fulfilled criteria for 'probable Alzheimer's disease',

and the majority had biomarker evidence of underlying Alzheimer's disease pathology from cerebrospinal fluid analyses. Given the increasing emphasis on biomarker evidence of Alzheimer's disease in research criteria, it would have been ideal for all patient participants to have supporting molecular biomarker evidence, but some individuals did not wish to have a lumbar puncture and there was no access to amyloid PET imaging, so where individuals otherwise met criteria they were recruited.

Individuals with young onset Alzheimer's disease are, in general, less likely to have significant co-existent confounding vascular disease. No participants with known cerebrovascular disease were recruited, and indirect evidence from results on the Hachinski score support this in the YOAD cohort. No patient had a modified Hachinski ischaemic score >3; a cut-off over 4 has been demonstrated to improve the differentiation of Alzheimer's disease from vascular dementia[278].

Weight loss is a well-recognised and consistent manifestation of Alzheimer's disease [279] and the lower BMI observed our patients participants relative to controls is in keeping with this. It is likely that reduction in food intake (forgetting to eat or decreased interest in food), or increased catabolism is responsible for this, although in the absence of premorbid weight it is not possible to explore the relationship between weight loss and disease onset.

There was no evidence in this small sample for blood pressure in patients to be either higher or lower than that of controls. This is in keeping with previous reports as although midlife systolic hypertension is a risk factor for the development of late onset Alzheimer's disease [280], by the time of diagnosis the blood pressure is either normal or low. Blood pressure in the aetiology of YOAD in less well studied due to the relative rarity of the disease, but these data albeit in a small sample does not suggest that there is aetiological link.

Within the patient cohort, two thirds had an amnestic presentation, and the remaining had atypical presentations, with posterior cortical atrophy being the most common. This is broadly consistent with previous studies that have reported approximately 1/3 of young onset Alzheimer's disease patients having a variant presentation [159].

Patient participants had a mean MMSE score of 21/30, with a wide range from 13 to 29. The patient who scored 29 was an individual with PCA who had had very focal symptoms for 3 years. Despite scoring 29/30 he was sufficiently impaired on activities of daily living to justify inclusion as a participant with Alzheimer's disease.

The mean age of clinical disease onset in the patient cohort was 56 years, nearly a decade younger than that required to meet the criteria for 'young onset', with some very young individuals (youngest age 42 years at symptom onset). No individual had a family history to suggest an autosomal dominant cause, but it is important to screen for these mutations in young onset cases due to the possibility of censored family histories, potential non-paternity, or de novo mutations. This is addressed in Chapter 7.

This cohort is a representative sample of patients with sporadic YOAD with evidence for Alzheimer's disease pathology, absence of significant vascular disease, absence of autosomal dominant family history, and a representative range of phenotypes including amnestic, PCA, LPA and frontal Alzheimer's disease, paving the way for the investigation of phenotypic diversity in subsequent chapters.

7 Genetic heterogeneity in the YOAD cohort

7.1 Introduction

Factors initiating and potentiating selective vulnerability and differential expression of pathology across the brain in sporadic YOAD are likely to be driven, at least in part, by genetic influences. This chapter describes work that I undertook to screen for any autosomal dominant mutations in the YOAD cohort, and look at *APOE* alleles and how this relates to age at clinical disease onset, leading symptom and neuropsychology results.

7.2 Methods

7.2.1 Participants

Participants were recruited to the YOAD cohort as outlined in Chapter 5. In addition to the study consent, specific consent was obtained from participants to enter a further genetic study being run at the DRC. Twenty millilitres of blood were collected by venepuncture and DNA extracted using standard techniques. Whilst individual results were not given, patients were given the option to know if their participation in the research led to the development of a clinical genetic test for their condition.

Control subjects did not have genetic analyses performed.

7.2.2 Dementia Panel NGS

Acknowledging the diagnostic challenges presented by atypical Alzheimer's disease phenotypes, all patient participants underwent next generation sequencing for autosomal dominant causes of neurodegenerative disease.

An Ion Torrent Personnel Genome Machine (PGM) sequencer (Life Technologies Corporation, CA, USA) was used with Ampliseq PCR amplicon-based library preparation (Life Technologies) to sequence approximately 17.7Kb across 16 dementia related genes (variants in *PRNP, PSEN1, PSEN2, APP, GRN, MAPT, TREM2, CHMP2B, CSF1R, FUS, ITM2B, NOTCH3, SERPINI1, TARDBP, TYROBP, VCP*)[281].

7.2.3 Sanger Sequencing

C9orf72 was Sanger sequenced to look for any pathological expansions, as this type of intronic expansion cannot be sequenced by the NGS dementia panel.

7.2.4 *APOE* ε4 status

APOE status for patient participants was ascertained by Minor Groove Binding probe and fluorescent polymerase chain reaction.

7.3 Results

7.3.1 Autosomal dominant variants

There were no pathological expansions in the C9orf72 gene in any members of the YOAD cohort. Three patients had variants identified in autosomal dominant genes known to cause neurodegenerative diseases (Table 7.1). These cases were all reviewed in the Dementia Research Centre neurogenetics multidisciplinary meeting. Neither the VCP nor the SQSTM1 variant had been previously reported, and on the basis of evolutionary conservation, predicted amino acid change and predicted possible impact of an amino acid substitution on the structure and function of the protein encoded [282] were not consider pathogenic. The PSEN1 variant was thought to be pathogenic (see 7.4 for details)

This individual found to have a pathogenic *PSEN1* variant had indicated on their consent form that they would not wish to be informed should a genetic cause for their dementia be identified. The other two individuals with non-pathogenic mutations were not notified of these findings as they are of no clinical significance.

Participant ID	*APOE* ε4 status	Variant	phenotype	AAO
01-037	34	PSEN1 Leu235Val	Memory led	52
01-004	34	VCP Pro137Ser	PCA	61
01-068	44	SQSTM1 Glu155Lys	LPA	56

Table 7.1 Variants identified in genes causing autosomal dominant Alzheimer's disease

7.3.2 *APOE* ε4 status

APOE genotyping was performed on all patient participants. 28/45 (62%) of patients had one or more ε4 allele (22 (49%) heterozygotes, 6 (13%) homozygotes). 6/45 (13%) possessed an ε2 allele. The individual with a PSEN1 variant was genotyped as ε3ε4 and was excluded from the analyses in the rest of this chapter.

Based on the allele frequency of the general population (ε2: 0.07; ε3: 0.79; ε4: 0.14; (meta-analysis http://www.alzgene.org/[28]), the expected frequency of each genotype was calculated and compared with that found in this patient cohort (Table 7.2). Patients with Alzheimer's disease were significantly less likely to have an E3E3 genotype than expected from population based results. Patients were significantly more likely to carry one or more ε4 alleles (ε2 ε4, ε3ε4 or ε4ε4 genotype) than expected (expected: 12/45, observed: 28/45, p=0.001).

Genotype	Expected frequency		Observed frequency		p[a]	Age at onset	
	n	(%)	n	(%)		Mean	(SD)
ε2ε2	0	(1)	0	(0)	-	-	-
ε2ε3	5	(12)	2	(4)	0.4	56.5	2.1
ε2ε4	1	(2)	4	(9)	0.4	57.5	2.4
ε3ε3	27	(61)	15	(33)	**0.02**	54.7	3.4
ε3ε4	10	(22)	17	(40)	0.2	55.4	5.3
ε4ε4	1	(2)	6	(13)	0.1	57.3	4.3

Table 7.2 Expected and observed *APOE* genotype and mean age at onset

[a] Fisher's exact test

7.3.2.1 APOE ε4 status and age at onset

Individuals with *APOE* ε3ε3 genotype had the earliest age of onset, with ε4 homozygotes having the latest age at onset (Table 7.2), despite ε4 being a major risk factor for developing Alzheimer's disease, and having been reported to reduce age at onset in late onset disease. Dividing the patient cohort into those with at least one ε4 allele (n=27) and those without (n=17) showed a similar directional but non-significant difference in age of onset (ε4–ve mean AAO 59.8 ± 3.8yrs, ε4+ve mean AAO 61.8 ± 5.0yrs, p=0.2 t test).

7.3.2.2 APOE ε4 and clinical phenotype

Memory impairment as a leading symptom was more common in individuals with at least one ε4 allele than those without: ε4+ve 18/27 (67%) vs ε4-ve 7/17 (41%), but this did not reach statistical significance (p=0.1, Fishers exact test). The majority of ε4-ve individuals (10/17, 59%) had non-amnestic presentations (language impairment, visuospatial or visuoperceptual, dyspraxia, executive impairment).

Phenotype according to research criteria was 9/17 (53%) typical amnestic Alzheimer's disease and 8/17 (47%) PCA in the ε4-ve group. Typical amnestic Alzheimer's disease represented a greater proportion of cases in the ε4+ve group: 18/27 (67%), with the remaining individuals having PCA (6/27, 22%), LPA (2/27, 7%) and frontal Alzheimer's disease (1/27, 4%). Of the 6 ε4 homozygotes, 4 had a typical amnestic presentation, 1 had a LPA phenotype and 1 had PCA.

There was no significant difference in neurological signs between the groups of individuals with and without an ε4 allele (Table 7.3), or in apraxia scores (ε4+ve mean 48.6 ± SD 2.4, ε4-ve 48.3 ± 2.5, p=0.6 Wilcoxon rank sum).

	ε4+ve n=27		**ε4-ve n=17**		**P†**
	n	**(%)**	**n**	**(%)**	
Field defect	3	11	2	12	1.0
Optic ataxia	5	19	4	24	0.7
Visual extinction	4	15	6	35	0.1
Eye movement abnormality	4	15	2	12	1.0
Myoclonus	3	11	2	12	1.0
Rest tremor	0	0	0	0	n/a
Postural tremor	4	15	4	24	0.7
Bradykinesia	1	4	0	0	1.0
Ataxia	3	11	0	0	0.3
Dystonia	0	0	0	0	n/a
UL spasticity	0	0	0	0	n/a
LL spasticity	0	0	1	6	0.4
UL hyper-reflexia	4	15	1	6	0.6
LL hyper-reflexia	2	7	0	0	0.5
Extensor plantars	0	0	0	0	n/a
Abnormal gait	0	0	0	0	n/a

Table 7.3 Neurological signs in YOAD cohort ε4+ve and ε4-ve individuals

† Fisher's exact test.

7.3.2.3 APOE ε4 status and neuropsychology profile

APOE ε4+ve individuals performed slightly better on the MMSE but this did not reach statistical significance (ε4+ve mean MMSE score 22/30 ± SD 4.7, ε4-ve 20/30 ± 4.5, p=0.2, Wilcoxon rank sum).

Neuropsychology results for YOAD patient participants by *APOE* ε4 status are show in Table 7.4. *APOE* ε4-ve individuals performed significantly less well than those with an ε4 allele on the digit symbol modalities test (DSMT) and the 'A' cancellation task, both of which reflect executive functioning. Poor performance on the 'A' cancellation test is indicated by taking a longer time to complete the task, this test is confounded by any co-existent visuospatial deficit impairing the 'visual search'. *APOE* ε4-ve individuals were also significantly more impaired on the written spelling task (GDST).

There was a trend for *APOE* ε4-ve individuals to perform significantly less well on the backward digit span (reflecting executive function and sequencing ability) and the shape detection and fragmented letters subtests of the visual object and space perception battery indicating inefficiency of higher visual processing by the parieto-occipital lobes.

Neuropsychological assessment	***APOE*ε4+ve Mean (SD)**	***APOE*ε4-ve Mean (SD)**	**P**
Episodic memory			
RMT words (short, /25)	18.7 (3.6)	18.2 (3.8)	0.68 [a]
RMT faces (short, /25)	18.9 (4.9)	20.5 (3.2)	0.22 [a]
Executive skills			
WASI matrices (/35)	11.1 (8.5)	7.4 (6.9)	0.14 [a]
WMS-R digit span forward (/12)	6.6 (2.7)	5.4 (2.3)	0.10 [a]
WMS-R digit span backwards (/12	4.4 (2.2)	3.1 (2.0)	0.05 [a]
DSMT (/93)	**22.9 (18.1)**	**10.0 (9.3)**	**0.01 [a]**
A cancellation (s)	**45.8 (22.7)**	**61 (20.7)**	**0.03 [a]**
Verbal skills			
NART (/50)	28.8 (13.8)	29.2 (9.7)	0.92 [a]
WASI vocabulary (/ 80)	53.4 (19.0)	51.7 (21.5)	0.80 [a]
GNT (/30)	16.7 (8.4)	14.6 (9.4)	0.46 [a]
Literacy and numeracy skills			
GDST written (/30)	**16.1 (8.4)**	**10.8 (7.0)**	**0.04 [a]**
GDST oral (/30)	15.5 (9.8)	11.4 (6.6)	0.11 [a]
GDA (/24)	4.0 (5.4)	1.9 (2.6)	0.23 [b]
Visuoperceptual skills			
VOSP object decision (/20)	14.9 (5.0)	13.8 (3.9)	0.44 [a]
VOSP shape detection (/20)	17.8 (4.1)	17.6 (1.3)	0.07 [b]
VOSP fragmented letters (/20)	13.2 (7.4)	8.8 (6.4)	0.05 [a]
VOSP dot counting (/10)	7.8 (2.8)	7.1 (3.5)	0.61 [b]

Table 7.4 Neuropsychological profiles of YOAD cohort patient participants by APOE ε4 status

Raw data are shown for neuropsychological tests (maximum scores in parentheses). Bold indicates significant difference in performance between patient groups ($p<0.05$).

[a] t test, [b] Wilcoxon rank sum.

7.4 Discussion

Only individuals without a family history suggesting autosomal dominant disease were recruited. However, one individual without a family history was found to harbour a PSEN1 variant. The PSEN1 variant identified (leu235val, rs63751130) is a missense point mutation in a coding region of exon 7 (Chr14:73659506 C>G) that results in a leucine being changed to a valine. This mutation has previously been reported in a UK family with 4 affected individuals with a mean age of onset at 52 years (range 44-59)[100], and the diagnosis has been confirmed post mortem in at least one case[283]. This L235V mutation has also been reported in a family from Mexico with a familial dementia, with age of onset around 48 years. Asymptomatic mutation carriers in this family had a higher incidence of depression than non-carriers, even when they did not know their mutation status, suggesting that depression may be an early clinical feature related to Alzheimer's disease pathology in this variant [284]. This association of L235V with depression has been explored in cell models using murine hippocampal cells suggesting that this variant in PSEN1 affects neurotransmitter metabolism through an interaction with mono-amine-oxidase-A, an enzyme that degrades serotonin and noradrenaline [285]. The individual carrying this variant in the YOAD cohort reported mild depression in the absence of any other psychiatric symptoms and was taking citalopram.

The individual with a pathogenic PSEN1 variant was excluded from the APOE analyses in this chapter, and has not been included in the VBM structural analysis (Chapter 9). However, the genetic results were not available at the time the DTI/NODDI (Chapter 10) and activation fMRI (Chapter 11) experiments were run, and so was included. The potential effect of including this individual is discussed further in the respective chapters.

Identifying novel variants of uncertain clinical significance, such as the SQSTM1 and VCP variants here described, is an increasingly common occurrence in both research and clinical genetic testing as genetic sequencing technology becomes increasingly sophisticated, accessible and inexpensive. However, predicting the significance of these variants and deciding what to do with this knowledge is challenging for researchers, clinicians and patients alike [286]. The genetic consent used in the YOAD study foresaw both the eventualities of variants of uncertain clinical significance, and identification of an (unexpected) autosomal dominant mutation. Participants were consented that they could chose at study entry whether they would want to be informed of clinically significant genetic results, and were informed that variants of no clinical significance would not be disclosed. The genetics multidisciplinary meeting was set up to discuss variants of uncertain significance to come to consensus opinion on the clinical relevance.

As expected, the *APOE* ε4 allele was over represented in the YOAD cohort relative to population data. However, individuals homozygous for ε4 did not have the youngest age of clinical disease onset, in keeping with previous observations that young onset Alzheimer's disease can also develop in the absence of an *APOE* ε4 allele and that individuals with one or two ε3 alleles may be even younger than ε4 carriers with early onset disease [196]. This suggests other genetic and/or environmental factors play a more significant role in young onset Alzheimer's disease.

There were no differences in neurological signs observed in the YOAD patient cohort. A larger cohort of 168 patients with YOAD has previously found that individuals carrying a ε4 allele were more likely to experience myoclonus and less likely to have tremor than individuals with a non-ε4 genotype [287]. A postural tremor was significantly associated with YOAD relative to controls (Table 6.2), but this was not present differentially between patient groups based on ε4 genotype. Perhaps the lack of difference in neurological

signs reported in this chapter reflects a smaller cohort being underpowered to detect subtle group differences.

A typical amnestic phenotype was more common in the group of individuals carrying an ε4 allele in the YOAD cohort although all 4 canonical phenotypes were represented, and variant AD presentations were more common in the ε4-ve cohort. This is consistent with previous studies which have consistently shown that patients who do not carry an *APOE* ε4 allele are more likely to present with a non-memory phenotype that those who do [160, 206, 288]. There was one individual in the YOAD cohort with a PCA phenotype who was homozygous for the ε4 allele. *APOE* is a risk factor for PCA, but a weaker risk factor than it is for more typical amnestic Alzheimer's disease [289].

There was no difference on neuropsychological tests of memory between ε4+ve and ε4-ve groups, although previous studies have shown carriers of the ε4 allele perform worse on memory tasks than non-carriers [197, 198]. *APOE* ε4-ve individuals were more impaired than ε4+ve individuals on neuropsychological tasks of executive function, speed, and literacy, with a trend to poorer performance on higher order visual processing tasks consistent with findings from several previous studies whereby ε4- patients were shown to be more impaired in non-memory cognitive domains [195, 288-290].

This chapter has demonstrated that *APOE* ε4 genotype may account for some of the observed heterogeneity in YOAD age of onset and cognitive profiles, but it cannot account for the full spectrum of phenotypic differences. Chapter 8 investigates another significant risk factor gene for Alzheimer's disease: the p.*R47H* variant of *TREM2* that was first identified whilst this PhD was being undertaken[39, 40]. Chapters 9 to 11 then explore the effect of *APOE* ε4 on macroscopic and microscopic brain structure in YOAD using brain volumes, voxel based morphometry, diffusion tensor imaging, and neurite orientation and dispersion imaging.

8 Rare genetic variants: *TREM2*

8.1 Introduction

In 2013, whole genome association analyses led to the identification of p.R47H (rs75932628), a rare variant in the triggering receptor expressed on myeloid cells 2 gene (*TREM2)* causing an arginine-47-histidine substitution in the extracellular immunoglobulin domain, as a significant risk factor for late onset Alzheimer's disease in two large cohorts of European descent [39, 40]. This variant increases the risk of developing Alzheimer's disease by two to three times, i.e. similar to that conferred by one copy of the *APOE* ε4 allele.

The associated phenotype of individuals with Alzheimer's disease carrying a p.R47H *TREM2* variant is relatively unknown. The presence of this variant has been associated with lower age of clinical disease onset: 3.18 years for individuals in an Icelandic population, and 3.65 years for those in at Dutch population[40]. The p.R47H *TREM2* has also been described as a risk factor specifically for young onset Alzheimer's disease [291].

The *TREM2* gene is located on chromosome 6p21.1 (chr6:41,126,244-41,130,924, hg19) and encodes a transmembrane receptor which is expressed on myeloid cells, including microglia and osteoclasts that participates in modulation of the immune system [292]. *TREM2* importance in brain function is also highlighted by its known involvement in other neurodegenerative diseases. p.R47H has since been associated with frontotemporal dementia (FTD) [293] and Parkinson's disease [293, 294]. Enrichment of other rare *TREM2* variants has also been observed in both individuals with Alzheimer's disease and FTD relative to controls [295, 296]. Polycystic lipomembranous osteodysplasia with sclerosing leukoencephalopathy (PLOSL), is a recessively inherited early onset frontal dementia with bone cysts and basal ganglia calcification [297, 298]

due to variants in either *TREM2* or *TYROBP* (TYRO protein tyrosine kinase binding protein) [37, 299, 300]. PLOSL associated homozygote *TREM2* variants (p.Q33X, p.T66M and p.Y38C) are also described in 3 individuals with typical cognitive impairment, white matter change and frontal atrophy, but without bone cysts [38]. Similar immune modulation is also proposed as pathological mechanism in other neurodegenerative diseases. Microglial proliferation and *CSF1R (*colony stimulating factor 1 receptor) activation, implicated in the same inflammatory pathway as the *TREM2*/*TYROBP* complex, are thought to be a major component of prion related neurodegeneration [301] and a partial loss of function variant in *CSF1R* causes hereditary diffuse leukoencephalopathy with spheroids [302]. Given that this microglial mediated inflammation is implicated in several dementias, p.R47H *TREM2* effects may be associated with neurodegeneration across multiple dementias.

In this chapter I aimed to examine the frequency of *TREM2* variants in an Alzheimer's disease cohort enriched for YOAD, comparing them to large a cohort of individuals with FTD, and to describe the clinical phenotype in individuals with p.R47H associated Alzheimer's disease.

8.2 Methods

8.2.1 Cohorts

8.2.1.1 YOAD cohort

Participants were recruited to the YOAD cohort as outlined in Chapter 5. In addition to the study consent, specific consent was obtained from participants to enter a further genetic study being run at the DRC. Twenty millilitres of blood were collected by venepuncture and DNA extracted using standard techniques. Whilst individual results were not given, patients were given the option to know if their participation in the research led to the development of a clinical genetic test for their condition.

Control subjects did not have genetic analyses performed.

8.2.1.2 DRC genetic cohort

DNA samples from individuals with clinical diagnoses of Alzheimer's disease (n=1002) and FTD (n=358), were identified from the Medical Research Council Prion Unit research sample database (1990 onwards). These individuals had been recruited via tertiary specialist clinics at the National Hospital for Neurology and Neurosurgery, London. Clinical diagnoses of Alzheimer's disease and FTD were supported by participation in longitudinal research studies at University College London and the University of Cambridge, however as these sample collections were acquired over two decades the comprehensive use of research diagnostic criteria cannot be confirmed and some samples were assigned to these diagnostic categories based on clinical diagnoses only.

All patients of known non-white ethnicity were excluded. Individuals known to have pathogenic disease-causing variants in the amyloid precursor protein, *APP*; Presenillin 1, *PSEN1*; Presenillin 2, *PSEN2*; prion protein, *PRNP*, chromosome 9 open reading frame 72, *C9orf72*; microtubule associated protein tau, *MAPT*; or progranulin, *PGRN* genes were excluded, although the entire sample collection was only partially screened for mutations in these genes.

Control samples were obtained from the Human Random Control panel (European Collection of Cell Cultures *n=534), and* the UK 1958 Birth cohort (n=2381) (University of Leicester).

8.2.2 Genetics

8.2.2.1 Sanger sequencing

Exon 2 of the *TREM2* gene was Sanger sequenced for individuals in the YOAD cohort who do not have any autosomal dominant mutations known to cause Alzheimer's disease (n=44), and from the DRC genetic cohort with Alzheimer's disease (n=971), FTD (n=358) and UK controls (n=534).

Polymerase-chain-reaction (PCR) amplification used 20ng of genomic DNA, 2xPCR MegaMix-Royal® (Microzone) and forward (5'-gaccatacgatgggttttcc3') and reverse (5'-ccgctcccaacttgtataagaa3') primers. PCR products were cleaned, and 5-20ng was sequenced in a reaction containing 5x Reaction Buffer, BigDye® (Applied Biosystems) and the forward primer. Sequencing reaction products were cleaned, and sequencing was performed on a 3730 DNA Analyzer (Applied Biosystems). Sequence traces were analysed using Seqscape software (version 2.7).

Genotyping

Controls from the UK 1958 Birth cohort (n=2381) (University of Leicester), were directly genotyped for p.R47H using a Taqman minor groove binding probe.
APOE status for cases of p.R47H variant associated Alzheimer's disease identified was ascertained by minor groove binding probe and fluorescent PCR.

8.2.3 Clinical phenotyping

To determine the clinical features of p.R47H Alzheimer's disease, I carried out a pseudo-case controls study. I established age at symptom onset (AAO), where available from the entire genetic cohort and reviewed medical records for p.R47H Alzheimer's cases (n=14) and a group of nil *TREM2* variant cases (n=33), matched for sex and age at

symptom onset (Table 8.1) to determine sex, annualised rates of decline on the mini-mental state examination (MMSE) based on the longest available interval, presenting clinical features (visual, language, behavioural/dysexecutive, memory), neurological and psychiatric signs and symptoms.

I extracted the following neuropsychometric data, where available from the clinical records: general intellectual function - Wechsler Adult Intelligence Scale-Revised or the Wechsler Abbreviated Scale of Intelligence [259, 303]; verbal and visual memory - Recognition Memory Test for words and faces respectively [260]; and visuospatial and visuoperceptual skills - Visual Object and Spatial Perception battery [266]. Raw scores were converted into percentiles for reporting.

Post mortem data reports for individuals with p.R47H variants held in the Queen Square brain bank (University College London) and Institute of Psychiatry brain bank (Kings College London) were also reviewed where available

		AD p.R47H variant	AD nil *TREM2* variants	P value
Leading symptom and neurological features	n	12	33	n/a
	M:F	5:7	9:24	0.47 [c]
	AAO (mean yrs ± SD yrs)	55.2 ± 8.5	56.1 ± 7.2	0.72 [a]
Rate MMSE decline	n	5	21	n/a
	M:F	2:3	9:12	1.0 [c]
	AAO (mean yrs ± SD yrs)	53.6 ± 6.5	56.6 ± 7.4	0.42 [a]
Volumetric imaging analysis	n	4	22	n/a
	M:F	3:1	7:15	0.26 [c]
	AAO (mean yrs ± SD yrs)	53.5 ± 4.8	56.0 ± 7.0	0.45 [b]
	Disease duration at time of scan (mean yrs±SD yrs)	5.0 ± 3.4	3.5 ± 2.3	0.33 [b]

Table 8.1 Demographics of age and sex matched p.R47H and nil TREM2 variant Alzheimer's disease cases

[a] P value calculated using T test for equal variance. [b] P values calculated using the Wilcoxon-Mann-Whitney test. [c] P values calculated using Fisher's exact test.

8.2.4 Imaging

T1 weighted volumetric brain MRI scans were reviewed retrospectively and volumetric region of interest comparisons performed for p.R47H variant individuals (3T n=3 and 1.5T n=1) and 22 AAO and disease duration matched Alzheimer's disease individuals with no *TREM2* variants (3T n=17, 1.5T n=5) (Table 8.1).

T1-weighted volumetric brain MRIs had been acquired using a Magnetization Prepared Rapid Gradient Echo sequence: 1.5T GE Signa scanner (General Electric Milwaukee, WI, USA) (256×256 matrix; 1.5mm slice thickness) and 3.0T Siemens Trio scanner (Siemens, Germany) (256×256 matrix; 1.1mm slice thickness).

MR images were corrected for intensity inhomogeneity using N3 [304, 305]. Whole brain volumes were generated using an automated segmentation technique (brain-MAPS) [306]. Hippocampi were delineated using the automated STEPS algorithm [307]. Both the brain regions and hippocampal regions were checked by experienced raters. Total intracranial volumes (TIV) were calculated by summing grey matter, white matter and cerebrospinal fluid volumes acquired using the new segmentation toolbox within Statistical Parametric Mapping – version 8 [308].

All analyses were performed blind to genetic status.

8.2.5 Statistics

The association between *TREM2* variants and each neurodegenerative condition was examined using odds ratios and Fisher exact test based on allelic frequencies.

The characteristics of the p.R47H variant and nil *TREM2* variant Alzheimer's disease cases were compared using two tailed T-tests or Wilcoxon-Mann-Whitney test where appropriate. Brain and total hippocampal volumes (expressed as ratio of TIV to correct

for head size) between p.R47H positive and *TREM2* negative Alzheimer's disease subjects were compared using the Wilcoxon-Mann-Whitney test.

All statistical tests were two-tailed, with significance set at $p<0.05$ without any correction for multiple hypothesis testing. Statistical analyses were performed using Stata (version 12).

8.3 Results

8.3.1 *TREM2* in YOAD cohort

There were no R47H variants identified in the YOAD cohort.

8.3.2 *TREM2* in DRC genetics cohort

TREM2 variants identified in exon 2 for Alzheimer's disease (n=1002) FTD (n=358) and UK controls (n=534) are show in Table 8.2.

There were fifteen non reference alleles causing p.R47H variants (13 heterozygote individuals and 1 homozygote) in the Alzheimer's disease population, and 2 in the FTD cohort. A number of other possible damaging variants were identified, including p.C51Y, p.D87N, p.T96K and A105V. Using the UK control cohort as a reference there were no *TREM2* variants significantly associated with disease.

Sanger Sequencing of Exon2						AD (n=971)		FTD (n=358)		Controls (n=534)	
Variant	SNP Number	Position†	Reference Allele	Minor allele	PolyPhen-2‡ ?damaging	No. non ref alleles	MAF	No. non ref alleles	MAF	No. non ref alleles	MAF
p.Q33R	n/a	41129296	A	G	Benign (0)	0	0.0000	1	0.0014	0	0.0000
p.D39E	rs200392967	41129275	G	C	Possibly (0.89)	1	0.0005	0	0.0000	1	0.0009
p.R47H	rs75932628	41129252	C	T	Probably (1.00)	15	0.0077	2	0.0028	5	0.0047
p.C51Y	n/a	41129264	G	A	Probably (1.00)	1	0.0005	0	0.0000	0	0.0000
p.R62H	rs143332484	41129207	C	T	Benign (0.02)	22	0.0113	8	0.0112	9	0.0084
p.R62C	n/a	41129208	G	A	Possibly (0.99)	1	0.0005	0	0.0000	0	0.0000
p.D87N	rs142232675	41129133	C	T	Probably (1.00)	0	0.0000	0	0.0000	1	0.0009
p.T96K	rs2234253	41129105	G	T	Probably (1.00)	8	0.0041	1	0.0014	1	0.0009
p.R98W	rs147564421	41129100	G	A	Probably (1.00)	1	0.0005	0	0.0000	1	0.0009
p.R98Q	n/a	41129099	C	T	Benign (0.02)	0	0.0000	0	0.0000	0	0.0000
p.A105V	rs145080901	41129078	G	A	Probably (1.00)	0	0.0000	0	0.0000	1	0.0009
Total						**49**		**12**		**19**	

Table 8.2 TREM2 coding variants identified using Sanger sequencing of exon 2

† Position denotes the location of the variant in base pairs in chromosome 6 (hg19). ‡ PolyPhen-2 refers to the pathogenicity prediction on Polymorphism Phenotyping, version 2. The numbers in brackets represent prediction scores ranging from 0 (benign) to 1 (damaging). The 15 non-reference alleles at 41129252 (R47H variant) in the AD cohort represent 13 heterozygote individuals and 1 homozygote individual. One further individual had two different variants (R62H and T96K).

Using a larger control cohort (n=534+2381) to calculate control minor allele frequencies there was an odds ratio of increased risk in Alzheimer's disease verses UK controls of 2.19 (95%CI=1.04-4.51, *P*=0.03) (Table 8.3), confirming the significant association demonstrated in previous studies [39, 40, 309-311]. There was no significant association for p.R47H with FTD.

	n	non reference alleles	MAF cases	MAF controls	OR	95% CI	P
AD	1002	15[†]	0.0075[†]	0.0034[†]	2.19	1.04-4.51	0.03 [a]
FTD	358	2[†]	0.0028[†]	0.0034[†]	0.81	0.09-3.36	1.00 [a]

Table 8.3 p.R47H TREM2 variants in Alzheimer's disease and frontotemporal dementia

MAF; minor allele frequency, OR; odds ratio, CI; confidence interval. MAF in cases were genotyped by Sanger Sequencing, MAF in controls were genotyped by Sanger Sequencing (n=534) or minor groove binding R47H probe (n=2381).[a] P values were calculated using 2 sided Fisher's exact test.

8.3.3 *TREM2* variants are associated with earlier disease onset in Alzheimer's disease

Age at disease onset was not available for all individuals in the genetic cohort, however where data was recorded individuals with p.R47H *TREM2* variants had significantly younger ages at onset than individuals with no *TREM2* variants (AAO=55.2±8.5yrs, n=12 vs. AAO=61.7±13.1yrs, n=551, P=0.024). 10/12 (83%) of these p.R47H variant individuals met criteria for YOAD, defined as symptom onset less than 65 years, with 4/12 (33%) of individuals having an age at onset <50 years, indicating very early onset disease.

8.3.4 R47H variants in Alzheimer's disease: clinical features and neuropsychological profiles

Disease duration (age from first reported symptom to death) was known for 6/14 individuals, for whom the mean was 11.3 years (range 7-15 years). 6/12 (50%) of the individuals with detailed clinical information had at least one first or second degree relative with a diagnosis of Alzheimer's disease. Case 1 (p.R47H homozygote) had a mother who developed Alzheimer's disease in her 70s who died in her 80s, and a brother with disease onset at 52 years, who died in his 60s. Their *TREM2* statuses are unknown.

The majority of p.R47H individuals (10/12, 83%) for whom clinical information was available had an amnestic presentation. This was supported by neuropsychology data, available on seven individuals (Table 8.4). The disease duration at time of testing varied from one to seven years. All cases had impairment (<5th percentile) on at least one recognition memory test at the time of testing. Three also had some evidence of visuospatial and/or visuoperceptual disturbance, but for no cases was this disproportionate to the degree of amnesia.

Anecdotally, none of the Alzheimer's disease p.R47H patients were reported to have had bone cysts or pathological fractures, but this was not examined or investigated for systematically.

Case	M/F	TREM2 R47H	Other gene variants	APOE	AAO (yrs)	DD (yrs)	Family history	Leading symptom	Neuropsychology						
									years since onset	*VIQ*	*PIQ*	*RMT-W*	*RMT-F*	*Visuo-Percept (VOSP)*	*Visuo spatia (VOS*
1	F	**homozygote**	nil	3 4	64	14	yes	frontal	-	-	-	-	-	-	-
2	F	heterozygote	nil	3 3	44	-	no	memory	3	86	77	<5	<5	-	-
3	M	heterozygote	nil	3 4	49	15	yes	memory	3	67	64	<5	<5	10-25	-
4	M	heterozygote	nil	3 3	49	-	no	memory	3	80	65	-	-	25-75	25-75
5	M	heterozygote	nil	3 3	54	-	yes	memory	4	55	63	<5	<5	<5	<5
6	M	heterozygote	nil	3 3	60	-	yes	memory	1	87	72	<5	10-25	<5	25-75
7	F	heterozygote	nil	3 4	71	8	yes	memory	-	-	-	-	-	-	-
8	F	heterozygote	nil	3 3	46	-	no	memory	-	-	-	-	-	-	-
9	M	heterozygote	nil	4 4	50	-	no	language	-	-	-	-	-	-	-
10	F	heterozygote	nil	4 4	51	15	no	memory	7	78	83	<5	<5	25-75	25-75
11	F	heterozygote	nil	3 3	59	7	yes	memory	4	-	-	<5	-	25-75	10-25
12	F	heterozygote	PS1 E318G	3 4	65	9	no	memory	5	73	62	<5	25-75	25-75	25-75
13	F	heterozygote	nil	-	unknown	-	unknown	unknown	-	-	-	-	-	-	-
14	F	heterozygote	nil	3 3	unknown	-	unknown	unknown	-	-	-	-	-	-	-

Table 8.4 Clinical features of Alzheimer's disease individuals with p.R47H variant

Positive family history denotes those with at least one secondary case of Alzheimer's disease diagnosed in a first or second degree relative; VIQ, verbal intelligence quotient; PIQ, performance intelligence quotient; RMT-W, Recognition Memory Test for words; RMT-F, Recognition Memory Test for faces; VOSP, Visual object and spatial perception battery. RMT and VOSP scores given as percentiles. '-' indicates no data available.

		AD p.R47H variant (n=12)		AD nil *TREM2* variant (n=33)		P value [a]
		n	**%**	**n**	**%**	
Leading symptom	memory	10	83.3	21	63.6	0.29
	language	1	8.3	1	3.0	0.47
	frontal	1	8.3	2	6.1	1.00
	parietal	0	0.0	9	27.3	0.09
Neurological signs	myoclonus	3	25.0	10	30.3	1.00
	seizures	2	16.7	2	6.1	0.29
	cerebellar signs	2	16.7	0	0.0	0.07
	extrapyramidal motor features	2	16.7	3	9.1	0.60
	pyramidal motor features	1	8.3	3	9.1	1.00
	dystonia	1	8.3	0	0.0	0.27
	hallucinations	1	8.3	3	9.1	1.00
	other psychiatric symptoms	1	8.3	12	36.4	0.13
	sleep disturbance	1	8.3	2	6.1	1.00
	dyspraxia	2	16.7	5	15.2	1.00

Table 8.5 Leading symptoms and neurological signs in AD patients by p.R47H genotype

[a] P values calculated using Fisher's exact test.

There was no significant difference in the annual rate of MMSE decline between the p.R47H variant (n=5) and nil *TREM2* variants (n=21) groups, albeit with small numbers (4.3 points/year ± 3.8 vs. 3.2 points/year ± 2.6 respectively, P=0.43). Most individuals in both the *TREM2* positive and negative variant groups had an amnestic presentation. No TREM2 p.R47H individual presented with cognitive deficits referable to parietal lobe dysfunction. (Table 3). There were no significant differences in neurological signs reported between the p.R47H variant positive (n=12) and nil *TREM2* variant (n=33) cases (Table 8.5).

8.3.5 Neuroimaging in p.R47H variants

MRI in the p.R47H cases (n=4) was typical for Alzheimer's disease, revealing generalised cerebral and symmetrical hippocampal atrophy (Figure 8.1). Other than case 10, who had participated in the AN1792 vaccination trial [312], none of the other individuals with neuroimaging had any white matter disease greater than would have been expected for age. No basal ganglia calcification was evident on any of the T1 sequences. Quantitative analysis of cross-sectional brain volumes revealed no difference in brain volume/TIV (median [IQR] = 0.69 [0.66-0.70] vs. 0.70 [0.66-0.73], p=0.40), or total hippocampal volume*1000/TIV (median [IQR] = 3.5 [3.2-3.6] vs. 3.3 [2.9-3.6], p=0.43), between p.R47H positive (n=4) and nil *TREM2* variant (n=22) Alzheimer's disease cases.

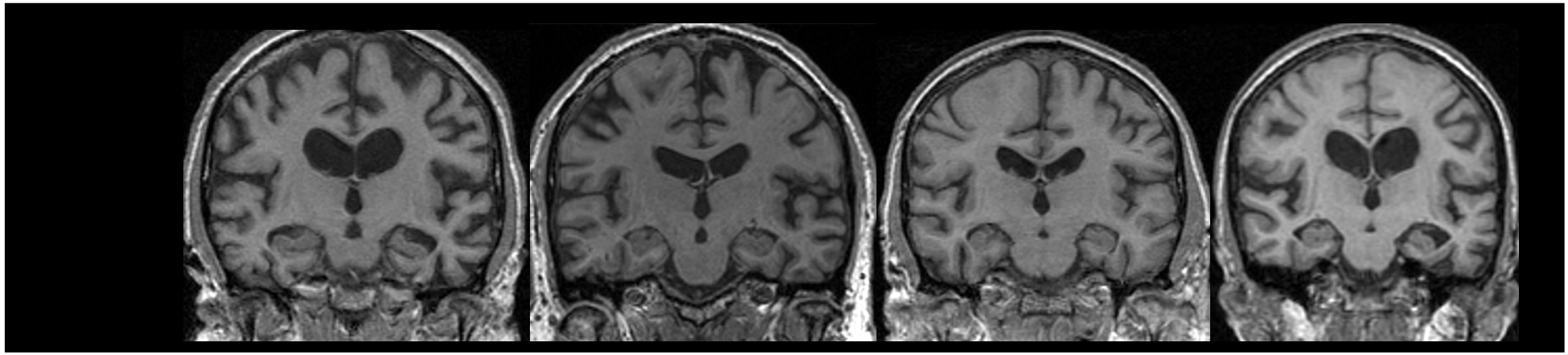

Case	4	5	6	10
Age at scan (yrs)	55	58	60	60
Disease duration (yrs)	6	4	1	9

Figure 8.1 Coronal MRI images in 4 individuals with Alzheimer's disease and p.R47H variant

Disease duration denotes time from first symptom to time of scan.

8.3.6 Pathology in p.R47H cases

Alzheimer's disease pathology was confirmed in all 4 p.R47H Alzheimer's disease individuals who had post mortem examination, and two had at least moderate cerebral amyloid angiopathy. Pathological slides for case 10, previously published elsewhere [39], showed mature diffuse amyloid plaques. Case 1 (p.R47H homozygote, behavioural/dysexecutive presentation) showed marked frontal atrophy macroscopically, as is typical in PLOSL cases [313], however the associated typical white matter lesions were absent. There was extensive formation of senile plaques, neurofibrillary tangles and neuropil threads throughout the grey matter, but relative preservation of the hippocampus histologically.

8.4 Discussion

This chapter reports a sequencing and genotyping survey of *TREM2* variants in a large cohort of individuals with Alzheimer's disease (including those from the YOAD study) and FTD. There a significant association for p.R47H with Alzheimer's disease, but not FTD. Several other exon 2 variants predicted to be damaging were identified: including p.C51Y, p.D87N, p.T96K and A105V. None of these were significantly associated with either Alzheimer's disease or FTD using the UK control cohort n=534. Of other *TREM2* variants only p.Arg62His has since shown genome wide association levels of significance independently of the p.R47H association [314].

Given that the frequency of R47H was around 1:70 it is arguably not surprising that there were no carriers of this variant in the YOAD patient cohort. Possession of a p.R47H *TREM2* variant in Alzheimer's disease is associated with a significantly younger age at symptom onset than nil *TREM2* variant cases, and p.R47H associated Alzheimer's

disease is otherwise usually indistinguishable from typical, amnestic Alzheimer's disease on clinical, imaging, and neuropsychometric grounds.

It remains unclear whether p.R47H is a risk factor for neurodegeneration in general, or is specific to Alzheimer's disease. This study did not find any evidence that p.R47H variants are associated with FTD. Whilst there were no p.R47H variants identified in either French (n=175) [315], or Spanish (n=628) [316] FTD populations, a North American cohort (n=609) found a significant association (OR=5.06, P=0.001) [293]. Data from this UK study was not consistent with an association as large as an OR=5, but does not rule out a more modest association between p.R47H and frontotemporal dementia (95% CI=0.09-3.36). Whether these differences reflect the underlying pathological heterogeneity of patients presenting with behavioural problems or population differences in risk remains to be determined and further studies are warranted, ideally with post mortem confirmation of the underlying pathology, or using other biomarkers (e.g. CSF tau and Aβ1-42, amyloid imaging) to improve the diagnostic certainty in life.

The majority of individuals with p.R47H had young onset Alzheimer's disease, with 4/12 of these cases identified having very young age at onset (<50yrs) in the absence of other known genetic variants, consistent with results from a French YOAD population showing p.R47H is a risk factor for young onset disease [311]. p.R47H has previously been found to correspond with earlier age of onset in both Icelandic (3.18 years, P=0.20) and Dutch populations (3.65 years, P=0.13) [40]. In this UK YOAD enriched Alzheimer's disease population the mean AAO for p.R47H variant Alzheimer's disease patients was *significantly* earlier than nil *TREM2* variant cases (6.5 years, P=0.024). In families with late onset Alzheimer's disease, carrying p.R47H did not affect the age of disease onset, however the disease duration was significantly shorter in individuals who carried the mutation that those who did not [317].

In the majority of cases, heterozygous p.R47H variants were associated with typical 'amnestic' Alzheimer's disease presentations. Whereas atypical presentations are more commonly seen in YOAD than late onset Alzheimer's disease, accounting for between 30-40% of cases [159, 318], these data suggest that, if anything, individuals with *TREM2* variants were less likely to have a non-memory presentation compared with other YOAD individuals. This p.R47H cohort had a mean disease duration fairly typical for sporadic Alzheimer's disease, rates of MMSE decline were within the published range [319, 320] and there were no specific neurological features that could reliably be useful in identifying p.R47H *TREM2* variants. A Spanish study examining a cohort of individuals with late onset Alzheimer's disease carrying p.R47H variants found more frequent apraxia, psychiatric symptoms (personality change, anxiety, paranoia) and parkinsonism than in individuals without the p.R47H variant, most notably in the first two years of clinically manifest disease [321]. Both of these studies have small numbers of p.R47H cases to report, so results must be considered preliminary, but it is possible that p.R47H variants modify phenotype differently in early and late onset disease.

Brain volume analysis revealed no differences between p.R47H carriers and non-carriers, which may reflect the small numbers in this study. Interestingly, data from ADNI has shown individuals with *TREM2* variants lose 1.4 to 3.3% more brain tissue per year than non-carriers, and p.R47H is significantly associated with smaller hippocampal volumes [322]. The individuals in the Spanish cohort with more apraxia and psychiatric symptoms had higher frontobasal grey-matter cortical loss [321].

All p.R47H Alzheimer's disease individuals with post mortem data available had Alzheimer's pathology confirmed, although the topography of atrophy seen in case 1, (p.R47H homozygote) was similar to the 'generalised cerebral gyral atrophy with frontal accentuation' pathologically observed in a case series of eight patients with PLOSL [313].

Due to the relative rarity of *TREM2* variants the numbers of individuals identified were small, and not all had post-mortem diagnostic confirmation. Statistical analyses were not corrected for multiple comparisons, so results should be considered exploratory. The retrospective nature meant clinical information was limited and collected in a non-standardised manner, hence limiting direct comparisons and inferences with respect to the whole cohort. Whilst very large multicentre prospective studies will be needed to establish the true spectrum of clinical features, neuroimaging and pathological signatures of *TREM2* variants in Alzheimer's disease, these findings suggest *p.R47H* confers specific risk for typical, amnestic and often very young onset Alzheimer's disease.

9 *APOE* and structural brain imaging: brain and grey matter volumes

9.1 Introduction

APOE genotype appears to exert regionally specific effects on brain atrophy. The first studies examining ε4 genotype and brain atrophy in late onset Alzheimer's disease found a dose-effect relationship between an increasing number of ε4 alleles and decreasing volume of the temporal lobe [200, 323]. They also suggested that possession of ε4 alleles was associated with increased whole brain volume, and hence that individuals with Alzheimer's disease who do not carry an ε4 allele have more marked generalised atrophy, which has been confirmed by several later studies [199, 201, 324].

It is possible that the modulating effect of *APOE* genotype on regional vulnerability varies by age at clinical disease onset. This chapter studies the disease associated grey matter atrophy in the YOAD cohort and investigates how *APOE* ε4 status affects regional brain atrophy in YOAD using hippocampal, ventricle and brain volumes, and voxel based morphometry.

9.2 Methods

9.2.1 Participants

This analyses in this chapter include the participants recruited into the YOAD study, as described in Chapter 5. All participants underwent MRI scanning and testing on the MMSE [108]. The individual with a pathogenic *PSEN1* variant was excluded from the analyses in this chapter.

9.2.2 *APOE* genotyoing

As per previous chapters, patient participants gave separate specific consent to donate blood for genetic analyses. DNA was extracted and *APOE* genotype was determined by PCR with 3'-minor groove binding probes.

9.2.3 Imaging acquisition

All imaging was acquired on a 3T TIM Trio whole-body MRI scanner (Siemens Healthcare, Erlangen, Germany) using a 32-channel phased-array head coil. T1-weighted volumetric brain images were acquired using a sagittal 3-D magnetization prepared rapid gradient echo sequence (repetition time/echo time = 2200/2.9ms, dimensions 256x 256x208, voxel size 1.1x1.1x1.1 mm).

Scans were assessed by experienced raters for quality control purposes, based on coverage and movement artefact.

9.2.4 Data analyses

9.2.4.1 Volumetric data

Raw MR images were pre-processed to correct for magnetic field bias (inhomogeneity) using a non-parametric non-uniform intensity normalization (N3) algorithm [304, 305].

Brains were automatically segmented using Multi-Atlas Propagation and Segmentation [306], followed by manual editing to give a brain region separated from dura and skill; i.e. a whole brain volume.

Ventricle and hippocampal analysis was carried out on images registered to standard space [325] using a rigid (6 degree of freedom, dof) transformation derived from 9dof registration. All region editing and volume measurements were carried out using the

Medical Information Display and Analysis (MIDAS) package [326]. Ventricle segmentation was performed in a semi-automated method (intensity thresholding, morphological operations and editing) using MIDAS. Hippocampal segmentation was performed automatically using STEPS [307] followed by manual editing using MIDAS.

9.2.4.2 Voxel based morphometry

Pre-processing of 3D T1 brain MRIs used the New Segment and DARTEL toolboxes [327, 328]. Normalisation, segmentation and modulation of grey and white matter images were performed using default parameter settings in statistical parametric mapping software (SPM12; http://www.fil.ion.ucl.ac.uk/spm) running under MATLAB 2012a, with a Gaussian smoothing kernel of 6mm full-width-at-half-maximum.

Total intracranial volume was calculated for each participant by summing grey matter, white matter and CSF volumes following segmentation of all three tissue classes and used to adjust for differences in participant head size during subsequent analyses.

The general linear model was applied at the level of each voxel using all images. Grey matter volume was modelled as a function of group and corrected for age, gender and total intracranial volume (TIV), included as nuisance covariates in the model.

Group differences were calculated using one-tailed t-tests (in both directions) between group parameter estimates for each group comparison. A mask was created based on the optimal threshold of the group average image, using the automatic mask creation strategy in the SPM toolbox [329]

Random field theory was used to correct for multiple comparisons, controlling the family-wise error (FWE) rate at a significance level of 0.05, unless otherwise stated.

In addition to the thresholded statistical parametric maps, differences in grey matter volume between groups that did not reach statistical significance are presented on effect maps (the t statistic for each contrast at each voxel is plotted without any threshold being applied) to provide more information about the patterns of cerebral atrophy associated with each group.

9.3 Results

40/44 patients and 21/24 control participants had scans that passed T1 quality control and are included in the analyses that follow. Those that failed were due to severe motion artefact, giving a failure rate of 11% for patients and 17% for controls. This is comparable to rates seen in other longitudinal studies running locally.

9.3.1 Demographics and clinical phenotypes

The groups included in these analyses, whilst not the full YOAD cohort, remained well matched based on sex, age, disease duration and MMSE score (Table 9.1).

	Controls	YOAD	ε4-ve	ε4+ve
n	21	40	16	24
Sex (M:F, %M)	8:13, 38	15:25, 38	6:10, 38	9:15, 38
Age (yrs)	60.3 (6.1)	61.9 (5.2)	60.5 (3.9)	62.8, (5.8)
Disease duration (yrs)	-	5.9 (3.0)	5.7 (2.7)	6.1 (3.2)
Phenotype (tAD:PCA:LPA:frontal)	-	26:12:1:1	9:7:0:0	17:5:1:1
MMSE (x/30)	29.4 (0.7)	21.4 (4.7)	20.1 (4.5)	22.3 (4.8)

Table 9.1 Demographics for YOAD study participants included in the grey matter atrophy analyses

Results are shown as mean (standard deviation) unless otherwise indicated.

9.3.2 Brain, ventricle and hippocampal volumes

Volumetric analyses showed that, as expected, there were significant differences between the patient and control group when considering brain, ventricle and hippocampal volumes, and the brain/total intracranial volume ratio (to correct for head size), but not TIV. However, none of these indices showed differences between *APOE* ε4+ve and ε4-ve groups (Table 9.2).

	Control n=21	YOAD n=40	P value	*APOE* ε4-ve n=16	*APOE* ε4+ve n=24	P [a]
Brain/TIV, mean (±SD)	0.75 (0.02)	0.69 (0.03)	<0.0001	0.68 (0.03)	0.69 (0.03)	0.5
Ventricles, mls, mean (±SD)	28.0 (13.6)	47.6 (21.5)	<0.0001	47.4 (23.7)	47.7 (20.4)	1.0
L hippocampus, mls, mean (±SD)	2.69 (0.2)	2.44 (0.4)	0.005	2.52 (0.4)	2.39 (0.5)	0.3
R hippocampus, mls, mean (±SD)	2.77 (0.3)	2.52 (0.4)	0.001	2.61 (0.4)	2.49 (0.4)	0.4
TIV, mls, mean (±SD)	1491 (141)	1504 (164)	0.73	1480 (135)	1521 (182)	0.4
Brain, mls, mean (±SD)	1121 (105)	1040 (124)	0.01	1017 (90)	1056 (142)	0.3

Table 9.2 Volumetric data for 40 YOAD patient participants and 21 controls

[a] unpaired T-test

9.3.3 Grey matter structural changes: VBM analyses

When the controls and patient cohorts were compared using VBM, there was a significant disease associated atrophy profile in the patient group affecting the hippocampi, posterior cingulate and precuneus and temporo-parietal lobes (Figure 9.1).

Relative to controls, ε4-ve individuals showed greatest atrophy in the right temporo-parietal junction, and ε4+ve individuals in the left inferior posterior temporal lobe (Figure 9.2). Comparing the ε4+ve and ε4-ve cohorts directly did not show any statistically significant differences in atrophy at the prescribed threshold. Uncorrected analyses confirmed that there was an area in the right parietal lobe where the ε4-ve group showed more atrophy that the ε4+ve. Examining effect maps for atrophy (where the T statistic for each contrast at each voxel is plotted without any threshold), ε4+ve patients show more atrophy in the medial temporal lobes, and ε4-ve individuals have more atrophy throughout the neocortex (Figure 9.3).

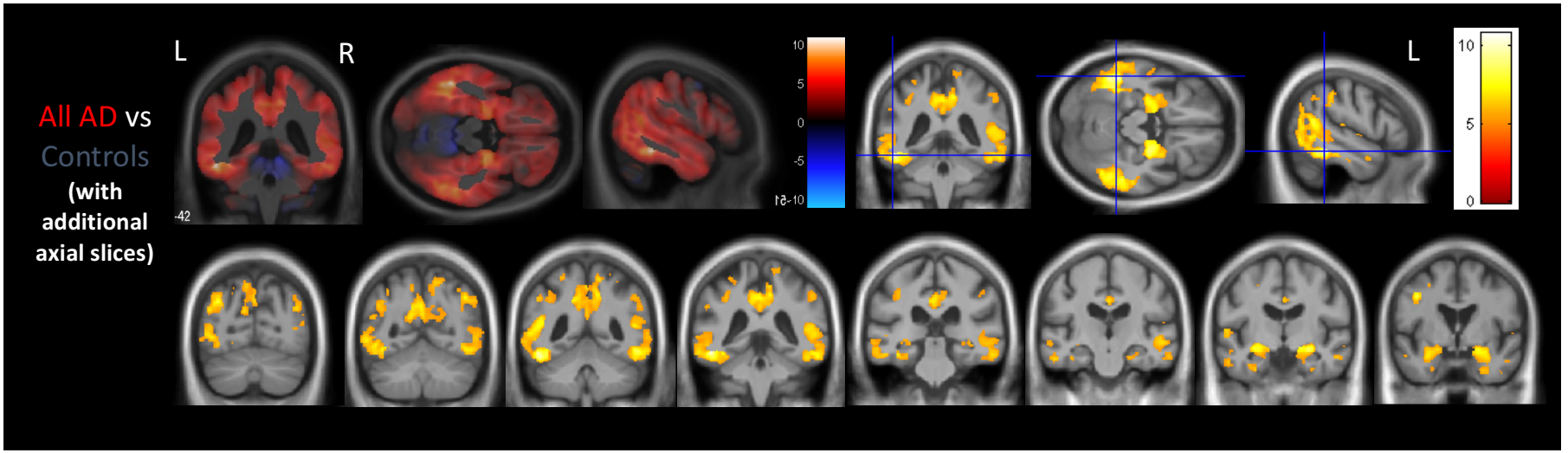

Figure 9.1 Atrophy in young onset Alzheimer's disease relative to controls. Top row: unthresholded t-statistic maps are shown on the left, statistical parametric maps on the right. Bottom row: additional coronal SPM slices

SPMs are corrected for multiple comparisons using random field theory to control the family-wise error (FWE) rate at a significance level of $p<0.05$. The crosshairs represent the global maximum difference. The right cerebral hemisphere is displayed on the right in coronal and axial sections.

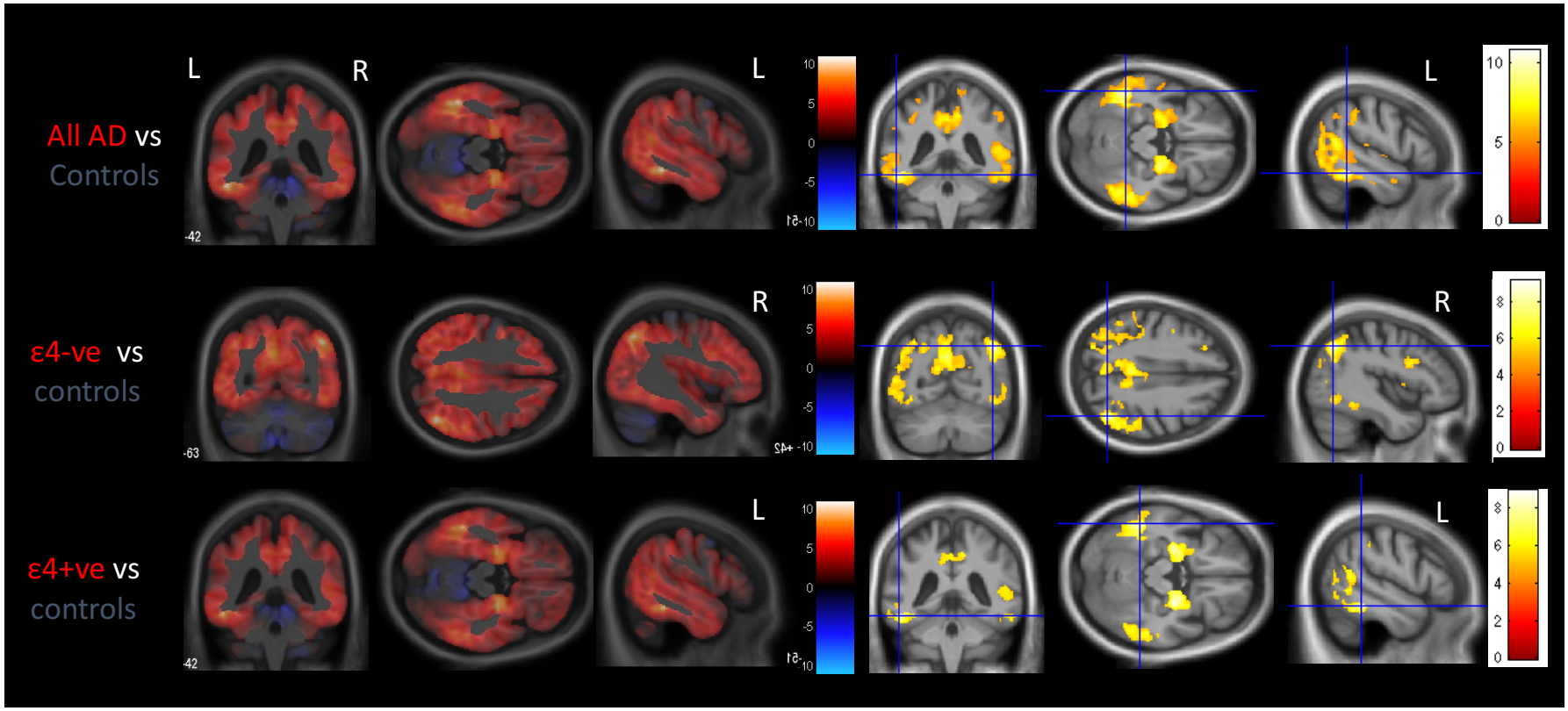

Figure 9.2 Atrophy in young onset APOE ε4 positive and negative individuals with Alzheimer's disease relative to controls

Effect size maps are shown on the left, statistical parametric maps on the right. Additional coronal SPM slices are presented for the whole Alzheimer's disease cohort vs control group comparison. SPMs are corrected for multiple comparisons using random field theory to control the family-wise error (FWE) rate at a significance level of 0.05. The crosshairs represent the global maximum difference. The right cerebral hemisphere is displayed on the right in coronal and axial sections.

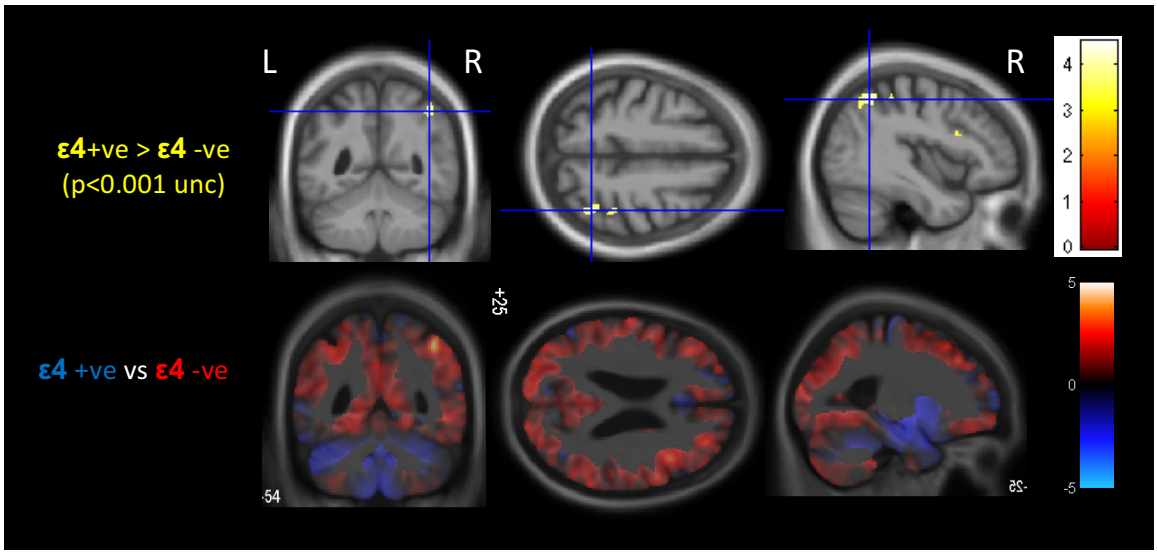

Figure 9.3 Atrophy differences between ε4–ve and ε4 +ve individuals

The top row demonstrates the regions where volume loss in the ε4–ve group was greater than in the ε4+ve group. There were no regions where the volume loss in the ε4+ve group was greater than in the ε4-ve group. The bottom row shows effect size maps, with regions in blue more atrophied in the ε4+ve group, and regions in red more atrophied in the ε4-ve group.

9.4 Discussion

This chapter investigates the pattern of grey matter atrophy in YOAD. As expected, individuals with YOAD had significantly smaller brain and hippocampal volumes and increased ventricle volumes relative to control participants, and the atrophy profile demonstrated in VBM analyses is fairly typical for YOAD with a hippocampal-parietal-posterior cingulate predominance [172, 180, 330].

Individuals with an *APOE* ε4 allele had smaller mean hippocampal volumes than individuals without an ε4 allele, but these differences did not reach statistical significance. It is possible that this is due to the YOAD study being relatively small and

these analyses being cross-sectional in nature. Longitudinal analyses of hippocampal atrophy rates may show a more marked differential effect of possession of an ε4 allele as previous studies have shown greater hippocampal atrophy rates in carriers of an ε4 allele [331]. The tendency for ε4+ve individuals to have more hippocampal involvement, and ε4-ve individuals to have more widespread neo-cortical atrophy was borne out on effect map comparisons, consistent with previous studies that have reported greater medial temporal lobe atrophy in *APOE* ε4+ve carriers, and greater fronto-parietal atrophy in non-carriers [290, 332]. These patterns of atrophy are congruent with the differences in neuropsychological profiles in the presence and absence of an ε4 allele described in Chapter 7.

This association of *APOE* ε4 status with regional atrophy profiles is also seen in other imaging modalities including PIB-PET amyloid burden and FDG-PET hypometabolism [203]. Despite primarily thought to be involved in amyloid metabolism, differential tau distribution is also seen in the presence of *APOE* ε4, mirroring the patterns of neurodegeneration. *ε4*-ve patients have greater ^{18}F-AV-1451 uptake in lateral parietal, medial parietal, occipital, and whole brain cortical areas compared with *APOE ε4*+ve patients [333]. The mechanisms why the neocortex, especially the frontal and parietal lobes, are more vulnerable to tau pathology and neurodegeneration in patients who develop Alzheimer's disease despite lacking *APOE* ε4 is unclear.

These data suggest that *APOE ε4* status affects regional susceptibility to molecular pathology and modulates the anatomic pattern of neurodegeneration in Alzheimer's disease. The greater degree of cortical damage in *ε4-ve* individuals likely results in more significant, wide-spread neurologic dysfunction, potentially explaining the observation that such individuals have a broader profile of clinically manifest cognitive dysfunction, as seen in Chapter 7, and can experience a more rapid clinical decline [334]. This 'hippocampal effect' of *APOE ε4* may also mask the influence of other genetic and

epigenetic factors, hence these factors may have a greater role in the absence of ε4; their variability in turn explaining the greater heterogeneity of non-ε4 young onset Alzheimer's disease.

10 *APOE* and structural brain imaging: microstructural white matter changes

10.1 Introduction

The imaging techniques explored thus far in the thesis have focussed on atrophy, i.e. neuronal loss, the end stage of neurodegeneration. As discussed in Chapter 2, there is considerable interest in exploring genetic influences on other aspects of the pathological process, and network breakdown in particular to understand how this relates to clinical heterogeneity.

Chapter 9 explored associations between *APOE* ε4 status and regional macrostructural brain damage. Patterns of microstructural white matter network damage, as evidenced by altered metrics on diffusion weighted imaging, may also affect the cognitive domains involved clinically and the severity of impairment, which is the subject of this chapter.

Diffusion tensor imaging (DTI) is a magnetic resonance (MR) technique for exploring the structural integrity of brain networks and white matter *in vivo* using water diffusion to distinguish different microstructural environments. As outlined in Chapter 3, DTI provides voxel-level estimates of fractional anisotropy (FA), axial diffusivity (AxD) and radial diffusivity (RD). Neurite orientation dispersion and density imaging (NODDI) [242] is an advanced diffusion MRI technique designed to probe tissue microstructure beyond a composite view of each voxel by modelling water diffusion in multiple compartments [243]: i.e. diffusion that is restricted in axons and dendrites, hindered in extra-neurite space and isotropic in cerebrospinal fluid. NODDI derives a neurite density index (NDI), orientation dispersion index(ODI) and the fraction of free water (F_{iso}). This model allows axonal loss in white matter (modelled by NDI) to be distinguished from altered patterns of axonal organization (modelled by ODI) on a voxel-by-voxel basis, thereby

disentangling two key factors contributing to changes in FA. A key strength of NODDI, compared to alternative multi-compartment techniques, is the use of standard MRI acquisition similar to DTI, making it accessible for routine clinical studies. To date, it is the only multi-compartment technique whose utility has been widely demonstrated in a broad range of applications, including Parkinson's disease [244], epilepsy [245], normal ageing [246], brain development [247], and neurogenetic disorders [248].

In this chapter, DTI and NODDI are employed in a population of patients with YOAD and healthy controls to investigate the nature of microstructural damage underpinning changes in FA, and test the hypothesis that (i) *APOE* ε4 status in YOAD modulates regional signatures of white matter network breakdown, and (ii) reduction in white matter NDI, reflecting neurite loss, influences the clinical phenotype of YOAD.

10.2 Methods

10.2.1 Participants

Forty-five patients meeting consensus criteria for probable Alzheimer's disease [117] with symptom onset <65 years and twenty-four healthy controls matched for mean age and gender were recruited in the YOAD study, as described in Chapter 5. None had a known mutation or family history suggestive of autosomal dominant inheritance at time of recruitment but dedicated screening for autosomal dominant mutations in genes known to cause Alzheimer's disease had not been performed at the time of analyses in this chapter. The presenting cognitive symptom was recorded for all patients, and patients were classified as having a typical [117] or atypical (PCA [165]) Alzheimer's disease phenotype according to published criteria.

All participants underwent MRI scanning, testing on the MMSE [108], assessment on the Hachinski Ischaemic Score [278] and an extensive neuropsychology battery (see Chapter 5 for details).

10.2.2 *APOE* genotyping

As per previous chapters, patient participants gave separate specific consent to donate blood for genetic analyses. DNA was extracted and *APOE* genotype was determined by PCR with 3'-minor groove binding probes.

10.2.3 Imaging acquisition

MRI imaging was performed on a Siemens Magnetom Trio (Siemens, Erlangen, Germany) 3T MRI scanner using a 32-channel phased array head coil.

Two identical Diffusion Weighted Imaging (DWI) acquisitions were performed using a single-shot, spin-echo echo planar imaging sequence (64 diffusion-weighted directions, b=1000 s/mm^2; 9 b=0 s/mm^2 images (referred to as 'b0' images); 55 slices; voxel size 2.5x2.5x2.5mm^3; TR/TE=6900/91ms; total acquisition time for both sequences=16:29 minutes).

A three-shell diffusion sequence optimised for NODDI was acquired (64, 32, and 8 diffusion-weighted directions at b=2000, 700 and 300 s/mm^2; 14 b=0 images; 55 slices; voxel size 2.5x2.5x2.5mm^3; TR/TE=7000/92ms; total acquisition time=16:13 minutes). Both single-shell (DTI) and multi-shell (NODDI) diffusion weighted sequences utilise twice-refocused spin echo to minimise distortion effects from eddy-currents.

All scans were visually assessed for quality control purposes by experienced raters based on coverage and movement artefact.

10.2.4 Data analyses

10.2.4.1 Demographic and neuropsychology

Statistical tests comparing clinical characteristics and neuropsychology scores were performed in Stata version 12. Patient neuropsychology raw scores (x) were converted to z scores using the formula $z=(x-\mu)/\sigma$ (σ - control population standard deviation, μ - control population mean). Mean z scores were calculated for each neuropsychological test within participant groups, and across neuropsychological tests (where applicable) to generate a composite score for each cognitive domain (Table 10.1).

10.2.4.2 Diffusion imaging data: DTI and NODDI

Sixty participants (37 YOAD, 23 controls) had both DTI and NODDI data that passed quality control criteria and were included for analysis. Images were confirmed to have minimal eddy-current distortion and were corrected for motion by rigidly registering each diffusion-weighted image to the first b0 image using FLIRT [270, 271]. Diffusion tensor volumes were spatially normalized with DTI-TK (http://dti-tk.sourceforge.net) which bootstraps a population-specific tensor template from the input tensor volumes and aligns them to the template in an iterative fashion [272] with a tensor-based registration algorithm [273]. This framework has been shown to improve white matter alignment compared to conventional FA-based registration [274]. DTI metrics (FA, AxD, RD) were estimated using FSL [275]. NODDI metrics (NDI, ODI, F_{iso}) were estimated using the NODDI Matlab toolbox (http://www.nitrc.org/projects/noddi_toolbox).

The Tract-Based Spatial Statistics [335] pipeline from FSL [336], optimised [337] by incorporating a population-specific template [338] with tensor-based registration [273, 339] was used to detect whole-brain white matter differences between YOAD groups as defined by *APOE* ε4 status relative to controls, including age and gender as covariates

(5000 permutations, corrected for multiple comparisons with Threshold-Free Cluster Enhancement [340], $p<0.05$).

10.2.5 Neurite density index region of interest analyses

To assess the relationship between microstructural tissue changes and clinical phenotype in YOAD patients, correlations between NDI and neuropsychological performance (z scores by cognitive domain) were assessed in four manually-defined regions of interest corresponding to left and right posterior quadrants (parieto-occipital lobe projections) and left and right anterior quadrants (fronto-temporal lobe projections) of the mean white matter skeleton. These ROIs were delineated by dividing the white matter skeleton into 4 areas at coordinates (x=112, y=88) in standard template space.

Mean NODDI metrics (NDI, ODI and Fiso) within each quadrant ROI were calculated for each individual, and for patient and control groups. Age and gender were included as covariates and correlations with a $p<0.05$ were reported.

10.3 Results

10.3.1 Demographics and clinical features

Demographic and clinical data for participant groups included in the analyses are summarised in Table 10.1. Mean age and gender did not differ significantly between patients and controls (age, p=0.3; gender, p=0.8), and no individual scored >4 on the Hachinski Ischaemic Score. *APOE* ε4 status was available for the 37 YOAD patients, of whom 22 (59%) were *APOE* ε4+ve (18 heterozygotes, 4 homozygotes). Patients who had an *APOE* ε4 allele (ε4+ve) were significantly older than those who did not (ε4-ve) at enrolment to the study (p=0.03). There were no significant differences between ε4+ and ε4-ve patients for age at clinical symptom onset, clinical disease duration at enrolment to the study, or MMSE. The majority of ε4+ve patients presented with a 'typical

Alzheimer's disease' amnestic phenotype (16/22, 73%) as did 3/4, (75%) of the ε4+ homozygotes. The ε4-ve patient group however contained approximately equal numbers of individuals with an amnestic (8/15, 53%) and atypical visual-led posterior cortical atrophy presentations (7/15, 47%); or alternatively expressed 67% of the amnestic patients carried one or more ε4 alleles while only 46% of the non-amnestic patients were ε4+ve.

10.3.2 Neuropsychological profiles

Neuropsychological analyses showed that as expected, patients with YOAD had multi-domain cognitive impairment, performing significantly less well than controls on measures of performance IQ; recognition memory for words; literacy and numeracy; visuospatial and visuoperceptual performance; speed of information processing and executive function (Table 10.1).

In keeping with Chapter 7, the ε4-ve patients included in this analysis were more impaired on tests of literacy and numeracy ($p=0.04$) and speed of information processing and executive function ($p=0.01$) than ε4+ve patients, despite there being no significant difference in the clinical disease durations between the patient groups.

	Controls n=23		YOAD n=37			*APOE*ε4- n=15		*APOE*ε4+ n=22		
	Mean	SD	Mean	SD	P	Mean	SD	Mean	SD	P
Demographic and Clinical										
Sex, M:F, n	10:13	-	18:19	-	0.8[a]	7:8	-	11:11	-	1.0[a]
Age (years)	60.7	6.0	62.3	4.9	0.3[b]	60.2	3.8	63.6	5.2	0.03[b]
Handedness, L:R, n	3:20	-	1:36	-	0.2[a]	0:15	-	1:21	-	1.0[a]
Years of education	16.7	3.1	14.9	2.8	0.03[a]	15.5	2.3	14.5	3.0	0.3[a]
MMSE (/30)	29.3	1.0	21.3	4.5	<0.0001[c]	19.9	4.4	22.3	4.4	0.1[c]
Age at onset (years)	-	-	56.8	4.4	n/a	55.4	4.3	57.8	4.4	0.1[b]
Disease Duration (years)	-	-	5.4	3.2	n/a	4.8	3.0	5.9	3.3	0.3[b]
Neuropsychology										
General intellect: Verbal IQ (WASI vocabulary), z score	-	-	-1.15	1.9	-	-1.56	2.3	-0.88	1.6	0.4[c]
General intellect: Performance IQ (WASI matrices), z score	-	-	**-5.80**	2.4	-	**-6.24**	2.3	**-5.43**	2.39	0.4[c]
Episodic memory for faces (RMT), z score	-	-	-1.90	1.8	-	-1.65	1.3	**-2.08**	2.1	0.6[c]
Episodic memory for words (RMT), z score	-	-	**-4.35**	2.6	-	**-4.38**	2.7	**-4.33**	2.5	0.8[c]
Literacy and numeracy (GDST, GDA), z score	-	-	**-2.04**	1.3	-	**-2.54**	1.0	-1.70	1.4	**0.04[b]**
Visuoperceptual and visuospatial (VOSP), z score	-	-	**-6.81**	6.5	-	**-8.34**	5.7	**-5.76**	7.0	0.09[c]
Processing speed and executive function (DKEFS, verbal fluency, DSMT), z score	-	-	**-2.23**	0.8	-	**-2.6**	0.7	**-1.97**	0.7	**0.01[c]**
Phenotype	n		N			n		n		
Leading symptom, memory / visual / language / behavioural	n/a		24/13/0/0		n/a	8/7/0/0		16/6/0/0		0.3[a]

Table 10.1 Study Participants' Demographic, Neuropsychological and Clinical Characteristics

Neuropsychology scores shown are mean z scores for each cognitive domain (a z score <- 1.96 indicates statistical difference from controls at p<0.05, indicated in bold). Probability values for neuropsychology scores show significance value comparing *APOE* ε4- and *APOE* ε4+ patient groups.

[a] two sided Fisher's exact, [b] two-tailed t-test, [c] Wilcoxon rank sum

10.3.3 White matter changes by *APOE* ε4 genotype: DTI and NODDI

DTI and NODDI metrics are shown for ε4-ve and ε4+ve patients relative to controls in Figure 10.1.

Both patient groups had decreased FA in white matter tracts projecting from the parieto-occipital lobes (inferior longitudinal fasciculus, inferior fronto-occipital fasciculus, superior longitudinal fasciculus, genu of corpus callosum, posterior thalamic radiation), with ε4- patients also having decreased FA in the splenium of the corpus callosum and anterior corona radiata. AxD and RD were increased in both patient groups relative to controls in the genu, body and splenium of the corpus callosum, and parieto-occipital white matter projections (those listed above and the internal capsules). ε4+ve patients additionally had increased RD in the white matter projections from the frontal lobes. There were no areas where patients had increased FA or decreased diffusivity relative to controls, and no significant differences in any DTI metric when APOE ε4+ve and ε4-ve groups were compared directly.

NDI was reduced in the parieto-occipital white matter projections (same as listed above) of both ε4-ve and ε4+ve patient groups relative to controls, but was more widespread in ε4+ve patients, additionally affecting the body and genu of the corpus callosum, and extending further into the frontal and temporal lobe white matter projections. ε4-ve and ε4+ve patient groups had a common signature of decreased ODI in the posterior parts of the corpus callosum and internal capsule. ε4-ve patients also had increased F_{iso} in the corpus callosum, whereas there were no significant differences in F_{iso} in ε4+ve patients relative to controls.

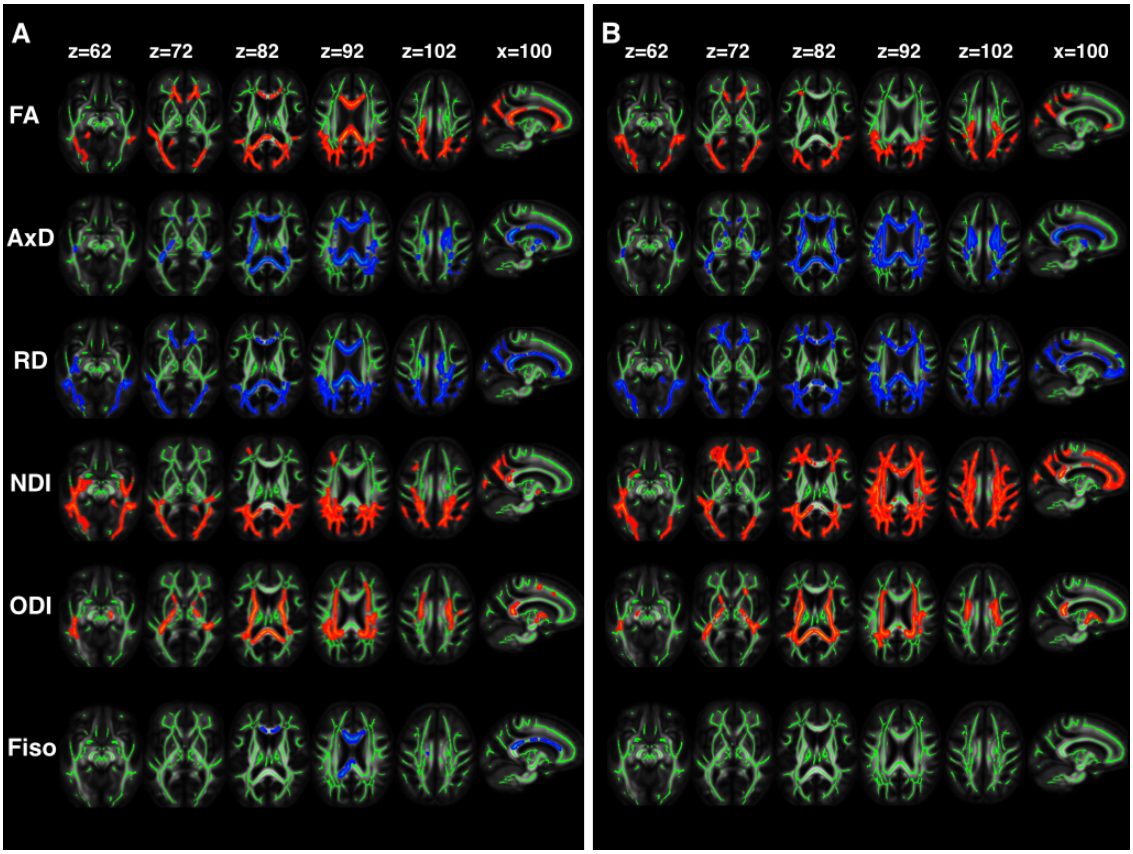

Figure 10.1 DTI and NODDI metrics in patients with (A) ε4-ve YOAD (n15) and (B) ε4+ve YOAD (n=22) relative to controls (n=23)

Voxel-wise group differences are shown in red for metrics that are decreased in patients and blue for those increased in patients. Results are overlaid on axial and sagittal sections of the group-specific white matter skeleton (shown in green) in neurologic convention (the left side appears on the left).

AxD, axial diffusivity; FA, fractional anisotropy; Fiso, fraction of isotropic water; L, left; NDI, neurite density index; ODI, orientation dispersion index; RD, radial diffusivity; R, right.

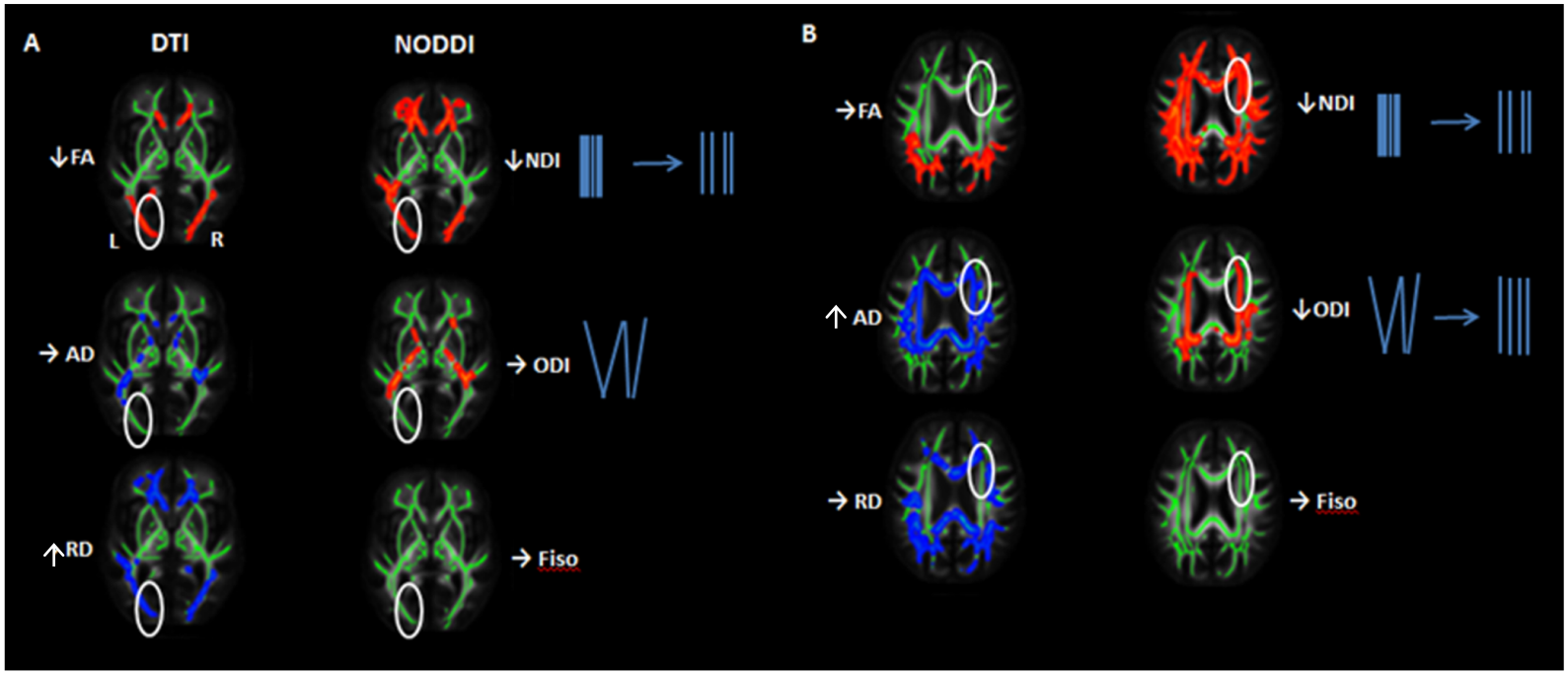

Figure 10.2 Added sensitivity and specificity of NODDI over DTI

(A) Left posterior white microstructural changes in ε4+ve (n=22) relative to controls (n=23). Patients with ε4+ve YOAD have lower FA and increased RD. NODDI metrics for this region suggest that the underlying microstructural change is decreased neurite density, rather than alteration in neurite orientation, illustrating the additional specificity of NODDI. (B) Right frontal white microstructural changes in ε4+ve (n=22) relative to controls (n=23). There is no significant change in FA. However, axial diffusivity increases suggesting underlying microstructural damage, which is corroborated by NODDI metrics revealing reduction in both NDI and ODI (which would tend to affect FA in opposite directions, and hence manifest as no overall change in FA). Here NODDI metrics are more sensitive than FA by avoiding cancelling effects.

The tissue specificity afforded by NODDI revealed a landscape of microstructural damage in YOAD underpinning these changes in DTI metrics; e.g. identifying areas of FA reduction specifically due to decreased NDI rather than changes in ODI (Figure 10.2). NODDI metrics could also be more sensitive to change; e.g. identifying regions where NDI and ODI reduction occurred in parallel, hence resulting in no overall FA change (Figure 10.2).

There were no significant differences in any NODDI metric when directly comparing ε4-ve and ε4+ve patient groups at the prescribed statistical threshold; however, plotting the NDI t-statistic maps (uncorrected) (Figure 10.3) revealed that ε4-ve patients had greatest NDI reduction relative to ε4+ve in the right parietal lobe white matter projections; and ε4+ve patients had greatest reduction in NDI relative to ε4-ve in the left temporal lobe projections.

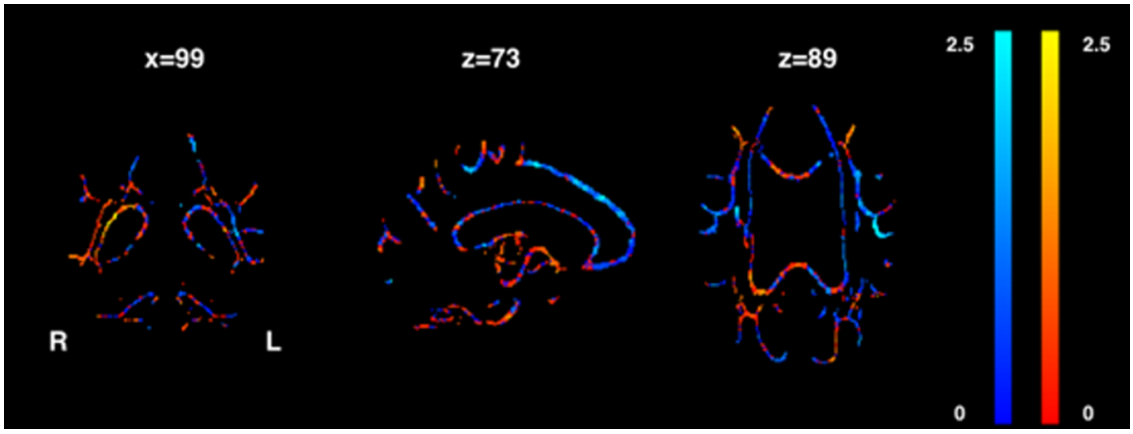

Figure 10.3 Coronal (left), sagittal (middle) and axial (right) neurite density index t-statistic maps

Areas where APOE ε4-ve patients have reduced NDI relative to ε4+ve patients are shown in warm colours, and where ε4+ve patients have reduced NDI relative to ε4-ve patients are shown in cool colours.

10.3.4 Region of interest NDI correlation with cognitive function

Mean values for NODDI metrics in each of the 4 regions of interest are shown in Table 10.2. There were borderline significant differences between patients and control NDI metrics in the two anterior quadrants, and strong evidence for differences in the posterior (particularly left) quadrants. There were no differences in ODI or FISO for any quadrant.

WM ROIs	YOAD **Mean** ± SD	Controls **Mean** ± SD	P[a]
NDI (mean±SD)			
Left anterior quadrant	0.554±0.022	0.538±0.031	0.043
Left posterior quadrant	0.559±0.029	0.518±0.031	<0.00002
Right anterior quadrant	0.555±0.022	0.539±0.036	0.067
Right posterior quadrant	0.552±0.029	0.511±0.052	0.001
ODI (mean±SD)			
Left anterior quadrant	0.214±0.015	0.214±0.007	0.95
Left posterior quadrant	0.202±0.023	0.201±0.007	0.76
Right anterior quadrant	0.213±0.014	0.211±0.008	0.54
Right posterior quadrant	0.195±0.013	0.194±0.008	0.68
FISO (mean±SD)			
Left anterior quadrant	0.105±0.017	0.108±0.016	0.67
Left posterior quadrant	0.107±0.024	0.111±0.017	0.58
Right anterior quadrant	0.099±0.017	0.106±0.018	0.22
Right posterior quadrant	0.101±0.023	0.111±0.034	0.26

Table 10.2 NODDI metrics in each region of interest

FISO, fraction of free water; NDI, neurite density index; NODDI, neurite orientation dispersion and density imaging; ODI, orientation dispersion index; P, probability; ROI, region of interest; SD, standard deviation; WM, white matter; YOAD, young onset Alzheimer's disease. [a] two-tailed T-test

Having demonstrated regional differences in NDI between patients and controls, I next correlated the neuropsychology profiles with the mean NDI values in each quadrant. As shown in Figure 10.4, in patients there were significant positive correlations between a visually-demanding measure of performance IQ (WASI matrices) and regional NDI in white matter projections from the right parieto-occipital lobe (10.4, A) and between visuospatial and visuoperceptual tasks and NDI in white matter projections from the parieto-occipital lobes bilaterally (Figures. 10.4 B and 10.4 C). There were no significant positive correlations between NDI and performance on other cognitive domains, and no significant negative correlations between regional NDI and any cognitive score.

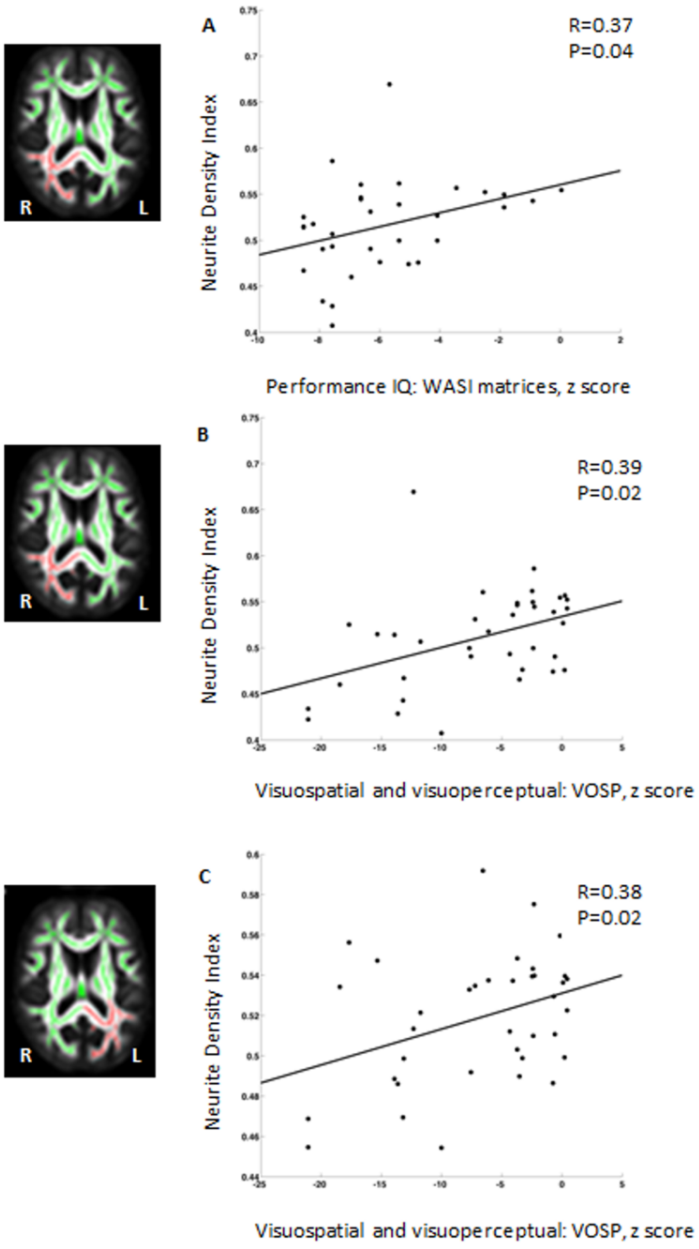

Figure 10.4 Significant correlations between regional neurite density index and neuropsychological measures in white matter projections from the right (A and B) and left (C) parieto-occipital cortices of patients with YOAD (n=37)

Regions of interest (red) are shown on the group mean white matter skeleton (green) to the left of each graph. L, left; IQ, intelligence quotient; R, right; VOSP, visual object and spatial perception battery; WASI, Wechsler Abbreviated Scale of Intelligence.

10.4 Discussion

This chapter uses DTI and NODDI to explore signatures of white matter structural brain damage and their biological underpinnings in patients with YOAD on the basis of *APOE* ε4 genotype. DTI metrics showed regions of altered white matter microarchitecture in both ε4+ve and ε4-ve patients relative to controls. NODDI, a multi-shell diffusion technique implemented on standard 3T clinical MR scanners, provided further insights into the commonalities and differences in white matter change associated with ε4 genotype; namely more widespread NDI reduction in ε4+ve individuals and more focal posterior reductions in patients without an ε4 allele.

Despite being the most important risk factor for Alzheimer's disease, the effects of *APOE* ε4 on clinical phenotype white matter damage are incompletely understood. The relatively few previous DTI studies in YOAD have shown decreased white matter FA and increased diffusivity, but have focussed on describing regional variation between phenotypes [239, 240, 341] or in YOAD relative to late onset Alzheimer's disease [238] rather than investigating potential differential effects of *APOE* ε4. Studies in late onset Alzheimer's disease have shown contradictory findings: *APOE* ε4 allele status was associated with an increase in parahippocampal white matter mean diffusivity [342], yet Kljajevic *et al.* found ε4 status affected mean diffusivity in controls, but not in participants with clinically-manifest Alzheimer's disease [343]. The observation here that axial and radial diffusivity changes are more prominent than FA in both the presence and absence of an ε4 allele is consistent with previous observations that these directional diffusivity metrics can be a more sensitive marker of structural change than FA [344]. The areas of increased RD and AxD, and FA reduction in bilateral parietal lobes, genu of the corpus callosum, frontal white matter lobe projections shown here are broadly in keeping with changes in DTI metrics reported in YOAD patients (ε4 status unspecified) previously

[238], and an additional possible modulating effect of ε4 status is shown: less anterior FA reduction in the presence of an ε4 allele.

The NODDI results allow more specific inferences about the nature of the underlying microstructural damage. Thus, as illustrated in Figure 10.2. NODDI metrics can explain different mechanisms underlying changes in FA; or indeed detect the effects of concomitant pathological processes that would individually affect FA in opposing ways and hence cancel one another out, resulting in no observable FA change.

White matter NDI reduction was more extensive anteriorly in ε4+ve than ε4-ve YOAD patients (Figure 10.1). Although differences did not survive the statistical threshold for multiple comparisons when comparing the patient groups directly, T-statistic maps (uncorrected) reveal potential subtle differences in regional NDI values between the ε4-ve and ε4+ve groups (Figure 10.3). The former appears to have more NDI loss in right parietal lobe white matter connections, in keeping with a trend for worse performance on visual tasks. Conversely the ε4+ve group tends to more NDI reduction in left temporal lobe connections. The similarities and differences could suggest there being a "generic" signature of network breakdown in Alzheimer's disease, with relatively subtle ε4 modulation of network dysfunction, perhaps influencing phenotype through differential propagation of pathology.

Histological evidence supports a relationship between MRI estimates of axonal density reduction and actual axon loss. *Ex vivo* studies in animals have demonstrated that diffusion MRI estimates of axon density, using a related diffusion model, show a high degree of correlation with optical staining intensity of myelin and stereological estimates of axonal volume fraction in white matter [345]. If reduced NODDI NDI truly reflects axon loss in YOAD, then it follows that even partial disconnection of brain regions should lead to functional consequences that manifest in the phenotype.

Whilst DTI metrics do not correspond to compartment-specific microstructural changes, previous studies have shown correlation with global measures of cognition. In patients with LOAD, fractional anisotropy in the corpus callosum has been shown to correlate with performance on the MMSE [238], and more specifically, radial diffusivity and fractional anisotropy in the splenium correlate with dementia severity on the ACE-R [346]. In YOAD, global cognitive performance on the Clinical Dementia Rating Sum of Boxes has been found to correlate with mean diffusivity in several brain regions including the corpus callosum, posterior cingulate, frontal and parietal parts of the superior longitudinal fasciculus bilaterally, and left temporal regions [238]. However, no correlation has been demonstrated between diffusion MRI metrics and performance on focal cognitive test scores sensitive to regional brain dysfunction.

In the analyses presented in the chapter, NDI in white matter projections from both left and right parieto-occipital lobes correlated with visuospatial and visuoperceptive cognitive performance, a sensitive marker of non-dominant parietal cortex function; bilateral correlations are likely to reflect that the parietal lobes are structurally closely inter-connected. Right parieto-occipital white matter NDI also correlated with a measure of performance (non-verbal) intelligence, reflecting right hemisphere dysfunction.

These correlations suggest that regional reductions in NDI can provide *in vivo* measures of cell loss and network breakdown, which in turn shape clinical phenotype. The lack of correlation of NDI with other neuropsychological scores may reflect these cognitive functions being underpinned by a more distributed white matter network, or relate to the dispersion of results on psychology testing - the tests that showed correlation were those with the largest range of patient performance.

NODDI has since been applied to studying cortical diffusion in grey matter where microstructural damage modelled by regional changes in NODDI metrics may be

expected to show closer correlation with performance on specific neuropsychological tests. Lower NDI was associated with lower MMSE scores, with the strongest associations seen in the precuneus, inferior temporal and middle temporal gyri [347], but regional correlation with focal cognitive scores has not been investigated.

Orientation dispersion is thought to relate to axonal organisation [348] and white matter orientation dispersion index has been shown to correlate with altered neurite morphology histologically [349]. White matter ODI has been reported to increase in normal aging [246]. The data presented here show ODI was reduced (i.e. the tracts were more coherent) in the corpus callosum and internal capsule of individuals in both ε4-ve and ε4+ve YOAD patients relative to controls, notably even in some regions unaffected by significant NDI change. The anatomical dissociation may suggest alterations in NDI and ODI reflect different pathophysiological phenomena in neurodegeneration. One possible histological explanation is that reduced orientation dispersion reflects loss of secondary crossing fibres to leave more aligned neurons in the primary tracts, perhaps mediated by selective axonal degeneration. Longitudinal NODDI studies will be needed to understand the temporal sequence of change, but it may be that reduction in orientation dispersion precedes reduction in neurite density.

The work presented in this chapter has a number of limitations. As with all biophysical models, and specifically multi-compartment diffusion models, NODDI requires a number of assumptions: modelling axon orientation does not account for crossing fibres, the value of intrinsic diffusivity is fixed over the whole brain, and intra-neurite diffusion is modelled as being completely restricted within a collection of impermeable sticks. It is conceivable that this does not fully characterise all pathological processes involved in neurodegenerative diseases (e.g. Alzheimer's disease) such as possible regional variation in intrinsic diffusivity, alterations in neurite membrane permeability or damage to intra-neurite architecture. Jesperson *et al.* have used a related multi-compartment

diffusion model [350] to examine the relationship between neurite density and orientation dispersion with histological measures in animal brains [345]. There is however, currently limited histopathological evidence to specifically validate NODDI model metrics in the human brain; however an ex vivo study of human spinal cord in multiple sclerosis showed NODDI replicated the trends of histological indices and could detect specific features of tissue pathology [351].

The potential presence of white matter hyperintensities is not accounted for. These have been shown to result in lower FA and higher MD relative to normal appearing white matter [352]. In Alzheimer's disease, white matter hyperintensities may be related to coexistent vascular burden, or be part of Alzheimer's disease pathogenesis. One of the advantages of studying patients with YOAD is that they are less likely to have significant coexistent vascular disease than individuals with late onset disease. All participants in this study scored 4 or less on the Hachinski ischaemic score indicating that on clinical grounds there was not a significant vascular component to their syndrome; and as shown in Chapter 6, no differences in blood pressure were seen between patients and controls in the wider YOAD study from which these participants were drawn. There may be more amyloid angiopathy observed in patients with ε4+ve disease than those who do not carry an ε4 allele [353] which could both explain some of the differences observed. It is unknown how the presence of white matter hyperintensities affect NODDI metrics – and indeed future studies with post-mortem verification are needed to see if NODDI may be a useful imaging technique to understand the microstructural changes underpinning these white matter alterations. If quantifiable, WMH lesions loads could be included as a covariate in the modelling.

The participant groups reported are relatively small, yet indicative of the relative rarity of YOAD, and may explain why direct comparisons of ε4+ve and ε4-ve groups were not sufficiently powered to reach statistical significance. The individual with a PSEN1 variant

had also been included as his autosomal dominant genetic status was not known at the time of these analyses. Ideally in studying the differential effect of *APOE* ε4, individuals with autosomal dominant disease would be excluded to try to remove a potential confounder for any differences found between groups being attributed to *APOE* ε4 status. It is possible, but unlikely that the presence of a single individual with an autosomal dominant mutation will have significantly changed the results.

Alzheimer disease is a complex genetic disease and any modulation of network breakdown due to *APOE* ε4 here observed likely occurs in the context of attenuation by a host of other genetic and environmental factors.

NODDI metrics in the healthy aging brain show good short interval reproducibility [354] but longitudinal studies, ideally with post mortem histological evaluation, are required to establish if NODDI metrics are robust, reproducible and capable of tracking Alzheimer's disease progression, characteristics that may give the technique utility in clinical trials. Given the interest in testing potential therapeutic agents at earlier stages of disease it is important to assess if, as predicted, NODDI metrics can detect white matter microstructural changes in people with very mild or pre-symptomatic stages of disease. A large longitudinal cohort study of healthy older adults is now underway investigating whether NODDI can detect microstructural changes in people with pre-symptomatic disease [355].

11 Investigating the functional basis of memory impairment in Alzheimer's disease

11.1 Introduction

Data presented in this thesis thus far have concentrated on the genetic, volumetric and diffusion imaging characteristics of YOAD, and presented indirect evidence for links between regional structural network breakdown and cognitive performance in individuals with different *APOE* ε4 genotypes. Activation fMRI can be used to study functional, rather than structural, connections between brain regions, and identify areas of both decreased activity, and disease mediated aberrant and compensatory increases in activity. This chapter describes a series of experiments using activation fMRI to investigate differences in aspects of memory processing and their functional neuroanatomical bases in patients with different phenotypes of Alzheimer's disease, using music as a stimulus.

As outlined in Chapter 2, substantial evidence has implicated a core neural network as the key target of pathogenic protein spread in Alzheimer's disease [177, 222, 356, 357]. This 'default mode' network links medial temporal lobe structures to lateral temporo-parietal and medial prefrontal regions via a 'hub' zone in postero-medial cortex (posterior cingulate and precuneus). Differential Involvement of this network is thought to underpin the variable clinical deficits seen in the major Alzheimer's disease variant phenotypes: typical memory led Alzheimer's disease (tAD) and posterior cortical atrophy (PCA) [101, 165, 222, 358-360].

Music is a very salient stimulus for studying default mode network function. In addition to mediating stimulus-independent thought [217] the DMN plays an active role in coordinating brain activity during other cognitive operations including the analysis of

auditory scenes and patterns [361, 362]. Components of the default mode network are also implicated in the processing of several aspects of musical memory processing. Impaired processing of complex auditory stimuli has been linked specifically to dysfunction and atrophy of the postero-medial hub region, and reported in both tAD and PCA [101, 222, 358-360, 363].

As a research stimulus, music also enables multiple fundamental aspects of information encoding and processing to be experimentally altered and studied. Musical processing involves appreciation of temporal information (regularity and irregularity in rhythms), pitch and timbre perception, spatial encoding of where a sound is coming from, emotional aspects (whether music sounds 'sad' or 'happy', depending on the key) and several aspects of memory processing. Music engages separable cognitive systems mediating procedural memory (playing an instrument), semantic memory (recognition of musical objects, such as familiar tunes) and episodic memory (encoding and recollection of specific musical events) [364, 365]. These musical memory systems are likely to be differentially vulnerable to the effects of Alzheimer's disease [364-367] with the balance of evidence suggesting that episodic memory for music becomes impaired early in the course of Alzheimer's disease, while effects on musical semantic and procedural memory are more variable and may become more evident only with advancing disease [366, 368-370] mirroring the variable susceptibility of memory functions in non-musical domains [222]. People with advanced dementia may still remember the tunes of their favourite songs from earlier in life and familiar music appears to be able to 'unlock' autobiographical memories and other cognitive capacities in Alzheimer's disease [371].

Functional neuroanatomical work in the healthy brain has identified separable, distributed, bi-hemispheric cerebral networks that support these different musical memory systems. Musical semantic memory has been shown to engage anterior temporal, inferior and supero-medial prefrontal cortices [367, 372-375] while musical

episodic memory engages precuneus, posterior cingulate, hippocampus and other medial temporal lobe structures [372, 376, 377]. The processing of unfamiliarity (novelty) in music and other sensory stimuli engages a distributed network of brain areas overlapping those implicated in musical semantic and episodic memory, including medial temporal lobes and temporo-parietal, inferior frontal, insula and anterior cingulate cortices [378-380].

Despite considerable interest however, the neural mechanisms underlying musical memory in Alzheimer's disease remain contentious. It has been proposed that preservation of musical memory (in particular, musical semantic memory) in Alzheimer's disease might be attributable to relative sparing of the medial prefrontal cortices implicated in mediating musical familiarity in healthy listeners [367]. However, changes in musical memory processing in Alzheimer's disease have not been studied directly in patients. It remains unclear if Alzheimer's disease affects processing in core musical memory systems differentially, and how this manifests in patients with variant AD syndromes who have DMNs with regionally different patterns of structural damage.

In this chapter I start to address these issues using activation fMRI in a cohort of patients representing the canonical syndromes of tAD and PCA, relative to healthy age-matched individuals. The neuropsychological and regional atrophy profiles of the YOAD cohort based on phenotype are described. Then a simple paradigm is used to capture disease-associated changes in the core semantic (familiarity) and episodic (tune repetition) dimensions of musical memory that might be relevant to any listener, including those without specific musical training. In everyday music listening, we are generally not called upon to analyse melodies explicitly but the sense that a tune is familiar, that musical motifs are repeating or that new material is being presented are common experiences that contribute importantly to the appreciation of music even among musically naïve listeners. These listening experiences are in turn likely to depend on semantic and

episodic musical memory systems: prior familiarity with a melody engages musical semantic memory while the incidental detection of repeating motifs engages (incidental) episodic memory for music. In the fMRI paradigm used these factors of prior familiarity and repetition are presented orthogonally in a stimulus set comprising short musical melodies.

Although familiarity decisions on melodies have been used as a model for musical semantic memory in previous studies [364], familiarity does not, of course, equate to detailed semantic knowledge of a musical piece; nor does incidental memory for music equate to explicit episodic recall. The objective was not to delineate fully the brain systems that mediate musical semantic and episodic memory, but rather to probe these systems using a paradigm relevant to listeners potentially varying widely in musical expertise and in particular, without the requirement for an overt task during scanning. Task effects are particularly problematic in fMRI studies of cognitively impaired individuals due to confounds from e.g. remembering what button to press, and when to do so. Therefore, in order to provide a behavioural reference for the neuroanatomical changes observed, all participants also completed tasks assessing aspects of musical semantic and episodic memory following the scanning session.

Based on behavioural and neuroanatomical evidence from previous studies [222, 364-367, 370, 372, 374-377], I hypothesized that Alzheimer's disease and PCA would be associated with a similar profile of abnormal activation of postero-medial cortices during incidental episodic processing of repeated melodies relative to healthy individuals, whereas these syndromes would show divergent activation profiles during semantic processing of prior melody familiarity, due to sparing of more anterior cortical regions in PCA relative to tAD [381].

11.2 Methods

11.2.1 Participants

A subset of thirty-four patients (mean age 60.9 years; 20 female) fulfilling consensus criteria for Alzheimer's disease [117] and 19 age-matched healthy individuals (60.5 years, 10 female) from the YOAD cohort participated in the experiments described in this chapter. Twenty-four of these patients presented with an amnestic clinical syndrome of tAD [116] and 10 patients presented with a syndrome meeting research criteria for PCA [165]. The clinical syndromic diagnosis was corroborated by neuropsychological assessment (for details of the neuropsychological battery, see Chapter 5). Patients had a compatible profile of regional atrophy and no significant associated burden of cerebrovascular disease on volumetric structural T1 brain MRI. No participant had a history of hearing loss or congenital amusia.

No participants had a known mutation or family history suggestive of autosomal dominant inheritance at time of recruitment but dedicated screening for autosomal dominant mutations in genes known to cause Alzheimer's disease had not been performed at the time of analyses in this chapter, hence the tAD participant harbouring a pathogenic *PSEN1* variant is included.

CSF examination was undertaken in 30 of these patients (23/24 with tAD, 7/10 with PCA), all of whom had a profile of neurodegeneration protein markers (tau and Aβ1-42) consistent with likely underlying Alzheimer's disease pathology [382].

At the time of participation, 32 patients were receiving symptomatic treatment with an acetylcholinesterase inhibitor (two were also taking memantine), one patient was taking memantine without a cholinesterase inhibitor and the remaining patient was taking no symptomatic treatment.

Demographic, clinical and neuropsychological details for all participant groups are summarised in Table 11.1.

11.2.2 Assessment of musical background and peripheral hearing function

All participants completed a questionnaire detailing their prior musical training and current music listening [383]. In order to assess peripheral hearing function, all participants had pure-tone audiometry using a procedure adapted from a commercial screening audiometry software package (http://www.digital-recordings.com/audiocd/audio.html). The test was administered via headphones from a laptop in a quiet room. Five frequency levels (500, 1000, 2000, 3000, 4000Hz) were assessed: at each frequency participants were presented with an intermittent tone that slowly and linearly increased in intensity. Participants were instructed to indicate as soon as they were sure they could detect the tone; this response time was measured and stored for offline analysis.

Characteristic	Healthy controls n=19	tAD n=24	PCA n=10
General			
Gender (M:F)	9:10	12:12	2:8
Age (years)	60.5 (6.0)	60.3 (4.4)	62.1 (5.6)
Handedness (L:R)	3:16	1:23	1:9
Education (years)	17.1 (3.1)	15.5 (2.9)	15.0 (2.9)
Musical training (years)	2.7 (5.2)	3.8 (5.3)	1.2 (2.1)
Music listening (hours/week	9.4 (10.5)	6.8 (7.4)	5.9 (8.1**)**
MMSE (/30)	29.5 (0.7)	19.7* (3.7)	22.9* (4.3)
Age at onset (years)	NA	55.2 (3.9)	55.8 (4.3)
Symptom duration (years)	NA	5.1 (2.6)	6.3 (3.3)
CSF examination	NA	23[§]	7[§]
Neuropsychological assessment			
Episodic memory			
RMT words (short, /25)	24.5 (0.8)	**16.8†* (2.5)**	20.0†* (4.0)
RMT faces (short, /25)	24.5 (1.0)	20.0† (4.6)	18.3† (4.7)
Executive skills			
WASI matrices (/35)	26.9 (2.3)	9.0 †*(6.6)	**3.6 †*(3.8)**
WMS-R digit span forward (/12)	8.9 (1.8)	5.8† (2.1)	6.2† (3.0)
WMS-R digit span backwards (/12	7.8 (1.6)	3.7† (1.6)	3.9† (2.7)
DSMT (/93)	54.6 (9.1)	**13.4 † (11.9)**	**5.8 † (8.7)**
A cancellation	20.7 (5.1)	**50.2†* (20.5)**	**74.5†* (18.0)**
Verbal skills			
NART (/50)	40.3 (5.1)	30.6† (10.3)	28.4† (12.4)
WASI vocabulary (/ 80)	69.7 (7.5)	53.0† (17.4)	55.5† (21.7)
GNT (/30)	25.7 (2.7)	**14.1† (9.3)**	17.6† (7.1)
Literacy and numeracy skills			
GDST (/30)	27.4 (3.0)	16.1† (8.6)	13.5† (8.1)
GDA (/24)	13.7 (6.7)	**1.8 † (2.8)**	**1.5† (2.0)**
Visuoperceptual skills			
VOSP object decision (/20)	18.2 (1.5)	15.6†* (3.0)	**10.4†* (4.5)**
VOSP shape detection (/20)	19.4 (0.8)	**18.3†* (1.4)**	**16.2†* (2.4)**
VOSP fragmented letters (/20)	19.4 (0.7)	**12.3†* (7.1)**	**5.3†* (5.6)**
VOSP dot counting (/10)	9.9 (0.3)	8.1†* (2.8)	**4.9†* (3.0)**
Post-scan musical tasks			
Melody familiarity judgement (d')	2.8 (0.7)	2.8 (0.8)	2.7 (0.8)
Melody episodic memory[#] (d')	1.6 (0.8)	**0.8 (0.7)**	**0.9 (0.6)**

Table 11.1 Demographic, clinical and behavioural characteristics of participants

Mean (standard deviation) values are presented unless otherwise indicated. Raw data are shown for neuropsychological tests (maximum scores in parentheses). Bold

indicates patient performance was significantly impaired (<5th percentile) relative to age matched published norms; †significant difference between patient group and healthy controls ($p<0.05$), *significant difference between patient syndromic groups ($p<0.05$); #18 controls, 14 tAD, eight PCA patients completed this test; §profile of neurodegeneration markers consistent with Alzheimer's disease pathology in all cases; CSF, cerebrospinal fluid; DSMT, Digit Symbol Modalities Test [268]; F, female; GDA, Graded Difficulty Arithmetic [264]; GDST, Graded Difficulty Spelling Test [265]; GNT, Graded naming test [263]; IQ, intelligence quotient; M, male; MMSE, Mini Mental State Examination [108]; n, number; NA, not applicable; NART, National Adult Reading Test [384]; P, probability; PCA, patient group with posterior cortical atrophy; RMT, Recognition Memory Test [260]; SD, standard deviation; verbal fluency [385]; tAD, patient group with typical amnestic presentation of Alzheimer's disease; VOSP, Visual Object and Spatial Perception battery [266]; WASI, Wechsler Abbreviated Scale of Intelligence [259]; WMS-R, Wechsler Memory Scale Revised [262].

11.2.3 Experimental stimuli and protocol

Two musical stimulus subsets were created, based respectively on previously familiar melodies (widely-known tunes that would be recognised based on long-term, general musical experience rather than specific autobiographical recall) and previously unfamiliar melodies (melodies created *de novo* for the experiment). During scanning, particular melodies from each set were either presented once only or twice, to vary the frequency of particular musical episodes over the experimental session. This yielded four stimulus conditions: familiar melodies, each presented once; unfamiliar melodies, each presented once; familiar melodies, each presented twice; unfamiliar melodies, each presented twice.

This experimental design allowed construction of key contrasts to assess musical semantic memory (previously familiar > unfamiliar melodies), musical novelty (the 'reverse' contrast, previously unfamiliar > familiar melodies), musical episodic memory (repeat [second] > first presentation of repeated melodies) and musical encoding (the 'reverse' contrast, first > repeat presentation of repeated melodies).

Musical stimuli were synthesised in MatlabR2012a® as digital wave files (sampling rate 44.1kHz) and comprised sequences of harmonic complexes (notes) with defined fundamental pitch and fixed inter-note gap (6ms). The total length of each stimulus sequence was fixed at eight seconds and mean sound intensity was fixed across stimuli.

Familiar melodies comprised excerpts from popular classical instrumental tunes widely known among older British individuals (details in Table 11.2), selected based on a pilot survey; the tune excerpts selected were classified as familiar (versus unfamiliar) by ≥ 80% of healthy older British participants (n=5, all >50 years), none of whom participated subsequently in the fMRI study. Non-vocal tunes were used to minimise implicit processing of verbal (song lyric) associations. Unfamiliar melodies were created by re-distributing the notes from each familiar melody to create a novel musical sequence with equivalent temporal and pitch interval structure. Repeated melodies (half familiar, half unfamiliar) were distributed such that repeats were separated by two intervening melodies (stimulus trials) which (in the 'sparse' (long TR) acquisition protocol used here) corresponded to an interval of approximately 33 seconds between repetitions of a given note sequence. This design was intended to maximise any effect from melody repetition while minimising musical short-term sensory trace memory or working memory processing. A silent 'rest' condition was also included to provide a low-level baseline for assessing the effect of auditory stimulation.

The complete stimulus set (144 trials) comprised 96 unique melodies (48 familiar, 48 unfamiliar) plus 48 repeat-presentation trials (24 familiar melodies, 24 unfamiliar melodies). The stimuli were delivered binaurally from a laptop using electrodynamic headphones (MR Confon GmbH, Magdeburg) at a comfortable listening level (approximately 70 dB). The presentation order of familiar and unfamiliar melody trials was randomised. In-house routines in Python (http://www.python.org) were used to integrate stimulus delivery with the scanner controls. Participants were instructed to listen to the sound stimuli; there was no output task and no participant responses were collected during the scanning session.

Composer	**Musical piece**	**Notes** (no.)	**Pitch range** (notes)	**Pitch change** (semitones)
Bach	Fugue in D minor	32	A0 - A1	7.07
Bach	Jesu Joy of Man's Desiring	32	D1 - G2	2.87
Bach	Minuet in G: excerpt 1	32	A1 - E2	1.67
Bach	Minuet in G: excerpt 2	32	F1# - G2	3.91
Bach	Toccata in D minor	32	F1 - A2#	2.58
Barber	Adagio for Strings	16	A1 - D2#	1.84
Beethoven	Fur Elise: excerpt 1	32	E0 - E3	8.44
Beethoven	Fur Elise: excerpt 2	32	E0 - E2	6.74
Beethoven	Moonlight Sonata	32	G0# -F1#	5.93
Beethoven	Ode to Joy	32	D1 - E2	3.67
Bizet	Toreador's Song (Carmen)	18	C1 - D2	3.18
Bizet	Habanera (Carmen): excerpt 1	35	D1 - C2#	2.40
Bizet	Habanera (Carmen): excerpt 2	29	D1 - D2	2.23
Boccherini	Minuet (String Quintet in E)	30	D1 - A2	4.12
Brahms	Hungarian Dance No 5	19	F1# - A2	3.27
Charpentier	Prelude (Te Deum)	21	G1 - G2	2.87
Delibes	Mazurka (Coppelia)	21	G1 - C3	4.61
Delibes	Flower Duet (Lakme)	32	G1 - D2#	1.74
Dvorak	Humoreske: excerpt 1	21	G1 - B2	3.35
Dvorak	Humoreske: excerpt 2	28	C1 - A2	2.70
Dvorak	New World Symphony, Adagio	16	F1 - C2	2.42
Grieg	Morning Mood (Peer Gynt): excerpt 1	32	F1 - D2	2.95
Grieg	Morning Mood (Peer Gynt): excerpt 2	32	E1 - C2#	3.43
Grieg	Hall of the Mountain King (Peer Gynt) excerpt 1	32	C1# - A1	3.03
Grieg	Hall of the Mountain King (Peer Gynt) excerpt 2	32	B0 - B1	3.60
Handel	Hornpipe (Water Music)	28	C1 - G1	2.87
Handel	Arrival of Queen of Sheba: excerpt 1)	32	B0 - E2	2.35
Handel	Arrival of Queen of Sheba: excerpt 2	32	G1 - G2	3.79
Joplin	The Entertainer: excerpt 1	36	D1 - E2	5.14
Joplin	The Entertainer: excerpt 2	48	D1 - E2	2.6
Mozart	Eine Kleine Nachtmusik	18	D1 - D2	4.25

Mozart	Piano Concerto No 21, Mov 2	26	C2 - D3	4.68
Mozart	Symphony No 40, Mov 1: excerpt 1	40	C1 - A1#	2.86
Mozart	Symphony No 40, Mov 1: excerpt 2	31	C2# - C3	2.96
Mozart	Turkish Rondo (Piano Sonata No 11)	43	G1# - C3	2.35
Offenbach	Infernal Gallop (Orpheus): excerpt 1	32	A1 - D3	3.94
Offenbach	Infernal Gallop (Orpheus): excerpt 2	32	G1 - G2	3.20
Prokofiev	Peter's theme (Peter and the Wolf)	25	G1 - C3	4.28
Puccini	Nessum Dorma	16	B1 - G2	2.52
Quilter	Upon St Paul's	16	D1 - D2	4.72
Ravel	Bolero	33	C1 - D2	1.99
Saint-Saens	Danse Macabre	32	D1 - A1#	2.26
Strauss	Radetsky March	43	C1 - B1	3.34
Strauss	Tritsch Tratsch Polka	38	B0 - E2	5.10
Tchaikovsky	Waltz of the Flowers (Nutcracker)	27	F1 - F2	4.17
Tchaikovsky	Dance of the Little Swans (Swan Lake)	32	F0# -F2#	4.84
Vivaldi	Spring (The Four Seasons)	32	B1 - B2	3.03
Wagner	Ride of the Valkyries	18	F0# - A1	5.02
Mean:		*29.4*		*3.6*

Table 11.2 Familiar melodies presented in the fMRI experiment

The 48 familiar melodies used are indicated, with relevant stimulus parameters; all stimuli were edited to duration 8 seconds and presented using a pleasant synthetic timbre with fixed overall (root-mean-square) intensity. Familiar melodies comprised 48 excerpts from tunes widely known among older British people. *standard deviation for inter-tone pitch variation across the 8 second excerpt.

11.2.4 Brain imaging acquisition

MRI data were acquired on a 3T TIM Trio whole-body MRI scanner (Siemens Healthcare, Erlangen, Germany). 92 gradient-echo echo-planar image (GE-EPI) volumes were acquired in each run using a 12-channel RF receive head and body transmit coil in sparse (TR 11.3 seconds) acquisition mode (to reduce any interaction between scanner acoustic noise and auditory stimulus presentations). Each EPI volume

comprised 48 oblique transverse slices with slice thickness 2mm, inter-slice gap 1mm and 2x2mm in-plane resolution (TR/TE=11340/30ms; echo spacing=0.69ms; matrix size=96x96 pixels; FoV=192x192mm, GRAPPA factor 2 in anterior-posterior phase encoding direction). The initial two brain volumes were discarded to allow for equilibrium of longitudinal T1 magnetization. B0 field-maps were acquired using two gradient echo sequences (TR=688ms; TE1/TE2=4.92/7.38ms, 3x3x3mm resolution, no inter-slice gap; matrix size=80x80pixels; FoV=192x192mm; phase encoding anterior-posterior) to allow correction of field inhomogeneity.

Volumetric structural brain MR images were also obtained in each participant. A sagittal 3-D magnetization prepared rapid gradient echo T1-weighted volumetric MRI (TR/TE=2200/2.9ms, dimensions 256x 256x208, voxel size 1.1x1.1x1.1 mm) was acquired on the same 3.0T Siemens scanner using a 32-channel phased-array head coil.

All structural and functional MR scans were visually assessed for quality control purposes by an experienced rater, based on coverage and movement artefact.

11.2.5 Post scan behavioural testing

Immediately after the scanning session two behavioural tests based on the fMRI conditions were administered, in order to assess each participant's ability to process relevant dimensions of musical memory.

To assess musical semantic memory, 24 (12 familiar, 12 unfamiliar) melodies from the set used during scanning were presented in randomised order and the task on each trial was to decide whether the tune was familiar or unfamiliar. The second test was designed to assess musical episodic recognition memory using novel musical stimuli. The participant was first asked to assess the pleasantness of three probe melodies (not

previously presented during scanning) and then, after a delay of 60 seconds, to identify these melodies among nine foil melodies (the task on each trial was to decide whether or not the melody had been presented earlier); this same procedure was repeated for a second set of probes and foils.

Participant responses were given verbally and recorded by the researcher. No feedback was given during either test and no time limits were imposed. Participant responses were recorded for off-line analysis.

11.2.6 Data analyses

11.2.6.1 Demographic and behavioural data

All statistical analyses were conducted using Stata version 12. Demographic characteristics and musical experience were compared between the control and patient groups using two sample t-tests and Wilcoxon rank sum; gender differences were assessed using a Pearson's chi-square test. Neuropsychological data were compared between study groups using Wilcoxon rank sum tests. Tone detection thresholds on audiometry screening and musical familiarity and repetition judgement results were analysed using linear regression models with clustered, robust standard error.

Performance data for the post-scan musical memory tasks were analysed using signal detection theory. Hit rate and false alarm rates were calculated and combined to create sensitivity measure d-prime (Z(Hit rate)–Z(False alarm rate). Two sample t-tests were used to compare d-prime values between participant groups on each task.

A threshold $p<0.05$ was accepted as the criterion of statistical significance for all tests.

11.2.6.2 Voxel-based morphometry data.

Structural brain MR images were compared between patient and control groups in a VBM analysis. Normalisation, segmentation and modulation of grey and white matter images were performed using default parameter settings in statistical parametric mapping software (SPM8; http://www.fil.ion.ucl.ac.uk/spm), with a Gaussian smoothing kernel of 6mm full-width-at-half-maximum. To help protect against voxel drop-out because of potentially marked local regional atrophy in particular scans, a customised explicit brain mask was derived by maximising the correlation between the binary mask and the average of the images to be analysed [329]. Regional grey matter volume was compared between patient and control groups and between syndromic groups using voxel-wise two sample t-tests, including covariates of age, gender and total intracranial volume. Statistical parametric maps of grey matter atrophy were thresholded at peak voxel level $p<0.05$ after family-wise-error (FWE) correction for multiple comparisons over the whole brain volume.

11.2.6.3 Functional MRI data.

Data from the fMRI experiment were pre-processed using SPM8. Scans for each participant were realigned using the first image as a reference, and unwarped incorporating field-map distortion information. DARTEL processing was used to spatially normalise individual scans to a group mean template image in MNI space. Normalised images were smoothed using a Gaussian smoothing kernel 6mm full-width at half-maximum.

Pre-processed images were entered into a first-level design matrix modelling each experimental condition as a separate regressor with boxcars of one-TR duration convolved with the canonical haemodynamic response function and six head movement regressors derived from the realignment process. First-level contrast images were

generated for effects of musical semantic memory (familiar > unfamiliar melody conditions), musical novelty (unfamiliar > familiar melody conditions), incidental musical episodic memory (repeat > first presentation of repeated melodies) and musical encoding (first > repeat presentation of repeated melodies). Contrast images for each participant were entered into a second-level random-effects analysis using T-tests to examine within- and between-group effects.

Contrasts were assessed at peak voxel level within small anatomical volumes of interest, as specified by our prior hypotheses based on previous functional neuroanatomical work in the healthy brain [367, 372-379, 386]. Relevant small volumes were derived from the Oxford Harvard Brain Atlas [387] in FSL view [275](Figure 11.1). These regions comprised an anterior peri-Sylvian region (combining inferior frontal gyrus, frontal operculum and anterior temporal cortex) and supplementary motor cortex, for the contrast assessing musical semantic memory; regions comprising posterior cingulate cortex, precuneus and hippocampi, for the contrasts assessing musical episodic memory and encoding; and the combination of these regions for the contrast assessing musical novelty (unfamiliarity) processing. A statistical threshold $p<0.05$ after family-wise error (FWE) correction for multiple comparisons ($p_{FWE}<0.05$) over the pre-specified region of interest was used in assessing all contrasts. For each contrast of interest showing a significant difference between patients and healthy controls, the voxel peak effect size (beta estimate value) was extracted for correlation with post-scan behavioural test performance.

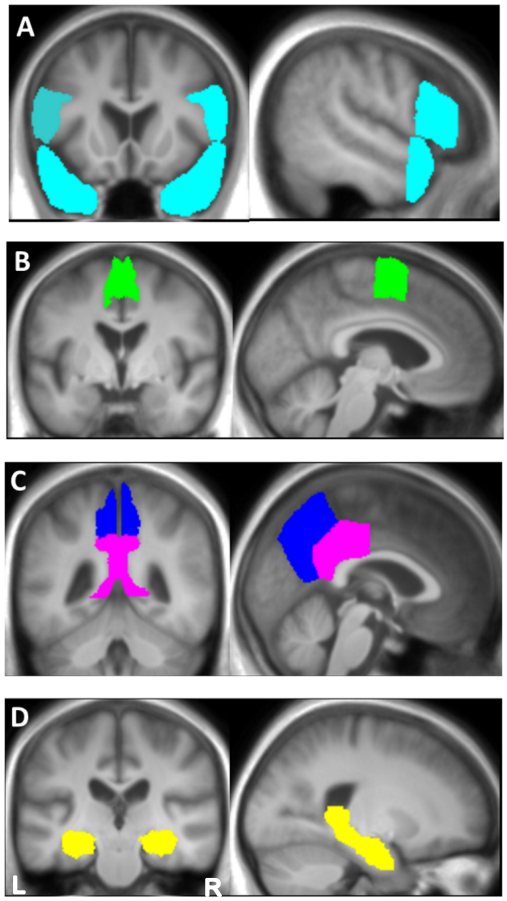

Figure 11.1 Anatomical small volumes used in analysis of fMRI data

Representative coronal (left) and sagittal (right) sections of the anatomically-defined small volumes used in the fMRI analysis are shown, projected on the study-specific group mean T1-weighted structural MR brain image. Anatomical regions were derived from the Oxford Harvard Brain Atlas [35] and created in FSL view [275], as follows: **A**, inferior frontal gyrus, frontal operculum and anterior temporal cortex (cyan); **B**, supplementary motor cortex (green); **C**, posterior cingulate cortex (magenta) and precuneus (blue); **D**, hippocampi (yellow). Volumes shown in **A** and **B** were used in analysis of the contrast assessing musical semantic memory; volumes shown in **C** and **D** were used in analysis of contrasts assessing musical episodic memory; and both regions were used in analysis of the contrast assessing musical novelty processing (see text).

11.3 Results

11.3.1 General characteristics of participant groups

Demographic, clinical and neuropsychological data for participant groups are summarised in Table 11.1. Patients and controls did not differ in age, gender, years of education, years of musical training or current musical listening. The patient groups did not differ significantly in symptom duration, but the tAD group had lower mean Mini-Mental State Examination score than the PCA group (p=0.04).

In keeping with the results presented previously, the syndromic groups showed the anticipated profiles of multi-domain cognitive impairment: relative to published norms, patients with tAD had deficits of verbal episodic memory, naming, arithmetic, visual processing and executive function while patients with PCA had markedly impaired visuoperceptual and visuospatial skills but relatively preserved episodic memory and verbal skills; comparing syndromic groups, the tAD group had significantly worse verbal episodic memory performance than the PCA group, and the PCA group had significantly worse visuoperceptual skills than the tAD group.

There were no significant effects of group membership on tone detection thresholds across frequencies ($F_{(2,53)}$=0.59, p=0.56).

11.3.2 Post scan behavioural data

Group performance data for the post scan behavioural tests are summarised in Table 11.1. Both patient groups performed significantly worse than the control group on the musical episodic memory task (tAD p=0.005, PCA p=0.03) but had unimpaired musical semantic memory (tAD p=0.7, PCA p=0.8). There were no significant performance differences between the patient groups. Performance on the musical episodic memory

test was correlated with performance on the musical semantic memory test (r=0.5, p=0.04) across the patient cohort. There were no significant correlations between any musical memory task and standard neuropsychological measures of memory (Recognition Memory Test for Words and Faces [260], all p>0.05).

11.3.3 Structural neuroanatomical data

The tAD and PCA groups showed the anticipated profiles of grey matter atrophy relative to the healthy control group (Figure 11.2). The tAD group showed widespread atrophy involving the hippocampi, temporo-parietal and postero-medial cortices, also extending to involve prefrontal cortices; while the PCA group showed relatively selective posterior atrophy preferentially affecting the parietal and occipital lobes.

There were no significant differences in grey matter atrophy profiles when the syndromic groups were directly compared (not shown).

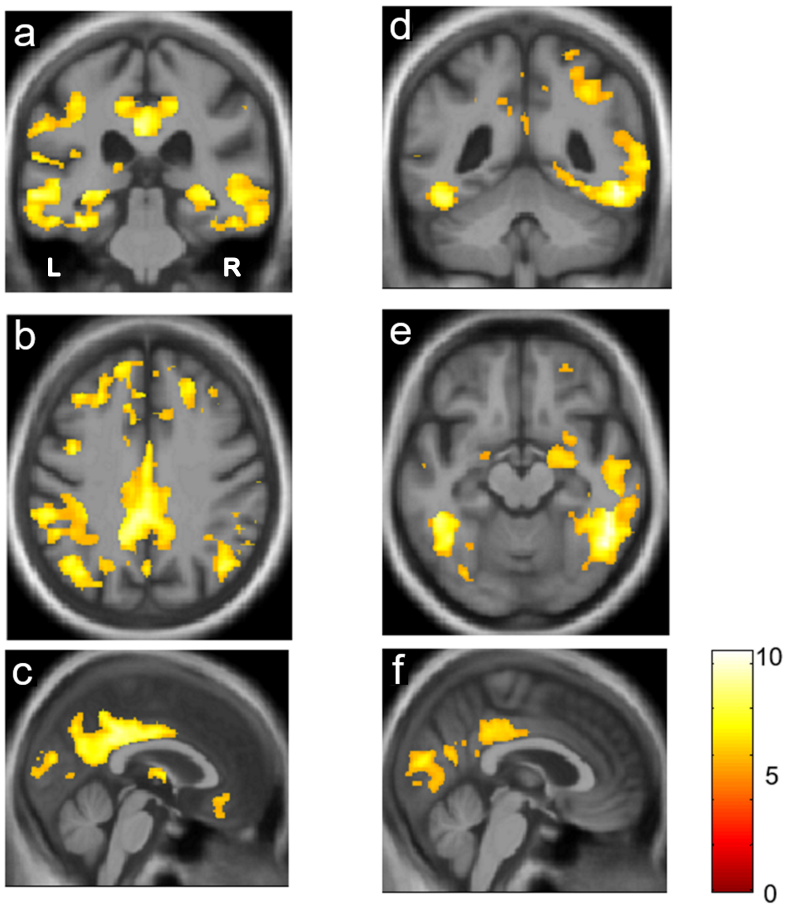

Figure 11.2 Regional grey matter atrophy profiles in the patient groups

Results of the voxel-based morphometry analysis showing statistical parametric maps (SPMs) of regional grey matter atrophy in the patient group with a memory-led syndrome of Alzheimer's disease (panels **a**, **b**, **c**) and the patient group with a syndrome of posterior cortical atrophy (panels **d**, **e**, **f**) relative to the healthy control group. SPMs are rendered on representative coronal (**a**,**d**), axial (**b**,**e**) and sagittal (**c**,**f**) sections of the group mean T1-weighted MR brain image in MNI space, thresholded at $p<0.05$ after family-wise-error correction for multiple voxel-wise comparisons over the whole brain volume. The colour bar codes voxel-wise t-scores of grey matter change across the patient cohort. Planes of sections have the following MNI coordinates (mm): **a**, y=-31; **b**, z=39; **c**, x=0; **d**, y=-49; **e**, z=-14; **f**, x=3. The right cerebral hemisphere is displayed on the right in coronal and axial sections.

11.3.4 Functional neuroanatomical data

Regional activation profiles for the musical contrasts of interest are summarised in Table 11.3. Statistical parametric maps are presented in Figure 11.3 (within participant groups) and Figure 11.4 (comparing patients and healthy controls). All contrasts were thresholded at $p<0.05_{FWE}$ after correction for multiple voxel-wise comparisons within the pre-specified anatomical small volume of interest.

Musical semantic processing (familiar > unfamiliar melody conditions) was associated in the healthy control group with significant activation of bilateral supplementary motor and anterior superior temporal cortices and right inferior frontal gyrus; and in the tAD group, with significant activation of bilateral supplementary motor cortex and left anterior superior temporal cortex. No significant activation for musical semantic processing was identified in the PCA group.

Musical novelty processing (unfamiliar > familiar melody conditions) was associated in the healthy control group with activation of right precuneus. There were no significant activations within either patient group for this contrast.

Comparing participant groups on the musical semantic memory contrasts revealed a significant activation difference (Figure 11.4) between the healthy control group and the tAD group in right inferior frontal gyrus. From inspection of plots of effect size (Figure 11.4), this interaction was driven chiefly by reduced activation to familiar melodies in the tAD group. There were no other significant activation differences between participant groups at the prescribed threshold.

Incidental musical episodic memory (repeat > first presentation of repeated melodies) and musical encoding (first > repeat presentation of repeated melodies) revealed no

significant activations within any participant group at $p<0.05_{FWE}$ within the pre-specified anatomical small volume of interest.

However, comparing groups revealed significant differences between the healthy control group and each of the patient groups for musical episodic memory processing: for the comparison between healthy control and tAD groups, this activation difference occurred in left precuneus while for the comparison between healthy control and PCA groups the activation difference occurred in right posterior cingulate cortex (Figure 11.4). From inspection of plots of effect size, the interaction versus healthy controls was driven for the tAD group chiefly by abnormal activation of precuneus (relative to baseline) during melody encoding; and for the PCA group, by abnormal activation of posterior cingulate cortex by repeated melodies. There were no significant activation differences between patient groups at the prescribed threshold.

In a regression analysis of out-of-scanner behavioural performance (d-prime) against peak effect size in the relevant anatomical regions, no significant correlations with output behaviour were found for the patient cohort for either the musical semantic memory or musical episodic memory contrasts (all $p>0.05$).

Group	Contrast	Region	Side	Cluster (voxels)	Peak (mm)			t-value	P
					x	y	z		
Healthy Controls	Familiar > unfamiliar	Supplementary motor	R	85	6	2	66	8.83	<0.001
		Supplementary motor	L	30	0	8	63	4.42	0.05
		Anterior superior temporal cortex	L	312	-54	14	6	6.78	0.003
		Anterior superior temporal cortex	R	90	58	14	-9	6.44	0.004
		Inferior frontal gyrus	R	55	58	26	18	6.28	0.006
	Unfamiliar > familiar	Precuneus	R	95	14	-58	18	7.43	0.006
tAD	Familiar > unfamiliar	Supplementary motor	L	49	-6	6	63	5.03	0.006
		Supplementary motor	R	25	8	6	63	4.89	0.008
		Anterior superior temporal cortex	L	38	-52	10	-12	4.91	0.033
Control > tAD	Familiar > unfamiliar	Inferior frontal gyrus	R	13	60	24	15	4.46	0.032
	Repeat > 1st presentation	Precuneus	L	13	-4	-56	42	4.21	0.049
PCA > Control	Repeat > 1st presentation	Posterior cingulate cortex	R	20	6	-22	33	5.73	0.002

Table 11.3 Summary of fMRI data within and between participant groups

Cerebral activations significant at peak voxel threshold $p<0.05_{FWE}$ after correction for multiple voxel-wise comparisons within the pre-specified anatomical volume of interest are shown, for clusters >10 voxels; coordinates of local maxima are in MNI space. Significant within-group contrasts are presented above and significant between-group comparisons below (the contrasts between familiar [widely-known] and unfamiliar [newly-created] melody conditions refer to familiarity prior to scanning, i.e., musical semantic memory or musical novelty; the contrasts between repeat [second] and first presentations refer to melodies heard [musical events] during scanning, i.e., musical episodic memory).

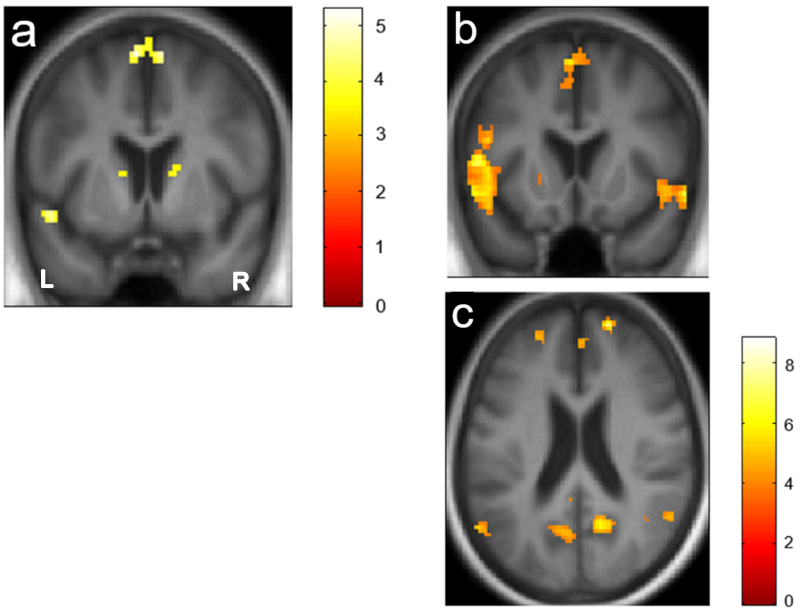

Figure 11.3 Functional neuroanatomy of musical memory: within-group correlates for patients and healthy controls

Statistical parametric maps (SPMs) show all significant regional brain activations for musical memory contrasts within participant groups; significant activations were demonstrated in the patient group with memory-led Alzheimer's disease (panel **a**) and in the healthy control group (panels **b**,**c**). Contrasts forming SPMs were as follows: **a,b** previously familiar [widely-known] > unfamiliar [newly-created] melody conditions (musical semantic memory); **c**, unfamiliar > previously familiar melody conditions (musical novelty). SPMs are rendered on coronal (**a,b**) and axial (**c**) sections of the group mean T1-weighted structural MR brain image, thresholded for display purposes at $p<0.001$ uncorrected over the whole brain volume; sections have been selected to show activations significant at $p<0.05$ after family-wise-error correction for multiple voxel-wise comparisons within the pre-specified small anatomical volumes of interest (see Table 3). Colour bars alongside panels **a** and **c** code voxel-wise activation t-scores in the AD group and the healthy control group. Planes of sections have the following MNI coordinates (mm): **a**, y=6; **b**, y=16; **c**, z=22. The right cerebral hemisphere is displayed on the right in all panels.

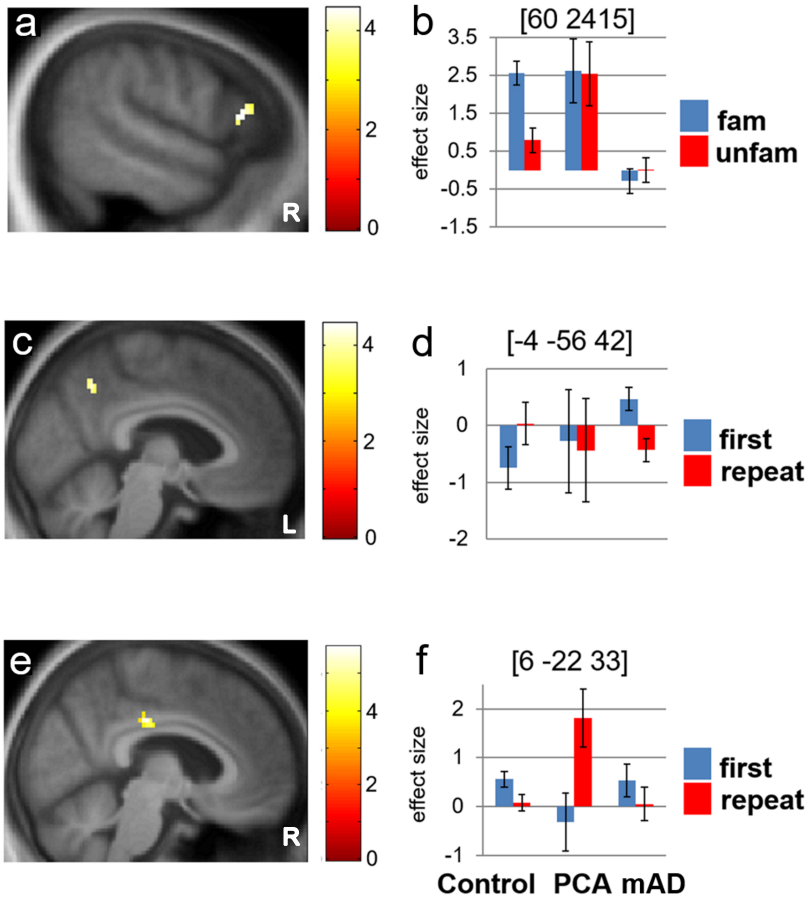

Figure 11.4 Functional neuroanatomy of musical memory: patients compared with healthy controls

Panels **a** and **b** compare the tAD and healthy control groups in the musical semantic memory contrast (previously familiar > unfamiliar melody conditions); panels **c** and **d** compare the tAD and healthy control groups in the musical episodic memory contrast (repeat > first melody presentations); panels **e** and **f** compare the PCA and healthy control groups in the musical episodic memory contrast (see also text and Table 11.3). Statistical parametric maps (SPMs) of significant differences in regional brain activation between groups are presented in panels **a**, **c**, **e**; plots of peak voxel condition effect size (mean beta parameter estimate ± standard error, with MNI coordinates of corresponding local maxima) are presented in panels **b**, **d**, and **f**. SPMs are rendered on sagittal sections of the group mean T1-weighted structural MR brain image, thresholded for display purposes at p<0.001 uncorrected over the whole brain volume; activations shown

were significant at $p<0.05$ after family-wise-error correction for multiple voxel-wise comparisons over the anatomical small volume of interest. Colour bars alongside panels **a**, **c** and **e** code voxel-wise activation t-values for each comparison. **Control,** healthy control group; **fam**, previously familiar melodies condition; **first**, first presentation of repeated melodies; **PCA**, patient group with a syndrome of posterior cortical atrophy; **repeat**, second presentation of repeated melodies; **tAD**, patient group with a syndrome of memory-led Alzheimer's disease; **unfam**, unfamiliar melodies condition.

11.4 Discussion

This chapter describes a functional neuroanatomical basis for alterations of musical memory in tAD and its major 'visual' variant syndrome, PCA. Both tAD and PCA groups showed neuropsychological profiles and regional atrophy patterns in line with previous studies [101, 381].

As per the prior experimental predictions, relative to the healthy control group both syndromic groups showed altered activation of postero-medial cortical regions during episodic processing of repeated melodies and the tAD group additionally showed altered activation of inferior frontal cortex during semantic processing of familiar (relative to unfamiliar) melodies.

Out-of-scanner behavioural testing demonstrated the anticipated neuropsychological profiles of impaired musical episodic memory but retained musical semantic memory in both patient groups: however, behavioural performance in the patient groups did not correlate with brain activation profiles, suggesting these profiles may represent true disease signatures rather than simply compensatory effects.

During processing of familiar melodies, both the control and tAD groups showed activation of a predominantly anterior fronto-temporal cortical network previously implicated in musical semantic memory in healthy brain [367, 372-375] (Figure 11.3). Involvement of anterior temporal cortex is consistent this region integrating domains of semantic knowledge and previous evidence that anterior temporal degeneration is associated with impaired recognition of familiar music [388, 389]. Inferior and dorso-medial prefrontal regions may be engaged in anticipating syntactical structure in familiar music and implicitly preparing motor responses [390, 391]. The healthy control group showed activation of right precuneus by previously unfamiliar melodies: this response was lost in the patient groups, consistent with Alzheimer's disease pathology affecting the hippocampus and linked temporo-parietal circuits that decode musical novelty [380, 390, 392].

The lack of a significant difference between patient and control groups on the musical novelty contrast may simply reflect the relatively small cohort size here; alternatively, it may imply that the neuroanatomical substrates of novelty processing within the distributed functional network vary widely between individuals, which could plausibly reflect the complex behavioural and experiential influences that modulate the novelty value of particular stimuli (i.e., musical novelty is not simply the cognitive 'mirror image' of familiarity [392]). Although inferior frontal cortex is not a classical site of pathological involvement in Alzheimer's disease and did not emerge as a site of significant disease-related atrophy in the present Alzheimer's disease cohort (Figure 11.2), reduced activation of this region by familiar melodies in the tAD group relative to the healthy control group here might reflect an abnormal interaction of fronto-temporo-parietal brain networks that decode novelty and familiarity [392]. In contrast, dorsal medial prefrontal cortex did not emerge as a functional locus of altered musical semantic processing in either Alzheimer's disease syndromic group: as proposed by Jacobsen and colleagues

[367]. This region may be relatively resistant to the effects of Alzheimer's disease pathology and may therefore provide a substrate for relative preservation of musical semantic memory in Alzheimer's disease.

No within-group functional neuroanatomical correlates of incidental episodic melody processing were identified at the prescribed threshold. This is in line with previous work employing a similar paradigm in the healthy brain [367]; melody repetition is likely to be less salient than prior familiarity, particularly where, (as here) there is deliberately no task demanding active recall or recognition during scanning. Nevertheless, incidental processing of repeated melodies left its traces in the comparison between patients and healthy controls (Figure 12.4). The tAD group failed to deactivate precuneus normally on first presentation of melodies (implicit melody encoding) while the PCA group showed abnormally increased activation of posterior cingulate cortex on second presentation of melodies (implicit melody recollection). Postero-medial cortex constitutes a principal projection zone of the hippocampal outflow [393] and a core target of Alzheimer's disease pathology, here as in previous studies [177] (Figure 11.2). However, the over-activation of this region in patients relative to healthy controls argues against this being simply signal attenuation due to atrophy. While information for melodies remains limited, these findings fit with previous fMRI evidence for the processing of other kinds of memory by postero-medial cortex. Task-induced deactivation of postero-medial cortex has been shown to predict successful memory formation in both younger and healthy older cohorts [394, 395], whereas memory impairment in Alzheimer's disease has been linked to impaired deactivation and paradoxical activation of postero-medial cortex [219, 396, 397].

The precise functions of the subregions composing postero-medial cortex and the impact of different Alzheimer's disease phenotypes on these subregions contine to be defined. However, the syndromic profiles for incidental musical episodic memory observed here

are consistent with findings from studies examining other cognitive domains. Behaviourally, tAD is associated with impaired memory encoding while PCA has been found to be particularly associated with impaired memory retrieval [398]; this would predict relatively greater disruption of melody encoding (first presentation of melodies) in tAD and relatively greater disruption of melody retrieval (second presentation of melodies) in PCA, as indexed by condition-specific activation profiles here (Figure 11.4). In tAD, dysfunction of the precuneus might impair the preparation of responses to external sensory events and encoding of those events into memory [395]; while in PCA, dysfunction of posterior cingulate cortex might underpin impaired attentional shifts across internal states (for example, during re-awakening of memories) as well as the external sensory environment [361, 399]. The correlation between musical semantic and episodic memory performance seen here argues for at least some functional inter-dependence of these two musical memory systems. The overall balance of effects observed may depend on the particular musical memory paradigm employed.

These findings substantiate previous evidence that musical memory in Alzheimer's disease is not one process. In the patient cohort in this study, behaviourally observed deficits of incidental musical episodic memory led deficits of musical semantic memory both in tAD and PCA. This differential vulnerability of musical memory is underpinned by separable functional neuroanatomical substrates: the core region for altered musical episodic processing in both Alzheimer's disease and PCA lies within the postero-medial cortical 'hub' zone of the core 'default-mode' network targeted by Alzheimer's disease pathology. The key functional neural substrate of musical semantic memory however lie in prefrontal cortex and the impact of different Alzheimer's disease phenotypes on this anterior substrate appears to be more variable. Taken together, these findings suggest that heteorogentity of musical memory deficits exist both in different memory systems and between individual patients with Alzheimer's disease [364-367, 369-371]. The

neuroanatomical profiles identified here and the complexity of functional alterations (in particular, abnormal increased activations) produced by Alzheimer's disease relative to the healthy brain underline the potential of music to capture dynamic disease-associated effects in vulnerable neural networks. The present findings add to a growing body of evidence suggesting that disordered analysis of complex auditory environments may be a robust and relevant functional marker of Alzheimer's disease pathology.

This study has several limations and raises important issues for future work. Most fundamentally, the deliberately simple, task-free fMRI paradigm deliberately does not model much of the complexity of musical semantic and episodic memory. These memory systems are likely to involve multiple components and levels to encoding and retrieval, for example, explicit melody recognition and recall of musical episodes often entails the activation of associated knowledge about musical objects and associated detail about musical events. Future studies should begin to disentangle this complexity and also address the effects of explicit memory tasks and dimensions such as musical emotion that are likely to have potent modulatory effects.

The PCA group here was relatively small; the findings described here should be further corroborated in larger cohorts, covering the full phenotypic spectrum of Alzheimer's disease, and ultimately with histopathological correlation. It will be important to assess the wider population of Alzheimer's disease and in particular the more frequent scenario of older age onset. It remains unclear how musical memory evolves over the clinical course of Alzheimer's disease: this will only be established by longitudinal study of episodic and semantic musical memory in Alzheimer's disease, ideally including presymptomatic carriers of pathogenic mutations.

It is also likely that profiles of musical memory (including the relative prominence of episodic and semantic deficits) differ between Alzheimer's disease and other

neurodegenerative proteinopathies [364, 369]. Therefore behavioural and neuroanatomical correlates of musical memory in these diseases should be compared directly and assessed in relation to other components of music cognition [364, 369, 400].

The roles played by particular components of the musical memory networks implicated here will only be fully elucidated by paradigms that incorporate techniques with high temporal resolution (such as magnetoencephalography) that can track dynamic connectivity shifts between memory phases and among brain regions.

Taking these limitations into account, musical memory may be a flexible, clinically relevant tool to define behavioural and functional neuroanatomical signatures of Alzheimer's disease that reflect the autobiographical and emotional resonance of music in everyday life. Improved understanding of musical memory in Alzheimer's disease may in turn inform rational music-based therapies. Music already provides a welcome source of comfort for patients and their caregivers. However, music-based therapies may have cognitive benefits beyond enjoyment and improved quality of life [401]. Work such as this has the potential to guide the development of such therapies, by suggesting relevant targets within the domain of music cognition and providing surrogate therapeutic markers of altered brain function.

12 General discussion

12.1 Summary of findings

This thesis has recruited a cohort of 45 individuals with YOAD across the phenotypic spectrum of Alzheimer's disease and 24 matched healthy controls to investigate clinical heterogeneity, evidence for selective vulnerability, and potential genetic factors underpinning this. The clinical, neuropsychological and regional grey matter atrophy profiles of individuals with YOAD are described by both *APOE* ε4 status (Chapters 7 and 9) and phenotype (Chapter 11). The effect of *APOE* ε4 status on microstructural white matter changes, and how alterations in white matter microstructure relate to clinically observed neuropsychological deficits is explored in Chapter 10. The effect of a rare TREM2 variant, p.R47H, on phenotype is investigated in Chapter 8. Mechanisms underpinning aspects of memory processing in different YOAD phenotypes are explored in Chapter 11 using musical stimuli and activation fMRI to study functional brain network changes.

Setting up and recruitment to the YOAD study

The YOAD study (methods described in Chapter 5, participant recruitment and clinical features described in Chapter 6) was set up to be a representative sample of patients with sporadic YOAD with evidence for Alzheimer's disease pathology where possible, in the absence of significant vascular disease, and to include a representative range of phenotypes including amnestic, posterior cortical atrophy, logopenic aphasia and frontal Alzheimer's disease. Participants were assessed using a range of clinical measures and neuropsychological batteries, and underwent multimodal MRI and genetic testing. This body of work paved the way for the investigation of phenotypic diversity in subsequent chapters.

Genetic heterogeneity in the YOAD study

In Chapter 7 I examined for the presence of any autosomal dominant mutations in genes known to cause dementia using next generation sequencing on a customised 'dementia panel'. Despite patient participants only being recruited in the absence of a family history suggestive of autosomal dominant disease, one individual was found to be harbouring a pathogenic *PSEN1* variant that has previously been described in families in the UK and Mexico. He was excluded from analyses of psychology, brain volumes and grey matter VBM, but had already been included in the analyses of Chapters 10 and 11.

The *APOE* ε4 allele, a low frequency variant with intermediate effect was over represented in the YOAD cohort relative to population data. However, individuals homozygous for ε4 did not have the youngest age of clinical disease onset, hence the common tenet that *APOE* ε4 reduces age at onset does not apply to patients with young onset disease.

Variant AD presentations were more common in the ε4-ve cohort, and these individuals were more impaired in non-memory cognitive domains than those who did carry an ε4 allele. Hence *APOE* ε4 contributes to, but does not fully explain heterogeneity in YOAD – there must be other factors yet to be determined. Importantly, I show that there is no clear relationship between the canonical AD syndromes – and PCA in particular – with *APOE* genotype.

Other rare genetic variants – TREM2

TREM2, a rare but significant risk factor for Alzheimer's disease may be one such other genetic factor, but provisional analyses presented in this thesis suggest it drives age at onset more than phenotype.

Chapter 8 uses sanger sequencing and p.R47H genotyping in cohorts of individuals with Alzheimer' disease, frontotemporal dementia and healthy controls to investigate whether this TREM2 variant is a risk factor or phenotypic modifier in patients for Alzheimer's disease alone, or a more general risk factor for neurodegeneration with other pathologies. I found it to be confirmed as a risk factor for Alzheimer's disease, but not for frontotemporal dementia. The individuals with p.R47H associated Alzheimer's disease had significantly earlier symptom onset than individuals with no TREM2 variants. Heterozygous p.R47H AD appeared to be memory led and otherwise indistinguishable from "typical" sporadic AD.

The role of APOE E4: brain volumes and grey matter atrophy

In Chapter 9 I investigated regionally specific effects of *APOE* genotype on brain atrophy using brain, hippocampal and ventricle volumes, and grey matter VBM analyses. ε4+ve patients tended towards having more atrophy in the medial temporal lobes, and ε4-ve individuals having more atrophy throughout the neocortex, broadly aligning with neuropsychological profiles described in Chapter 7. Whilst *APOE ε4* status is associated with regional vulnerability to neurodegeneration the reasons why the neocortex, especially the frontal and parietal lobes, are more vulnerable to tau pathology and neurodegeneration in patients who develop Alzheimer's disease despite lacking *APOE* ε4 is unclear and warrants further study. Other genetic risk factors may have an unmasked disproportionate effect in the absence of ε4, with their variability explaining the greater heterogeneity in ε4-ve YOAD.

The role of APOE and microstructural WM changes

Chapter 10 looked at whether considering Alzheimer's disease as a network disease and examining at microstructural white matter track damage may provide further insights to clinical heterogeneity. DTI and NODDI with tract-based spatial statistics were used to

investigate *APOE* ε4 modulation of white-matter damage in a subset of 37 patients with YOAD and 23 age-matched controls.

In contrast to the grey matter VBM analyses in Chapter 9, microscopic white-matter disruption tended towards being more widespread in ε4+ individuals and more focal (posterior predominant) in the absence of an ε4 allele, however there were no significant differences between groups when compared directly. NDI effect maps showed ε4-ve patients had greatest NDI reduction relative to ε4+ve in the right parietal lobe white matter projections; and ε4+ve patients had greatest reduction in NDI relative to ε4-ve in the left temporal lobe projections which was more consistent with grey matter analyses showing ε4+ve as a more hippocampal disease.

NODDI metrics also indicated that observed changes in fractional anisotropy are underpinned by combinations of axonal loss and morphological change. Regional NDI correlated with some measures of focal neuropsychological deficit, giving indirect evidence that the model of neurite density loss reflects disconnection and loss of function.

Investigating the functional basis of memory impairment in Alzheimer's disease variants

In Chapter 11 I set out to explore how phenotype in the YOAD cohort relates to changes in brain function using activation fMRI. Both the atrophy profile and neuropsychological profiles by phenotype were consistent with current formulations of typical memory led Alzheimer's disease and PCA. Music was used to study brain function with activation fMRI as characteristics of music can be augmented to study different aspects of information processing. The paradigm used explored memory processing, for melodies that are 'familiar' well-known tunes to model semantic memory for music, and motifs that were repeated during the scanning session to model 'episodic memory' processing.

Both typical memory led Alzheimer's disease and PCA groups showed significant functional neuroanatomical alterations relative to the control group. For musical semantic memory, disease-associated activation group differences were localised to right inferior frontal cortex (reduced activation in the group with memory-led Alzheimer's disease); while for incidental musical episodic memory, disease-associated activation group differences were localised to precuneus and posterior cingulate cortex (abnormally enhanced activation in the syndromic groups). In post-scan behavioural testing, both patient groups had a deficit of musical episodic memory relative to healthy controls whereas musical semantic memory was unimpaired

This demonstrates functional neuroanatomical substrates for the differential involvement of musical semantic and incidental episodic memory in major phenotypes of Alzheimer's disease and suggests that musical memory is a useful paradigm to probe neural network function in Alzheimer's disease. Different activation profiles in the hub of the default mode network in typical Alzheimer's disease and posterior cortical atrophy suggests there is differential vulnerability within a common 'faulty' network, that is consequently (mis)behaving in different ways, and manifests as different clinical phenotypes.

12.2 Limitations

Cohorts

The YOAD study cohort recruited for this thesis was relatively small, reflecting the rarity of young onset Alzheimer's disease. This may account for the lack of significant differences when comparing imaging metrics between patient groups directly. Logopenic and frontal Alzheimer's disease phenotypes were also relatively under-represented, as patients with these phenotypes were often recruited for other studies running concurrently at the Dementia Research Centre.

Given the increasing emphasis on biomarker evidence of Alzheimer's disease in research criteria, it would have been ideal for all patient participants in the study to have supporting molecular biomarker evidence, but some individuals did not wish to have a lumbar puncture and there was no access to amyloid PET imaging at the time of recruitment.

The genetic cohort used in Chapter 8 to investigate the frequency of TREM2 variants in Alzheimer's disease and frontotemporal dementia was acquired over two decades and so comprehensive use of research diagnostic criteria could not be confirmed. Age of clinical disease onset for individuals was also not universally recorded. Some samples were classified based on clinical diagnoses only, and hence it is possible that clinical diagnoses did not reflect the underlying pathology (for example, an individual with frontal presentation of Alzheimer's disease could easily have been clinically (mis)diagnosed with frontotemporal dementia). This may account for the differences observed in strength of association between p.R47H and frontotemporal dementia observed across other studies. Further studies are warranted, ideally with post mortem confirmation of the underlying pathology, or using other biomarkers (e.g. CSF tau and Aβ1-42 or amyloid imaging) to corroborate clinical diagnoses. The clinical information reviewed retrospectively for individuals found to have p.R47H variants in Alzheimer's disease was also limited and had been collected and recorded in a non-standardised manner, making my conclusions preliminary and in need of corroboration from large multicentre prospective studies to establish the true spectrum of clinical features, neuroimaging and pathological signatures of *TREM2* variants in Alzheimer's disease.

Sample size calculations

As outlined in the previous section, this study was small and exploratory. Formal sample size calculations were not performed. There is empirical evidence in activation fMRI

[402], voxel based morphometry [403] and theoretical data [404] to suggest a sample size of as few as ~10-20 subjects is sufficient to detect group differences in key primary neuroimaging outcome measures ($p<0.05$ corrected for multiple comparisons over the entire brain). However, these sample sizes are for detecting differences between patient and control groups, the sample size for detecting differences with a disease group will be much higher.

Given the number of techniques used in this thesis it would potentially require many sample size calculations for each chapter: e.g. in Chapter 10 calculations could be done for each of the DTI indices between the groups.

For novel techniques the expected measured effect size attributable to disease (or specific genetic risk factor within two disease groups), is unknown and would also need to be estimated.

The lack of power calculations used in this body of work means that a negative statistical result when comparing two groups does not differentiate between (i) there being no true effect and (ii) there being an effect that is present but not detected due to the study being underpowered. In taking this work forward I would consider using an approach similar to that employed in Mahoney *et al*., 2015 [405] whereby longitudinal data is collected and sample sizes required for future clinical trials calculated using annualised change scores in potential outcome measures (e.g. NDI in a region of interest).

Genetics

Genetic analyses for autosomal dominant causes of Alzheimer's disease were not available until after the diffusion MRI and activation fMRI analyses had been completed. Whilst no individual included had a family history supportive of an autosomal dominant cause, the lack of genetic screening at entry to the study resulted in the one individual

with a *PSEN1* variant being included in Chapters 10 and 11. He presented with a memory led phenotype and was an ε4 heterozygote. It is possible, but unlikely, that the inclusion of a single individual with an autosomal dominant mutation in a subgroup of 22 patients with an ε4 allele significantly changed the results presented in Chapter 10. Ideally in studying the differential effect of *APOE* ε4, individuals with autosomal dominant disease would be excluded to try to remove a potential confounder for any differences found between groups being attributed to *APOE* ε4 status. The activation fMRI experiment described in Chapter 11 set out to investigate how phenotype related to regional brain activation changes, so arguably the effect of this individual (with a typical memory-led phenotype) being included in this chapter is less marked than in Chapter 10, as differences were not being associated with a genotype.

Finally, Alzheimer's disease is a complex genetic disease, and any associations of *APOE* ε4 with clinical features or neuropsychological profile (Chapter 7) and changes in brain structure (Chapters 9 and 10) observed here are likely an oversimplification and occur in the context of attenuation by a milieu of other genetic and environmental factors, the contribution of which has not been studied.

Imaging techniques and models

The MRI techniques used in this thesis each have a number of limitations. Individuals with severe claustrophobia or other physical restrictions (e.g. morbidly obese, severe kyphoscoliosis) are unable to tolerate the physical restriction of MRI scanning. During YOAD cohort recruitment this resulted in one control and one participant not entering the study (in both cases due to claustrophobia), however this was a small number overall. Furthermore, a small number of both controls and patient participants moved during certain MRI sequence acquisitions, resulting in movement artefact precluding use of the scans for some analyses.

As with all biophysical models, the structural and functional imaging techniques used in this thesis all require a number of assumptions. The imaging metrics may not perfectly reflect the underlying pathological changes in Alzheimer's disease, but can give insight and estimates of atrophy, changes in brain microstructure, and brain activation. Voxel based morphometry includes a number of pre-processing steps, namely tissue classification, spatial normalisation and spatial smoothing (required due to not being able to perfectly warp one brain so that it matches another), followed by statistical analysis. Whilst a model, it has become a widely used and accepted method. DTI models each voxel as a single compartment to give an estimate of the fraction of anisotropic water from which inferences about brain microstructure are made. DTI cannot model crossing fibres. NODDI modelling is arguably more reflective of underlying brain microstructure as it models three different diffusion compartments. However, it's model of axon orientation still cannot account for crossing fibres, the value of intrinsic diffusivity is fixed over the whole brain, and intra-neurite diffusion is modelled as being completely restricted within a collection of impermeable sticks. It is likely that this also does not fully characterise all pathological processes involved in neurodegenerative diseases (e.g. Alzheimer's disease) but starts to explain some of the factors underpinning changes in fractional anisotropy seen on DTI. White matter hyperintensities are also not accounted for in either of the diffusion models used in this thesis. Future work should look at whether white matter lesion loads can be quantified and included as a covariate in the analyses. Activation fMRI cannot measure the magnetic fields associated with neural activity directly as they are too small to be localised using MRI. The MRI signal associated with the vascular response to the neural activity (the BOLD signal) depends on the blood's velocity, volume fraction and oxygenation, and is only qualitative rather than quantitative. Activation fMRI is also vulnerable to the presence of physiological noise and physiological data was not separately accquired during scanning, instead relying on processing to remove this from the model. The application of task based fMRI

to patients with cognitive impairment can be challenging, so the paradigm I used was kept deliberately simple and task-free to make it accesbile to people with cognitive impairment. Whilst the music paradigm employed does not model all of the complexity of musical semantic and episodic memory, within these limitations it appears to be useful for investigating aspects of memory processing in individuals with Alzheimer's disease.

12.3 Why clinical heterogeneity matters: Future Directions

As outlined in Chapter 2, diagnostic criteria developed for both clinical and research purposes have attempted to include and define atypical presentations of Alzheimer's disease. However, in view of the challenges posed by defining clinical heterogeneity, the most recent NIA-AA 2018 Research Framework acknowledge the difficulty of defining disease based on clinical features and have moved to a purely biological construct using biomarkers of Aβ1-42 deposition, pathologic tau, and neurodegeneration [169]. Whilst defining disease based on biomarkers is important, recognising, characterising and understanding rarer Alzheimer's disease variants is also important and should not be overlooked. Studying common and discordant genetic (and environmental) risk factors for typical and atypical Alzheimer's disease, combined with neuroimaging, cerebrospinal fluid and other biomarkers, may provide fundamental insights into Alzheimer's disease pathogenesis. It is entirely plausible that different risk factors modulate the rate, timing and site of amyloid deposition; whether or when amyloid deposition leads to neurodegeneration; and which neuronal networks bear the brunt of the disease. This in turn may influence how pathology spreads through the brain, and what symptoms predominate.

Cohorts

Findings from this thesis should be further corroborated in larger cohorts, covering the full phenotypic spectrum of Alzheimer's disease, ideally with biomarker evidence of

underlying Alzheimer's disease pathology and ultimately, with histopathological correlation. It will be important to also assess how applicable my findings are to the more frequent scenario of Alzheimer's disease occurring with late age of onset.

Longitudinal studies

Whilst the YOAD study set up as part of this thesis included a one year follow up visit with repeat clinical, neuropsychological assessments, and neuroimaging, only cross-sectional analyses are presented here. Longitudinal analyses are required to assess how heterogeneity evolves over time, whether the MRI techniques employed here are reproducible and capable of detecting interval change, and over what periods of time this change can be detected. For example, if NODDI can reliably detect microstructural brain changes over shorter intervals than volumetric MRI can track macrostructural brain atrophy, this could enable clinical trials to be conducted over shorted time periods. Equally, it is important to understand whether these imaging techniques can be useful in the pre-symptomatic period of Alzheimer's disease, and help define the optimal point in the disease course for a disease modifying therapy to be given.

Polygenic risk scores

The genetic architecture of Alzheimer's disease likely includes many common variants with small effect that are likely to reflect a large number of susceptibility genes and a complex set of biological pathways related to disease. The effect of these have not been studied or accounted for in the *APOE* and *TREM2* analyses in this thesis. A way forward may be to look at 'polygenic' risk scores and consider how they are associated with clinical heterogeneity.

In addition to identifying susceptibility alleles for complex diseases, GWAS can identify common single nucleotide polymorphisms that show disease association but do not

meet genome wide significance. Considering these weak effect loci significantly increases the estimated heritability detected in AD [406]. Polygenic risk scores are estimated using both the genome-wide-significant polymorphisms and other nominally associated variants (typically thousands) at a lower significance threshold. Their use can increase the accuracy of Alzheimer's disease prediction models [407], so may in the future prove useful for calculating the genetic risk profile of an individual for developing Alzheimer's disease. Measures of polygenic disease burden in Alzheimer's disease could also help clinical trial design, and lead to better understanding of how gene-environment interactions affect the development of AD.

Neuroimaging

Advances in neuroimaging techniques, MRI physics and image analysis techniques including machine learning will all aid our study of clinical heterogeneity in Alzheimer's disease in the future.

The development of ultra-high field 7T MRI offers superior signal-to-noise and spatial resolution relative to the 3T MRI used in this thesis. Whilst not currently widely available, the increase in image resolution afforded by 7T MRI gives the potential for brain microstructure, such as cortical layers, hippocampal subfields, and potentially even amyloid plaques, to be imaged *in vivo* [408].

Amyloid and tau molecular PET imaging is also transforming neuroimaging in Alzheimer's disease research by making it possible to assess the regional distribution of proteinopathy and how it changes over time *in vivo* during life [409]. It will be possible to better understand how amyloid and tau pathology relate to each other, and to the associated phenotype and underlying genotype.

Multimodal imaging, including techniques to combining PET and MRI [410]. and large multicentre studies using multimodal imaging protocols, such as the Human Connectome Project [411], are studying how molecular and metabolic changes relate to the anatomy and function of the brain and clinical presentation.

New therapeutic targets in Alzheimer's disease

Identifying *TREM2* variants as risk factors for AD has led to research into the pathobiological mechanisms this microglial receptor mediates. *p.*R47H variants cause partial loss of function of *TREM2* in *in vitro* studies [412]. This is thought to impair the response of microglia to amyloid pathology by preventing a switch from a homeostatic to neuroprotective disease-associated phenotype, and/or interfering with tonic TREM2 signalling required to support microglial metabolism and the ability to respond to stressors. As more is understood about the pathways involved, therapeutic targets to augment this inflammatory response may be identified.

Towards a unifying model for understanding heterogeneity in YOAD

Whilst each individual technique used in this thesis offers insights into heterogeneity, methods to combine modalities are described [413] but not well established. These multimodal techniques need to be further refined in order to study how genetic variation interplays with structural and functional brain networks, and clinical manifestation.

Nexopathies [207] and the network paradigm of neurodegenerative disease [357] as outlined in Chapter 2 offer hypotheses that can potentially be tested to better understand the basis clinical heterogeneity. For example, the molecular nexopathy paradigm makes specific predictions about the sequence of regional involvement with particular proteinopathies. The 'problem' of heterogenetiy may be resolved in part by mapping disease evolution using neuroimaging longitudinally. This is where fMRI and diffusion

weighted imaging techniques, such as DTI and NODDI, could be used to examine for convergent structural and/or functional changes across the brain over time Specifically, in variant forms of Alzheimer's disease, differential involvement of cortico-cortical projection zones that are part of a core Alzheimer's disease vulnerable network may explain the atypical phenotypes that characterise posterior cortical atrophy and logopenic aphasia.

We will also need to understand how genetic differences not only relate to these structural and functional imaging metrics, but the mechanisms by which they do so, and how this is augmented by environmental factors. Innoculation studies and tracer studies in animal and stem cell models, will continue to further our understanding of how proteins can spread through a brain network. The basis of the interaction between proteins and specific brain networks, or parts of a network, can be studied by developing model neural circuits in vitro [414] to examine effects on cellular transport, morphology and cell-cell interactions, and computational modelling of artificial neural networks.

Implications for clinical trials

The diversity of Alzheimer's disease may in part account for the failure to date to develop effective disease modifying therapies. Better understanding of syndromic inhomogeneity may disentangle its confounding effects in clinical trials. We may also use heterogeneity to our advantage by using it to enrich study populations for specific interventions, or selecting individuals with certain genotypes or phenotypes to allow clinical trials to be powered using smaller cohorts. Improved understanding of the determinants and natural history of network disintegration would enable more accurate tracking of disease evolution and potentially enable prediction of clinical course.

Furthermore, understanding the factors that influence the initiation, spread and differential vulnerability seen in atypical Alzheimer's disease variants may lead to new

targets for therapy and allow for better tailoring of existing therapies to individuals. Just as treatments in other fields of medicine have moved towards a more personalised approach, such as Herceptin for individuals with breast cancer overexpressing the *HER2* gene [415], a similar approach is likely to be possible, and perhaps necessary, in Alzheimer's disease therapy. There are already examples of how *APOE* ε4 status affects response to potential new therapeutic agents in clinical trials, such as the increased risk of intracerebral vasogenic oedema and haemorrhage seen in relation to *APOE* genotype in a trial of bapineuzamab, a monoclonal antibody against amyloid [139]. This is hypothesized to be related to the presence of more cerebral amyloid angiopathy in ε4 carriers. Equally, genetic differences between familial Alzheimer's disease and apparent sporadic disease are likely to be important. For example, *in vitro* studies suggest that some presenilin variants are associated with resistance to inhibitors of γ-secretase inhibitors [416]. Hence, if a clinical trial did not show efficacy using a familial Alzheimer's disease cohort, it does not necessarily follow that the agent would also be ineffective for individuals with sporadic Alzheimer's disease. Clinical trial participant selection on genetic basis is also being used in studies of individuals 'at risk' for Alzheimer's disease, offering an opportunity to intervene before Alzheimer's pathological changes become clinically manifest disease, with certain studies recruiting individuals with autosomal dominant familial Alzheimer' disease [132, 133], *APOE* ε4 homozygotes [133] and Downs Syndrome [417].

Implications for clinical practice

As a clinician faced with a patient, it is important to recognise that Alzheimer's disease can present with non-memory symptoms and signs, and that these other cognitive domains can also be affected in individuals with a more typical amnestic presentation, as the disease progresses. Early and more accurate diagnosis will become ever more

important should a disease modifying therapy become available, and tailored support and guidance is important for symptomatic management regardless.

12.4 Conclusions

This thesis has explored the clinical heterogeneity in young onset Alzheimer's disease and investigated some of the genetic factors underpinning this. *APOE* ε4 genotype contributes to, but does not fully explain clinical heterogeneity, with the youngest ages of onset and most atypical presentations seen in ε4-ve individuals. Heterozygosity of the rare p.R47H *TREM2* genetic variant for late-onset Alzheimer's disease is shown to confer risk for young onset Alzheimer's disease but drives younger age of onset rather than clinical phenotype. Regional brain atrophy profiles in *APOE* ε4 genotypes are shown to broadly align with the associated neuropsychological deficits. Microstructural damage studied using Diffusion Tensor Imaging, and Neurite Orientation Dispersion and Density Imaging provides a fine-grained profile of white matter network breakdown, revealing regional differences based on *APOE* ε4 genotype, and correlations with focal neuropsychological deficits. Finally, activation fMRI using a music paradigm to probe relationships between cognitive performance and brain function shows different patterns of brain activation during memory tasks in different Alzheimer's disease phenotypes.

Statement of contribution

I have conducted the work described in this thesis in collaboration with other researchers at the MRC Prion Unit, Department of Neurodegenerative Disease, UCL Institute of Neurology (Gary Adamson, GA; Simon Mead, SM; James Uphill, JU) and the Dementia Research Centre, Department of Neurodegenerative Disease, UCL Institute of Neurology (Jen Agustus, JA; Suzie Barker, SB; Amelia Carton, AC; Sebastian Crutch, SC; Alex Foulkes, AF; Nick Fox, NF; Susie Henley, SH; Kirsty MacPherson, KM; Ian Malone, IM; Ross Paterson, RP; Jonathan Schott, JS; Jason Warren, JW; Felix Woodward, FW).

Contributions made by other for each chapter are detailed below:

Chapters 5 and 6: Study design and recruitment

I designed the YOAD study including writing the protocol, information sheets, consent forms and designing the data collection and entry forms with RP, supervised by the Principal Investigators JS and NF. I wrote the ethics application form and attended the ethics meeting, and wrote the NHS sponsorship application with RP and guidance from SB. I recruited patients to the study, organised and ran the research visits with RP and AF. The neuropsychology battery was devised by SC and SH. Neuropsychology assessments were performed by FW, AC or KM. Blood samples for genetics were taken myself, RP or AF and tested by the University College London Neurogenetics department. CSF samples were taken by myself, RP, AF and processed by the UCL CSF laboratory. MRI brain scans were imported by the Dementia Research Centre Trials team and I then uploaded them to XNAT (an imaging software platform for uploading, storing and processing imaging data). I performed all the statistical analyses presented in this thesis

Chapters 7 and 8: Genetics

I did the *TREM2* R47H sanger sequencing for all AD, FTD patients and controls, and analysed the variants with laboratory and technical support from JU, GA and SM. I reviewed the medical records and obtained the MRI scans for all the individuals carrying R47H variants. GA, SM and JU ran the next generation sequencing for autosomal dominant variants using the dementia panel, did the sanger sequencing for *C9or72* variants, and analysed the *APOE* ε4 genotype of participants. The brain volumes were run by the DRC trials team, namely IM. I performed all the analyses, supported by JS and SM.

Chapter 9: VBM

I performed all the VBM analyses independently. The brain, hippocampal and ventricle volumes were calculated by the Dementia Research Centre Clinical Trials imaging team.

Chapter 10

I performed all the DTI and NODDI analyses supported by GZ, JY (who assisted with the data processing) and JS. SC assisted with the methods for generating z scores from neuropsychology data.

Chapter 11

The activation paradigm was devised by JA and JDW. It had previously been trialled in a cohort of healthy individuals. I collected all the activation fMRI and behavioural data for the YOAD cohort and processed and analysed it with assistance from JA and JW.

Acknowledgements

First and foremost, I would like to thank all of our study participants for their involvement.

I am grateful to the following organisations and charities for funding this work: the Alzheimer's Society, Alzheimer's Research UK, the Wellcome Trust, the UK Medical Research Council, the NIHR Queen Square Dementia Biomedical Research Unit.

I would also like to thank the following people, without whom this body of work would not have been possible:

Gary Adamson, Jen Agustus, Suzie Barker, Amelia Carton, Seb Crutch, Susie Henley, Kirsty MacPherson, Ian Malone, Simon Mead, James Uphill, and Felix Woodward.

A special thank you to my supervisors Professor JM Schott, Professor NC Fox and Professor JD Warren for their guidance, support and patience.

I am also indebted to Dr RW Paterson and Dr AJW Foulkes whom I worked most closely with on the YOAD study. Thank you for your help and friendship.

Publications

Publications arising as a direct result of the work presented in this thesis:

- **Slattery CF**, Beck JA, Harper L, *et al.* R47H *TREM2* variant increases risk of typical early-onset Alzheimer's disease but not of prion or frontotemporal dementia. *Alzheimer's & Dementia*, 2014. 10(6): p. 602-608.

- **Slattery CF**, Crutch SJ, Schott JM. Phenotypical variation in Alzheimer's disease: insights from posterior cortical atrophy. *Practical Neurology,* 2015. 15(1): 2-4.

- **Slattery CF**, Zhang J, Paterson RW, et al, *APOE* influences regional white-matter axonal density loss in Alzheimer's disease. *Neurobiology of Aging*, 2017. 57: 8-17.

- **Slattery CF**, Agustus JL, Paterson RW, *et al*, The functional neuroanatomy of musical memory in Alzheimer's disease. In press, *Cortex,* 2019.

Other publications related to the YOAD cohort and work carried out for this thesis:

- Paterson RW, **Slattery CF**, *et al*., Cerebrospinal fluid in the differential diagnosis of Alzheimer's disease: clinical utility of an extended panel of biomarkers in a specialist cognitive clinic. *Alzheimers Res Ther.* 2018 Mar 20;10(1):32.

- Wellington H, Paterson RW, Suárez-González A, Poole T, Frost C, Sjöbom U, **Slattery CF**, *et al.,* CSF neurogranin or tau distinguish typical and atypical Alzheimer disease. *Ann Clin Transl Neurol*. 2018 Jan 11;5(2):162-171. 3.

- Pavisic IM, Firth NC, Parsons S, Rego DM, Shakespeare TJ, Yong KXX, **Slattery CF**, *et al.,* Eyetracking Metrics in Young Onset Alzheimer's Disease: A Window into Cognitive Visual Functions. *Front Neurol.* 2017 Aug 7;8:377

- Golden HL, Clark CN, Nicholas JM, Cohen MH, **Slattery CF**, et al, Music Perception in Dementia. *J Alzheimers Dis*. 2017;55(3):933-949.

- Suárez-González A, Lehmann M, Shakespeare TJ, Yong KXX, Paterson RW, **Slattery CF**, *et al,* Effect of age at onset on cortical thickness and cognition in posterior cortical atrophy. *Neurobiol Aging*. 2016;44:108-113

- Paterson RW, Toombs J, **Slattery CF**, et al, Dissecting IWG-2 typical and atypical Alzheimer's disease: insights from cerebrospinal fluid analysis. *J Neurol*. 2015;262(12):2722-30.

- Fletcher PD, Downey LE, Golden HL, Clark CN, **Slattery CF**, *et al.* Auditory hedonic phenotypes in dementia: A behavioural and neuroanatomical analysis. *Cortex*. 2015;67:95-105.

- Shakespeare TJ, Kaski D, Yong KX, Paterson RW, **Slattery CF**, *et al.* Abnormalities of fixation, saccade and pursuit in posterior cortical atrophy. *Brain*. 2015;138(7):1976-91.

Prizes

Prizes awarded arising directly from the work conducted in this thesis

2015 Platform Presentation Prize, awarded by the NIHR Biomedical Research Units for Dementia at the trainees' Networking Event (London UK).

Platform presentation: Neurite orientation dispersion and density imaging (NODDI) in Young Onset Alzheimer's Disease and its Syndromic Variants.

2015 Best Poster Prize, awarded by the Alzheimer's Imaging Consortium, at the Alzheimer's Association International, Conference (Washington, USA).

Poster title: Neurite orientation dispersion and density imaging (NODDI) in Young Onset Alzheimer's Disease and its Syndromic Variants.

2014 The Alwyn Lishman Prize, awarded at the British Neuropsychiatry Association Annual Conference (London, UK).

Platform presentation: TREM2 – a study of clinical phenotype.

Appendices

Appendix 1: YOAD cohort characteristics and participation by imaging modality

Appendix 2: Items used in the musical experience questionnaire

Appendix 3: Young onset Alzheimer's disease study- participant folder

Appendix 1: YOAD cohort characteristics and participation by imaging modality

subject ID	phenotype	sex	Years education	handedness	age	age at symptom onset	MMSE	E4 status	Volumes	VBM	NODDI / DTI	act FMRI
01-001	control	F	17	R	51		29		√	√	√	√
01-002	tAD	M	15	R	63	56	24	4 4	√	√	√	√
01-003	tAD	F	16	R	63	61	20	3 4	√	√	√	√
01-004	PCA	F	12	R	65	61	27	3 4	√	√	√	√
01-005	tAD	F	12	R	64	60	26	3 4	√	√	√	√
01-006	control	F	16	R	64		30		√	√	√	√
01-007	control	M	17	L	68		30		√	√	√	√
01-008	tAD	F	18	R	53	50	24	3 4	√	√	√	√
01-009	tAD	M	17	R	65	57	16	3 3	√	√	√	√
01-010	tAD	F	18	R	62	53	17	3 3	√	√	√	√
01-011	control	M	22	R	63		30		√	√	√	√
01-012	tAD	M	18	R	61	58	24	2 3	√	√	√	√
01-013	control	F	12	R	62		28		√	√	√	√
01-014	PCA	F	12	R	67	59	21	2 4	√	√	√	√
01-015	control	M	20	R	66		29				√	√
01-016	control	M	16	R	66		30		√	√	√	

01-017	tAD	F	10	R	73	62	27	3 4	√	√	√	
01-018	tAD	M	10	R	64	57	13	3 4	√	√	√	√
01-019	tAD	M	12	R	62	56	25	2 4	√	√	√	√
01-020	control	F	12	R	65		30		√	√	√	√
01-021	tAD	M	18	R	59	54	20	3 3	√	√	√	√
01-022	tAD	F	14	R	58	57	15	3 3	√	√	√	√
01-023	control	M	17	R	60		30		√	√	√	√
01-024	control	M	15	R	59		30				√	√
01-025	tAD	F	12	R	58	55	18	2 4	√	√	√	√
01-026	control	M	17	R	58		30		√	√	√	
01-027	PCA	F	13	R	57	54	21	3 3	√	√	√	√
01-028	control	M	17	R	60		30					√
01-029	tAD	F	12	R	60	50	20	3 3	√	√	√	√
01-030	control	M	15	R	63		30		√	√	√	√
01-031	frontal	M	14	R	53	42	15	3 4	√	√		
01-032	tAD	F	16	R	66	63	16	3 4	√	√	√	√
01-033	control	M	18	R	52		29		√	√	√	√
01-034	tAD	F	17	R	51	47	19	3 4	√	√		√
01-035	PCA	F	17	R	57	49	22	3 3	√	√	√	√
01-036	control	M	20	R	59		28		√	√	√	√
01-037	tAD	M	20	R	55	52	22	3 4			√	√

01-038	control	F	21	R	51		30		√	√	√	√
01-039	control	F	19	L	48		29		√	√	√	√
01-040	control	F	20	R	67		30		√	√	√	√
01-041	control	F	18	R	63		29		√	√	√	√
01-042	PCA	F	20	L	65	60	27	3 3	√	√		√
01-043	PCA	F	12	R	60	56	25	3 3			√	√
01-044	tAD	M	17	R	55	53	16	3 3	√	√	√	√
01-045	tAD	F	12	R	64	58	17	3 3	√	√	√	√
01-046	control	F	12	R	66		28		√	√	√	
01-047	PCA	F	14	R	70	56	22	3 4	√	√	√	√
01-048	PCA	F	15	R	58	53	24	3 4			√	√
01-049	tAD	F	17	R	57	53	15	4 4	√	√		√
01-050	PCA	M	18	R	67	60	27	3 3	√	√	√	√
01-051	control	F	11	L	62		30	.	√	√	√	√
01-052	tAD	M	17	R	52	49	23	3 4	√	√	√	
01-053	tAD	F	17	R	59	55	22	3 3	√	√		√
01-054	LPA	M	20	R	65	62	23	3 4				
01-055	tAD	M	11	L	67	60	23	2 4	√	√	√	√
01-056	control	F	17	R	60		29	.	√	√	√	√
01-057	tAD	M	19	R	59	57	16	3 4			√	√
01-058	tAD	M	17	R	64	54	22	4 4	√	√	√	√

01-059	PCA	M	17	R	53	50	13	3 3	√	√	√	√
01-060	PCA	M	15	R	65	62	29	3 4	√	√	√	
01-061	tAD	F	10	R	59	55	25	3 4	√	√		
01-062	control	F	13	R	58		29	.	√	√	√	
01-063	PCA	F	15	R	59	55	18	2 3	√	√	√	
01-064	control	F	18	R	51		30	.	√	√	√	
01-065	PCA	M	14	R	57	55	27	3 3	√	√	√	
01-066	PCA	M	12	R	64	61	16	4 4	√	√	√	
01-067	tAD	F	17	R	64	63	27	3 4	√	√	√	
01-068	LPA	F	14	R	62	56	29	4 4	√	√		
01-069	tAD	M	18	R	68	64	28	4 4	√	√	√	

Appendix 2: Items used in the musical experience questionnaire

The questionnaire items used in Chapter 11 are taken from Hailstone *et al.*, (2009).

1. Have you ever had any musical training (music lessons at school, lessons on an instrument, etc)? (yes/no)

1a. If yes, what kind and for how long?

2. Have you ever played a musical instrument? (yes/no – if no, skip to question 6)

3. If yes, which instrument(s)?

3a. How did you play it (them) for?

3b. What standard did you reach (grade, etc)?

4. Do you still play an instrument regularly? (yes/no – if no, skip to question 6.)

If yes, which instrument?

5a. Approximately how many hours per week do you play?

5b. Where do you play (at home, band, orchestra etc.)?

6. Do you listen to music regularly? (yes/no)

If yes, approximately how many hours per week do you listen to music?

7. What kind of music do you mainly listen to (pop, easy listening, jazz, classical etc.)?

Appendix 3: YOAD study – participant folder

Patient details and research schedule		
Participant Name		
Hospital Number		
DOB		
YOAD _ _	Participant Code _ _ _ _ _ _	
Address		
Telephone number		
Support / carer		
Address (if different)		
Telephone number (if different)		
GP name and address		
	Date	**Transport**
Visit 1 Day 1		
Visit 1 Day 2		
Visit 2		
Visit 3 Day 1		
Visit 3 Day 2		
Post LP telephone call		
Annual telephone call F/U		

Drug History		
Aspirin	0 never taken 1 currently taking 2 previously taking	
Clopidogrel	0 never taken 1 currently taking 2 previously taking	
Warfarin	0 never taken 1 currently taking 2 previously taking	
HRT	0 never taken 1 currently taking 2 previously taking	
AChE inhibitor	0 never taken 1 currently taking 2 previously taking	If yes, name and dose:
Memantine	0 never taken 1 currently taking 2 previously taking	
Neuroleptics	0 never taken 1 currently taking 2 previously taking	If yes, name and dose:
Antidepressants	0 never taken 1 currently taking 2 previously taking	If yes, name and dose:
Other	If yes, name and dose:	
Personal and Social History		
Smoking history	0 Never 1 Current 2 Previous	If 1 or 2, Pack years:
Alcohol history	1 nil 2 <14 units per week 3 14 to 21 units per week 4 >21 units per week	
Employment	1 Employed 2 Unemployed 3 Retired (including medically)	
Occupation		

Family History Did any of the following members of the subject's family have dementia?		1 AD, 2 VaD, 3 bv FTD, 4 PPA, 5 CBS, 6 DLB, 7 PD, 8 PSP, 9 HD, 10 Dementia NOS, 11 Other, 12 Unknown	Age of onset 00 unknown 01 for N/A	Age of death 00 unknown 01 for N/A
Father	No 0 Yes 1			
Mother	No 0 Yes 1			
Maternal Grandfather	No 0 Yes 1			
Maternal Grandmother	No 0 Yes 1			
Paternal Grandfather	No 0 Yes 1			
Paternal Grandmother	No 0 Yes 1			
How many **siblings does the subject** have?				
Do any have dementia? *If yes, please specify.*				No 0 Yes 1

No. in pedigree	Diagnosis	Age of onset	Age of death

Draw pedigree

Predominant first symptom *notes: code symptoms as below* *e.g. A1 - memory impairment*	
Age of first symptom onset	_ _ years
A. Cognitive	
1. Memory impairment "forgets conversations and/or dates; repeats questions and/or statements; forgets names of people etc."	0 Absent 0.5 Questionable / very mild 1 Mild 2 Moderate 3 Severe
2. Language impairment "difficulty naming, long pauses, poor grammar, impaired comprehension, impaired reading or writing etc."	0 Absent 0.5 Questionable / very mild 1 Mild 2 Moderate 3 Severe
3. Visuoperceptual / visuospatial "difficulty interpreting visual stimuli, finding way round, judging distances etc."	0 Absent 0.5 Questionable / very mild 1 Mild 2 Moderate 3 Severe
4. Dyspraxia "difficulty in using hands to manipulate objects, hands do not seem to follow commands"	0 Absent 0.5 Questionable / very mild 1 Mild 2 Moderate 3 Severe
5. Executive: impaired judgement and problem solving "trouble handling money, paying bills, shopping, preparing meals etc."	0 Absent 0.5 Questionable / very mild 1 Mild 2 Moderate 3 Severe
6. Impaired attention / concentration "short attention span, difficulty concentrating, easily distracted etc"	0 Absent 0.5 Questionable / very mild 1 Mild 2 Moderate 3 Severe
B. Behavioural Symptoms	
1. Disinhibition "socially inappropriate behaviour; loss of manners; impulse, rash or careless actions"	0 Absent 0.5 Questionable / very mild 1 Mild 2 Moderate 3 Severe
2. Apathy "loss of interest, drive and motivation"	0 Absent 0.5 Questionable / very mild 1 Mild 2 Moderate

1. Loss of sympathy / empathy "diminished response to other people's needs or feelings, diminished social interest or personal warmth"	0 Absent 0.5 Questionable / very mild 1 Mild 2 Moderate 3 Severe
2. Ritualistic / compulsive behaviour "simple repetitive movements or complex compulsive or ritualistic behaviours"	0 Absent 0.5 Questionable / very mild 1 Mild 2 Moderate 3 Severe
3. Hyperorality / appetite changes "altered food preferences, binge eating, increased consumption of cigarettes and alcohol"	0 Absent 0.5 Questionable / very mild 1 Mild 2 Moderate 3 Severe
A. Neuropsychiatric symptoms	
1. Visual hallucinations	0 Absent 0.5 Questionable / very mild 1 Mild 2 Moderate 3 Severe
2. Auditory hallucinations	0 Absent 0.5 Questionable / very mild 1 Mild 2 Moderate 3 Severe
3. Tactile hallucinations	0 Absent 0.5 Questionable / very mild 1 Mild 2 Moderate 3 Severe
4. Delusions	0 Absent 0.5 Questionable / very mild 1 Mild 2 Moderate 3 Severe
5. Depression	0 Absent 0.5 Questionable / very mild 1 Mild 2 Moderate 3 Severe
6. Anxiety	0 Absent 0.5 Questionable / very mild 1 Mild 2 Moderate 3 Severe

A. Motor Symptoms	
1. Dysarthria "problems with articulation"	0 Absent 0.5 Questionable / very mild 1 Mild 2 Moderate 1 Severe
2. Tremor "rhythmic shaking, especially in hands, arms, legs or head"	0 Absent 0.5 Questionable / very mild 1 Mild 2 Moderate 3 Severe
3. Slowness "noticeably slowed down in walking or moving or writing, other than due to acute illness or injury"	0 Absent 0.5 Questionable / very mild 1 Mild 2 Moderate 3 Severe
4. Weakness "weakness of arms or legs"	0 Absent 0.5 Questionable / very mild 1 Mild 2 Moderate 3 Severe
5. Gait disorder "has the participant's walking changed, not specifically due to arthritis or injury? Are they unsteady, or shuffle when walking, or drag a foot?"	0 Absent 0.5 Questionable / very mild 1 Mild 2 Moderate 3 Severe
6. Falls "does the subject fall more than usual?"	0 Absent 0.5 Questionable / very mild 1 Mild 2 Moderate 3 Severe
7. Alien Limb "does either limb seem to have a mind of it's own, or grab onto things unexpectedly without the person intending to?"	0 Absent 0.5 Questionable / very mild 1 Mild 2 Moderate 3 Severe

Cranial Nerve Examination		
Visual fields on confrontation	0 normal 1 abnormal	if abnormal - details:
Optic ataxia	0 No 1 Yes - L>R 2 Yes - R>L 3 Yes - no major asymmetry	
Visual inattention	0 No 1 Yes - L 2 Yes - R 3 Yes - bilaterally	
Eye movements	0 normal 1 abnormal	if abnormal - details:

Limb Examination			
Myoclonus	0 No 1 Yes - L>R 2 Yes - R>L 3 Yes - no major asymmetry	Spasticity - upper limbs	0 No 1 Yes - L>R 2 Yes - R>L 3 Yes - no major asymmetry
Rest tremor	0 No 1 Yes - L>R 2 Yes - R>L 3 Yes - no major asymmetry	Spasticity - lower limbs	0 No 1 Yes - L>R 2 Yes - R>L 3 Yes - no major asymmetry
Postural tremor	0 No 1 Yes - L>R 2 Yes - R>L 3 Yes - no major asymmetry	Hyperreflexia - upper limbs	0 No 1 Yes - L>R 2 Yes - R>L 3 Yes - no major asymmetry
Bradykinesia	0 No 1 Yes - L>R 2 Yes - R>L 3 Yes - no major asymmetry	Hyperreflexia - lower limbs	0 No 1 Yes - L>R 2 Yes - R>L 3 Yes - no major asymmetry
Ataxia	0 No 1 Yes - L>R 2 Yes - R>L 3 Yes - no major asymmetry	Plantars	0 Normal 1 Abnormal - L extensor 2 Abnormal - R extensor 3 Abnormal - bilateral extens
Dystonia	0 No 1 Yes - L>R 2 Yes - R>L 3 Yes - no major asymmetry	Gait	0 Normal 1 Slight alteration in speed o fluidity of gait 2 Walks with difficulty but re no assistance 3 Severe gait disturbance 4 Cannot walk

Limb Apraxia	
5: an accurate, prompt, complete and readable gesture 4: an ambiguous or incorrect gesture, but self corrects to an accurate response 3: the gesture is basically correct, but crude and defective in amplitude, speed or accuracy. If the subject makes no response for 10 seconds, or attempts a response but is unsuccessful, demonstrate the gesture. Then: 2: performs correctly after demonstration 1: gesture, after demonstration, is basically correct, but crude and defective in amplitude, speed or accuracy 0: even after demonstration, unable to perform the correct gesture	
Score using the scale above:	
Make a fist	R score _ L score _
Wave goodbye	R score _ L score _
Snap your fingers	R score _ L score _
Throw a ball	R score _ L score _
Hide your eyes	R score _ L score _
Make a hitch-hiking sign	R score _ L score _
Make a pointing sign	R score _ L score _
Salute	R score _ L score _
Play the piano	R score _ L score _
Scratch	R score _ L score _
Orofacial Apraxia *Score using the scale above:*	
Stick out your tongue	_
Whistle	_
Puff out your cheeks	_
Pretend to kiss	_
Clear your throat	_
Bite your lower lip	_
Show me your teeth	_
Take a deep breath in and hold it	_
Lick your lips	_
Open your mouth	_

General Examination	
Supine Blood Pressure	___/___mmHg
Standing Blood Pressure	___/___mmHg
Resting Heart Rate	_ _beats per minute
Height	_ _ m
Weight	_ _kg
BMI	_ _

Hachinski Score *circle number as appropriate*	
Abrupt onset	0 No 2 Yes
Stepwise deterioration	0 No 1 Yes
Fluctuating course	0 No 2 Yes
Nocturnal confusion	0 No 1 Yes
Relative preservation of personality	0 No 1 Yes
Depression	0 No 1 Yes
Somatic complaints	0 No 1 Yes
Emotional incontinence	0 No 1 Yes
History or presence of hypertension	0 No 1 Yes
History of strokes	0 No 2 Yes
Evidence of atherosclerosis	0 No 1 Yes
Focal neurological symptoms	0 No 2 Yes
Focal neurological signs	0 No 2 Yes
Total Score	__/18

Mini Mental State Examination

"I would like to go through a few questions with you. These questions are a brief assessment of memory and concentration."

ORIENTATION	Correct?	
1 What is the year?	Yes 1	No 0
2 What is the season?	Yes 1	No 0
3 What is the date?	Yes 1	No 0
4 What is the day of the week?	Yes 1	No 0
5 What is the month?	Yes 1	No 0
6 Can you tell me where you are now? For instance what country are we in?	Yes 1	No 0
7 What is the name of this city?	Yes 1	No 0
8 What are the names of two main streets nearby (or near your home)? *Are both streets correct (or plausibly correct?)*	Yes 1	No 0
9 What floor of the building are we on?	Yes 1	No 0
10 What is the name of this place?	Yes 1	No 0
REGISTRATION		
11. **I am now going to name three objects. The three objects are:** **Bus, Door, Rose. Please repeat the name of these three objects back to me.** *Record the FIRST responses (order of object recall does NOT matter):*		
First object named? ……..	Yes 1	No 0
Second object named? ……..	Yes 1	No 0
Third object named? ……..	Yes 1	No 0
If all three objects are repeated correctly (in any order) go to Q12. If the participant does not repeat all three words exactly then allow them two further attempts but DO NOT change their first responses or scores. Attempt 2: **I'm going to repeat once more the three objects, APPLE, TABLE, PENNY. Please say them back to me.** Attempt 3: **Can we try one more time? The names are, APPLE, TABLE, PENNY. Please say them back to me.**		

ATTENTION AND CALCULATION			
12a. **Please take seven away from one hundred** *(Answer: 93)*			
Answer 1		YES 1	No 0
Now I'm going to ask you to take seven away from what you have left over, and then keep taking seven away until I stop you. *(Answers: 86, 79, 72 and 65. If the participant gets an answer wrong but then takes seven away correctly from that answer you should score as correct).*			
Answer 2		Yes 1	No 0
Answer 3		Yes 1	No 0
Answer 4		Yes 1	No 0
Answer 5		Yes 1	No 0
T /5 e for 1 to 5 of 12a			
If the participant scores 5/5 then go to Q13.			
If the participant scores less than 5/5 for 12a then complete question 12b.			
12b. **Please spell "WORLD" backwards** *(Answer: D L R O W)*			
TOTAL number of letters in correct order for 12b /5			
Highest score for 12a **or** 12b			
RECALL		Correct?	
13. **Please name the three objects that I mentioned to you earlier?**			
First object named? ……..……..		Yes 1	No 0
Second object named?.....		Yes 1	No 0
Third object named?.....		Yes 1	No 0
NAMING			
14. **What is this called?** (show watch)……		Yes 1	No 0
15. **What is this called?** (show pen) ……		Yes 1	No 0
REPETITION			

THREE STAGE COMMAND	Correct?	
17. **Please take this paper with your right hand, fold it in half and put it on your lap**. *Do not repeat the sentence. If necessary say:* ***I'm sorry, I'm only allowed to read that out once.*** *Did the participant take the paper in their right hand?*	Yes 1	No 0
Did the participant fold the paper in half or quarter (both allowed)?	Yes 1	No 0
Did the participant put the paper on their lap?	Yes 1	No 0
READING		
18. Now give the sheet called "MMSE CLOSE YOUR EYES" to the participant and say: **Please read the sentence at the top of this sheet and do what it says.** *Did the participant close their eyes?*	Yes 1	No 0
WRITING		
19. **Please write a sentence in the space here**. Indicate the space under "Write a sentence". *Did the participant write a sentence?*	Yes 1	No 0
20. **Please copy this drawing**. Indicate the space to the right of the design. *Did the participant copy the drawing correctly?*	Yes 1	No 0
Score		/30

Urine Sample – Prion ethics form

Hand the urine sample, and the corresponding tracking form, to the lab staff.
Please initial the box to confirm you have done this.

☐

Blood Samples

Complete Dementia Genetics consent form (03/N049) and DRC research sample record form.

Collect blood in the following tubes:

20mls EDTA

15 mls citrate

5 mls serum (white)

1x PAX gene tube

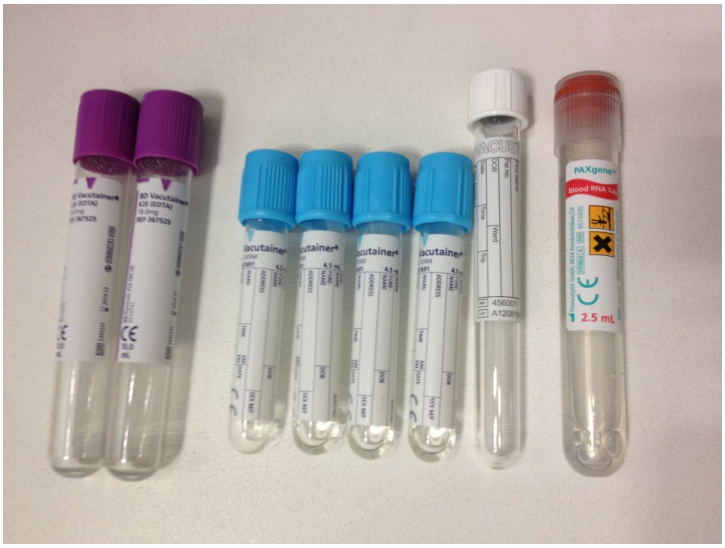

Hand the blood sample, and the corresponding tracking form, to the lab staff.
Please initial the box to confirm you have done this.

☐

Scan the consent form and save in U:\CONSENT FORMS\03N049_Dementia Genetics

Give original consent forms to Suzie Barker.

Complete and send out GP letter with a copy of Dementia Genetics 03N049 information sheet.

Smell Testing

Head injury with LOC or skull fracture?	No	0	Yes	1
Recurrent upper respiratory infection or allergic rhinitis?	No	0	Yes	1
Surgery on the face or nose?	No	0	Yes	1
Other diseases involving the nose?	No	0	Yes	1

Instruction: "Sniff each label and choose one of four alternatives that best describes the presented odou
If no smell is present, please guess."

No	Target	Response Options (Circle One)				Correct?
		A	B	C	D	
1	**Pizza**	Petrol	**Pizza**	Peanuts	Lilac	Yes 1 No 0
2	**Bubblegum**	Chutney	**Bubblegum**	Liniment	Watermelon	Yes 1 No 0
3	**Menthol**	Tomato	Baby powder	Strawberry	**Menthol**	Yes 1 No 0
4	**Cherry**	Whiskey	Honey	Lime	**Cherry**	Yes 1 No 0
5	**Motor oil**	Grass	Pizza	**Motor oil**	Pineapple	Yes 1 No 0
6	**Mint**	Dog	**Mint**	Peach	Cola	Yes 1 No 0
7	**Banana**	**Banana**	Garlic	Cherry	Motor oil	Yes 1 No 0
8	**Clove**	Baby powder	**Clove**	Spaghetti	Banana	Yes 1 No 0
9	**Leather**	Clove	Lilac	**Leather**	Apple	Yes 1 No 0
10	**Coconut**	Dog	**Coconut**	Cedar	Honey	Yes 1 No 0
11	**Onion**	Chocolate	Banana	**Onion**	Peach	Yes 1 No 0
12	**Grapefruit**	Soap	**Grapefruit**	Menthol	Nutmeg	Yes 1 No 0
13	**Baby powder**	**Baby powder**	Pineapple	Cheese	Cherry	Yes 1 No 0
14	**Coffee**	Paint thinner	Cherry	Coconut	**Coffee**	Yes 1 No 0
15	**Cinnamon**	Cola	**Cinnamon**	Pine	Coconut	Yes 1 No 0
16	**Petrol**	Rose	Lemon	Peach	**Petrol**	Yes 1 No 0
17	**Strawberry**	**Strawberry**	Chutney	Chocolate	Cedar	Yes 1 No 0
18	**Cedar**	**Cedar**	Petrol	Lemon	Liquorice	Yes 1 No 0
19	**Chocolate**	Lemon	**Chocolate**	Liquorice	Black pepper	Yes 1 No 0
20	**Apple**	Menthol	Gingerbread	**Apple**	Cheese	Yes 1 No 0
21	**Lilac**	**Lilac**	Spaghetti	Coconut	Whiskey	Yes 1 No 0
22	**Turpentine**	**Turpentine**	Soap	Dog	Spaghetti	Yes 1 No 0
23	**Peach**	Chocolate	**Peach**	Leather	Pizza	Yes 1 No 0
24	**Liquorice**	**Liquorice**	Watermelon	Banana	Smoke	Yes 1 No 0

25	**Chutney**	Pineapple	**Chutney**	Liquorice	Rose	Yes 1 No 0
26	**Pineapple**	Smoke	Whiskey	**Pineapple**	Onion	Yes 1 No 0
27	**Lime**	Musk	Garlic	Turpentine	**Lime**	Yes 1 No 0
28	**Orange**	Cheddar cheese	**Orange**	Bubblegum	Turpentine	Yes 1 No 0
29	**Rubber tyre**	Lime	**Rubber tyre**	Nutmeg	Leather	Yes 1 No 0
30	**Watermelon**	Spaghetti	Menthol	Orange	**Watermelon**	Yes 1 No 0
31	**Paint thinner**	Watermelon	Peanuts	Rose	**Paint thinner**	Yes 1 No 0
32	**Grass**	Mint	Gingerbread	**Grass**	Strawberry	Yes 1 No 0
33	**Smoke**	Chutney	Grass	**Smoke**	Peach	Yes 1 No 0
34	**Pine**	**Pine**	Smoke	Peanuts	Orange	Yes 1 No 0
35	**Raspberry**	Pizza	Turpentine	Clove	**Raspberry**	Yes 1 No 0
36	**Lemon**	Motor oil	Nutmeg	Rose	**Lemon**	Yes 1 No 0
37	**Soap**	**Soap**	Black pepper	Baby powder	Peanuts	Yes 1 No 0
38	**Natural gas**	Orange	Musk	Cola	**Natural gas**	Yes 1 No 0
39	**Rose**	Lime	**Rose**	Mint	Bubblegum	Yes 1 No 0
40	**Peanuts**	**Peanuts**	Lemon	Apple	Liquorice	Yes 1 No 0
					Total Score	**/40**

Imaging Protocol: ICELAND 1 (32 channel head coil)

- Localiser
- 3D T1-volumetric
- 3D T2-volumetric
- Field map
- Resting state fMRI (32 channel)
- DTIx2
- ASL

Comments: e.g. incomplete acquisition, excess participant movement etc

Please ask radiographers to send scan to the "DRC DICOM server" ☐ Initial when done

Check details updated on Research Scans Requested spreadsheet ☐ Initial when done

Imaging Protocol: ICELAND 2 (32 channel head coil)

- Localiser
- Field map
- Resting state fMRI
- MPM
- NODDI

Comments: e.g. incomplete acquisition, excess participant movement etc

Please ask radiographers to send scan to the "DRC DICOM server" ☐ Initial when done

Check details updated on Research Scans Requested spreadsheet ☐ Initial when done

Imaging Protocol: ICELAND 3 (12 channel head coil)

- Localiser
- Field map
- Activation fMRI
- T2*-weighted

Comments: e.g. incomplete acquisition, excess participant movement etc

Please ask radiographers to send scan to the "DRC DICOM server" ☐ Initial when done

Check details updated on Research Scans Requested spreadsheet ☐ Initial when done

References

1. Maignen, F., *Estimation of future cases of dementia from those born in 2015: updated analysis using CFAS II study; Consultation report for Alzheimer's Research UK.* Aug 2016.
2. *About a peculiar disease of the cerebral cortex. By Alois Alzheimer, 1907 (Translated by L. Jarvik and H. Greenson).* Alzheimer Dis Assoc Disord, 1987. **1**(1): p. 3-8.
3. E., K., *Psychiatrie: Ein Lehrbuch für Studierende und Ärzte. Leipzig: Barth* 1910.
4. Amaducci, L.A., W.A. Rocca, and B.S. Schoenberg, *Origin of the distinction between Alzheimer's disease and senile dementia: how history can clarify nosology.* Neurology, 1986. **36**(11): p. 1497-9.
5. Bachman, D.L., et al., *Incidence of dementia and probable Alzheimer's disease in a general population: the Framingham Study.* Neurology, 1993. **43**(3 Pt 1): p. 515-9.
6. Prince, M., Albanese E., Guerchet, M., *World Alzheimer Report 2014: Dementia and Risk Reduction an Analysis of Protective and Modifiable Factors.* 2014.
7. Prince, M.e.a., *Dementia UK: Update Second Edition report produced by King's College London and the London School of Economics for the Alzheimer's Society.* 2014.
8. Serrano-Pozo, A., et al., *Neuropathological alterations in Alzheimer disease.* Cold Spring Harb Perspect Med, 2011. **1**(1): p. a006189.
9. Paglini, G., et al., *Tau protein function in axonal formation.* Neurochem Res, 2000. **25**(1): p. 37-42.
10. Schneider, J.A., et al., *The neuropathology of probable Alzheimer disease and mild cognitive impairment.* Ann Neurol, 2009. **66**(2): p. 200-8.
11. James, B.D., et al., *TDP-43 stage, mixed pathologies, and clinical Alzheimer's-type dementia.* Brain, 2016. **139**(11): p. 2983-2993.
12. Ingelsson, M., et al., *Early Abeta accumulation and progressive synaptic loss, gliosis, and tangle formation in AD brain.* Neurology, 2004. **62**(6): p. 925-31.
13. Braak, H. and E. Braak, *Neuropathological stageing of Alzheimer-related changes.* Acta Neuropathol, 1991. **82**(4): p. 239-59.
14. Mirra, S.S., et al., *The Consortium to Establish a Registry for Alzheimer's Disease (CERAD). Part II. Standardization of the neuropathologic assessment of Alzheimer's disease.* Neurology, 1991. **41**(4): p. 479-86.
15. Thal, D.R., et al., *Phases of A beta-deposition in the human brain and its relevance for the development of AD.* Neurology, 2002. **58**(12): p. 1791-800.
16. Braak, H., et al., *Staging of Alzheimer disease-associated neurofibrillary pathology using paraffin sections and immunocytochemistry.* Acta Neuropathol, 2006. **112**(4): p. 389-404.
17. Geddes, J.W., et al., *Comparison of neuropathologic criteria for the diagnosis of Alzheimer's disease.* Neurobiol Aging, 1997. **18**(4 Suppl): p. S99-105.

18. Hyman, B.T. and J.Q. Trojanowski, *Consensus recommendations for the postmortem diagnosis of Alzheimer disease from the National Institute on Aging and the Reagan Institute Working Group on diagnostic criteria for the neuropathological assessment of Alzheimer disease.* J Neuropathol Exp Neurol, 1997. **56**(10): p. 1095-7.

19. Hyman, B.T., et al., *National Institute on Aging-Alzheimer's Association guidelines for the neuropathologic assessment of Alzheimer's disease.* Alzheimers Dement, 2012. **8**(1): p. 1-13.

20. Olson, M.I. and C.M. Shaw, *Presenile dementia and Alzheimer's disease in mongolism.* Brain, 1969. **92**(1): p. 147-56.

21. Goate, A., et al., *Segregation of a missense mutation in the amyloid precursor protein gene with familial Alzheimer's disease.* Nature, 1991. **349**(6311): p. 704-6.

22. Sherrington, R., et al., *Cloning of a gene bearing missense mutations in early-onset familial Alzheimer's disease.* Nature, 1995. **375**(6534): p. 754-60.

23. Rogaev, E.I., et al., *Familial Alzheimer's disease in kindreds with missense mutations in a gene on chromosome 1 related to the Alzheimer's disease type 3 gene.* Nature, 1995. **376**(6543): p. 775-8.

24. Rovelet-Lecrux, A., et al., *APP locus duplication causes autosomal dominant early-onset Alzheimer disease with cerebral amyloid angiopathy.* Nat Genet, 2006. **38**(1): p. 24-6.

25. Hardy, J.A. and G.A. Higgins, *Alzheimer's disease: the amyloid cascade hypothesis.* Science, 1992. **256**(5054): p. 184-5.

26. Saunders, A.M., et al., *Association of apolipoprotein E allele epsilon 4 with late-onset familial and sporadic Alzheimer's disease.* Neurology, 1993. **43**(8): p. 1467-72.

27. Siest, G., et al., *Apolipoprotein E: an important gene and protein to follow in laboratory medicine.* Clin Chem, 1995. **41**(8 Pt 1): p. 1068-86.

28. Bertram, L., et al., *Systematic meta-analyses of Alzheimer disease genetic association studies: the AlzGene database.* Nat Genet, 2007. **39**(1): p. 17-23.

29. Ashford, J.W., *APOE genotype effects on Alzheimer's disease onset and epidemiology.* J Mol Neurosci, 2004. **23**(3): p. 157-65.

30. Corder, E.H., et al., *Gene dose of apolipoprotein E type 4 allele and the risk of Alzheimer's disease in late onset families.* Science, 1993. **261**(5123): p. 921-3.

31. Mahley, R.W., *Apolipoprotein E: cholesterol transport protein with expanding role in cell biology.* Science, 1988. **240**(4852): p. 622-30.

32. Mahley, R.W. and S.C. Rall, Jr., *Apolipoprotein E: far more than a lipid transport protein.* Annu Rev Genomics Hum Genet, 2000. **1**: p. 507-37.

33. Kim, J., J.M. Basak, and D.M. Holtzman, *The role of apolipoprotein E in Alzheimer's disease.* Neuron, 2009. **63**(3): p. 287-303.

34. Daw, E.W., et al., *The number of trait loci in late-onset Alzheimer disease.* Am J Hum Genet, 2000. **66**(1): p. 196-204.

35. Cuyvers, E. and K. Sleegers, *Genetic variations underlying Alzheimer's disease: evidence from genome-wide association studies and beyond.* Lancet Neurol, 2016. **15**(8): p. 857-868.

36. Guerreiro, R., J. Bras, and J. Hardy, *SnapShot: genetics of Alzheimer's disease.* Cell, 2013. **155**(4): p. 968-968 e1.

37. Paloneva, J., et al., *Mutations in Two Genes Encoding Different Subunits of a Receptor Signaling Complex Result in an Identical Disease Phenotype.* The American Journal of Human Genetics, 2002. **71**(3): p. 656-662.

38. Guerreiro, R.J., et al., *Using exome sequencing to reveal mutations in TREM2 presenting as a frontotemporal dementia-like syndrome without bone involvement.* JAMA Neurol, 2013. **70**(1): p. 78-84.

39. Guerreiro, R., et al., *TREM2 variants in Alzheimer's disease.* N Engl J Med, 2013. **368**(2): p. 117-27.

40. Jonsson, T., et al., *Variant of TREM2 associated with the risk of Alzheimer's disease.* N Engl J Med, 2013. **368**(2): p. 107-16.

41. Zhang, B., et al., *Integrated systems approach identifies genetic nodes and networks in late-onset Alzheimer's disease.* Cell, 2013. **153**(3): p. 707-20.

42. Forabosco, P., et al., *Insights into TREM2 biology by network analysis of human brain gene expression data.* Neurobiol Aging, 2013. **34**(12): p. 2699-714.

43. Lane, C.A., J. Hardy, and J.M. Schott, *Alzheimer's disease.* Eur J Neurol, 2018. **25**(1): p. 59-70.

44. Kivipelto, M., et al., *Obesity and vascular risk factors at midlife and the risk of dementia and Alzheimer disease.* Arch Neurol, 2005. **62**(10): p. 1556-60.

45. Debette, S., et al., *Midlife vascular risk factor exposure accelerates structural brain aging and cognitive decline.* Neurology, 2011. **77**(5): p. 461-8.

46. Anstey, K.J., et al., *Smoking as a risk factor for dementia and cognitive decline: a meta-analysis of prospective studies.* Am J Epidemiol, 2007. **166**(4): p. 367-78.

47. Rusanen, M., et al., *Heavy smoking in midlife and long-term risk of Alzheimer disease and vascular dementia.* Arch Intern Med, 2011. **171**(4): p. 333-9.

48. Solomon, A., et al., *Midlife serum cholesterol and increased risk of Alzheimer's and vascular dementia three decades later.* Dement Geriatr Cogn Disord, 2009. **28**(1): p. 75-80.

49. Larson, E.B., et al., *Exercise is associated with reduced risk for incident dementia among persons 65 years of age and older.* Ann Intern Med, 2006. **144**(2): p. 73-81.

50. Laurin, D., et al., *Physical activity and risk of cognitive impairment and dementia in elderly persons.* Arch Neurol, 2001. **58**(3): p. 498-504.

51. Wang, H.X., W. Xu, and J.J. Pei, *Leisure activities, cognition and dementia.* Biochim Biophys Acta, 2012. **1822**(3): p. 482-91.

52. Stern, Y., et al., *Influence of education and occupation on the incidence of Alzheimer's disease.* Jama, 1994. **271**(13): p. 1004-10.

53. Fleminger, S., et al., *Head injury as a risk factor for Alzheimer's disease: the evidence 10 years on; a partial replication.* J Neurol Neurosurg Psychiatry, 2003. **74**(7): p. 857-62.

54. Weiner, M.W., et al., *Effects of traumatic brain injury and posttraumatic stress disorder on development of Alzheimer's disease in Vietnam Veterans using the*

Alzheimer's Disease Neuroimaging Initiative: Preliminary Report. Alzheimers Dement (N Y), 2017. **3**(2): p. 177-188.

55. Crane, P.K., et al., *Association of Traumatic Brain Injury With Late-Life Neurodegenerative Conditions and Neuropathologic Findings.* JAMA Neurol, 2016. **73**(9): p. 1062-9.

56. Hardy, J., *Amyloid, the presenilins and Alzheimer's disease.* Trends Neurosci, 1997. **20**(4): p. 154-9.

57. Mudher, A. and S. Lovestone, *Alzheimer's disease-do tauists and baptists finally shake hands?* Trends Neurosci, 2002. **25**(1): p. 22-6.

58. De Strooper, B., et al., *Deficiency of presenilin-1 inhibits the normal cleavage of amyloid precursor protein.* Nature, 1998. **391**(6665): p. 387-90.

59. Wolfe, M.S., et al., *Two transmembrane aspartates in presenilin-1 required for presenilin endoproteolysis and gamma-secretase activity.* Nature, 1999. **398**(6727): p. 513-7.

60. Jonsson, T., et al., *A mutation in APP protects against Alzheimer's disease and age-related cognitive decline.* Nature, 2012. **488**(7409): p. 96-9.

61. Selkoe, D.J. and J. Hardy, *The amyloid hypothesis of Alzheimer's disease at 25 years.* EMBO Mol Med, 2016. **8**(6): p. 595-608.

62. Shankar, G.M., et al., *Amyloid-beta protein dimers isolated directly from Alzheimer's brains impair synaptic plasticity and memory.* Nat Med, 2008. **14**(8): p. 837-42.

63. Esparza, T.J., et al., *Amyloid-beta oligomerization in Alzheimer dementia versus high-pathology controls.* Ann Neurol, 2013. **73**(1): p. 104-19.

64. Mitchell, T.W., et al., *Parahippocampal tau pathology in healthy aging, mild cognitive impairment, and early Alzheimer's disease.* Ann Neurol, 2002. **51**(2): p. 182-9.

65. Heutink, P., *Untangling tau-related dementia.* Hum Mol Genet, 2000. **9**(6): p. 979-86.

66. Jin, M., et al., *Soluble amyloid beta-protein dimers isolated from Alzheimer cortex directly induce Tau hyperphosphorylation and neuritic degeneration.* Proc Natl Acad Sci U S A, 2011. **108**(14): p. 5819-24.

67. Nelson, P.T., et al., *Correlation of Alzheimer disease neuropathologic changes with cognitive status: a review of the literature.* J Neuropathol Exp Neurol, 2012. **71**(5): p. 362-81.

68. Karran, E. and J. Hardy, *A critique of the drug discovery and phase 3 clinical programs targeting the amyloid hypothesis for Alzheimer disease.* Ann Neurol, 2014. **76**(2): p. 185-205.

69. Karran, E. and J. Hardy, *Antiamyloid therapy for Alzheimer's disease--are we on the right road?* N Engl J Med, 2014. **370**(4): p. 377-8.

70. Wang, J., et al., *ADCOMS: a composite clinical outcome for prodromal Alzheimer's disease trials.* J Neurol Neurosurg Psychiatry, 2016. **87**(9): p. 993-9.

71. Satlin, A., et al., *Design of a Bayesian adaptive phase 2 proof-of-concept trial for BAN2401, a putative disease-modifying monoclonal antibody for the treatment of Alzheimer's disease.* Alzheimers Dement (N Y), 2016. **2**(1): p. 1-12.

72. *A Study to Evaluate Safety, Tolerability, and Efficacy of BAN2401 in Subjects With Early Alzheimer's Disease,* https://clinicaltrials.gov/ct2/show/NCT01767311*, accessed 11/08/2018.*

73. Olsson, B., et al., *CSF and blood biomarkers for the diagnosis of Alzheimer's disease: a systematic review and meta-analysis.* Lancet Neurol, 2016. **15**(7): p. 673-684.

74. Seppala, T.T., et al., *CSF biomarkers for Alzheimer disease correlate with cortical brain biopsy findings.* Neurology, 2012. **78**(20): p. 1568-75.

75. de Souza, L.C., et al., *CSF tau markers are correlated with hippocampal volume in Alzheimer's disease.* Neurobiol Aging, 2012. **33**(7): p. 1253-7.

76. Tapiola, T., et al., *Cerebrospinal fluid beta-amyloid 42 and tau proteins as biomarkers of Alzheimer-type pathologic changes in the brain.* Arch Neurol, 2009. **66**(3): p. 382-9.

77. Ost, M., et al., *Initial CSF total tau correlates with 1-year outcome in patients with traumatic brain injury.* Neurology, 2006. **67**(9): p. 1600-4.

78. Buerger, K., et al., *CSF phosphorylated tau protein correlates with neocortical neurofibrillary pathology in Alzheimer's disease.* Brain, 2006. **129**(Pt 11): p. 3035-41.

79. Blennow, K., et al., *Cerebrospinal fluid and plasma biomarkers in Alzheimer disease.* Nat Rev Neurol, 2010. **6**(3): p. 131-44.

80. Freeborough, P.A. and N.C. Fox, *The boundary shift integral: an accurate and robust measure of cerebral volume changes from registered repeat MRI.* IEEE Trans Med Imaging, 1997. **16**(5): p. 623-9.

81. Clark, C.M., et al., *Use of florbetapir-PET for imaging beta-amyloid pathology.* Jama, 2011. **305**(3): p. 275-83.

82. Ikonomovic, M.D., et al., *Post-mortem histopathology underlying beta-amyloid PET imaging following flutemetamol F 18 injection.* Acta Neuropathol Commun, 2016. **4**(1): p. 130.

83. Sabri, O., et al., *Florbetaben PET imaging to detect amyloid beta plaques in Alzheimer's disease: phase 3 study.* Alzheimers Dement, 2015. **11**(8): p. 964-74.

84. Jack, C.R., Jr., J.R. Barrio, and V. Kepe, *Cerebral amyloid PET imaging in Alzheimer's disease.* Acta Neuropathol, 2013. **126**(5): p. 643-57.

85. Klunk, W.E., et al., *Imaging brain amyloid in Alzheimer's disease with Pittsburgh Compound-B.* Ann Neurol, 2004. **55**(3): p. 306-19.

86. Roher, A.E., et al., *Bapineuzumab alters abeta composition: implications for the amyloid cascade hypothesis and anti-amyloid immunotherapy.* PLoS One, 2013. **8**(3): p. e59735.

87. Jagust, W.J., et al., *The Alzheimer's Disease Neuroimaging Initiative positron emission tomography core.* Alzheimers Dement, 2010. **6**(3): p. 221-9.

88. Xia, C.F., et al., *[(18)F]T807, a novel tau positron emission tomography imaging agent for Alzheimer's disease.* Alzheimers Dement, 2013. **9**(6): p. 666-76.

89. Schwarz, A.J., et al., *Regional profiles of the candidate tau PET ligand 18F-AV-1451 recapitulate key features of Braak histopathological stages.* Brain, 2016. **139**(Pt 5): p. 1539-50.

90. Ossenkoppele, R., et al., *Tau PET patterns mirror clinical and neuroanatomical variability in Alzheimer's disease.* Brain, 2016. **139**(Pt 5): p. 1551-67.

91. Dronse, J., et al., *In vivo Patterns of Tau Pathology, Amyloid-beta Burden, and Neuronal Dysfunction in Clinical Variants of Alzheimer's Disease.* J Alzheimers Dis, 2017. **55**(2): p. 465-471.

92. Bateman, R.J., et al., *Clinical and biomarker changes in dominantly inherited Alzheimer's disease.* N Engl J Med, 2012. **367**(9): p. 795-804.

93. Villemagne, V.L., et al., *Amyloid beta deposition, neurodegeneration, and cognitive decline in sporadic Alzheimer's disease: a prospective cohort study.* Lancet Neurol, 2013. **12**(4): p. 357-67.

94. Jack, C.R., Jr., et al., *Hypothetical model of dynamic biomarkers of the Alzheimer's pathological cascade.* Lancet Neurol, 2010. **9**(1): p. 119-28.

95. Jack, C.R., Jr. and D.M. Holtzman, *Biomarker modeling of Alzheimer's disease.* Neuron, 2013. **80**(6): p. 1347-58.

96. Cerejeira, J., L. Lagarto, and E.B. Mukaetova-Ladinska, *Behavioral and psychological symptoms of dementia.* Front Neurol, 2012. **3**: p. 73.

97. Jost, B.C. and G.T. Grossberg, *The natural history of Alzheimer's disease: a brain bank study.* J Am Geriatr Soc, 1995. **43**(11): p. 1248-55.

98. Rossor, M.N., et al., *The diagnosis of young-onset dementia.* Lancet Neurol, 2010. **9**(8): p. 793-806.

99. Vieira, R.T., et al., *Epidemiology of early-onset dementia: a review of the literature.* Clin Pract Epidemiol Ment Health, 2013. **9**: p. 88-95.

100. Ryan, N.S., et al., *Clinical phenotype and genetic associations in autosomal dominant familial Alzheimer's disease: a case series.* Lancet Neurol, 2016. **15**(13): p. 1326-1335.

101. Crutch, S.J., et al., *Posterior cortical atrophy.* Lancet Neurol, 2012. **11**(2): p. 170-8.

102. Gorno-Tempini, M.L., et al., *Classification of primary progressive aphasia and its variants.* Neurology, 2011. **76**(11): p. 1006-14.

103. Binetti, G., et al., *Executive dysfunction in early Alzheimer's disease.* J Neurol Neurosurg Psychiatry, 1996. **60**(1): p. 91-3.

104. Stopford, C.L., et al., *Variability in cognitive presentation of Alzheimer's disease.* Cortex, 2008. **44**(2): p. 185-95.

105. Johnson, J.K., et al., *Clinical and pathological evidence for a frontal variant of Alzheimer disease.* Arch Neurol, 1999. **56**(10): p. 1233-9.

106. Ossenkoppele, R., et al., *The behavioural/dysexecutive variant of Alzheimer's disease: clinical, neuroimaging and pathological features.* Brain, 2015.

107. Bouchard, R.W.a.R., M.N., *Typical clinical features, Clinical Diagnosis and management of AD, London: Dunitz.* 1996.

108. Folstein, M.F., S.E. Folstein, and P.R. McHugh, *"Mini-mental state". A practical method for grading the cognitive state of patients for the clinician.* J Psychiatr Res, 1975. **12**(3): p. 189-98.

109. Nasreddine, Z.S., et al., *The Montreal Cognitive Assessment, MoCA: a brief screening tool for mild cognitive impairment.* J Am Geriatr Soc, 2005. **53**(4): p. 695-9.

110. Mathuranath, P.S., et al., *A brief cognitive test battery to differentiate Alzheimer's disease and frontotemporal dementia.* Neurology, 2000. **55**(11): p. 1613-20.

111. *Dementia: supporting people with dementia and their carers in health and social care (2006 updated 2016) NICE guideline CG42.*

112. Keshavan, A., et al., *Blood Biomarkers for Alzheimer's Disease: Much Promise, Cautious Progress.* Mol Diagn Ther, 2017. **21**(1): p. 13-22.

113. Frisoni, G.B., et al., *The clinical use of structural MRI in Alzheimer disease.* Nat Rev Neurol, 2010. **6**(2): p. 67-77.

114. Meeter, L.H., et al., *Imaging and fluid biomarkers in frontotemporal dementia.* Nat Rev Neurol, 2017. **13**(7): p. 406-419.

115. Kato, T., et al., *Brain fluorodeoxyglucose (FDG) PET in dementia.* Ageing Res Rev, 2016. **30**: p. 73-84.

116. Dubois, B., et al., *Advancing research diagnostic criteria for Alzheimer's disease: the IWG-2 criteria.* Lancet Neurol, 2014. **13**(6): p. 614-29.

117. McKhann, G.M., et al., *The diagnosis of dementia due to Alzheimer's disease: recommendations from the National Institute on Aging-Alzheimer's Association workgroups on diagnostic guidelines for Alzheimer's disease.* Alzheimers Dement, 2011. **7**(3): p. 263-9.

118. *AMYPAD.* http://amypad.eu/ *(accessed 02/04/2018).*

119. *IDEAS* https://www.ideas-study.org/ *(accessed 02/04/2018).*

120. Slattery, C.F., S.J. Crutch, and J.M. Schott, *Phenotypical variation in Alzheimer's disease: insights from posterior cortical atrophy.* Pract Neurol, 2015. **15**(1): p. 2-4.

121. Knopman, D.S., et al., *Practice parameter: diagnosis of dementia (an evidence-based review). Report of the Quality Standards Subcommittee of the American Academy of Neurology.* Neurology, 2001. **56**(9): p. 1143-53.

122. Waldemar, G., et al., *Diagnosis and management of Alzheimer's disease and other disorders associated with dementia. The role of neurologists in Europe. European Federation of Neurological Societies.* Eur J Neurol, 2000. **7**(2): p. 133-44.

123. Hort, J., et al., *EFNS guidelines for the diagnosis and management of Alzheimer's disease.* Eur J Neurol, 2010. **17**(10): p. 1236-48.

124. Blennow, K., *Cerebrospinal fluid protein biomarkers for Alzheimer's disease.* NeuroRx, 2004. **1**(2): p. 213-25.

125. Birks, J., *Cholinesterase inhibitors for Alzheimer's disease.* Cochrane Database Syst Rev, 2006(1): p. Cd005593.

126. Howard, R., et al., *Nursing home placement in the Donepezil and Memantine in Moderate to Severe Alzheimer's Disease (DOMINO-AD) trial: secondary and post-hoc analyses.* Lancet Neurol, 2015. **14**(12): p. 1171-81.

127. McShane, R., A. Areosa Sastre, and N. Minakaran, *Memantine for dementia.* Cochrane Database Syst Rev, 2006(2): p. Cd003154.

128. Schmidt, R., et al., *EFNS-ENS/EAN Guideline on concomitant use of cholinesterase inhibitors and memantine in moderate to severe Alzheimer's disease.* Eur J Neurol, 2015. **22**(6): p. 889-98.

129. *The Trajectory of Dementia in the UK – Making a Difference.* https://www.alzheimersresearchuk.org/wp-content/uploads/2015/01/OHE-report-Full.pdf *(accessed 27/05/2018).*

130. Sevigny, J., et al., *The antibody aducanumab reduces Abeta plaques in Alzheimer's disease.* Nature, 2016. **537**(7618): p. 50-6.

131. Ruthirakuhan, M., et al., *Beyond immunotherapy: new approaches for disease modifying treatments for early Alzheimer's disease.* Expert Opin Pharmacother, 2016. **17**(18): p. 2417-2429.

132. Mills, S.M., et al., *Preclinical trials in autosomal dominant AD: implementation of the DIAN-TU trial.* Rev Neurol (Paris), 2013. **169**(10): p. 737-43.

133. Reiman, E.M., et al., *Alzheimer's Prevention Initiative: a plan to accelerate the evaluation of presymptomatic treatments.* J Alzheimers Dis, 2011. **26 Suppl 3**: p. 321-9.

134. https://www.generationprogram.com/ *(accessed 27/05/2018).*

135. Sperling, R.A., et al., *The A4 study: stopping AD before symptoms begin?* Sci Transl Med, 2014. **6**(228): p. 228fs13.

136. Aisen, P.S., et al., *Tramiprosate in mild-to-moderate Alzheimer's disease - a randomized, double-blind, placebo-controlled, multi-centre study (the Alphase Study).* Arch Med Sci, 2011. **7**(1): p. 102-11.

137. Green, R.C., et al., *Effect of tarenflurbil on cognitive decline and activities of daily living in patients with mild Alzheimer disease: a randomized controlled trial.* Jama, 2009. **302**(23): p. 2557-64.

138. Doody, R.S., et al., *A phase 3 trial of semagacestat for treatment of Alzheimer's disease.* N Engl J Med, 2013. **369**(4): p. 341-50.

139. Salloway, S., et al., *Two phase 3 trials of bapineuzumab in mild-to-moderate Alzheimer's disease.* N Engl J Med, 2014. **370**(4): p. 322-33.

140. Doody, R.S., et al., *Phase 3 trials of solanezumab for mild-to-moderate Alzheimer's disease.* N Engl J Med, 2014. **370**(4): p. 311-21.

141. Relkin, N.R., et al., *A phase 3 trial of IV immunoglobulin for Alzheimer disease.* Neurology, 2017. **88**(18): p. 1768-1775.

142. Hung, S.Y. and W.M. Fu, *Drug candidates in clinical trials for Alzheimer's disease.* J Biomed Sci, 2017. **24**(1): p. 47.

143. Calsolaro, V. and P. Edison, *Neuroinflammation in Alzheimer's disease: Current evidence and future directions.* Alzheimers Dement, 2016. **12**(6): p. 719-32.

144. Cummings, J., et al., *Alzheimer's disease drug development pipeline: 2018.* Alzheimers Dement (N Y), 2018. **4**: p. 195-214.

145. Muller, U., P. Winter, and M.B. Graeber, *A presenilin 1 mutation in the first case of Alzheimer's disease.* Lancet Neurol, 2013. **12**(2): p. 129-30.

146. McDonald, C., *Clinical heterogeneity in senile dementia.* Br J Psychiatry, 1969. **115**(520): p. 267-71.

147. Ritchie, K. and J. Touchon, *Heterogeneity in senile dementia of the Alzheimer type: individual differences, progressive deterioration or clinical sub-types?* J Clin Epidemiol, 1992. **45**(12): p. 1391-8.

148. Foster, N.L., et al., *Alzheimer's disease: focal cortical changes shown by positron emission tomography.* Neurology, 1983. **33**(8): p. 961-5.

149. Haxby, J.V., et al., *Relations between neuropsychological and cerebral metabolic asymmetries in early Alzheimer's disease.* J Cereb Blood Flow Metab, 1985. **5**(2): p. 193-200.

150. Grady, C.L., et al., *Stability of metabolic and neuropsychological asymmetries in dementia of the Alzheimer type.* Neurology, 1986. **36**(10): p. 1390-2.

151. Seltzer, B. and I. Sherwin, *A comparison of clinical features in early- and late-onset primary degenerative dementia. One entity or two?* Arch Neurol, 1983. **40**(3): p. 143-6.

152. Filley, C.M., J. Kelly, and R.K. Heaton, *Neuropsychologic features of early- and late-onset Alzheimer's disease.* Arch Neurol, 1986. **43**(6): p. 574-6.

153. Fisher, N.J., et al., *Neuropsychological subgroups of patients with Alzheimer's disease.* J Clin Exp Neuropsychol, 1996. **18**(3): p. 349-70.

154. Fisher, N.J., B.P. Rourke, and L.A. Bieliauskas, *Neuropsychological subgroups of patients with Alzheimer's disease: an examination of the first 10 years of CERAD data.* J Clin Exp Neuropsychol, 1999. **21**(4): p. 488-518.

155. Fisher, N.J., et al., *Unmasking the heterogeneity of Alzheimer's disease: case studies of individuals from distinct neuropsychological subgroups.* J Clin Exp Neuropsychol, 1997. **19**(5): p. 713-54.

156. Schott, J.M. and J.D. Warren, *Alzheimer's disease: mimics and chameleons.* Pract Neurol, 2012. **12**(6): p. 358-66.

157. Butters, M.A., O.L. Lopez, and J.T. Becker, *Focal temporal lobe dysfunction in probable Alzheimer's disease predicts a slow rate of cognitive decline.* Neurology, 1996. **46**(3): p. 687-92.

158. Armstrong, R.A., D. Nochlin, and T.D. Bird, *Neuropathological heterogeneity in Alzheimer's disease: a study of 80 cases using principal components analysis.* Neuropathology, 2000. **20**(1): p. 31-7.

159. Koedam, E.L., et al., *Early-versus late-onset Alzheimer's disease: more than age alone.* J Alzheimers Dis, 2010. **19**(4): p. 1401-8.

160. Snowden, J.S., et al., *Cognitive phenotypes in Alzheimer's disease and genetic risk.* Cortex, 2007. **43**(7): p. 835-45.

161. Ryan, N.S., et al., *Motor features in posterior cortical atrophy and their imaging correlates.* Neurobiol Aging, 2014. **35**(12): p. 2845-2857.

162. Renner, J.A., et al., *Progressive posterior cortical dysfunction: a clinicopathologic series.* Neurology, 2004. **63**(7): p. 1175-80.

163. Formaglio, M., et al., *In vivo demonstration of amyloid burden in posterior cortical atrophy: a case series with PET and CSF findings.* J Neurol, 2011. **258**(10): p. 1841-51.

164. Seguin, J., et al., *CSF biomarkers in posterior cortical atrophy.* Neurology, 2011. **76**(21): p. 1782-8.

165. Tang-Wai, D.F., et al., *Clinical, genetic, and neuropathologic characteristics of posterior cortical atrophy.* Neurology, 2004. **63**(7): p. 1168-74.

166. Crutch, S.J., et al., *Consensus classification of posterior cortical atrophy.* Alzheimers Dement, 2017. **13**(8): p. 870-884.

167. Grossman, M., *Primary progressive aphasia: clinicopathological correlations.* Nat Rev Neurol, 2010. **6**(2): p. 88-97.

168. Rohrer, J.D., M.N. Rossor, and J.D. Warren, *Alzheimer's pathology in primary progressive aphasia.* Neurobiol Aging, 2012. **33**(4): p. 744-52.

169. Jack, C.R., Jr., et al., *NIA-AA Research Framework: Toward a biological definition of Alzheimer's disease.* Alzheimers Dement, 2018. **14**(4): p. 535-562.

170. Mattsson, N., et al., *Selective vulnerability in neurodegeneration: insights from clinical variants of Alzheimer's disease.* J Neurol Neurosurg Psychiatry, 2016. **87**(9): p. 1000-4.

171. Cavedo, E., et al., *Medial temporal atrophy in early and late-onset Alzheimer's disease.* Neurobiol Aging, 2014. **35**(9): p. 2004-12.

172. Moller, C., et al., *Different patterns of gray matter atrophy in early- and late-onset Alzheimer's disease.* Neurobiol Aging, 2013. **34**(8): p. 2014-22.

173. Whitwell, J.L., et al., *Imaging correlates of posterior cortical atrophy.* Neurobiol Aging, 2007. **28**(7): p. 1051-61.

174. Rohrer, J.D., et al., *Patterns of longitudinal brain atrophy in the logopenic variant of primary progressive aphasia.* Brain Lang, 2013. **127**(2): p. 121-6.

175. Mesulam, M., et al., *Alzheimer and frontotemporal pathology in subsets of primary progressive aphasia.* Ann Neurol, 2008. **63**(6): p. 709-19.

176. Gorno-Tempini, M.L., et al., *The logopenic/phonological variant of primary progressive aphasia.* Neurology, 2008. **71**(16): p. 1227-34.

177. Lehmann, M., et al., *Reduced cortical thickness in the posterior cingulate gyrus is characteristic of both typical and atypical Alzheimer's disease.* J Alzheimers Dis, 2010. **20**(2): p. 587-98.

178. Whitwell, J.L., et al., *Temporoparietal atrophy: a marker of AD pathology independent of clinical diagnosis.* Neurobiol Aging, 2011. **32**(9): p. 1531-41.

179. Lehmann, M., et al., *Global gray matter changes in posterior cortical atrophy: a serial imaging study.* Alzheimers Dement, 2012. **8**(6): p. 502-12.

180. Migliaccio, R., et al., *Mapping the Progression of Atrophy in Early- and Late-Onset Alzheimer's Disease.* J Alzheimers Dis, 2015. **46**(2): p. 351-64.

181. Madhavan, A., et al., *FDG PET and MRI in logopenic primary progressive aphasia versus dementia of the Alzheimer's type.* PLoS One, 2013. **8**(4): p. e62471.

182. Woodward, M.C., et al., *Differentiating the frontal presentation of Alzheimer's disease with FDG-PET.* J Alzheimers Dis, 2015. **44**(1): p. 233-42.

183. Lehmann, M., et al., *Diverging patterns of amyloid deposition and hypometabolism in clinical variants of probable Alzheimer's disease.* Brain, 2013. **136**(Pt 3): p. 844-58.

184. de Souza, L.C., et al., *Similar amyloid-beta burden in posterior cortical atrophy and Alzheimer's disease.* Brain, 2011. **134**(Pt 7): p. 2036-43.

185. Rosenbloom, M.H., et al., *Distinct clinical and metabolic deficits in PCA and AD are not related to amyloid distribution.* Neurology, 2011. **76**(21): p. 1789-96.

186. Teng, E., et al., *Cerebrospinal fluid biomarkers in clinical subtypes of early-onset Alzheimer's disease.* Dement Geriatr Cogn Disord, 2014. **37**(5-6): p. 307-14.

187. Paterson, R.W., et al., *Dissecting IWG-2 typical and atypical Alzheimer's disease: insights from cerebrospinal fluid analysis.* J Neurol, 2015. **262**(12): p. 2722-30.

188. Gefen, T., et al., *Clinically concordant variations of Alzheimer pathology in aphasic versus amnestic dementia.* Brain, 2012. **135**(Pt 5): p. 1554-65.

189. Greene, J.D., et al., *Alzheimer disease and nonfluent progressive aphasia.* Arch Neurol, 1996. **53**(10): p. 1072-8.

190. Ossenkoppele, R., et al., *Cerebrospinal fluid biomarkers and cerebral atrophy in distinct clinical variants of probable Alzheimer's disease.* Neurobiol Aging, 2015. **36**(8): p. 2340-7.

191. Bennett, D.A., et al., *Overview and findings from the rush Memory and Aging Project.* Curr Alzheimer Res, 2012. **9**(6): p. 646-63.

192. Ryan, N.S. and M.N. Rossor, *Correlating familial Alzheimer's disease gene mutations with clinical phenotype.* Biomark Med, 2010. **4**(1): p. 99-112.

193. Larner, A.J. and M. Doran, *Clinical phenotypic heterogeneity of Alzheimer's disease associated with mutations of the presenilin-1 gene.* J Neurol, 2006. **253**(2): p. 139-58.

194. Blacker, D., et al., *ApoE-4 and age at onset of Alzheimer's disease: the NIMH genetics initiative.* Neurology, 1997. **48**(1): p. 139-47.

195. van der Flier, W.M., et al., *Early-onset versus late-onset Alzheimer's disease: the case of the missing APOE varepsilon4 allele.* Lancet Neurol, 2011. **10**(3): p. 280-8.

196. Davidson, Y., et al., *Apolipoprotein E epsilon4 allele frequency and age at onset of Alzheimer's disease.* Dement Geriatr Cogn Disord, 2007. **23**(1): p. 60-6.

197. Marra, C., et al., *Apolipoprotein E epsilon4 allele differently affects the patterns of neuropsychological presentation in early- and late-onset Alzheimer's disease patients.* Dement Geriatr Cogn Disord, 2004. **18**(2): p. 125-31.

198. Lehtovirta, M., et al., *Clinical and neuropsychological characteristics in familial and sporadic Alzheimer's disease: relation to apolipoprotein E polymorphism.* Neurology, 1996. **46**(2): p. 413-9.

199. Pievani, M., et al., *Mapping the effect of APOE epsilon4 on gray matter loss in Alzheimer's disease in vivo.* Neuroimage, 2009. **45**(4): p. 1090-8.

200. Hashimoto, M., et al., *Apolipoprotein E epsilon 4 and the pattern of regional brain atrophy in Alzheimer's disease.* Neurology, 2001. **57**(8): p. 1461-6.

201. Filippini, N., et al., *Anatomically-distinct genetic associations of APOE epsilon4 allele load with regional cortical atrophy in Alzheimer's disease.* Neuroimage, 2009. **44**(3): p. 724-8.

202. Ossenkoppele, R., et al., *Differential effect of APOE genotype on amyloid load and glucose metabolism in AD dementia.* Neurology, 2013. **80**(4): p. 359-65.

203. Lehmann, M., et al., *Greater medial temporal hypometabolism and lower cortical amyloid burden in ApoE4-positive AD patients.* J Neurol Neurosurg Psychiatry, 2014. **85**(3): p. 266-73.

204. Tiraboschi, P., et al., *Impact of APOE genotype on neuropathologic and neurochemical markers of Alzheimer disease.* Neurology, 2004. **62**(11): p. 1977-83.

205. Schott, J.M., et al., *Apolipoprotein e genotype modifies the phenotype of Alzheimer disease*. 2006: Arch Neurol. 2006 Jan;63(1):155-6.

206. van der Flier, W.M., et al., *The effect of APOE genotype on clinical phenotype in Alzheimer disease.* Neurology, 2006. **67**(3): p. 526-7.

207. Warren, J.D., et al., *Molecular nexopathies: a new paradigm of neurodegenerative disease.* Trends Neurosci, 2013. **36**(10): p. 561-9.

208. Pievani, M., et al., *Functional network disruption in the degenerative dementias.* Lancet Neurol, 2011. **10**(9): p. 829-43.

209. Zhou, J., et al., *Predicting regional neurodegeneration from the healthy brain functional connectome.* Neuron, 2012. **73**(6): p. 1216-27.

210. Greicius, M.D., et al., *Functional connectivity in the resting brain: a network analysis of the default mode hypothesis.* Proc Natl Acad Sci U S A, 2003. **100**(1): p. 253-8.

211. Kamenetz, F., et al., *APP processing and synaptic function.* Neuron, 2003. **37**(6): p. 925-37.

212. Bero, A.W., et al., *Neuronal activity regulates the regional vulnerability to amyloid-beta deposition.* Nat Neurosci, 2011. **14**(6): p. 750-6.

213. Brody, D.L., et al., *Amyloid-beta dynamics correlate with neurological status in the injured human brain.* Science, 2008. **321**(5893): p. 1221-4.

214. Buckner, R.L., et al., *Molecular, structural, and functional characterization of Alzheimer's disease: evidence for a relationship between default activity, amyloid, and memory.* J Neurosci, 2005. **25**(34): p. 7709-17.

215. Jagust, W.J. and E.C. Mormino, *Lifespan brain activity, beta-amyloid, and Alzheimer's disease.* Trends Cogn Sci, 2011. **15**(11): p. 520-6.

216. Raichle, M.E., et al., *A default mode of brain function.* Proc Natl Acad Sci U S A, 2001. **98**(2): p. 676-82.

217. Fox, M.D., et al., *The human brain is intrinsically organized into dynamic, anticorrelated functional networks.* Proc Natl Acad Sci U S A, 2005. **102**(27): p. 9673-8.

218. Zhou, J., et al., *Divergent network connectivity changes in behavioural variant frontotemporal dementia and Alzheimer's disease.* Brain, 2010. **133**(Pt 5): p. 1352-67.

219. Rombouts, S.A., et al., *Altered resting state networks in mild cognitive impairment and mild Alzheimer's disease: an fMRI study.* Hum Brain Mapp, 2005. **26**(4): p. 231-9.

220. Filippini, N., et al., *Distinct patterns of brain activity in young carriers of the APOE-epsilon4 allele.* Proc Natl Acad Sci U S A, 2009. **106**(17): p. 7209-14.

221. Ridgway, G.R., et al., *Early-onset Alzheimer disease clinical variants: multivariate analyses of cortical thickness.* Neurology, 2012. **79**(1): p. 80-4.

222. Warren, J.D., P.D. Fletcher, and H.L. Golden, *The paradox of syndromic diversity in Alzheimer disease.* Nat Rev Neurol, 2012. **8**(8): p. 451-64.

223. Lehmann, M., et al., *Intrinsic connectivity networks in healthy subjects explain clinical variability in Alzheimer's disease.* Proc Natl Acad Sci U S A, 2013. **110**(28): p. 11606-11.

224. Polymenidou, M. and D.W. Cleveland, *Prion-like spread of protein aggregates in neurodegeneration.* J Exp Med, 2012. **209**(5): p. 889-93.

225. Warren, J.D., J.D. Rohrer, and J. Hardy, *Disintegrating brain networks: from syndromes to molecular nexopathies.* Neuron, 2012. **73**(6): p. 1060-2.

226. Kang, J.E., et al., *Amyloid-beta dynamics are regulated by orexin and the sleep-wake cycle.* Science, 2009. **326**(5955): p. 1005-7.

227. Wirths, O., et al., *Axonopathy in an APP/PS1 transgenic mouse model of Alzheimer's disease.* Acta Neuropathol, 2006. **111**(4): p. 312-9.

228. Hardy, J., *Catastrophic cliffs: a partial suggestion for selective vulnerability in neurodegenerative diseases.* Biochem Soc Trans, 2016. **44**(2): p. 659-61.

229. Hardy, J. and E. Rogaeva, *Motor neuron disease and frontotemporal dementia: sometimes related, sometimes not.* Exp Neurol, 2014. **262 Pt B**: p. 75-83.

230. National Institute for Health and Care Excellence (2018) Dementia: assessment, m.a.s.f.p.l.w.d.a.t.c.s.p.w.d.a.t.c.i.

231. Mugler, J.P., 3rd and J.R. Brookeman, *Three-dimensional magnetization-prepared rapid gradient-echo imaging (3D MP RAGE).* Magn Reson Med, 1990. **15**(1): p. 152-7.

232. Scheltens, P., et al., *Atrophy of medial temporal lobes on MRI in "probable" Alzheimer's disease and normal ageing: diagnostic value and neuropsychological correlates.* J Neurol Neurosurg Psychiatry, 1992. **55**(10): p. 967-72.

233. Smith, S.M., et al., *Normalized accurate measurement of longitudinal brain change.* J Comput Assist Tomogr, 2001. **25**(3): p. 466-75.

234. Hua, X., et al., *Unbiased tensor-based morphometry: improved robustness and sample size estimates for Alzheimer's disease clinical trials.* Neuroimage, 2013. **66**: p. 648-61.

235. Reuter, M., et al., *Within-subject template estimation for unbiased longitudinal image analysis.* Neuroimage, 2012. **61**(4): p. 1402-18.

236. Ciccarelli, O., et al., *Diffusion-based tractography in neurological disorders: concepts, applications, and future developments.* Lancet Neurol, 2008. **7**(8): p. 715-27.

237. Basser, P.J., J. Mattiello, and D. LeBihan, *MR diffusion tensor spectroscopy and imaging.* Biophys J, 1994. **66**(1): p. 259-67.

238. Canu, E., et al., *White matter microstructural damage in Alzheimer's disease at different ages of onset.* Neurobiol Aging, 2013. **34**(10): p. 2331-40.

239. Caso, F., et al., *White Matter Degeneration in Atypical Alzheimer Disease.* Radiology, 2015: p. 142766.

240. Madhavan, A., et al., *Characterizing White Matter Tract Degeneration in Syndromic Variants of Alzheimer's Disease: A Diffusion Tensor Imaging Study.* J Alzheimers Dis, 2015.

241. Enzinger, C., et al., *Nonconventional MRI and microstructural cerebral changes in multiple sclerosis.* Nat Rev Neurol, 2015. **11**(12): p. 676-86.

242. Zhang, H., et al., *NODDI: practical in vivo neurite orientation dispersion and density imaging of the human brain.* Neuroimage, 2012. **61**(4): p. 1000-16.

243. Ferizi, U., et al., *A ranking of diffusion MRI compartment models with in vivo human brain data.* Magn Reson Med, 2014. **72**(6): p. 1785-92.

244. Kamagata, K., et al., *Neurite orientation dispersion and density imaging in the substantia nigra in idiopathic Parkinson disease.* Eur Radiol, 2015.

245. Winston, G.P., et al., *Advanced diffusion imaging sequences could aid assessing patients with focal cortical dysplasia and epilepsy.* Epilepsy Res, 2014. **108**(2): p. 336-9.

246. Billiet, T., et al., *Age-related microstructural differences quantified using myelin water imaging and advanced diffusion MRI.* Neurobiol Aging, 2015. **36**(6): p. 2107-21.

247. Kunz, N., et al., *Assessing white matter microstructure of the newborn with multi-shell diffusion MRI and biophysical compartment models.* Neuroimage, 2014. **96**: p. 288-99.

248. Timmers, I., et al., *White matter microstructure pathology in classic galactosemia revealed by neurite orientation dispersion and density imaging.* J Inherit Metab Dis, 2015. **38**(2): p. 295-304.

249. Raichle, M.E., *Neuroscience. The brain's dark energy.* Science, 2006. **314**(5803): p. 1249-50.

250. Elman, J.A., et al., *Neural compensation in older people with brain amyloid-beta deposition.* Nat Neurosci, 2014. **17**(10): p. 1316-8.

251. Machulda, M.M., et al., *Comparison of memory fMRI response among normal, MCI, and Alzheimer's patients.* Neurology, 2003. **61**(4): p. 500-6.

252. Rombouts, S.A., et al., *Functional MR imaging in Alzheimer's disease during memory encoding.* AJNR Am J Neuroradiol, 2000. **21**(10): p. 1869-75.

253. Schroder, J., et al., *Patterns of cortical activity and memory performance in Alzheimer's disease.* Biol Psychiatry, 2001. **49**(5): p. 426-36.

254. Sperling, R.A., et al., *fMRI studies of associative encoding in young and elderly controls and mild Alzheimer's disease.* J Neurol Neurosurg Psychiatry, 2003. **74**(1): p. 44-50.

255. Putcha, D., et al., *Hippocampal hyperactivation associated with cortical thinning in Alzheimer's disease signature regions in non-demented elderly adults.* J Neurosci, 2011. **31**(48): p. 17680-8.

256. Duits, F.H., et al., *Diagnostic impact of CSF biomarkers for Alzheimer's disease in a tertiary memory clinic.* Alzheimers Dement, 2015. **11**(5): p. 523-32.

257. Dabul, B., *Apraxia battery for adults, Second edn. Pro-Ed, Austin.* 2000.

258. Rosen, W.G., et al., *Pathological verification of ischemic score in differentiation of dementias.* Ann Neurol, 1980. **7**(5): p. 486-8.

259. Wechsler, D., *Abbreviated Scale of Intelligence. The Psychological Corporation; San Antonio, Texas.* 1999.

260. Warrington, E.K., *Manual for the Recognition Memory Test for Words and Faces; Windsor, UK: NFER-Nelson.* 1984.

261. Warrington, E.K., *The Camden Memory Test Battery.* Psychology Press, Hove, UK (1996), 1996.

262. Wechsler, D., *Wechsler Memory Scale: Revised.* The Psychological Corporation, San Antonio, TX, 1987.

263. McKenna, P. and E.K. Warrington, *GradedNamingTest. NFER-Nelson,Windsor, UK.* 1983.

264. Jackson, M. and E.K. Warrington, *Arithmetic skills in patients with unilateral cerebral lesions.* Cortex, 1986. **22**(4): p. 611-20.

265. Baxter, D.M. and E.K. Warrington, *Measuring dysgraphia: a graded-difficulty spelling test.* Behav Neurol, 1994. **7**(3): p. 107-16.

266. Warrington, E. and M. James, *The Visual Object and Space Perception Battery* Bury St Edmunds, UK: Thames Valley Test Company, 1991.

267. Delis, D.C., Kaplan, E., Kramer, J.H., *Delis-Kaplan Executive Function System. .* The Psychological Corporation, San Antonio, TX., 2001.

268. Smith, A., *The symbol-digit modalities test: a neuropsychologic test of learning and other cerebral disorders.* In J. Helmuth (Ed.), Learning disorders. Seattle: Special Child Publications, 1986: p. 83–91.

269. Mugler, J.P., 3rd and J.R. Brookeman, *Rapid three-dimensional T1-weighted MR imaging with the MP-RAGE sequence.* J Magn Reson Imaging, 1991. **1**(5): p. 561-7.

270. Jenkinson, M., et al., *Improved optimization for the robust and accurate linear registration and motion correction of brain images.* Neuroimage, 2002. **17**(2): p. 825-41.

271. Jenkinson, M. and S. Smith, *A global optimisation method for robust affine registration of brain images.* Med Image Anal, 2001. **5**(2): p. 143-56.

272. Zhang, H., et al., *High-dimensional spatial normalization of diffusion tensor images improves the detection of white matter differences: an example study using amyotrophic lateral sclerosis.* IEEE Trans Med Imaging, 2007. **26**(11): p. 1585-97.

273. Zhang, H., et al., *Deformable registration of diffusion tensor MR images with explicit orientation optimization.* Med Image Anal, 2006. **10**(5): p. 764-85.

274. Wang, Y., et al., *DTI registration in atlas based fiber analysis of infantile Krabbe disease.* Neuroimage, 2011. **55**(4): p. 1577-86.

275. Jenkinson, M., et al., *FSL.* Neuroimage, 2012. **62**(2): p. 782-90.

276. Sanger, F., S. Nicklen, and A.R. Coulson, *DNA sequencing with chain-terminating inhibitors. 1977.* Biotechnology, 1992. **24**: p. 104-8.

277. National Institute for Health and Care Excellence (2011, u.D., galantamine, rivastigmine and memantine for the treatment of Alzheimer's disease (Technology appraisal guidance TA217). Available at: https://www.nice.org.uk/guidance/ta217 [Accessed 18.08.2018].

278. Moroney, J.T., et al., *Meta-analysis of the Hachinski Ischemic Score in pathologically verified dementias.* Neurology, 1997. **49**(4): p. 1096-105.

279. Gillette-Guyonnet, S., et al., *Weight loss in Alzheimer disease.* Am J Clin Nutr, 2000. **71**(2): p. 637s-642s.

280. Kivipelto, M., et al., *Midlife vascular risk factors and Alzheimer's disease in later life: longitudinal, population based study.* Bmj, 2001. **322**(7300): p. 1447-51.

281. Beck, J., et al., *Validation of next-generation sequencing technologies in genetic diagnosis of dementia.* Neurobiol Aging, 2014. **35**(1): p. 261-5.

282. Adzhubei, I.A., et al., *A method and server for predicting damaging missense mutations.* Nat Methods, 2010. **7**(4): p. 248-9.

283. Janssen, J.C., et al., *Early onset familial Alzheimer's disease: Mutation frequency in 31 families.* Neurology, 2003. **60**(2): p. 235-9.

284. Ringman, J.M., et al., *Female preclinical presenilin-1 mutation carriers unaware of their genetic status have higher levels of depression than their non-mutation carrying kin.* J Neurol Neurosurg Psychiatry, 2004. **75**(3): p. 500-2.

285. Pennington, P.R., et al., *Alzheimer disease-related presenilin-1 variants exert distinct effects on monoamine oxidase-A activity in vitro.* J Neural Transm (Vienna), 2011. **118**(7): p. 987-95.

286. Hoffman-Andrews, L., *The known unknown: the challenges of genetic variants of uncertain significance in clinical practice.* J Law Biosci, 2017. **4**(3): p. 648-657.

287. Bronzova, J., et al., *Apolipoprotein E genotype and concomitant clinical features in early-onset Alzheimer's disease.* J Neurol, 1996. **243**(6): p. 465-8.

288. Schott, J.M., et al., *Apolipoprotein e genotype modifies the phenotype of Alzheimer disease.* Arch Neurol, 2006. **63**(1): p. 155-6.

289. Schott, J.M., et al., *Genetic risk factors for the posterior cortical atrophy variant of Alzheimer's disease.* Alzheimers Dement, 2016. **12**(8): p. 862-71.

290. Wolk, D.A. and B.C. Dickerson, *Apolipoprotein E (APOE) genotype has dissociable effects on memory and attentional-executive network function in Alzheimer's disease.* Proc Natl Acad Sci U S A, 2010. **107**(22): p. 10256-61.

291. Pottier, C., et al., *TREM2 R47H variant as a risk factor for early-onset Alzheimer's disease.* J Alzheimers Dis, 2013. **35**(1): p. 45-9.

292. Colonna, M. and Y. Wang, *TREM2 variants: new keys to decipher Alzheimer disease pathogenesis.* Nat Rev Neurosci, 2016. **17**(4): p. 201-7.

293. Rayaprolu, S., et al., *TREM2 in neurodegeneration: evidence for association of the p.R47H variant with frontotemporal dementia and Parkinson's disease.* Mol Neurodegener, 2013. **8**(1): p. 19.

294. Benitez, B.A. and C. Cruchaga, *TREM2 and neurodegenerative disease.* N Engl J Med, 2013. **369**(16): p. 1567-8.

295. Borroni, B., et al., *Heterozygous TREM2 mutations in frontotemporal dementia.* Neurobiology of Aging, (0).

296. Cuyvers, E., et al., *Investigating the role of rare heterozygous TREM2 variants in Alzheimer's disease and frontotemporal dementia.* Neurobiology of Aging, 2014. **35**(3): p. 726.e11-726.e19.

297. Hakola, H.P., *Neuropsychiatric and genetic aspects of a new hereditary disease characterized by progressive dementia and lipomembranous polycystic osteodysplasia.* Acta Psychiatr Scand Suppl, 1972. **232**: p. 1-173.

298. Nasu, T., Y. Tsukahara, and K. Terayama, *A lipid metabolic disease-"membranous lipodystrophy"-an autopsy case demonstrating numerous peculiar membrane-structures composed of compound lipid in bone and bone marrow and various adipose tissues.* Acta Pathol Jpn, 1973. **23**(3): p. 539-58.

299. Paloneva, J., et al., *Loss-of-function mutations in TYROBP (DAP12) result in a presenile dementia with bone cysts.* Nat Genet, 2000. **25**(3): p. 357-61.

300. Klunemann, H.H., et al., *The genetic causes of basal ganglia calcification, dementia, and bone cysts: DAP12 and TREM2.* Neurology, 2005. **64**(9): p. 1502-7.

301. Gomez-Nicola, D., et al., *Regulation of microglial proliferation during chronic neurodegeneration.* J Neurosci, 2013. **33**(6): p. 2481-93.

302. Rademakers, R., et al., *Mutations in the colony stimulating factor 1 receptor (CSF1R) gene cause hereditary diffuse leukoencephalopathy with spheroids.* Nat Genet, 2011. **44**(2): p. 200-5.

303. Wechsler, D., *Manual for the Wechsler Adult Intelligence Scale New York: Psychological Corporation.* 1981.

304. Sled, J.G., A.P. Zijdenbos, and A.C. Evans, *A nonparametric method for automatic correction of intensity nonuniformity in MRI data.* IEEE Trans Med Imaging, 1998. **17**(1): p. 87-97.

305. Boyes, R.G., et al., *Intensity non-uniformity correction using N3 on 3-T scanners with multichannel phased array coils.* Neuroimage, 2008. **39**(4): p. 1752-62.

306. Leung, K.K., et al., *Brain MAPS: an automated, accurate and robust brain extraction technique using a template library.* Neuroimage, 2011. **55**(3): p. 1091-108.

307. Jorge Cardoso, M., et al., *STEPS: Similarity and Truth Estimation for Propagated Segmentations and its application to hippocampal segmentation and brain parcelation.* Med Image Anal, 2013. **1**(13): p. 00020-0.

308. http://www.fil.ion.ucl.ac.uk/spm, *Interactive algorithms for theStatistical Parametric Mapping.*

309. Benitez, B.A., et al., *TREM2 is associated with the risk of Alzheimer's disease in Spanish population.* Neurobiol Aging, 2013. **34**(6): p. 5.

310. Giraldo, M., et al., *Variants in triggering receptor expressed on myeloid cells 2 are associated with both behavioral variant frontotemporal lobar degeneration and Alzheimer's disease.* Neurobiol Aging, 2013. **9**(13): p. 016.

311. Pottier, C., et al., *TREM2 R47H Variant as a Risk Factor for Early-Onset Alzheimer's Disease.* J Alzheimers Dis, 2013. **4**: p. 4.

312. Gilman, S., et al., *Clinical effects of Abeta immunization (AN1792) in patients with AD in an interrupted trial.* Neurology, 2005. **64**(9): p. 1553-62.

313. Paloneva, J., et al., *CNS manifestations of Nasu-Hakola disease: a frontal dementia with bone cysts.* Neurology, 2001. **56**(11): p. 1552-8.

314. Sims, R., et al., *Rare coding variants in PLCG2, ABI3, and TREM2 implicate microglial-mediated innate immunity in Alzheimer's disease.* Nat Genet, 2017. **49**(9): p. 1373-1384.

315. Lattante, S., et al., *TREM2 mutations are rare in a French cohort of patients with frontotemporal dementia.* Neurobiol Aging, 2013. **4**(13): p. 030.

316. Ruiz, A., et al., *Assessing the role of the TREM2 p.R47H variant as a risk factor for Alzheimer's disease and frontotemporal dementia.* Neurobiology of Aging, 2014. **35**(2): p. 444.e1-444.e4.

317. Korvatska, O., et al., *R47H Variant of TREM2 Associated With Alzheimer Disease in a Large Late-Onset Family: Clinical, Genetic, and Neuropathological Study.* JAMA Neurol, 2015. **72**(8): p. 920-7.

318. Balasa, M., et al., *Clinical features and APOE genotype of pathologically proven early-onset Alzheimer disease.* Neurology, 2011. **76**(20): p. 1720-5.

319. Tan, K.S., et al., *Differential Longitudinal Decline on the Mini-Mental State Examination in Frontotemporal Lobar Degeneration and Alzheimer Disease.* Alzheimer Dis Assoc Disord, 2013. **14**: p. 14.

320. van der Vlies, A.E., et al., *Most rapid cognitive decline in APOE epsilon4 negative Alzheimer's disease with early onset.* Psychol Med, 2009. **39**(11): p. 1907-11.

321. Luis, E.O., et al., *Frontobasal gray matter loss is associated with the TREM2 p.R47H variant.* Neurobiol Aging, 2014. **35**(12): p. 2681-2690.

322. Rajagopalan, P., D.P. Hibar, and P.M. Thompson, *TREM2 and neurodegenerative disease.* N Engl J Med, 2013. **369**(16): p. 1565-7.

323. Geroldi, C., et al., *APOE-epsilon4 is associated with less frontal and more medial temporal lobe atrophy in AD.* Neurology, 1999. **53**(8): p. 1825-32.

324. Gutierrez-Galve, L., et al., *Patterns of cortical thickness according to APOE genotype in Alzheimer's disease.* Dement Geriatr Cogn Disord, 2009. **28**(5): p. 476-85.

325. Evans, A.C., et al., *3D statistical neuroanatomical models from 305 MRI volumes, in: Nuclear Science Symposium and Medical Imaging Conference, 1993., 1993 IEEE Conference Record. Presented at the Nuclear Science Symposium and Medical Imaging Conference, 1993., 1993 IEEE Conference Record., pp. 1813–1817 vol.3. doi:10.1109/NSSMIC.1993.373602.* 1993.

326. Freeborough, P.A., N.C. Fox, and R.I. Kitney, *Interactive algorithms for the segmentation and quantitation of 3-D MRI brain scans.* Comput Methods Programs Biomed, 1997. **53**(1): p. 15-25.

327. Ashburner, J., *A fast diffeomorphic image registration algorithm.* Neuroimage, 2007. **38**(1): p. 95-113.

328. Ridgway, G.R., et al., *Ten simple rules for reporting voxel-based morphometry studies.* Neuroimage, 2008. **40**(4): p. 1429-35.

329. Ridgway, G.R., et al., *Issues with threshold masking in voxel-based morphometry of atrophied brains.* Neuroimage, 2009. **44**(1): p. 99-111.

330. Frisoni, G.B., et al., *The topography of grey matter involvement in early and late onset Alzheimer's disease.* Brain, 2007. **130**(Pt 3): p. 720-30.

331. Manning, E.N., et al., *APOE epsilon4 is associated with disproportionate progressive hippocampal atrophy in AD.* PLoS One, 2014. **9**(5): p. e97608.

332. Agosta, F., et al., *Apolipoprotein E epsilon4 is associated with disease-specific effects on brain atrophy in Alzheimer's disease and frontotemporal dementia.* Proc Natl Acad Sci U S A, 2009. **106**(6): p. 2018-22.

333. Mattsson, N., et al., *Greater tau load and reduced cortical thickness in APOE epsilon4-negative Alzheimer's disease: a cohort study.* Alzheimers Res Ther, 2018. **10**(1): p. 77.

334. Murray, M.E., et al., *Neuropathologically defined subtypes of Alzheimer's disease with distinct clinical characteristics: a retrospective study.* Lancet Neurol, 2011. **10**(9): p. 785-96.

335. Smith, S.M., et al., *Tract-based spatial statistics: voxelwise analysis of multi-subject diffusion data.* Neuroimage, 2006. **31**(4): p. 1487-505.

336. Smith, S.M., et al., *Advances in functional and structural MR image analysis and implementation as FSL.* Neuroimage, 2004. **23 Suppl 1**: p. S208-19.

337. Bach, M., et al., *Methodological considerations on tract-based spatial statistics (TBSS).* Neuroimage, 2014. **100**: p. 358-69.

338. Keihaninejad, S., et al., *The importance of group-wise registration in tract based spatial statistics study of neurodegeneration: a simulation study in Alzheimer's disease.* PLoS One, 2012. **7**(11): p. e45996.

339. Keihaninejad, S., et al., *An unbiased longitudinal analysis framework for tracking white matter changes using diffusion tensor imaging with application to Alzheimer's disease.* Neuroimage, 2013. **72**: p. 153-63.

340. Winkler, A.M., et al., *Permutation inference for the general linear model.* Neuroimage, 2014. **92**: p. 381-97.

341. Cerami, C., et al., *Brain changes within the visuo-spatial attentional network in posterior cortical atrophy.* J Alzheimers Dis, 2015. **43**(2): p. 385-95.

342. Wang, C., et al., *Atrophy and dysfunction of parahippocampal white matter in mild Alzheimer's disease.* Neurobiol Aging, 2012. **33**(1): p. 43-52.

343. Kljajevic, V., et al., *The epsilon4 genotype of apolipoprotein E and white matter integrity in Alzheimer's disease.* Alzheimers Dement, 2014. **10**(3): p. 401-4.

344. Acosta-Cabronero, J., et al., *Absolute diffusivities define the landscape of white matter degeneration in Alzheimer's disease.* Brain, 2010. **133**(Pt 2): p. 529-39.

345. Jespersen, S.N., et al., *Neurite density from magnetic resonance diffusion measurements at ultrahigh field: comparison with light microscopy and electron microscopy.* Neuroimage, 2010. **49**(1): p. 205-16.

346. Acosta-Cabronero, J., et al., *Diffusion tensor metrics as biomarkers in Alzheimer's disease.* PLoS One, 2012. **7**(11): p. e49072.

347. Parker, T.D., et al., *Cortical microstructure in young onset Alzheimer's disease using neurite orientation dispersion and density imaging.* Hum Brain Mapp, 2018. **39**(7): p. 3005-3017.

348. Jespersen, S.N., et al., *Determination of axonal and dendritic orientation distributions within the developing cerebral cortex by diffusion tensor imaging.* IEEE Trans Med Imaging, 2012. **31**(1): p. 16-32.

349. Grussu, F., et al., *Neurite dispersion: a new marker of multiple sclerosis spinal cord pathology?* Ann Clin Transl Neurol, 2017. **4**(9): p. 663-679.

350. Jespersen, S.N., et al., *Modeling dendrite density from magnetic resonance diffusion measurements.* Neuroimage, 2007. **34**(4): p. 1473-86.

351. Grussu F, S.T., Yates RL, Tachrount M, Newcombe J, Zhang H, Alexander DC, DeLuca GC, and Wheeler-Kingshott CAM., *Histological metrics confirm microstructural characteristics of NODDI indices in multiple sclerosis spinal cord.* Poster session presented at ISMRM 23rd Annual Meeting & Exhibition 2015. **30 May-05 June 2015, Toronto, Ontario, Canada**.

352. Maniega, S.M., et al., *White matter hyperintensities and normal-appearing white matter integrity in the aging brain.* Neurobiol Aging, 2015. **36**(2): p. 909-18.

353. Shinohara, M., et al., *Impact of sex and APOE4 on cerebral amyloid angiopathy in Alzheimer's disease.* Acta Neuropathol, 2016. **132**(2): p. 225-34.

354. Chang, Y.S., et al., *White Matter Changes of Neurite Density and Fiber Orientation Dispersion during Human Brain Maturation.* PLoS One, 2015. **10**(6): p. e0123656.

355. Lane, C.A., et al., *Study protocol: Insight 46 - a neuroscience sub-study of the MRC National Survey of Health and Development.* BMC Neurol, 2017. **17**(1): p. 75.

356. Buckner, R.L., J.R. Andrews-Hanna, and D.L. Schacter, *The brain's default network: anatomy, function, and relevance to disease.* Ann N Y Acad Sci, 2008: p. 011.

357. Seeley, W.W., et al., *Neurodegenerative diseases target large-scale human brain networks.* Neuron, 2009. **62**(1): p. 42-52.

358. Goll, J.C., et al., *Impairments of auditory scene analysis in Alzheimer's disease.* Brain, 2012. **135**(Pt 1): p. 190-200.

359. Golden, H.L., et al., *Functional neuroanatomy of auditory scene analysis in Alzheimer's disease.* Neuroimage Clin, 2015. **7**: p. 699-708.

360. Golden, H.L., et al., *Functional neuroanatomy of spatial sound processing in Alzheimer's disease.* Neurobiol Aging, 2016. **39**: p. 154-64.

361. Leech, R. and D.J. Sharp, *The role of the posterior cingulate cortex in cognition and disease.* Brain, 2014. **137**(Pt 1): p. 12-32.

362. Zundorf, I.C., J. Lewald, and H.O. Karnath, *Neural correlates of sound localization in complex acoustic environments.* PLoS One, 2013. **8**(5): p. e64259.

363. Golden, H.L., et al., *Auditory spatial processing in Alzheimer's disease.* Brain, 2015. **138**(Pt 1): p. 189-202.

364. Omar, R., Hailstone, J.C., Warren, J.D., *Semantic memory for music in dementia.* Music Perception, 2012. **29: 467-477**.

365. Baird, A. and S. Samson, *Music and dementia.* Prog Brain Res, 2015. **217**: p. 207-35.

366. Groussard, M., C. Mauger, and H. Platel, *[Musical long-term memory throughout the progression of Alzheimer disease].* Geriatr Psychol Neuropsychiatr Vieil, 2013. **11**(1): p. 99-109.

367. Jacobsen, J.H., et al., *Why musical memory can be preserved in advanced Alzheimer's disease.* Brain, 2015.

368. Baird, A. and S. Samson, *Memory for music in Alzheimer's disease: unforgettable?* Neuropsychol Rev, 2009. **19**(1): p. 85-101.

369. Omar, R., et al., *The cognitive organization of music knowledge: a clinical analysis.* Brain, 2010. **133**(Pt 4): p. 1200-13.

370. Vanstone, A.D., Sikka, R., Tangness, L., Sham, R., Garcia, A., Cuddy, L.L., *Episodic and semantic memory for melodies in Alzheimer's disease.* Music Perception, 2012. **29: 501-507**.

371. Cuddy, L.L., R. Sikka, and A. Vanstone, *Preservation of musical memory and engagement in healthy aging and Alzheimer's disease.* Ann N Y Acad Sci, 2015. **1337**: p. 223-31.

372. Platel, H., et al., *Semantic and episodic memory of music are subserved by distinct neural networks.* Neuroimage, 2003. **20**(1): p. 244-56.

373. Groussard, M., et al., *When music and long-term memory interact: effects of musical expertise on functional and structural plasticity in the hippocampus.* PLoS One, 2010. **5**(10).

374. Groussard, M., et al., *The neural substrates of musical memory revealed by fMRI and two semantic tasks.* Neuroimage, 2010. **53**(4): p. 1301-9.

375. Sikka, R., et al., *An fMRI comparison of neural activity associated with recognition of familiar melodies in younger and older adults.* Front Neurosci, 2015. **9**: p. 356.

376. Watanabe, T., S. Yagishita, and H. Kikyo, *Memory of music: roles of right hippocampus and left inferior frontal gyrus.* Neuroimage, 2008. **39**(1): p. 483-91.

377. Burunat, I., et al., *Dynamics of brain activity underlying working memory for music in a naturalistic condition.* Cortex, 2014. **57**: p. 254-69.

378. Hunkin, N.M., et al., *Novelty-related activation within the medial temporal lobes.* Neuropsychologia, 2002. **40**(8): p. 1456-64.

379. Downar, J., et al., *A cortical network sensitive to stimulus salience in a neutral behavioral context across multiple sensory modalities.* J Neurophysiol, 2002. **87**(1): p. 615-20.

380. Herdener, M., et al., *Musical training induces functional plasticity in human hippocampus.* J Neurosci, 2010. **30**(4): p. 1377-84.

381. Ossenkoppele, R., et al., *Atrophy patterns in early clinical stages across distinct phenotypes of Alzheimer's disease.* Hum Brain Mapp, 2015. **36**(11): p. 4421-37.

382. Weston, P.S., et al., *Using florbetapir positron emission tomography to explore cerebrospinal fluid cut points and gray zones in small sample sizes.* Alzheimers Dement (Amst), 2015. **1**(4): p. 440-446.

383. Hailstone, J.C., et al., *It's not what you play, it's how you play it: timbre affects perception of emotion in music.* Q J Exp Psychol (Hove), 2009. **62**(11): p. 2141-55.

384. Nelson, H.E., *National Adult Reading Test.* NEFR-Nelson, Windsor., 1982.

385. Gladsjo, J.A., et al., *Norms for letter and category fluency: demographic corrections for age, education, and ethnicity.* Assessment, 1999. **6**(2): p. 147-78.

386. Strange, B.A., et al., *Information theory, novelty and hippocampal responses: unpredicted or unpredictable?* Neural Netw, 2005. **18**(3): p. 225-30.

387. Desikan, R.S., et al., *An automated labeling system for subdividing the human cerebral cortex on MRI scans into gyral based regions of interest.* Neuroimage, 2006. **31**(3): p. 968-80.

388. Hsieh, S., et al., *Neural basis of music knowledge: evidence from the dementias.* Brain, 2011. **134**(Pt 9): p. 2523-34.

389. Golden, H.L., et al., *Identification of environmental sounds and melodies in syndromes of anterior temporal lobe degeneration.* J Neurol Sci, 2015. **352**(1-2): p. 94-8.

390. Demorest, S.M., et al., *An fMRI investigation of the cultural specificity of music memory.* Soc Cogn Affect Neurosci, 2010. **5**(2-3): p. 282-91.

391. Pereira, C.S., et al., *Music and emotions in the brain: familiarity matters.* PLoS One, 2011. **6**(11): p. e27241.

392. Kafkas, A. and D. Montaldi, *Two separate, but interacting, neural systems for familiarity and novelty detection: a dual-route mechanism.* Hippocampus, 2014. **24**(5): p. 516-27.

393. Leech, R., et al., *Fractionating the default mode network: distinct contributions of the ventral and dorsal posterior cingulate cortex to cognitive control.* J Neurosci, 2011. **31**(9): p. 3217-24.

394. Daselaar, S.M., S.E. Prince, and R. Cabeza, *When less means more: deactivations during encoding that predict subsequent memory.* Neuroimage, 2004. **23**(3): p. 921-7.

395. Cavanna, A.E. and M.R. Trimble, *The precuneus: a review of its functional anatomy and behavioural correlates.* Brain, 2006. **129**(Pt 3): p. 564-83.

396. Lustig, C., et al., *Functional deactivations: change with age and dementia of the Alzheimer type.* Proc Natl Acad Sci U S A, 2003. **100**(24): p. 14504-9.

397. Celone, K.A., et al., *Alterations in memory networks in mild cognitive impairment and Alzheimer's disease: an independent component analysis.* J Neurosci, 2006. **26**(40): p. 10222-31.

398. Tsai, P.H., et al., *Posterior cortical atrophy: evidence for discrete syndromes of early-onset Alzheimer's disease.* Am J Alzheimers Dis Other Demen, 2011. **26**(5): p. 413-8.

399. Shakespeare, T.J., et al., *Reduced modulation of scanpaths in response to task demands in posterior cortical atrophy.* Neuropsychologia, 2015. **68**: p. 190-200.

400. Golden, H.L., et al., *Music Perception in Dementia.* J Alzheimers Dis, 2017. **55**(3): p. 933-949.

401. Sarkamo, T., et al., *Cognitive, emotional, and social benefits of regular musical activities in early dementia: randomized controlled study.* Gerontologist, 2014. **54**(4): p. 634-50.

402. Goll, J.C., et al., *Nonverbal sound processing in semantic dementia: a functional MRI study.* Neuroimage, 2012. **61**(1): p. 170-80.

403. Whitwell, J.L., et al., *VBM signatures of abnormal eating behaviours in frontotemporal lobar degeneration.* Neuroimage, 2007. **35**(1): p. 207-13.

404. Mumford, J.A. and T.E. Nichols, *Power calculation for group fMRI studies accounting for arbitrary design and temporal autocorrelation.* Neuroimage, 2008. **39**(1): p. 261-8.

405. Mahoney, C.J., et al., *Longitudinal diffusion tensor imaging in frontotemporal dementia.* Ann Neurol, 2015. **77**(1): p. 33-46.

406. Lee, S.H., et al., *Estimation and partitioning of polygenic variation captured by common SNPs for Alzheimer's disease, multiple sclerosis and endometriosis.* Hum Mol Genet, 2013. **22**(4): p. 832-41.

407. Escott-Price, V., et al., *Common polygenic variation enhances risk prediction for Alzheimer's disease.* Brain, 2015. **138**(Pt 12): p. 3673-84.

408. McKiernan, E.F. and J.T. O'Brien, *7T MRI for neurodegenerative dementias in vivo: a systematic review of the literature.* J Neurol Neurosurg Psychiatry, 2017. **88**(7): p. 564-574.

409. Villemagne, V.L., et al., *Imaging tau and amyloid-beta proteinopathies in Alzheimer disease and other conditions.* Nat Rev Neurol, 2018. **14**(4): p. 225-236.

410. Zhang, X.Y., et al., *PET/MR Imaging: New Frontier in Alzheimer's Disease and Other Dementias.* Front Mol Neurosci, 2017. **10**: p. 343.

411. Glasser, M.F., et al., *The Human Connectome Project's neuroimaging approach.* Nat Neurosci, 2016. **19**(9): p. 1175-87.

412. Carmona, S., et al., *The role of TREM2 in Alzheimer's disease and other neurodegenerative disorders.* Lancet Neurol, 2018. **17**(8): p. 721-730.

413. Javad, F., et al., *Auditory tracts identified with combined fMRI and diffusion tractography.* Neuroimage, 2014. **84**: p. 562-74.

414. Shi, Y., et al., *Human cerebral cortex development from pluripotent stem cells to functional excitatory synapses.* Nat Neurosci, 2012. **15**(3): p. 477-86, s1.

415. Hudis, C.A., *Trastuzumab--mechanism of action and use in clinical practice.* N Engl J Med, 2007. **357**(1): p. 39-51.

416. Czirr, E., et al., *Insensitivity to Abeta42-lowering nonsteroidal anti-inflammatory drugs and gamma-secretase inhibitors is common among aggressive presenilin-1 mutations.* J Biol Chem, 2007. **282**(34): p. 24504-13.

417. Ness, S., et al., *Down's syndrome and Alzheimer's disease: towards secondary prevention.* Nat Rev Drug Discov, 2012. **11**(9): p. 655-6.